

A Model-based Assessment of Ocean Carbon Sequestration with Macroalgae Mariculture

Dissertation

zur Erlangung des Doktorgrades
der Mathematisch-Naturwissenschaftlichen Fakultät
der Christian-Albrechts-Universität zu Kiel

vorgelegt von

Jiajun Wu

Kiel
November, 2023

Erster Gutachter und Betreuer: Professor Andreas Oshlies

Zweiter Gutachter: Professor Arne Körtzinger

Tag der Disputation: 09. February. 2024

.....
gez. Prof. Dr. Frank Kempken, Dekan

"For a successful technology, reality must take precedence over public relations, for Nature cannot be fooled."

– Richard P. Feynman

Summary

The Paris Agreement, adopted in 2015, sets a clear goal to limit the average global temperature rise to well below 2°C, and ideally, to 1.5°C above pre-industrial levels by the end of the 21st century. This is expected to prevent the most severe consequences of human-induced climate change. However, the current efforts towards emission reduction and other climate mitigation efforts have not yielded sufficient results for the set temperature limits. In light of this, Carbon Dioxide Removal (CDR) methodologies, entailing the artificial/human-made capture and long-term storage of carbon dioxide from the atmosphere, have emerged as unavoidable/necessary and pivotal measures to achieve proclaimed net-zero emissions targets by nations around the world.

The ocean, as the Earth's largest long-term repository for anthropogenic CO₂, possesses a carbon storage capacity significantly surpassing that of the atmosphere and terrestrial biosphere, prompting the exploration of ocean-based CDR strategies. The utilization of macroalgae for ocean-based CDR has attracted notable attention due to their high photosynthetic efficiency, carbon-rich biomass, and well-established breeding and cultivation techniques. In this thesis, I present the assessment of the ocean-based CDR with macroalgae as carbon courier, named macroalgae-based CDR strategies. Macroalgae-based CDR has been studied in both open oceans and nearshore regions via numerical modeling within an Earth sys-

tem climate model (Chapter 2 & 3). The assessment concerned its carbon sequestration capacity and efficiency, as well as the interactions between macroalgae-based CDR and the global carbon cycle and marine biogeochemistry. Meanwhile, macroalgae-based CDR is evaluated as a viable component of Germany's Net-Zero 2050 target (Chapter 4), bridging the theoretical assessments with practical, region-specific applications, further contributing to the broader understanding and increased feasibility of macroalgae-based CDR strategies in addressing climate change goals.

In Chapter 2, the focus is on the Macroalgae Open-ocean Mariculture and Sinking (MOS) methodology as a viable macroalgae-based CDR strategy. Through a synergistic approach that integrates a macroalgae growth model into the University of Victoria Earth System Model (UVic ESCM), the theoretical efficacy of MOS in carbon sequestration is explored, alongside its potential biogeochemical implications. The findings reveal that MOS, particularly when enhanced with Artificial Upwelling (AU), holds substantial promise in sequestering carbon. However, this CDR potential comes with significant repercussions on marine ecosystems, notably a reduction in Phytoplankton Net Primary Production (PNPP) due to nutrient competition and canopy shading, and downstream alterations in Oxygen-Minimum Zones (OMZs).

Chapter 3 transitions to evaluating the Nearshore Macroalgae Aquaculture for Carbon Sequestration (N-MACS) strategy, which facilitates macroalgae cultivation in nearshore ocean surfaces. The assessment covers the CDR potential of N-MACS, its implications on the global carbon cycle, marine biogeochemistry, and marine ecosystems. The macroalgae model, initially established, is adapted to nearshore areas to align with the span of Exclusive Economic Zones (EEZs). The simulations underscore that while N-MACS holds promise in carbon sequestration, it also curtails marine net primary productivity due to nutrient depletion and canopy shading, with

a cascade of effects that diminish organic carbon export and alter certain biogeochemical processes in upwelling regions.

In Chapter 4, the narrative extends to proposing macroalgae-based CDR as a viable component of Germany's Net-Zero 2050 target. The proposition underscores macroalgae, with its rapid growth rates and optimal biochemical composition, as a sustainable feedstock for third-generation biofuels. The concept of offshore macroalgae cultivation coupled with maturity of macroalgae cultivation technologies opens up sustainable alternatives for biofuel production while potentially sequestering substantial amounts of CO₂.

Throughout this dissertation, a systematic evaluation of macroalgae-based CDR methodologies is carried out, encompassing various deployment locations, combinations with artificial upwelling, and a case study within Germany's EEZ. The findings, in conjunction with existing research, underline the significant trade-offs involved, particularly the suppression of marine primary production which could have broader ecological ramifications. Despite being based on certain idealized assumptions, the thesis lays a solid groundwork for further investigations, advocating for a diversified approach in the assessment of climate mitigation strategies and emphasizing the urgency for further research, implementation, and global collaboration in addressing the climate change crisis.

Zusammenfassung

Das Pariser Klimaschutzabkommen, das im Jahr 2015 verabschiedet wurde, setzt das klare Ziel, den durchschnittlichen globalen Temperaturanstieg bis zum Ende des 21. Jahrhunderts auf deutlich unter 2°C, idealerweise auf unter 1.5°C gegenüber dem vorindustriellen Niveau zu begrenzen. Diese Begrenzung soll die schwerwiegendsten Folgen des vom Menschen verursachten Klimawandels abwenden. Die bisherigen Bemühungen zur Emissionsreduktion und andere Klimaschutz-MaSSnahmen sind allerdings nicht ausreichend um die deklarierten Temperatur-Ziele einzuhalten. In Anbetracht dessen haben sich Methoden zur Entfernung von Kohlendioxid (CDR), welche eine künstliche/mensch-gemachte Entnahme aus der Atmosphäre und langfristige Speicherung von Kohlendioxid umfassen, zu unvermeidlich/notwenige und zentrale MaSSnahmen entwickelt, um die weltweit deklarierten Netto-Null Ziele zu erreichen.

Der Ozean ist das grösSste Reservoir der Erde für die langfristige Speicherung von anthropogenem CO₂. Seine Kohlenstoffspeicherkapazität, welche die der Atmosphäre und der terrestrischen Biosphäre deutlich übertrifft, legt somit die Erforschung ozeanbasierter CDR-Strategien nahe. Die Nutzung von Makroalgen für ozeanbasiertes CDR hat aufgrund der hohen photosynthetischen Effizienz, der kohlenstoffreichen Biomasse und gut etablierter Züchtungs- und Anbautechniken groSSes Interesse erregt. In dieser Arbeit stelle ich Ergebnisse bezüglich ozeanbasiertem CDR mit

Makroalgen als Kohlenstoffträger vor, die als Makroalgen-basierte CDR-Strategien bezeichnet werden. Makroalgen-basiertes CDR wurde sowohl im offenen Ozean als auch in küstennahen Regionen mittels numerischer Modellierung innerhalb eines Erdsystem-Klimamodells untersucht (Kapitel 2 & 3). Die Bewertung betraf die Kohlenstoff-Sequestrierungskapazität und -effizienz sowie die Wechselwirkungen zwischen Makroalgen-basierten CDR und dem globalen Kohlenstoffkreislauf und der marinen Biogeochemie. Unterdessen wird die Makroalgen-basierte CDR als mögliche Komponente des Netto-Null-Ziels Deutschlands für 2050 bewertet (Kapitel 4), wobei die theoretischen Bewertungen mit praktischen und regionsspezifischen Anwendungen verknüpft werden. Diese Arbeit trägt somit zu einem tieferen Verständnis und einer höheren Realisierbarkeit von Makroalgen-basierten CDR-Strategien und deren Beitrag zum Erreichen der Klimaziele bei.

In Kapitel 2 liegt der Fokus auf der Methodik der Makroalgen-Offshore-Marikultur und Versenkung (MOS) als mögliche Makroalgen-basierte CDR-Strategie. Durch einen synergetischen Ansatz, bei dem ein Makroalgen-Wachstumsmodell in das Earth System Model der University of Victoria (UVic ESCM) integriert wurde, wird die theoretische Effizienz von MOS bezüglich der Kohlenstoffsequestrierung sowie potenzieller biogeochemische Auswirkungen erforscht. Die Ergebnisse zeigen, dass MOS, insbesondere wenn es mit künstlicher Aufwärtsströmung (AU) verstärkt wird, erhebliches Potenzial zur Kohlenstoffsequestrierung bietet. Gleichzeitig finden sich jedoch erhebliche Auswirkungen auf marine Ökosysteme, insbesondere einer Reduzierung der Nettoprimärproduktion von Phytoplankton (PNPP) aufgrund von Nährstoffkonkurrenz und Schattierung sowie Veränderungen in den Sauerstoff-Minimum-Zonen (OMZs).

Kapitel 3 wechselt zur Bewertung von küstennahen-Makroalgen-Aquakulturen für Kohlenstoffsequestrierung (N-MACS), welche den Makroalgenanbau

in küstennahen Ozeanflächen ermöglicht. Die Bewertung umfasst das CDR-Potenzial von N-MACS, seine Auswirkungen auf den globalen Kohlenstoffkreislauf, die marine Biogeochemie und marine Ökosysteme. Das ursprünglich etablierte Makroalgenmodell wird an küstennahe Gebiete angepasst, um sich an den Umfang der Ausschließlichen Wirtschaftszonen (EEZs) anzulehnen. Die Simulationen verdeutlichen, dass N-MACS zwar Potenzial für die Kohlenstoffsequestrierung hat, aber auch die marine Netto-primärproduktion aufgrund von Nährstoffverarmung und Schattierung verringert, gefolgt von einer Reihe von Auswirkungen, die den organischen Kohlenstoffexport verringern und bestimmte biogeochemische Prozesse in Auftriebsregionen verändern.

In Kapitel 4 wird die Darstellung erweitert, um Makroalgen-basierte CDR als mögliche Komponente für das Erreichen des Netto-Null-Ziels von Deutschland für 2050 vorzuschlagen. Der Vorschlag stützt sich auf Makroalgen, welche sich aufgrund ihrer schnellen Wachstumsraten und ihrer optimalen biochemischen Zusammensetzung als nachhaltigen Rohstoff für Biokraftstoffe der dritten Generation eignen. Das Konzept des Offshore-Makroalgenanbaus in Verbindung mit ausgereiften Makroalgenanbau-Technologien, eröffnet nachhaltige Alternativen für die Biokraftstoffproduktion, während potenziell erhebliche Mengen an CO₂ sequestriert werden könnten.

In dieser Dissertation wird eine systematische Bewertung von auf Makroalgen basierenden CDR-Methoden durchgeführt, die verschiedene Einsatzorte, Kombinationen mit künstlicher Aufwärtsströmung und eine Fallstudie innerhalb der Ausschließlichen Wirtschaftszone (EEZ) Deutschlands umfassen. Die Ergebnisse, in Verbindung mit vorgegangenen Forschungsarbeiten, unterstreichen bedeutende Zielkonflikte, insbesondere die Unterdrückung der marinen Primärproduktion, welche weitreichendere ökologische Auswirkungen haben könnte. Obwohl diese Arbeit auf einigen

idealisierten Annahmen basiert, legt sie eine solide Grundlage für weitere Untersuchungen und befürwortet dabei einen diversifizierten Ansatz bei der Bewertung von Klimaschutzstrategien. Die Dringlichkeit für weiterführende Forschung, der Umsetzung von Maßnahmen und der globalen Zusammenarbeit bei der Bewältigung der Klimakrise wird betont.

Contents

1	Introduction	1
1.1	Scientific Background: The Global Carbon Cycle and Climate Change . . .	1
1.1.1	Climate Change: Human-Induced Perturbations of the Global Carbon Cycles	1
1.1.2	The Role of the Ocean in the Global Carbon Cycle Amidst Climate Change	8
1.2	Unlocking the Blue Potential for Climate Change Mitigation: the Potential of Ocean-Based CDR Strategies	14
1.2.1	Carbon Dioxide Removal (CDR): a promising and vital option for combating climate change	14
1.2.2	Ocean-based CDR: unleashing the Blue Potential	17
1.3	Research motivation: evaluating the potential and consequences of macroalgae-based CDR through Earth system climate model simulations	21
1.4	Macroalgae-based CDR	21
1.5	Why simulating macroalgae-based CDR in an Earth system climate model?	23
1.6	Chapter synopsis and author contributions	25
1.7	References	27
2	Carbon dioxide removal via macroalgae open-ocean mariculture and sinking: an Earth system modeling study	53
2.1	Introduction	55
2.2	Methods	58
2.2.1	Model description	58
2.2.2	Modeling MOS in the UVic ESCM	59
2.3	Experiment design	67
2.3.1	Deployment strategies of MOS	67

2.3.2	Sensitivity studies	69
2.4	Results	71
2.4.1	Evaluation of MOS	71
2.4.2	Evaluation of MOS with artificial upwelling (AU)	74
2.4.3	MOS deployment until year 2100	75
2.4.4	Long-term effects of MOS	86
2.4.5	Termination effects	90
2.4.6	Leakage of MOS-sequestered carbon	91
2.5	Concluding discussions	92
2.6	References	96
3	Nearshore macroalgae cultivation for carbon sequestration by biomass harvesting: evaluating potential and impacts with an Earth system model	111
3.1	Introduction	112
3.2	Methods	113
3.2.1	Experimental design	115
3.3	Results & Discussions	115
3.3.1	Macroalgae model validation	115
3.3.2	CDR capacity and impacts on carbon cycle	118
3.3.3	Impacts on global marine biogeochemistry	120
3.4	Conclusion & Outlook	125
3.5	References	126
4	Scoping carbon dioxide removal options for Germany What is their potential contribution to Net-Zero CO₂?	137
4.1	Introduction	138
4.2	Materials and Methods	142
4.2.1	Selection of CDR options available in Germany	142
4.2.2	CDR concepts development	142
4.2.3	Data collection review and quality control	144
4.2.4	Calculation of CO ₂ removal potential	144
4.3	Results	146
4.3.1	CDR concepts portfolio	146
4.3.2	Data collection	160
4.3.3	Technical potential of options deployment	160

4.4	Discussion	163
4.4.1	Bringing CDR options closer to deployment - bottlenecks and open questions	163
4.4.2	Distribution patterns	167
4.4.3	Setting the CO ₂ removal potential in context	170
4.4.4	Limitations and further research demand	171
4.5	Conclusion	171
4.6	References	174
5	Conclusion and Outlook	187
5.1	Summary and Conclusion	187
5.2	Outlook	190
5.3	References	192
A.	Supporting Information for Chapter 2	195
A.1	MOS validations	195
A.1.1	MOS yield calculation	195
A.1.2	MOS NPP	196
A.2	Impacts of MOS on global biogeochemistry	196
B.	Supporting Information for Chapter 3	209
C.	Supporting Information for Chapter 4	221
	List of Figures	222
	List of Tables	230
	Erklärung	235

Chapter 1

Introduction

1.1 Scientific Background: The Global Carbon Cycle and Climate Change

The introduction of this dissertation begins by briefly introducing the global carbon cycle and human-induced climate change, highlighting the significant role of the ocean within the carbon cycle in the context of a changing climate. Following this, the Introduction presents the promising and essential strategy for addressing climate change, Carbon Dioxide Removal (CDR), with a specific focus on ocean-based CDR approaches. This forms the basis for the research explored in the forthcoming chapters. The idea of using macroalgae in ocean-based CDR, known as macroalgae-based CDR, is introduced, along with the significance of numerical models in assessing these strategies. This sets the foundation for the comprehensive investigations conducted in this study. The introduction concludes with a preview of the upcoming chapters and an acknowledgment of the respective contributors.

1.1.1 Climate Change: Human-Induced Perturbations of the Global Carbon Cycles

The advent of the steam engine in the 18th century marked the beginning of the industrial era, propelling humanity toward rapid industrialization. However, as modernization progressed, it became increasingly evident that human activities significantly impacted Earth's climate and ecological systems. A primary consequence of these anthropogenic activities is climate change, fundamentally driven by increased concentrations of greenhouse

gases (GHGs) in the atmosphere of the Earth due to human activities, such as fossil fuel combustion, deforestation, livestock farming, industrial processes, and land-use changes (IPCC, 2018, 2022). Climate change is now widely recognized as one of the most pressing global challenges of the 21th century. The human-caused global surface temperature increase in 2010-2019 is approximately 1.07°C higher than in 1850-1900, leading to far-reaching repercussions for ecosystems, human health, and socio-economic systems (IPCC, 2018).

The most important greenhouse gases in Earth's atmosphere are water vapor (H₂O), carbon dioxide (CO₂), methane (CH₄), nitrous oxide (N₂O) and fluorinated gases (United States Environmental Protection Agency, 2023; Ehhalt et al., 2001). These gases are capable of trapping heat because they absorb infrared radiation emitted by the Earth's surface and atmosphere before re-emitting a portion of that energy back toward the surface, known as the greenhouse effect. Greenhouse effect helps maintain the Earth's surface at a warmer temperature than it would be otherwise (National Aeronautics and Space Administration, 2023). Water vapor is recognized primarily as a feedback mechanism rather than an anthropogenic GHG, since its concentration in the atmosphere is mainly dependent on temperature and not human activities (Held and Soden, 2000; National Aeronautics and Space Administration, 2008). Carbon dioxide (CO₂) is widely considered the primary anthropogenic GHG for its substantial warming effect and long atmospheric lifetime (IPCC, 2014; Archer et al., 2009; Friedlingstein et al., 2022a). The role of CO₂ in the greenhouse effect was first proposed by the Swedish scientist Svante Arrhenius in the late 19th century (Arrhenius, 1896). About 40 years later, G. S. Callendar built on Arrhenius' work and established a scientific link between human activities, atmospheric CO₂ accumulation, and global warming (Callendar, 1938). Regrettably, it was not until nearly half a century later that society became acutely aware of the reality of human-induced climate change (e.g., Keeling (1958); Broecker (1975)), and its increasingly severe consequences are now starkly evident, such as extreme weather events, melting polar ice caps, and rising sea levels (IPCC, 2018). Since the onset of the industrial era, approximately 2,500 Gt of CO₂ have been emitted, of which around 40% has resulted in an increase in atmospheric CO₂ concentration, while the remainder has been absorbed by terrestrial and oceanic sinks (Pörtner et al., 2022; Friedlingstein et al., 2022b).

While the anthropogenic emission of CO₂ has received numerous attention due to its critical pivotal role in climate change, the element constituting CO₂, carbon, does not persist stationary in the atmosphere. Instead, carbon circulates throughout the Earth system in a process known as the global carbon cycle. This cycle is a key component of the Earth's

climate system, significantly influencing global climate by regulating atmospheric CO₂ concentrations (Allen et al., 2009; Kump et al., 2000; Matthews et al., 2009). Therefore, a comprehensive understanding of the global carbon cycle is essential in addressing the climate change crisis (Falkowski et al., 2000; Ciais et al., 2013).

Table 1.1: Conversions between the weight of carbon (C) and carbon dioxide (CO₂) for commonly used units. The conversion factor is based on the molecular weight ratio of CO₂ (44.01 g/mol) to C (12.01 g/mol), approximately 3.67.

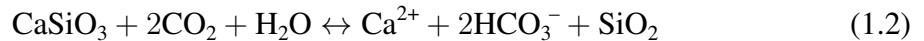
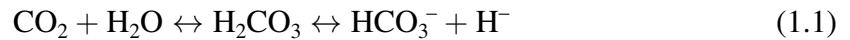
Unit	C Weight	CO ₂ Weight
ton	1 tC	3.67 tCO ₂
kilogram (kg)	1 kgC	3.67 kgCO ₂
Gigaton (Gt)	1 × 10 ⁹ tC (GtC)	3.67 × 10 ⁹ tCO ₂ (GtCO ₂)

Given that our planet and its atmosphere form a closed system, the total amount of carbon within this system remains unchanged. The carbon cycle is usually divided into two main components: the *endogenic* (deep) cycle and the *exogenic* (surface) cycle (Berner, 2003; Mackenzie and Lerman, 2006, pp7).

The vast majority of Earth's carbon (nearly 99.9%, equal to approximately 1×10^{23} grams) is sequestered within the lithosphere (Williams and Follows, 2011; Sarmiento and Gruber, 2002; Mackenzie and Lerman, 2006). This carbon is stored primarily in sedimentary rocks in the form of inorganic carbonate minerals (for example, CaCO₃, MgCO₃), and organic compounds such as oil, natural gas, and coal, which are collectively termed fossil fuels (currently known and exploitable: 3,400 to 3,700 GtCO₂, Canadell et al. (2021); Scott et al. (2015); Williams and Follows (2011, pp7)). The *endogenic* carbon cycle connects the lithosphere with the deeper mantle and core through geological processes such as subduction (where one tectonic plate moves under another and sinks into the mantle) and volcanic eruptions (Fig.1.1, Orcutt et al. (2019); Foley and Fischer (2017); Williams et al. (1992); Mackenzie and Lerman (2006)). On the surface of the lithosphere, carbon is gradually redistributed to other carbon reservoirs over millions of years through slow geological processes such as chemical and biological weathering and sedimentation.

When CO₂ dissolves in water, it forms a weak carbonic acid (Eq.1.1), which can further react with silicate minerals (such as CaSiO₃ and MgSiO₃, Eq.1.2). Bicarbonate and cations, derived from the weathering of silicate minerals, are water-soluble and thus transported to the ocean via continental runoff. On geological timescales, these dissolved minerals have contributed to the slightly alkaline nature of the ocean. The precipitation of carbonate rocks (Eq.1.3) balances the ocean chemistry by removing alkalinity, thus achiev-

ing a relatively steady state. Historically, the global average surface pH of the ocean was 8.2 in the preindustrial era, which has since decreased to 8.1 due to anthropogenic CO₂ emissions (Jiang et al., 2019; Caldeira and Wickett, 2003). In the ocean, marine calcifiers absorb calcium bicarbonate to form shells and skeletons that contain insoluble calcium carbonate (CaCO₃). Death and subsequent sinking of these organisms and detritus results in sequestration of calcium carbonate in the sediment (Eq.1.3). Therefore, chemical weathering of silicate minerals facilitates the burial of an equivalent amount of CO₂ in CaCO₃, effectively acting as a carbon sink (Eq.1.4). This process plays an important role in the long-term regulation of Earth's climate by maintaining the balance of carbon in the atmosphere (Penman et al., 2020; Winnick and Maher, 2018; Berner and Berner, 1997).



The rock weathering (Eq.1.2) and marine carbonate precipitation (Eq.1.3) can be collectively expressed as follows:



These slow carbon cycles influences the Earth's climate over timescales ranging from millions to billions of years (Dasgupta and Hirschmann, 2010; Sleep and Zahnle, 2001), rendering lithosphere a relatively inactive component of the global carbon cycle (Bates, 2019). However, human-induced extraction and burning of fossil fuels have noticeably increased carbon release from this passive reservoir.

Here we primarily focus on the naturally and anthropologically influenced processes of the *exogenic* cycle, which incorporates active carbon reservoirs on Earth's surface, including the atmosphere, the hydrosphere (comprising oceanic and continental waters), the terrestrial and aquatic biosphere, and the surface sediment layer of the lithosphere.

Carbon in the atmosphere remains in the major form of carbon dioxide (CO₂) and methane (CH₄). Methane is the second most important greenhouse gas after CO₂ with a significantly stronger global warming potential (GWP = 29 in 100 years compared to 1 for CO₂, Stocker et al. (2013)) than CO₂ due to its superior efficiency in trapping radiation (Shindell et al., 2009). The main source of natural methane is the anaerobic biolog-

ical process named as *methano-genesis* by methanogenic *archaea* in wetlands, rice fields, oceans, ruminant and termite digestive systems (Conrad, 2009; Nazaries et al., 2013). Human activities, including the combustion of biomass and fossil fuel, livestock farming, and waste management, have significantly increased atmospheric methane concentrations (IPCC, 2018). Methane is removed from the atmosphere primarily through reactions with hydroxyl radicals (OH) in the troposphere to form CO₂ and water, together with other minor sinks, including oxidation through tropospheric chlorine radicals and microbial consumption in soils Conrad (2009); Myhre et al. (2013). These fast removal processes limit the atmospheric lifetime of methane to about 12 years (Myhre et al., 2013; Abernethy et al., 2021; Canadell et al., 2021). Understanding the methane cycle is vital for climate change research.

Compared to methane, the cycle of atmospheric CO₂ is more complex. Atmospheric CO₂ interacts with other active reservoirs in the ocean and on land through a combination of physio-chemical and biological pathways. In this section, we will briefly overview the cycles between atmospheric and terrestrial carbon reservoirs, reserving a detailed discussion on the oceanic reservoir for the subsequent section.

In addition to the relatively slow and long-term carbon exchange facilitated by the chemical weathering of silicate rocks and the endogenic cycle, terrestrial ecosystems play a pivotal role in carbon exchanges between atmospheric and terrestrial carbon pools. The atmosphere-land carbon cycle is a complex system influenced by a myriad of factors, both natural and anthropogenic. Understanding these influences is crucial to predict future changes in atmospheric CO₂ level and developing effective strategies for mitigation and adaptation of climate change.

The primary mechanism of carbon uptake in terrestrial ecosystems is photosynthesis, a process by which plants convert atmospheric CO₂ into organic compounds such as sugars and starches. This process is estimated to account for a global gross primary production (GPP) of approximately 123 PgC per year, and tropical forests and savannas contribute to 60% of this uptake (Canadell et al., 2021). However, the carbon absorbed through photosynthesis is not permanently sequestered in plant biomass. According to Fig.1.1 (taken from Ciais et al. (2013)), approximately 118.7 PgC, which accounts for over 95% of the carbon captured by GPP, is reintroduced into the atmosphere through autotrophic respiration by plants and heterotrophic respiration by herbivores, as well as combustion resulting from natural events or human-initiated fires (Keenan and Williams, 2018; Canadell et al., 2021). Therefore, the carbon dynamics of terrestrial vegetation can be roughly defined by the balance between carbon uptake through Gross Primary Production (GPP) and the car-

bon flux back through total respiration, combined with factors such as harvesting, erosion, and the export of Dissolved Organic Carbon (DOC) by runoffs to the oceans (Prentice et al., 2001).

Another critical component of the terrestrial ecosystem carbon reservoir is the soil, which stores approximately 1,700 PgC (range: 1,500 to 2,400 PgC), more than the combined carbon content of the atmosphere and terrestrial vegetation (Canadell et al., 2021; Friedlingstein et al., 2022b). Soil organic carbon primarily originates from the decomposition of dead plant and animal material by soil microbes and root exudates (Keenan and Williams, 2018). Meanwhile, the respiration of soil microbial decomposers, such as bacteria and fungi, also releases CO₂ back into the atmosphere.

The dynamics of the terrestrial carbon reservoir are shaped by a multitude of natural processes, including solar radiation, seasonal temperature fluctuations, nutrient availability, precipitation, and soil moisture (Hari and Tyagi, 2022; Tharammal et al., 2019; Schulze, 2006), as well as large-scale climatic phenomena, such as *El Niño* AND *La Niña* (Teckenstrup et al., 2021; Friedlingstein et al., 2022b).

However, human activities and climate change have significantly impacted the terrestrial carbon reservoir, leading to a complex interplay of both amplifying (positive) and decelerating (negative) feedbacks to atmospheric CO₂.

Anthropogenic CO₂ emissions have stimulated terrestrial plant photosynthesis due to elevated atmospheric CO₂ levels, an effect known as 'CO₂ fertilization' Walker et al. (2021); Reich et al. (2014). This process has dominantly enhanced the terrestrial carbon sink, providing a negative feedback to the atmospheric carbon pool (Friedlingstein et al., 2022b; Canadell et al., 2021). Another negative feedback arises from the deposition of nutrients, particularly reactive nitrogen, resulting from fossil fuel combustion and fertilizer use. This process enhances the terrestrial carbon sink by providing additional nutrients for plant growth (Wang et al., 2017; White et al., 1999) and by suppressing soil microbial respiration (Janssens et al., 2010).

Conversely, positive feedbacks that augment carbon outgassing from land include the enhanced respiration of both plants and soil microbes due to rising surface temperatures (Luo, 2007; Friedlingstein et al., 2001). Moreover, the terrestrial carbon pool is also influenced by climate change-induced global warming, extended growth seasons, alterations in botanical community structure, surface radiation, and changes in the hydrological cycle, such as rainfall patterns and permafrost thawing (Anderegg et al., 2013; Friedlingstein et al., 2020; Walvoord and Kurylyk, 2016). According to the estimation by Friedlingstein et al. (2022b), climate change has reduced the land sink by 17 % during the decade of 2012

to 2021.

Furthermore, human activities related to Land Use, Land-Use Change, and Forestry (LULUCF) significantly influence the carbon flux between terrestrial ecosystems and the atmosphere. These activities, which primarily involve forests but also extend to croplands, grasslands, wetlands and etc., can either donate or sink CO₂, thereby altering the balance of the global carbon cycle (IPCC, 2019). LULUCF activities, dominated by deforestation, have been reported to contribute an emission of 205 ± 60 GtC between 1850 and 2021, representing about 30% of the total anthropogenic CO₂ emissions in this period (Friedlingstein et al., 2022b). Meanwhile, the sequestration of the CO₂ emissions can be achieved through strategic planning and management of future LULUCF activities, such as afforestation & reforestation and re-wetting peatlands (Sha et al., 2022; Zomer et al., 2008; Günther et al., 2020; Schlamadinger et al., 2007).

Since the industrial era, the terrestrial carbon reservoir has sequestered about 210 GtC, or 31% of total anthropogenic CO₂ emissions (Friedlingstein et al., 2022b). The terrestrial carbon sink has grown in line with increasing anthropogenic CO₂ emissions (Friedlingstein et al., 2022b; Walker et al., 2021; White et al., 1999; Schimel et al., 2015). However, it is uncertain whether terrestrial ecosystems will remain a net carbon sink or become a net carbon source due to complex feedback mechanisms within the terrestrial ecosystem, its interactions with other carbon reservoirs, the climate change and the unpredictable trajectory of human activities (Cox et al., 2000; Smith and Shugart, 1993; Joos et al., 2001; Friedlingstein et al., 2001).

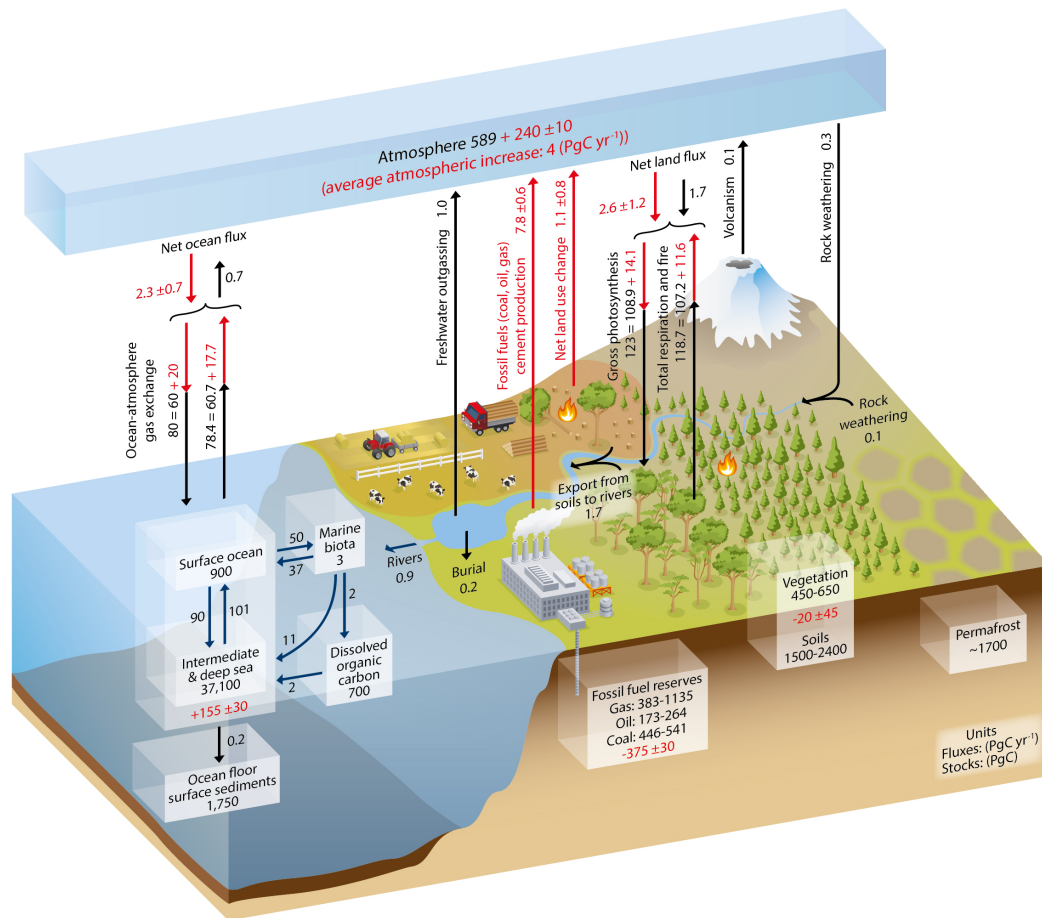


Figure 1.1: Simplified schematic of the global carbon cycle. Numbers represent reservoir mass in PgC ($1 \text{ PgC} = 10^{15} \text{ gC}$) and annual carbon exchange (in Pg yr^{-1}). Black numbers and arrows indicate reservoir mass and exchange fluxes estimated for the time prior to the Industrial Era. Red arrows and numbers indicate annual anthropogenic fluxes averaged over the 2000–2009 time period. Reprinted from Figure 6.1 in Ciais et al. (2013)

1.1.2 The Role of the Ocean in the Global Carbon Cycle Amidst Climate Change

Covering over 71% of the Earth's surface and containing 91% of the planet's total water, the ocean is a critical component of the Earth's energy budget and the global carbon cycle (Charette and Smith, 2010). The ocean is estimated to store approximately 38,000 GtC, with approximately 900 GtC in the surface ocean (0-1,000m) and over 37,000 GtC in the deep ocean (>1,000m, Fig.1.1). The carbon reservoir in the surface ocean alone is comparable to the carbon content in the atmosphere (600 to 800 GtC). Consequently, even minor perturbations in the oceanic carbon cycle and its exchange with the atmosphere could

have significant implications for the atmospheric carbon pool and thereby influence the climate (Bindoff et al., 2019). In this context, our primary focus will be on elucidating the ocean's pivotal role in the global carbon cycle and its connection with the human-induced climate change.

The exchange of carbon between the ocean and the atmosphere is distinct from that between the land and the atmosphere, owing to the unique physio-chemical interactions between seawater and CO_2 , dynamic ocean circulations, and marine biochemical processes. Generally, atmospheric CO_2 , including anthropogenic emissions, is absorbed by the surface ocean through physio-chemical and biological processes and further sequestered in the deep ocean interior via ocean vertical downward transportation and the export of organic/inorganic carbon particles. These carbon sequestration processes are referred to as oceanic carbon pumps (referred to 'solubility pump' and 'biological pump', Volk and Hofert (1985)).

The Solubility Carbon Pump (SCP)

The primary route for atmosphere-ocean carbon exchange is through air-sea CO_2 fluxes on the ocean surface, which are controlled by the gradient in air-sea CO_2 partial pressure ($p\text{CO}_2$). The $p\text{CO}_2$ signifies the CO_2 vapor pressure. Factors such as temperature, total dissolved CO_2 , and seawater alkalinity influence the $p\text{CO}_2$ in seawater, while the concentration at the gas exchange interface largely affects the atmospheric $p\text{CO}_2$. To maintain the air-sea equilibrium, CO_2 dissolves when the seawater $p\text{CO}_2$ is lower than that the atmospheric $p\text{CO}_2$, and vice versa. According to Eq.1.1 and Eq.1.5, dissolved CO_2 reacts with H_2O to form carbonic acid (H_2CO_3), which further dissociates into bicarbonate (HCO_3^-) and a hydrogen ion (H^+). This reaction sequence ultimately yields carbonate (CO_3^{2-}) and another H^+ . Some of the H^+ ions react with carbonate ions (CO_3^{2-}) to form an additional bicarbonate ion (Eq.1.5). This carbonate buffer system enhances the ocean's capacity to absorb CO_2 beyond what would be possible based solely on solubility, thereby helping to maintain the ocean's pH balance. The ensemble of bicarbonate (HCO_3^- , ~90%), carbonate (CO_3^{2-} , ~10%) and dissolved $\text{CO}_{2(\text{aq})}$ (<1%) constitutes the total dissolved inorganic carbon (DIC) in the ocean (Dickson, 2010). Meanwhile, the influx of cations and bicarbonates from terrestrial carbon weathering to the ocean over geological timescales have resulted in a slightly alkaline ocean with an averaged surface pH exceeding 8 (Caldeira and Wickett, 2003; Jiang et al., 2019). This alkalinity contributes to the ocean chemical carbon uptake.

Another critical component of the solubility pump is the ocean thermohaline circula-

tion, also known as the global conveyor belt (Broecker, 1991), a large-scale oceanic process driven by global density gradients created by surface heat and freshwater fluxes. It begins in high-latitude regions such as the North Atlantic and Southern Ocean (not in the North Pacific due to its lower surface salinity), where reduced solar radiation and increased salinity, resulting from sea ice formation and evaporation, cause the surface seawater to become denser and cooler (Raven and Falkowski, 1999; Weaver et al., 1999; Clark et al., 2002). Additionally, the solubility of CO_2 is enhanced in cooler water, facilitating greater CO_2 dissolution. Consequently, this denser, cooler water sinks and forms deep water masses (e.g., the North Atlantic Deep Water (NADW)), transporting the dissolved inorganic carbon (DIC) into the deep ocean. Given the thermohaline circulation's cycle time of nearly 1,000 years (Döös et al., 2012), the downwelled DIC can substantially be sequestered from the atmosphere for a long period, which plays a dominant role in the ocean carbon sink (negative feedback) of the anthropogenic CO_2 emission (Heinze et al., 2015).



The Biological Carbon Pump (BCP)

The 'biological carbon pump (BCP)' is another critical component of the ocean carbon cycle. It involves the fixation of dissolved inorganic carbon (DIC) by marine autotrophs in the upper ocean and its vertical transport to and sequestration in the deeper ocean interior ($\geq 1,000\text{m}$) for periods ranging from years to millennia. The BCP accounts for approximately 90% of the surface-to-deep gradient in DIC in the ocean (Sarmiento and Gruber, 2002; Passow and Carlson, 2012). Although most marine primary producers use carbon ions (HCO_3^- , CO_3^{2-}) in seawater rather than directly absorbing CO_2 , the carbon export by BCP significantly contributes to the removal of DIC from the surface ocean. This sustains the air-sea carbon exchange into the ocean and provides a negative feedback on the atmospheric CO_2 pool. Without the BCP, model predictions suggest that atmospheric $p\text{CO}_2$ levels could be nearly twice as high as current levels (Maier-Reimer et al., 1996), meanwhile a sudden hypothetical cessation of marine biology would increase the atmospheric CO_2 concentration by 200–300 ppm (Heinze et al., 2015).

Similar to their terrestrial counterparts, marine primary producers convert inorganic carbon into organic matter through photosynthesis within the euphotic layer (0 - 200m), utilizing nutrients such as nitrogen, phosphorus, and iron. The Net Primary Production (NPP) by marine photosynthesis is estimated to be approximately 50 to 60 GtC yr^{-1} , which

accounts for nearly half of the Earth's total annual primary production (Ciais et al., 2013; Nowicki et al., 2022; Heinze et al., 2015). The sinking mechanism of the BCP is driven by a combination of physical and biological processes, such as gravitational sinking of aggregated phytoplankton and zooplankton fecal pellets, active vertical migration of zooplankton and larger animals, and physical transportation such as mixed layer deepening and eddy subduction (Claustre et al., 2021). The export of POC out of the euphotic layer is estimated to be 5-25% of the total euphotic annual NPP of ~ 50 to 60 GtC yr^{-1} with large variations between polar regions (30% to 100%) and central gyres (1% to 10%, Ciais et al. (2013); Nowicki et al. (2022); Heinze et al. (2015); Buesseler (1998); De La Rocha and Passow (2007) and references within). Approximately 90% of the exported POC is reduced during the sinking route through the mesopelagic layer via microbial decomposition, solubilization, and feeding by zooplankton (Passow and Carlson, 2012; Turner, 2015). Therefore, the transportation and remineralization of POC contribute significantly to the vertical oceanic DIC gradient, which is dominated by the carbon redistribution by the BCP.

On the other hand, DOC, composed of tiny organic particles that are dissolved in seawater, is a type of passive tracer that can be transported as the DIC. Despite the fact that the export of DOC from the euphotic layer is only around 2 GtC yr^{-1} , it constitutes the largest organic carbon reservoir in the ocean, holding approximately 700 GtC with an estimated sequestration period ranging from centuries to millennia (Hansell et al., 2009; Hansell, 2013; Canadell et al., 2021; Nowicki et al., 2022). Approximately 95% of the dissolved organic matter (DOM) in the ocean is refractory dissolved organic matter (RDOM), which cannot be used as food by marine organisms. The RDOM is converted from bioavailable DOC by marine microbes, a process known as the 'microbial carbon pump' (Jiao et al., 2010; Legendre et al., 2015).

However, due to the significant reduction between the base of the euphotic and mesopelagic zones, the efficiency of the BCP in sequestering carbon in the deeper ocean (greater than 1,000m) is relatively low. Only a small fraction of the exported carbon, approximately 3% (ranging from 1% to 5%) of the NPP in the euphotic zone, or about 0.2 PgC yr^{-1} as shown in Fig.1.1, reaches the seafloor where it can be sequestered in sediments for longterm sequestration (Menon et al., 2007; Ciais et al., 2013; Heinze et al., 2015; De La Rocha and Passow, 2007). The BCP's high efficiency in primary production but low efficiency in carbon sequestration has led to the proposition of enhancing the BCP to sequester more carbon, such as cultivating macroalgae, marine macrophyte photosynthesizers, on the ocean surface with quick deep sinking of their carbon-rich biomass (e.g., Wu et al. (2023)).

The Carbonate Pump

In addition to the solubility pump and biological carbon pump, the carbonate pump also plays a significant role in the ocean's carbon cycle. This process, which is considered a subset of the biological pump, involves the sequestration of particulate inorganic carbon (PIC) by marine calcifiers, primarily coccolithophores. Coccolithophores are marine phytoplankton and a globally abundant calcifiers with contribution to roughly 50% of the pelagic CaCO_3 deposition in ocean sediments (Raven and Crawford, 2012; Bach et al., 2015). These organisms form their shells or skeletons by converting two bicarbonate ions (HCO_3^-) and one calcium ion (Ca^{2+}) into one calcium carbonate (CaCO_3) molecule. Notably, one CO_2 molecule is released during calcification (Eq.1.6), the carbonate pump therefore is also known as 'the carbonate counter pump' (Passow and Carlson, 2012; Frankignoulle et al., 1994; Heinze et al., 2015). Nevertheless, this carbon counter pump does not entirely offset the biological carbon pump, given the fact that the ratio of PIC : POC is approximately 15% on global scale (Heinze et al., 2015; Mekik et al., 2007) and less than 1 in coccolithophores (Zondervan et al., 2002; Findlay et al., 2011).



Some of the CO_2 released during this process can be utilized by coccolithophores for photosynthesis. The calcification process consumes two carbon atoms, trapping one within the mineral. Over time, coccolithophores significantly contribute to reducing atmospheric CO_2 levels by precipitating carbonate in the deep ocean. Similar to their terrestrial counterparts involved in weathering, the burial of sunken CaCO_3 in deep-ocean sediment serves as a primary buffer, mediating the CO_2 -rich deep waters and subsequently reducing atmospheric CO_2 over geological timescales. This process provides a crucial negative feedback to climate change. Furthermore, as the denser CaCO_3 platelets ('coccoliths') always combine with organic carbon, the 'ballast hypothesis' suggests that coccoliths could enhance organic carbon sequestration through accelerated precipitation and reduced remineralization (Hofmann and Schellnhuber, 2009; De La Rocha and Passow, 2007; Klaas and Archer, 2002).

Climate Change and the Ocean Carbon Cycle

Anthropogenic CO_2 emissions and the ensuing climate change have been, and will continue to influence various facets of the Earth's system. The ocean carbon cycle, being an

integral part of this system, is not immune to these effects. A multitude of climate change-induced impacts on oceanic carbon cycle have been identified and extensively studied.

The ocean's primary response to the ongoing emissions of CO₂, a process that is well-understood, is **ocean acidification** (Doney et al., 2009; Gattuso et al., 2015). The escalating partial pressure of CO₂ in the atmosphere has resulted in the ocean absorbing more CO₂, which alters the carbonate chemistry of seawater (Sect.1.1.2). Observations indicate that the pH of open ocean surface water has declined by approximately 0.1 relative to pre-industrial levels, and projections suggest a further decrease of 0.04 to 0.29 by 2100, contingent on future emission scenarios (Caldeira and Wickett, 2003; Pörtner et al., 2019). Ocean acidification not only diminishes the ocean's equilibrium carbon capacity (DeVries, 2022) but also undermines the stability of mineral forms of calcium carbonate (CaCO₃) by reducing carbonate ion concentrations, especially in upwelling and high-latitude regions of the ocean (Pörtner et al., 2019). Concurrently, it poses substantial threats to marine ecosystems and organisms, particularly calcifying species such as corals, shellfish, and certain types of plankton (Orr et al., 2005; Riebesell et al., 2000).

The second most significant factor influencing the ocean carbon cycle is **ocean warming and stratification**. As the Earth's climate warms, the ocean has absorbed more than 90% of the excess heat trapped in the climate system since the 1970s, leading to a rise in sea surface temperatures (Myhre et al., 2013; Levitus et al., 2000). The impacts of ocean warming on the oceanic carbon cycle are profound and multifaceted. Warmer ocean temperatures can decrease the solubility of carbon dioxide in seawater, reducing the ocean's capacity to absorb CO₂ from the atmosphere and thus exacerbating global warming. Additionally, ocean warming can lead to increased stratification of ocean layers, which can disrupt the vertical mixing of waters and the transport of carbon to the deep ocean (Pörtner et al., 2019). Increased ocean stratification and reduced overturning also decrease the supply of nutrients to surface waters from the mixing and upwelling of deep waters. This reduction in nutrient supply, combined with warmer ocean surface temperatures, will lead to declining biological productivity in the surface ocean and declining carbon export, which will weaken the BCP. Furthermore, ocean warming can have significant impacts on marine life, including changes in species distribution and productivity, which can further alter the oceanic carbon cycle. Ocean warming and stratification, in conjunction with various biogeochemical feedbacks, instigate a process known as **ocean deoxygenation**. This term refers to the decrease in oxygen levels within the world's oceans (Keeling et al., 2010; Oschlies et al., 2018; Falkowski et al., 2011). As the ocean's surface waters become warmer, their capacity to hold oxygen diminishes, leading to an overall reduction in oceanic oxygen

content. Furthermore, the stratification of the ocean, a consequence of warming, disrupts the vital mixing of surface and deep waters. This disruption hinders the transfer of oxygen from the atmosphere into the ocean's deeper layers. The ensuing ocean deoxygenation has significant implications for the ocean carbon cycle, particularly through its effects on nutrient cycling and the BCP (Pörtner, 2008).

The ocean has already absorbed 175 ± 35 GtC CO_2 , more than 25% of the total anthropogenic emissions (Friedlingstein et al., 2022b). In the future, the ocean carbon sink is projected to continuously grow with increasing atmospheric CO_2 concentrations, mainly driven by the solubility pump by ocean circulation and carbonate chemistry (Canadell et al., 2021). However, the fraction of atmospheric emissions taken up by the ocean is expected to decline due to the decreased ocean buffering effects (Pörtner et al., 2019).

1.2 Unlocking the Blue Potential for Climate Change Mitigation: the Potential of Ocean-Based CDR Strategies

1.2.1 Carbon Dioxide Removal (CDR): a promising and vital option for combating climate change

The escalating threat of climate change necessitates the implementation of both adaptation and mitigation strategies to alleviate its impacts and risks. Adaptation measures, encompassing technological, social, and institutional options, aim to bolster the resilience of human and natural systems against climate change effects, such as rising sea levels, extreme weather events, and shifting ecosystems (IPCC, 2014).

Mitigation strategies, on the other hand, directly address the issue by reducing greenhouse gas (GHG) emissions and enhancing atmospheric GHG sinks. These strategies contribute to the deceleration of global warming and its associated impacts (IPCC, 2014). The proliferation of renewable energy sources, such as solar and wind power, has significantly reduced reliance on fossil fuels, contributing to a more sustainable energy sector (REN21, 2022; Agency, 2021). The electrification of transportation, particularly in the automotive industry, has also gained momentum, supported by major companies' commitments and government policies (Agency, 2020).

Besides mitigation and adaptation approaches, one proposed geoengineering approach to address climate change is the Solar Radiation Modification (SRM). SRM techniques

aim at increasing surface albedo to reflect solar radiation (e.g., stratospheric aerosol injection (SAI, Smith and Wagner); marine cloud brightening (MCB, Latham et al.)) and enhancing Earth's long-wave radiation emissions (e.g., thinning cirrus clouds via ice nucleating particles seeding (TCC, Ulrike Lohmann)). Thus, SRM cools the Earth by altering its radiation budget (Shepherd, 2009). However, SRM only masks global warming without addressing the root cause, rising GHG concentrations. It also does not mitigate other effects of high atmospheric CO₂, such as ocean acidification. Meanwhile, SRM carries potential risks, including abrupt climate changes and severe impacts after termination (IPCC, 2018; Pathak et al., 2022). Therefore, SRM can only be involved as a complement to efforts to achieve sustained Net Zero or Net Negative emission globally (Pörtner et al., 2022; Shepherd, 2009).

The Paris Agreement, adopted in 2015, underscores the need for deep and rapid reductions in gross emissions (UNFCCC, 2015). This agreement introduced the concept of '**Net Zero**', referring to the balance between the amount of GHGs emitted and removed from the atmosphere. The achievement of Net Zero is a key target for many countries under the Paris Agreement, with more than 100 countries having adopted, announced, or are discussing Net Zero GHGs/CO₂ emissions commitments, covering more than two-thirds of global GHG emissions.

Carbon Dioxide Removal (CDR), also known as Negative Emission Technologies (NETs), plays an indispensable role in the achievement of Net Zero. CDR refers to anthropogenic activities removing CO₂ from the atmosphere and securely store it in geological, terrestrial, or oceanic reservoirs, or incorporate it into products (Pathak et al., 2022). CDR techniques remove CO₂ from the atmosphere, thus reducing the overall greenhouse effect and stabilizing the global surface temperature induced by emissions of CO₂ and other GHGs (IPCC, 2022). The necessity of CDR arises from the fact that even with aggressive mitigation strategies, it is unlikely that the world can achieve the necessary reductions in GHG emissions to limit global warming to 1.5°C or even well below 2° C, as described in the Paris Agreement, without some form of CDR (Pathak et al., 2022). This is due to the cumulative nature of CO₂ in the atmosphere, which means that even if all emissions were to stop immediately, the already emitted CO₂ would continue to drive global warming for some time. Therefore, to achieve the temperature goals of the Paris Agreement, it is not enough to simply reduce the emissions of GHG, but it is also necessary to actively remove CO₂ from the atmosphere (Pathak et al., 2022).

The IPCC has highlighted the importance of CDR in its 2018 report, stressing that a large-scale deployment of these technologies would be necessary to achieve the goals of the

Paris Agreement (IPCC, 2018). More recently, the IPCC AR6 report reiterates the growing urgency of mitigation and adaptation measures, accentuating the critical role of CDR in combating climate change (IPCC, 2022). Most pathways to reach the Paris Agreement targets involve not only urgent and deep decarbonization, but also large-scale CDR implementation on scales of 100 to 1,000 GtCO₂ by 2050 (Rogelj et al., 2018; Fuss et al., 2020; IPCC, 2022). CDR can fulfill three complementary functions: lowering net CO₂ or net GHG emissions in the near term; counterbalancing 'hard-to-abate' residual emissions (i.e., some emissions from agriculture, aviation, shipping, industrial processes) to help reach Net Zero CO₂ or GHG emissions, and achieving net negative CO₂ or GHG emissions if deployed at levels exceeding annual residual emissions (IPCC, 2022). The amount of CDR required to meet the Paris Agreement targets varies depending on the emission reduction pathways. However, according to IPCC AR6, in most pathways that limit global warming to 1.5° C, the median deployment of CDR is 730 GtCO₂ over the 21st century, with a wide range of 100–1200 GtCO₂ across different scenarios (Pathak et al., 2022). This underscores the significant role that CDR is expected to play in future climate change mitigation efforts.

The concept of CDR has can be traced back to the 1960s, when initial ideas emerged about extracting CO₂ from the atmosphere to counteract the rising concentrations of greenhouse gases (GHGs) (e.g., Marchetti (1977)). As climate change concerns have intensified over time, research into CDR has broadened, resulting in the evolution of diverse natural and technological methods. CDR strategies include existing and potential anthropogenic enhancement of biological, geochemical, or chemical carbon sinks. In this dissertation, CDR methods are categorized based on the enhancement of their target carbon reservoirs, specifically **land-based CDR** and **ocean-based CDR**.

Land-based (or terrestrial) CDR strategies leverage carbon sinks within geological or ecological systems on land. These strategies can be categorized into those that utilize chemical processes and those that are biomass-based, with some strategies combining both.

Chemical process-based strategies include direct air capture and carbon storage (DACCS) and enhanced weathering (EW). DACCS employs specialized machinery to capture CO₂ from ambient air using chemical reactions with sorbents or alkaline aqueous solutions (Keith et al., 2018; Kumar et al., 2015). EW, on the other hand, accelerates the breakdown of minerals that react with CO₂ to form stable carbonates (see Eq.1.1 - Eq.1.4), effectively sequestering CO₂ from the atmosphere (Taylor et al., 2016b; Goll et al., 2021).

Biomass-based terrestrial CDR strategies, such as afforestation and reforestation, peatland and wetland restoration, soil carbon sequestration and biochar, increase the carbon storage potential of ecosystems (Lal, 2004; Griscom et al., 2017; Günther et al., 2020;

Lenton, 2010; Lehmann et al., 2021). These strategies also offer co-benefits, including enhanced biodiversity, water quality, and soil health (Smith, 2016; Griscom et al., 2017).

Other terrestrial CDR strategies integrate both chemical and biological processes. For instance, Bioenergy with Carbon Capture and Storage (BECCS) combines the growth of bioenergy crops, which absorb CO₂ from the atmosphere, with carbon capture and storage (CCS) technologies. The biomass of these crops is used as fuel material and the CO₂ emissions generated during energy production are captured and stored in a deep geological burial (Hanssen et al., 2020; Fridahl and Lehtveer, 2018).

Land-based CDR strategies offer significant CDR potential, with biomass-based terrestrial CDR strategies currently capable of sequestering 1-1.5 PgC per year and potentially increasing to 4-6 PgC per year by 2050 (Lenton, 2010). However, these strategies are constrained by factors such as the availability of suitable land and water resources, and the potential for competition with food production. These limitations underscore the importance of a balanced and diversified approach to addressing climate change, incorporating a combination of strategies to reduce GHG emissions and enhance carbon sequestration (Pathak et al., 2022).

1.2.2 Ocean-based CDR: unleashing the Blue Potential

Encompassing 70% of the Earth's surface, the ocean is the most substantial active carbon sink, serving as a long-term repository for anthropogenic CO₂. Its capacity for carbon storage is significantly higher than those of the atmosphere and terrestrial ecosystems, positioning it as a crucial asset in combating climate change. Consequently, there is growing interest in ocean-based CDR strategies. In contrast to terrestrial CDR strategies, ocean-based CDR does not compete for land space, thus avoiding potential conflicts with agricultural or urban development. Most ocean-based CDR strategies primarily enhance the natural carbon sequestration processes that already exist in the ocean. Additionally, certain ocean-based CDR methods can locally mitigate ocean acidification. This dual benefit for climate mitigation and marine ecosystem health underscores the importance and timeliness of investigating the ocean-based CDR potential (Keller et al., 2018; Bach and Boyd, 2021; Gattuso et al., 2018). Therefore, the exploration and development of ocean-based CDR strategies are both essential and opportune in the context of global climate change mitigation. Fig.1.2 depicts a selection of representative ocean-based CDR strategies. These strategies can be broadly divided into two primary categories: biological and abiotic. Each category targets specific ocean carbon pumps, namely the biological carbon

pump and the solubility carbon pump, as discussed in Section 1.1.2 (Gattuso et al., 2021; Taylor et al., 2016b; Goll et al., 2021; Lenton et al., 2018b).

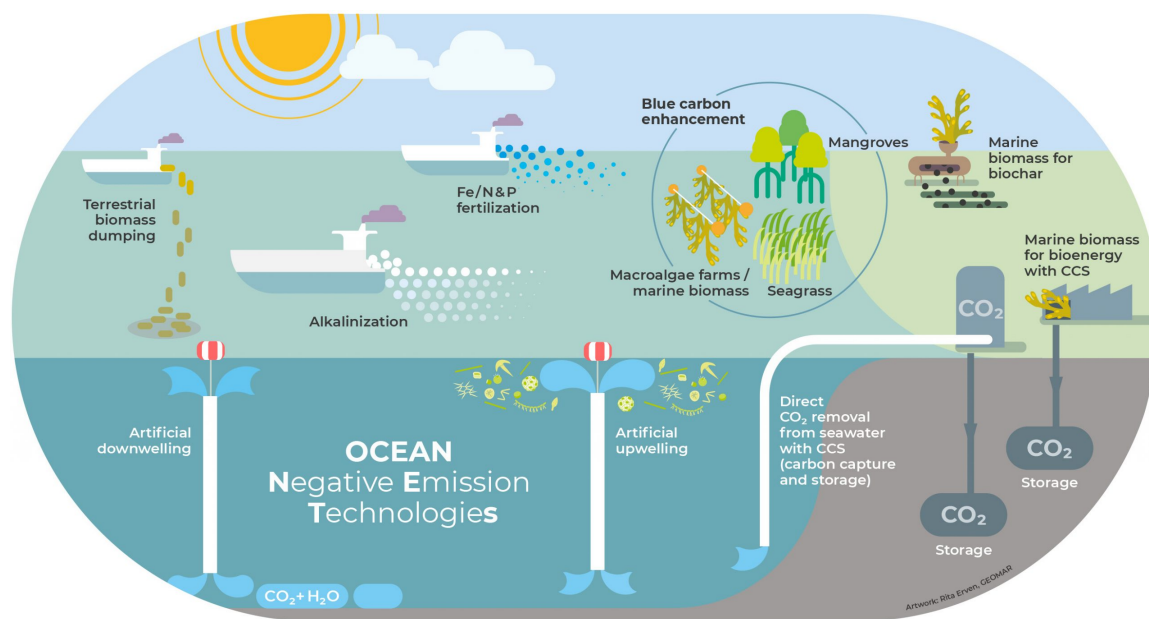


Figure 1.2: An illustrative diagram showcasing the conceptual approaches of Ocean-based Carbon Dioxide Removal (CDR), or Ocean Negative Emission Technologies (Ocean NETs). The artwork is credited to Rita Erven, OceanNETs/GEOMAR

Abiotic ocean-based CDR focuses on enhancing the solubility carbon pump, which represents the physical and chemical mechanisms facilitating inorganic carbon sequestration in the ocean. Several strategies have been proposed within this category, including ocean alkalization enhancement (OAE) and direct CO₂ injection.

Ocean alkalization enhancement (OAE), depicted as ocean alkalization in Fig.1.2, is a proposed ocean-based CDR strategy by increasing the alkalinity of the ocean, thereby enhancing its capacity to absorb and store CO₂. The concept of OAE is inspired by the Earth's natural regulation of alkalinity over geological timescales (Kheshgi, 1995). The process involves the addition of carbonate-containing minerals or alkaline solutions to the ocean, which react with CO₂ and water to form bicarbonate (HCO₃⁻) and carbonate (CO₃²⁻) ions. This not only increases the ocean's CO₂ uptake but also mitigates the acidity of seawater caused by excess anthropogenic CO₂ (Köhler et al., 2010; Ilyina et al., 2013; Taylor et al., 2016a; Lenton et al., 2018a; Bach et al., 2021a). OAE has been suggested to sequester more than 1.0 Gt CO₂/yr when implemented globally, and nearly double the CO₂ uptake after 30 years since implementation (Butenschön et al., 2021; National Academies of Sciences, Engineering, and Medicine, 2022, Table 7.3). Additionally, the increase in

CO_3^{2-} ion concentration enhances the calcium carbonate (CaCO_3) saturation state of seawater, which is crucial for promoting and maintaining the precipitation of calcium carbonate in shell-producing organisms (Riebesell et al., 2007). However, OAE also presents several challenges. The mining and transportation of the necessary alkaline materials require substantial infrastructure, potentially leading to significant environmental impacts. Furthermore, the potential impacts of alkalinity addition on marine ecosystems are not fully understood, necessitating further research (Gattuso et al., 2018; Bach et al., 2019; Taylor et al., 2016b; Lenton et al., 2018a).

Direct CO_2 injection is a more direct approach to augmenting the ocean's inorganic carbon pool (Orr et al., 2001; Reith et al., 2016a). This technique captures CO_2 from the atmosphere or point sources and injects it into deep ocean waters or sub-seabed geological formations, where it can be stored long-term without re-entering the atmosphere. The high pressure and low temperature at these depths promote the formation of CO_2 hydrates or dissolution in seawater, thus effectively storing CO_2 (Reith et al., 2016a). However, this method raises concerns about potential leakage, ecological impacts on deep-sea ecosystems, and long-term storage stability, requiring additional research and careful monitoring (Reith et al., 2016a; Seibel and Walsh, 2001; Haugan and Drange, 1992).

Conversely, biological ocean-based CDR strategies aim to augment the ocean's organic carbon pool by enhancing the biological carbon pump. These strategies primarily involve boosting the primary production by supplying exogenous nutrients to marine primary producers, such as phytoplankton. These methods also involve restoration or intentional expansion of productive ecosystems in coastal regions or open oceans, such as mangroves, salt marshes and macroalgae.

Nutrient fertilization involves the addition of micro (e.g., iron (Fe) and/or macro (e.g., phosphorus (P), nitrogen (N) nutrients to the ocean, in order to increase photosynthesis by marine phytoplankton, and thus enhance uptake of carbon dioxide (CO_2) from surface waters. The purpose of this strategy is to stimulate photosynthesis in marine phytoplankton, thereby enhancing the uptake of carbon dioxide (CO_2) from surface waters. Subsequently, it facilitates the transfer of newly formed organic carbon to the deep sea, effectively sequestering it away from the surface layer in immediate contact with the atmosphere (Boyd (2008); Keller et al. (2014b); Harrison (2017)). Several large-scale iron fertilization experiments have shown that the addition of iron to high-nutrient, low-chlorophyll (HNLC) regions can lead to substantial increases in primary production and carbon export to the deep ocean (Aumont and Bopp, 2006; Boyd, 2008; Buesseler et al., 2004). Nutrient fertilization is estimated to have a CDR potential in the order of GtCO_2 per year

(Keller et al., 2014b; Oschlies et al., 2010a; National Academies of Sciences, Engineering, and Medicine, 2022, Table 3.3). However, concerns about potential unintended ecological consequences, scalability, and the efficiency of carbon sequestration have led to calls for further research and careful regulation (Keller et al., 2014b; Oschlies et al., 2010a; Gattuso et al., 2021).

Restoration and protection of blue carbon ecosystems: Blue carbon ecosystems, such as mangroves, seagrass meadows, and salt marshes, are highly efficient carbon sinks due to their high rates of primary production and carbon sequestration in sediments Nellemann et al. (2009); McLeod et al. (2011). The restoration and protection of these ecosystems could significantly enhance the ocean's organic carbon reservoir while providing co-benefits such as habitat provision, coastal protection, and water quality improvement (Macreadie et al., 2021; Duarte et al., 2013). It is estimated that the restoration and protection of blue carbon ecosystems could potentially draw down 841 GtCO₂ by 2030 (Macreadie et al., 2021).

Artificial upwelling and downwelling represent ocean-based CDR strategies that effectively combine both abiotic and biological methods. Artificial upwelling aims to bring nutrient-rich deep waters to the surface, promoting phytoplankton growth and increasing primary production (Oschlies et al., 2010b; Keller et al., 2014a; National Academies of Sciences, Engineering, and Medicine, 2022, Sect. 4). These systems can potentially enhance the biological carbon pump by stimulating the growth of phytoplankton in nutrient-limited surface waters. Artificial downwelling, on the other hand, involves the use of engineered systems to increase the downward transport of carbon that has been taken up in the surface ocean water, potentially enhancing the sequestration of carbon in the deep ocean for long geological period. Both Artificial upwelling and downwelling require further research to assess their potential CDR efficacy, impacts on ecosystem, and optimal operational parameters (Jürchott et al., 2023; Keller et al., 2014b; Oschlies et al., 2010c; Feng et al., 2020).

Other ocean-based CDR strategies encompass methods such as terrestrial biomass dumping, which involves the harvesting of terrestrial biomass with sequestered carbon through photosynthesis during growth. The harvested biomass is then either deposited in the deep ocean or buried within coastal sediments, effectively sequestering the carbon away from the atmosphere (Fig.1.2). While ocean-based CDR strategies hold significant potential for mitigating climate change, they also necessitate further research. A comprehensive understanding of the environmental impacts and long-term efficacy of these approaches is crucial to ensure their sustainable and effective implementation (Gattuso et al., 2018; Keller et al., 2021).

1.3 Research motivation: evaluating the potential and consequences of macroalgae-based CDR through Earth system climate model simulations

1.4 Macroalgae-based CDR

As described in the previous section, ocean-based CDR strategies primarily function by enhancing the photosynthetic activity of primary producers, thereby facilitating the sequestration of carbon in organic forms. In this context, macroalgae, a type of marine macrophyte primary producer, emerges as a potential carbon fixer. This expands the scope of ocean-based CDR strategies beyond microphytes such as phytoplankton, offering a broader range of options for carbon sequestration in the marine environment. In this dissertation, the term 'macroalgae-based CDR' is specifically used to denote ocean-based CDR strategies involve the macroalgae cultivation or augmentation of natural macroalgae for carbon sequestration purposes.

Macroalgae, commonly known as seaweed, are highly efficient natural carbon fixers, characterized by a high carbon-to-nitrogen (C:N) ratio and elevated net primary production (NPP) rates (Pessarrodona et al., 2022; Fernand et al., 2017a; Atkinson and Smith, 1983; Buck and Buchholz, 2004; Zhang et al., 2016). Global estimates of natural macroalgae NPP reach up to 1.32 PgC yr^{-1} (Duarte et al., 2022), and it is suggested that carbon storage through the transport and subsequent sinking of macroalgal biomass to ocean sediments could account for approximately 0.17 PgC yr^{-1} (Canals et al., 2006; Krause-Jensen and Duarte, 2016; Luo et al., 2019; Macreadie et al., 2019). This process can be viewed as an enhancement of the biological carbon pump, aiming to sequester more carbon by circumventing the significant loss (around 70% to 85%) of particulate organic carbon due to consumption and respiration during its slow descent through the mesopelagic zone (Ducklow et al., 2001; Riebesell et al., 2009; Briggs et al., 2020). Furthermore, macroalgal biomass has been identified as resistant to microbial degradation, suggesting the potential for long-term carbon storage (Sichert et al., 2020). These characteristics underscore the potential of macroalgae cultivation for CDR in terms of its efficacy, scalability, and the durability of carbon sequestration.

Moreover, the technologies for macroalgae breeding and aquaculture are well-established and have been refined over the years (Tseng, 1987; Qin et al., 2005; Kim et al., 2017). This is evidenced by the impressive global production of macroalgae, which reached 34.7

million tonnes in 2019 (Cai et al., 2021). Many cultivated macroalgae species possess rhizoids, root-like structures that enable the macroalgae to anchor themselves to substrates (FAO, 2023). This characteristic simplifies the operational aspects of macroalgae cultivation, making it a more feasible option for CDR compared to methods involving microalgae cultivation or open ocean fertilization.

In addition, macroalgae-based CDR offers a range of enticing co-benefits. Similar to other proposed ocean-based CDR strategies, it does not directly compete with land, freshwater or fertilizer resources (Cai et al., 2021). It also offers potential ecological advantages, including mitigation against ocean acidification, helping to alleviate heavy metal contamination, deoxygenation and eutrophication (Xiao et al., 2017; Kim et al., 2019; Jiang et al., 2020). Other co-benefits with potential greenhouse gas reductions include the use of macrophyte biomass in animal feeds, which could reduce methane emissions (Maia et al., 2019).

The idea of employing macroalgae cultivation as a strategy for climate change mitigation has been under consideration for an extended period (e.g., Gao and McKinley (1994); Chen et al. (2015); Fernand et al. (2017b); Jung et al. (2013); Chung et al. (2013)). Meanwhile, the implementation of such practices has also been initiated in various parts of the world. For instance, the U.S. Department of Energy's Advanced Research Project Agency-e (ARPA-e) MARINER program is developing prototypes for scalable farmed systems that can be deployed in deeper waters to grow biomass stocks for biofuels (ARPA-e, 2023). Navarrete et al. (2021) tested the depth-cycling strategy, in which macroalgae are physically towed into the deep nutrient-rich water at night. Several organizations, including companies such as Running Tide (www.runningtide.com) and MACROCARBON (www.macrocarbon.world), as well as non-profits such as Ocean Visions (www.oceanvisions.org), are focusing on the development and commercialization of macroalgae-based CDR. On a global scale, seaweed aquaculture production surpasses 30 million wet metric tons, with a market value exceeding \$5.6 billion (Cai et al., 2021; National Academies of Sciences, Engineering, and Medicine, 2022, Sect. 5.3). As such, macroalgae-based CDR is transitioning from a theoretical concept to a promising and practical carbon sequestration approach, warranting further research and exploration.

1.5 Why simulating macroalgae-based CDR in an Earth system climate model?

Modeling has been widely employed as an essential tool for analyzing CDR approaches due to its ability to handle the scale and complexity of the various interacting components of the Earth's climate system, including the atmosphere, oceans, terrestrial carbon cycles and ecosystems, as well as human activities such as land-use and GHG emissions. Models provide a platform for virtual experimentation and intercomparison for various CDR methods and climate change scenarios, circumventing the practicalities of conducting real-world, large-scale experiments (e.g., the Carbon Dioxide Removal Model Intercomparison Project (CDRMIP) by Keller et al. (2018)), which is vital for assessing the potential of various CDR strategies and planning future climate mitigation efforts. They also aid in understanding the potential and possible side effects or risks (e.g., Oschlies et al. (2010c); Keller et al. (2014b); Siegel et al. (2021)). Additionally, the integration of CDR models with other types of models, such as economic or energy system models, offers a more comprehensive view of the potential impacts and benefits of CDR methods (e.g., Rickels et al. (2018); Schenuit et al. (2021); Hepburn et al. (2019)). Thus, models are a critical tool in the analysis of CDR methods, providing a means to understand, predict, and experiment with these methods in a way that would be otherwise impossible.

The research conducted in this dissertation utilizes the University of Victoria Earth system climate model (UVic ESCM), an Earth System Model of intermediate complexity (EMIC), fully integrated with a carbon cycle, and cutting-edge Integrated Assessment Models (IAMs). EMICs serve as a bridge between the most basic and the most intricate climate models (Claussen et al., 2002). EMICs are sufficiently complex to simulate crucial climate processes and feedbacks, but they often simplify one or more components of the climate model, such as the atmosphere and marine sediments (Keller et al., 2012). Nevertheless, EMICs are capable of integrating processes that operate within the Earth System over extremely long timescales. The primary benefit of EMICs, in comparison to more complex models, is their computational efficiency. They can run simulations several orders of magnitude faster and can be operated on standard computers. As such, these models are particularly suitable for studying the efficacy and impacts of CDR strategies over extended timescales (e.g., Keller et al. (2014b); Reith et al. (2016b); Mengis et al. (2016); Oschlies et al. (2010c)).

Similar to other CDR strategies, modeling studies can be employed to investigate the potential and impacts of macroalgae-based CDR on the Earth system carbon cycle, marine

biogeochemistry, and ecosystems prior to large-scale real-world deployments (Boyd et al., 2022; Berger et al., 2023; Ricart et al., 2022). Several processes involved in macroalgae-based CDR require further investigation, such as carbon capture capacity, impacts on phytoplankton and the fate of cultivated macroalgae biomass. Indeed, several modeling studies, apart from those presented in this dissertation, have been undertaken to explore this topic. For instance, Berger et al. (2023) modified a high-resolution ocean biogeochemical model, revealing that Eastern boundary upwelling systems, the Northeast Pacific and the Southern Ocean as potentially promising locations. However, the macroalgae-based CDR efficiency is limited to 58% (0.21 PgC yr^{-1}) considering physiochemical, nutrient limitations and depression on phytoplankton primary production. Bach et al. (2021b) analyzed the CDR potential of the belts of the floating macroalgae *Sargassum* in the (sub)tropical North Atlantic (GASB) as a natural analogue for ocean afforestation. The research revealed that: 1) two biogeochemical feedbacks, nutrient reallocation and calcification by encrusting marine life, can reduce the macroalgae-based CDR efficacy by 20% to 100%; 2) the atmospheric CO_2 influx into the surface seawater takes longer time than the CO_2 -deficient seawater's contact time with the atmosphere, and 3) the increased ocean albedo due to floating *Sargassum* could have a greater impact on climate radiative forcing than *Sargassum*-CDR. The study concludes that the efficacy of macroalgae-based CDR is determined by multifaceted Earth-system feedbacks. Arzeno-Soltero et al. (2023) utilized a dynamic seaweed growth model, incorporating growth-limiting mechanisms like nitrate supply, to estimate the global potential yield of four different seaweed species. Their findings suggest that to sequester 1 GtC through macroalgae-based CDR, farming would be required in approximately 1 million km^{-2} of the most productive Exclusive Economic Zones (EEZs) in the equatorial Pacific. However, they also noted a significant decrease in carbon harvest efficiency beyond these highly productive waters.

The existing modeling studies evaluating macroalgae-based CDR exhibit several limitations. Firstly, the simulation time length in these studies is often short (e.g., 1 to 5 years (Berger et al., 2023; Arzeno-Soltero et al., 2023)), which is not sufficient to assess the long-term impacts of deploying and terminating macroalgae-based CDR. Secondly, these studies do not simulate the fate of macroalgae biomass and the associated impacts, which typically involve sinking to the deep ocean or harvesting for further CDR purposes such as Bioenergy with Carbon Capture and Storage (BECCS) or biochar (Wu et al., 2023; National Academies of Sciences, Engineering, and Medicine, 2022, Sect. 5). Moreover, some of the macroalgae growth models used in these studies are overly simplified, lacking dynamic interactions with marine biogeochemical systems or the global carbon cycle. In addition,

the ocean-only models employed in some of these studies lack a land component, thereby excluding a fully coupled carbon cycle from their simulations (e.g., Berger et al. (2023)), which is crucial as a comprehensive evaluation of any ocean-based CDR must account for alterations in carbon fluxes between the Earth's carbon reservoirs.

The primary impetus for the research undertaken in this dissertation is to scrutinize the potential and repercussions of macroalgae-based CDR from a global and long-term standpoint. This encompasses an examination of its scalability, efficacy in terms of carbon sequestration, and potential impacts on various facets of the marine environment, including marine ecosystems, marine biogeochemistry, and the oceanic and global carbon cycles. Comprehending these factors is crucial for assessing the overall feasibility and sustainability of macroalgae-based CDR. The macroalgae-based CDR strategies in this dissertation include deployments in both global open ocean (Chapter 2) and global coastal regions (Chapter 3), specifically the Exclusive Economic Zones (EEZs). Additionally, an estimation of utilizing macroalgae cultivation as BECCS feedstock for the Net Zero 2050 target in Germany has also been conducted as part of this research (Chapter 4).

1.6 Chapter synopsis and author contributions

In **Chapter 2** we introduce and investigate the maximum physical and biogeochemical potential of a macroalgae-based CDR strategy: macroalgae open-ocean mariculture and sinking (MOS). The concept of MOS is to cultivate macroalgae in the open ocean and sink the carbon-rich macroalgal biomass to the deep seafloor for long-time carbon sequestration. For this purpose, we for the first time embed and validate a dynamic macroalgae growth model into the UVic ESCM. We also explore the combination of MOS with artificial upwelling (AU), which fertilizes the macroalgae by pumping nutrient-rich deeper water to the surface. The model simulated remineralization of the sunk biomass in the deep ocean, as well as the further physical and biogeochemical processes of the released carbon and nutrients. The simulations are under a moderate-emissions pathway, RCP 4.5. MOS is simulated to be deployed from the years 2020, either with termination at 2100 or continuous till 3000. Our results indicate that the carbon captured and exported by MOS is 270 PgC, which is further boosted by AU to 447 PgC. However, due to feedbacks in the Earth system, the oceanic carbon inventory only increases by 171.8 PgC (283.9 PgC with AU) in the idealized simulations. Our simulations also reveal the major side effects of MOS, including reducing the atmospheric and terrestrial carbon reservoirs while enhancing the ocean carbon reservoir, depression on pelagic phytoplankton, nutrients distribution

and alleviated middle depth oxygen concentrations. We conclude that while MOS holds considerable theoretical CDR potential, its large-scale deployment would have significant impacts on marine ecosystems.

Chapter 2 is based on the paper Wu, J., Keller, D. P., & Oschlies, A. (2023), *Carbon dioxide removal via macroalgae open-ocean mariculture and sinking: an Earth system modeling study* published in the journal *Earth System Dynamics*. JW, DPK and AO conceived and designed the experiments. JW implemented and performed the experiments and analyzed the data. JW wrote the paper with contributions from DPK and AO.

In **Chapter 3**, we analyse the CDR potential and impacts of macroalgae-based CDR in coastal regions, that is, the Nearshore Macroalgae Aquaculture for Carbon Sequestration (N-MACS). The macroalgae growth model in the UVic ESCM established in **Chapter 2** is migrated to the global ocean Exclusive Economic Zones (EEZs), where macroalgae biomass is cultivated and harvested from the ocean. To explore the theoretical maximum potential of N-MACS with macroalgae species from global coastal regions, we carry out an additional sensitivity simulation where the growth of macroalgae is not influenced by water temperature. Our findings suggest that N-MACS could potentially sequester between 0.71 to 1.10 GtC per year. However, the implementation of N-MACS also leads to a significant reduction in marine net primary productivity (NPP) due to nutrient competition and canopy shading effects, which in turn reduces the CDR capacity of N-MACS by about 30%. This suppression of surface NPP decreases organic carbon export to the deeper ocean, leading to increased dissolved oxygen concentrations and reduced denitrification in the middle layers. It also results in a decrease in surface ocean alkalinity due to nutrient removal. Several effects, such as the removal of phosphate and a reduction in global oceanic net primary production, persist for centuries even after the discontinuation of N-MACS. The chapter concludes by emphasizing the need for a careful evaluation of the potential benefits and impacts of macroalgae-based CDR, given the significant alterations it can cause in marine biogeochemistry and ecosystems.

Chapter 3 is based on the paper Wu, J., Keller, D. P., Yao, W & Oschlies, A. (2023), *Nearshore Macroalgae Cultivation for Carbon Sequestration by Biomass Harvesting: Evaluating Potential and Impacts with An Earth System Model* submitted to the journal *Geophysical Research Letters*. JW, DPK and AO conceived and designed the experiments. JW implemented and performed the experiments and analyzed the data. JW wrote the paper with contributions from DPK, WY and AO.

In **Chapter 4**, we explore the concept of using macroalgae cultivation as a feedstock for bioenergy with carbon capture and storage (BECCS with macroalgae) in the context of

Germany's Net Zero 2050 target. Our analysis suggests that the maximum theoretical CDR potential of BECCS with macroalgae is approximately 0.79 million tonnes of CO₂ per year, a significant contribution to the overall BECCS CDR potential in Germany. However, we also highlight several challenges and uncertainties, including the scalability of macroalgae cultivation, the efficiency of carbon sequestration, and the potential impacts on marine ecosystems and biogeochemistry. In comparison with 12 other CDR concepts available in Germany, BECCS with macroalgae is at the pilot-scale maturity level. We emphasize the need for further research, socio-economic analysis, clear regulations, and policy incentives to fully realize the potential of this approach.

Chapter 4 is based on the paper Borchers, M., ..., Wu, J. et al., (2022), *Scoping carbon dioxide removal options for Germany – What is their potential contribution to Net-Zero CO₂?* published in the journal *Frontiers in Climate*. JW and NM contributed to section BECC–macroalgae farming for biogas production for co-generation of heat and power (concept 6) and associated content about utilization of macroalgae.

1.7 References

- S. Abernethy, F. M. O'Connor, C. D. Jones, and R. B. Jackson. Methane removal and the proportional reductions in surface temperature and ozone. *Philosophical Transactions of the Royal Society A: Mathematical, Physical and Engineering Sciences*, 379(2210):20210104, September 2021. doi: 10.1098/rsta.2021.0104. URL <https://royalsocietypublishing.org/doi/10.1098/rsta.2021.0104>. Publisher: Royal Society.
- International Energy Agency. Energy efficiency 2020, 2020. URL <https://www.iea.org/reports/energy-efficiency-2020>.
- International Renewable Energy Agency. Renewable power generation costs in 2020. Technical report, International Renewable Energy Agency, 2021. URL <https://www.irena.org/publications/2021/Jun/Renewable-Power-Costs-in-2020>. Accessed: 2023-04-06.
- Myles R. Allen, David J. Frame, Chris Huntingford, Chris D. Jones, Jason A. Lowe, Malte Meinshausen, and Nicolai Meinshausen. Warming caused by cumulative carbon emissions towards the trillionth tonne. *Nature*, 458(7242):1163–1166, April 2009. ISSN 0028-0836, 1476-4687. doi: 10.1038/nature08019. URL <http://www.nature.com/articles/nature08019>.
- William R. L. Anderegg, Jeffrey M. Kane, and Leander D. L. Anderegg. Consequences of widespread tree mortality triggered by drought and temperature stress. *Nature Climate Change*, 3(1):30–36, January

2013. ISSN 1758-6798. doi: 10.1038/nclimate1635. URL <https://www.nature.com/articles/nclimate1635>. Number: 1 Publisher: Nature Publishing Group.
- David Archer, Michael Eby, Victor Brovkin, Andy Ridgwell, Long Cao, Uwe Mikolajewicz, Ken Caldeira, Katsumi Matsumoto, Guy Munhoven, Alvaro Montenegro, and Kathy Tokos. Atmospheric Lifetime of Fossil Fuel Carbon Dioxide. *Annual Review of Earth and Planetary Sciences*, 37(1):117–134, May 2009. ISSN 0084-6597, 1545-4495. doi: 10.1146/annurev.earth.031208.100206. URL <https://www.annualreviews.org/doi/10.1146/annurev.earth.031208.100206>.
- ARPA-e. Macroalgae research inspiring novel energy resources, 2023. URL <https://arpa-e.energy.gov/technologies/programs/mariner>. Accessed: 2023-3-15.
- Svante Arrhenius. On the influence of carbonic acid in the air upon the temperature of the ground. *Philosophical Magazine and Journal of Science*, 41(251):237–276, 1896. doi: 10.1080/14786449608620846. URL <https://www.tandfonline.com/doi/abs/10.1080/14786449608620846>.
- Isabella B. Arzeno-Soltero, Benjamin T. Saenz, Christina A. Frieder, Matthew C. Long, Julianne DeAngelo, Steven J. Davis, and Kristen A. Davis. Large global variations in the carbon dioxide removal potential of seaweed farming due to biophysical constraints. *Communications Earth & Environment*, 4(1):1–12, June 2023. ISSN 2662-4435. doi: 10.1038/s43247-023-00833-2. URL <https://www.nature.com/articles/s43247-023-00833-2>. Number: 1 Publisher: Nature Publishing Group.
- M. J. Atkinson and S. V. Smith. C:N:P ratios of benthic marine plants. *Limnology and Oceanography*, 28(3): 568–574, 1983. ISSN 19395590. doi: 10.4319/lo.1983.28.3.0568. URL <http://onlinelibrary.wiley.com/doi/10.4319/lo.1983.28.3.0568/abstract>.
- O. Aumont and L. Bopp. Globalizing results from ocean in situ iron fertilization studies: GLOBALIZING IRON FERTILIZATION. *Global Biogeochemical Cycles*, 20(2):n/a–n/a, June 2006. ISSN 08866236. doi: 10.1029/2005GB002591. URL <http://doi.wiley.com/10.1029/2005GB002591>.
- Lennart T. Bach and Philip W. Boyd. Seeking natural analogs to fast-forward the assessment of marine CO₂ removal. *Proceedings of the National Academy of Sciences*, 118(40):e2106147118, October 2021. ISSN 0027-8424, 1091-6490. doi: 10.1073/pnas.2106147118. URL <https://pnas.org/doi/full/10.1073/pnas.2106147118>.
- Lennart T. Bach, Sophie J. Gill, Rosalind E. M. Rickaby, Sarah Gore, and Phil Renforth. CO₂ Removal With Enhanced Weathering and Ocean Alkalinity Enhancement: Potential Risks and Co-benefits for Marine Pelagic Ecosystems. *Frontiers in Climate*, 1:7, October 2019. ISSN 2624-9553. doi: 10.3389/fclim.2019.00007. URL <https://www.frontiersin.org/article/10.3389/fclim.2019.00007/full>.
- Lennart T. Bach, Veronica Tamsitt, Jim Gower, Catriona L. Hurd, John A. Raven, and Philip W. Boyd. Testing the climate intervention potential of ocean afforestation using the Great Atlantic Sargassum Belt. *Nature Communications*, 12(1):2556, 5 2021a. ISSN 20411723. doi: 10.1038/s41467-021-22837-2. URL <http://dx.doi.org/10.1038/s41467-021-22837-2> <https://www.nature.com/articles/s41467-021-22837-2>.

- Lennart T. Bach, Veronica Tamsitt, Jim Gower, Catriona L. Hurd, John A. Raven, and Philip W. Boyd. Testing the climate intervention potential of ocean afforestation using the Great Atlantic Sargassum Belt. *Nature Communications*, 12(1):2556, May 2021b. ISSN 2041-1723. doi: 10.1038/s41467-021-22837-2. URL <https://www.nature.com/articles/s41467-021-22837-2>.
- Lennart Thomas Bach, Ulf Riebesell, Magdalena A. Gutowska, Luisa Federwisch, and Kai Georg Schulz. A unifying concept of coccolithophore sensitivity to changing carbonate chemistry embedded in an ecological framework. *Progress in Oceanography*, 135:125–138, June 2015. ISSN 0079-6611. doi: 10.1016/j.pocean.2015.04.012. URL <https://www.sciencedirect.com/science/article/pii/S0079661115000725>.
- Nicholas R. Bates. Ocean Carbon Cycle. In *Encyclopedia of Ocean Sciences*, pages 418–428. Elsevier, 2019. ISBN 978-0-12-813082-7. doi: 10.1016/B978-0-12-409548-9.11598-2. URL <https://linkinghub.elsevier.com/retrieve/pii/B9780124095489115982>.
- Manon Berger, Lester Kwiatkowski, David T Ho, and Laurent Bopp. Ocean dynamics and biological feedbacks limit the potential of macroalgae carbon dioxide removal. *Environmental Research Letters*, 18(2):024039, February 2023. ISSN 1748-9326. doi: 10.1088/1748-9326/acb06e. URL <https://iopscience.iop.org/article/10.1088/1748-9326/acb06e>.
- Robert A. Berner. The long-term carbon cycle, fossil fuels and atmospheric composition. *Nature*, 426(6964): 323–326, November 2003. ISSN 1476-4687. doi: 10.1038/nature02131. URL <https://www.nature.com/articles/nature02131>. Number: 6964 Publisher: Nature Publishing Group.
- Robert A. Berner and Elizabeth K. Berner. Silicate Weathering and Climate. In William F. Ruddiman, editor, *Tectonic Uplift and Climate Change*, pages 353–365. Springer US, Boston, MA, 1997. ISBN 978-1-4615-5935-1. doi: 10.1007/978-1-4615-5935-1_15. URL https://doi.org/10.1007/978-1-4615-5935-1_15.
- N.L. Bindoff, W.W.L. Cheung, J.G. Kairo, J. Arístegui, V.A. Guinder, R. Hallberg, N. Hilmi, N. Jiao, M.S. Karim, L. Levin, S. O’ Donoghue, S.R. Purca Cuicapusa, B. Rinkevich, T. Suga, A. Tagliabue, and P. Williamson. *Changing Ocean, Marine Ecosystems, and Dependent Communities*, pages 447–587. Cambridge University Press, Cambridge, UK and New York, NY, USA, 2019. doi: 10.1017/9781009157964.007.
- Philip W. Boyd. Ranking geo-engineering schemes. *Nature Geoscience*, 1(11):722–724, 2008. ISSN 17520894. doi: 10.1038/ngeo348.
- Philip W. Boyd, Lennart T. Bach, Catriona L. Hurd, Ellie Paine, John A. Raven, and Veronica Tamsitt. Potential negative effects of ocean afforestation on offshore ecosystems. *Nature Ecology & Evolution*, 6(6):675–683, April 2022. ISSN 2397-334X. doi: 10.1038/s41559-022-01722-1. URL <https://www.nature.com/articles/s41559-022-01722-1>.
- Nathan Briggs, Giorgio Dall’Olmo, and Hervé Claustre. Major role of particle fragmentation in regulating biological sequestration of CO₂ by the oceans. *Science*, 367(6479):791–793, 2020. ISSN 10959203. doi: 10.1126/science.aay1790.

- Wallace S Broecker. Climatic change: are we on the brink of a pronounced global warming? *Science*, 189 (4201):460–463, 1975.
- Wallace S. Broecker. The Great Ocean Conveyor. *Oceanography*, 4(2):79–89, 1991. ISSN 1042-8275. URL <https://www.jstor.org/stable/43924572>. Publisher: Oceanography Society.
- Bela Hieronymus Buck and Cornelia Maria Buchholz. The offshore-ring: A new system design for the open ocean aquaculture of macroalgae. *Journal of Applied Phycology*, 16(5):355–368, October 2004. ISSN 0921-8971. doi: 10.1023/B:JAPH.0000047947.96231.ea. URL <http://link.springer.com/10.1023/B:JAPH.0000047947.96231.ea>.
- Ken O. Buesseler. The decoupling of production and particulate export in the surface ocean. *Global Biogeochemical Cycles*, 12(2):297–310, 1998. ISSN 1944-9224. doi: 10.1029/97GB03366. URL <https://onlinelibrary.wiley.com/doi/abs/10.1029/97GB03366>. _eprint: <https://onlinelibrary.wiley.com/doi/pdf/10.1029/97GB03366>.
- Ken O. Buesseler, John E. Andrews, Steven M. Pike, and Matthew A. Charette. The Effects of Iron Fertilization on Carbon Sequestration in the Southern Ocean. *Science*, 304(5669):414–417, April 2004. doi: 10.1126/science.1086895. URL <https://www.science.org/doi/full/10.1126/science.1086895>. Publisher: American Association for the Advancement of Science.
- Momme Butenschön, Tomas Lovato, Simona Masina, Stefano Caserini, and Mario Grosso. Alkalinization Scenarios in the Mediterranean Sea for Efficient Removal of Atmospheric CO₂ and the Mitigation of Ocean Acidification. *Frontiers in Climate*, 3:614537, March 2021. ISSN 2624-9553. doi: 10.3389/fclim.2021.614537. URL <https://www.frontiersin.org/articles/10.3389/fclim.2021.614537/full>.
- Junning Cai, Alessandro Lovatelli, José Aguilar-Manjarrez, Lynn Cornish, Lionel Dabbadie, Anne Desrochers, Simon Diffey, Esther Garrido Gamarro, James Geehan, Anicia Hurtado, et al. Seaweeds and microalgae: an overview for unlocking their potential in global aquaculture development. *FAO Fisheries and Aquaculture Circular*, 1229, 2021.
- Ken Caldeira and Michael E. Wickett. Anthropogenic carbon and ocean pH. *Nature*, 425(6956):365–365, September 2003. ISSN 1476-4687. doi: 10.1038/425365a. URL <https://www.nature.com/articles/425365a>. Number: 6956 Publisher: Nature Publishing Group.
- G. S. Callendar. The artificial production of carbon dioxide and its influence on temperature. *Quarterly Journal of the Royal Meteorological Society*, 64(275):223–240, 1938. doi: 10.1002/qj.49706427503.
- Josep G Canadell, Pedro MS Monteiro, Marcos H Costa, Leticia Cotrim Da Cunha, Peter M Cox, Alexey V Eliseev, Stephanie Henson, Masao Ishii, Samuel Jaccard, Charles Koven, et al. Global carbon and other biogeochemical cycles and feedbacks, 2021.
- Miquel Canals, Pere Puig, Xavier Durrieu De Madron, Serge Heussner, Albert Palanques, and Joan Fabres. Flushing submarine canyons. *Nature*, 444(7117):354–357, 11 2006. ISSN 14764687. doi: 10.1038/nature05271. URL <http://www.nature.com/articles/nature05271>.

- Matthew Charette and Walter Smith. The Volume of Earth's Ocean. *Oceanography*, 23(2):112–114, June 2010. ISSN 10428275. doi: 10.5670/oceanog.2010.51. URL <https://tos.org/oceanography/article/the-volume-of-earths-ocean>.
- Huihui Chen, Dong Zhou, Gang Luo, Shicheng Zhang, and Jianmin Chen. Macroalgae for biofuels production: Progress and perspectives. *Renewable and Sustainable Energy Reviews*, 47:427–437, July 2015. ISSN 13640321. doi: 10.1016/j.rser.2015.03.086. URL <https://linkinghub.elsevier.com/retrieve/pii/S1364032115002397>.
- Ik Kyo Chung, Jung Hyun Oak, Jin Ae Lee, Jong Ahm Shin, Jong Gyu Kim, and Kwang-Seok Park. Installing kelp forests/seaweed beds for mitigation and adaptation against global warming: Korean Project Overview. *ICES Journal of Marine Science*, 70(5):1038–1044, September 2013. ISSN 1095-9289, 1054-3139. doi: 10.1093/icesjms/fss206. URL <https://academic.oup.com/icesjms/article/70/5/1038/644026>.
- P. Ciais, C. Sabine, G. Bala, L. Bopp, V. Brovkin, J. Canadell, A. Chhabra, R. DeFries, J. Galloway, M. Heimann, C. Jones, C. LeãQuere, R.B. Myneni, S. Piao, and P. Thornton. Carbon and other biogeochemical cycles. In T.F. Stocker, D. Qin, G.-K. Plattner, M. Tignor, S.K. Allen, J. Boschung, A. Nauels, Y. Xia, V. Bex, and P.M. Midgley, editors, *Climate Change 2013: The Physical Science Basis. Contribution of Working Group I to the Fifth Assessment Report of the Intergovernmental Panel on Climate Change*, book section 6, page 465–570. Cambridge University Press, Cambridge, United Kingdom and New York, NY, USA, 2013. ISBN ISBN 978-1-107-66182-0. doi: 10.1017/CBO9781107415324.015. URL <http://www.climatechange2013.org>.
- Peter U. Clark, Nicklas G. Piasias, Thomas F. Stocker, and Andrew J. Weaver. The role of the thermohaline circulation in abrupt climate change. *Nature*, 415(6874):863–869, February 2002. ISSN 1476-4687. doi: 10.1038/415863a. URL <https://www.nature.com/articles/415863a>. Number: 6874 Publisher: Nature Publishing Group.
- M. Claussen, L. Mysak, A. Weaver, M. Crucifix, T. Fichefet, M.-F. Loutre, S. Weber, J. Alcamo, V. Alexeev, A. Berger, R. Calov, A. Ganopolski, H. Goosse, G. Lohmann, F. Lunkeit, I. Mokhov, V. Petoukhov, P. Stone, and Z. Wang. Earth system models of intermediate complexity: closing the gap in the spectrum of climate system models. *Climate Dynamics*, 18(7):579–586, March 2002. ISSN 1432-0894. doi: 10.1007/s00382-001-0200-1. URL <https://doi.org/10.1007/s00382-001-0200-1>.
- Hervé Claustre, Louis Legendre, Philip W. Boyd, and Marina Levy. The Oceans' Biological Carbon Pumps: Framework for a Research Observational Community Approach. *Frontiers in Marine Science*, 8:780052, November 2021. ISSN 2296-7745. doi: 10.3389/fmars.2021.780052. URL <https://www.frontiersin.org/articles/10.3389/fmars.2021.780052/full>.
- Ralf Conrad. The global methane cycle: recent advances in understanding the microbial processes involved. *Environmental Microbiology Reports*, 1(5):285–292, 2009. ISSN 1758-2229. doi: 10.1111/j.1758-2229.2009.00038.x. URL <https://onlinelibrary.wiley.com/doi/abs/10.1111/j.1758-2229.2009.00038.x>. [_eprint: https://onlinelibrary.wiley.com/doi/pdf/10.1111/j.1758-2229.2009.00038.x](https://onlinelibrary.wiley.com/doi/pdf/10.1111/j.1758-2229.2009.00038.x).

- Peter M. Cox, Richard A. Betts, Chris D. Jones, Steven A. Spall, and Ian J. Totterdell. Acceleration of global warming due to carbon-cycle feedbacks in a coupled climate model. *Nature*, 408(6809):184–187, November 2000. ISSN 1476-4687. doi: 10.1038/35041539. URL <https://www.nature.com/articles/35041539>. Number: 6809 Publisher: Nature Publishing Group.
- Rajdeep Dasgupta and Marc M. Hirschmann. The deep carbon cycle and melting in Earth’s interior. *Earth and Planetary Science Letters*, 298(1-2):1–13, September 2010. ISSN 0012821X. doi: 10.1016/j.epsl.2010.06.039. URL <https://linkinghub.elsevier.com/retrieve/pii/S0012821X10004140>.
- Christina L. De La Rocha and Uta Passow. Factors influencing the sinking of POC and the efficiency of the biological carbon pump. *Deep Sea Research Part II: Topical Studies in Oceanography*, 54(5-7):639–658, March 2007. ISSN 09670645. doi: 10.1016/j.dsr2.2007.01.004. URL <https://linkinghub.elsevier.com/retrieve/pii/S0967064507000392>.
- Tim DeVries. The Ocean Carbon Cycle. *Annual Review of Environment and Resources*, 47(1):317–341, 2022. doi: 10.1146/annurev-environ-120920-111307. URL <https://doi.org/10.1146/annurev-environ-120920-111307>. _eprint: <https://doi.org/10.1146/annurev-environ-120920-111307>.
- Andrew G Dickson. The carbon dioxide system in seawater: equilibrium chemistry and measurements. *Guide to best practices for ocean acidification research and data reporting*, 1:17–40, 2010.
- Scott C. Doney, Victoria J. Fabry, Richard A. Feely, and Joanie A. Kleypas. Ocean acidification: The other co2 problem. *Annual Review of Marine Science*, 1:169–192, 2009. doi: 10.1146/annurev.marine.010908.163834.
- Carlos M. Duarte, Iñigo J. Losada, Iris E. Hendriks, Inés Mazarrasa, and Núria Marbà. The role of coastal plant communities for climate change mitigation and adaptation. *Nature Climate Change*, 3(11):961–968, 11 2013. ISSN 1758678X. doi: 10.1038/nclimate1970. URL <http://www.nature.com/articles/nclimate1970>.
- Carlos M. Duarte, JeanPierre Gattuso, Kasper Hancke, Hege Gundersen, Karen FilbeeDexter, Morten F. Pedersen, Jack J. Middelburg, MichaeläT. Burrows, Kira A. Krumhansl, Thomas Wernberg, Pippa Moore, Albert Pessarrodona, Sarah B. Ørberg, Isabel S. Pinto, Jorge Assis, AnaãM. Queirós, Dan A. Smale, Trine Bekkby, EsterãA. Serrão, Dorte KrauseJensen, and Richard Field. Global estimates of the extent and production of macroalgal forests. *Global Ecology and Biogeography*, 31(7):1422–1439, July 2022. ISSN 1466-822X, 1466-8238. doi: 10.1111/geb.13515. URL <https://onlinelibrary.wiley.com/doi/10.1111/geb.13515>.
- Hugh W. Ducklow, Deborah K. Steinberg, and Ken O. Buesseler. Upper ocean carbon export and the biological pump. *Oceanography*, 14(SPL.ISS. 4):50–58, 2001. ISSN 10428275. doi: 10.5670/oceanog.2001.06. URL <https://tos.org/oceanography/article/upper-ocean-carbon-export-and-the-biological-pump>.
- Kristofer Döös, Johan Nilsson, Jonas Nycander, Laurent Brodeau, and Maxime Ballarotta. The World Ocean Thermohaline Circulation. *Journal of Physical Oceanography*, 42(9):1445–1460, September 2012.

ISSN 0022-3670, 1520-0485. doi: 10.1175/JPO-D-11-0163.1. URL <https://journals.ametsoc.org/view/journals/phoc/42/9/jpo-d-11-0163.1.xml>. Publisher: American Meteorological Society Section: Journal of Physical Oceanography.

D Ehhalt, M Prather, F Dentener, R Derwent, E Dlugokencky, E Holland, I Isaksen, J Katima, V Kirchhoff, P Matson, et al. Atmospheric chemistry and greenhouse gases, 2001.

P. Falkowski, R. J. Scholes, E. Boyle, J. Canadell, D. Canfield, J. Elser, N. Gruber, K. Hibbard, P. Högberg, S. Linder, F. T. Mackenzie, B. Moore Iii, T. Pedersen, Y. Rosenthal, S. Seitzinger, V. Smetacek, and W. Steffen. The Global Carbon Cycle: A Test of Our Knowledge of Earth as a System. *Science*, 290 (5490):291–296, October 2000. ISSN 0036-8075, 1095-9203. doi: 10.1126/science.290.5490.291. URL <https://www.science.org/doi/10.1126/science.290.5490.291>.

Paul G. Falkowski, Thomas Algeo, Lou Codispoti, Curtis Deutsch, Steven Emerson, Burke Hales, Raymond B. Huey, William J. Jenkins, Lee R. Kump, Lisa A. Levin, Timothy W. Lyons, Norman B. Nelson, Oscar S. Schofield, Roger Summons, Lynne D. Talley, Ellen Thomas, Frank Whitney, and Carl B. Pilcher. Ocean deoxygenation: Past, present, and future. *Eos, Transactions American Geophysical Union*, 92(46):409–410, 2011. ISSN 2324-9250. doi: 10.1029/2011EO460001. URL <https://onlinelibrary.wiley.com/doi/abs/10.1029/2011EO460001>. _eprint: <https://onlinelibrary.wiley.com/doi/pdf/10.1029/2011EO460001>.

FAO. Cultured aquatic species information programme. *laminaria japonica*, 2023. URL https://firms.fao.org/fi/website/FIRRetrieveAction.do?dom=culturespecies&xml=Laminaria_japonica.xml&lang=en. Accessed: 2023-07-11.

Ellias Y. Feng, Yvonne Sawall, Marlene Wall, Mario Lebrato, and Yao Fu. Modeling Coral Bleaching Mitigation Potential of Water Vertical Translocation –An Analogue to Geengineered Artificial Upwelling. *Frontiers in Marine Science*, 7, 2020. ISSN 2296-7745. URL <https://www.frontiersin.org/articles/10.3389/fmars.2020.556192>.

Francois Fernand, Alvaro Israel, Jorunn Skjermo, Thomas Wichard, Klaas R. Timmermans, and Alexander Golberg. Offshore macroalgae biomass for bioenergy production: Environmental aspects, technological achievements and challenges. *Renewable and Sustainable Energy Reviews*, 75(November 2016):35–45, 8 2017a. ISSN 18790690. doi: 10.1016/j.rser.2016.10.046. URL <https://linkinghub.elsevier.com/retrieve/pii/S1364032116307018>.

Francois Fernand, Alvaro Israel, Jorunn Skjermo, Thomas Wichard, Klaas R. Timmermans, and Alexander Golberg. Offshore macroalgae biomass for bioenergy production: Environmental aspects, technological achievements and challenges. *Renewable and Sustainable Energy Reviews*, 75:35–45, August 2017b. ISSN 13640321. doi: 10.1016/j.rser.2016.10.046. URL <https://linkinghub.elsevier.com/retrieve/pii/S1364032116307018>.

Helen S. Findlay, Piero Calosi, and Katharine Crawford. Determinants of the PIC : POC response in the coccolithophore *Emiliania huxleyi* under future ocean acidification scenarios. *Limnology and Oceanography*, 56(3):1168–1178, 2011. ISSN 1939-5590. doi: 10.4319/lo.

- 2011.56.3.1168. URL <https://onlinelibrary.wiley.com/doi/abs/10.4319/lo.2011.56.3.1168>. _eprint: <https://onlinelibrary.wiley.com/doi/pdf/10.4319/lo.2011.56.3.1168>.
- Stephen F. Foley and Tobias P. Fischer. An essential role for continental rifts and lithosphere in the deep carbon cycle. *Nature Geoscience*, 10(12):897–902, December 2017. ISSN 1752-0894, 1752-0908. doi: 10.1038/s41561-017-0002-7. URL <https://www.nature.com/articles/s41561-017-0002-7>.
- Michel Frankignoulle, Christine Canon, and Jean-Pierre Gattuso. Marine calcification as a source of carbon dioxide: Positive feedback of increasing atmospheric CO₂. *Limnology and Oceanography*, 39(2):458–462, 1994. ISSN 1939-5590. doi: 10.4319/lo.1994.39.2.0458. URL <https://onlinelibrary.wiley.com/doi/abs/10.4319/lo.1994.39.2.0458>. _eprint: <https://onlinelibrary.wiley.com/doi/pdf/10.4319/lo.1994.39.2.0458>.
- Mathias Fridahl and Mariliis Lehtveer. Bioenergy with carbon capture and storage (BECCS): Global potential, investment preferences, and deployment barriers. *Energy Research & Social Science*, 42:155–165, August 2018. ISSN 2214-6296. doi: 10.1016/j.erss.2018.03.019. URL <https://www.sciencedirect.com/science/article/pii/S2214629618302998>.
- P. Friedlingstein, M. W. Jones, M. O’Sullivan, R. M. Andrew, D. C. E. Bakker, J. Hauck, C. Le Quéré, G. P. Peters, W. Peters, J. Pongratz, S. Sitch, J. G. Canadell, P. Ciais, R. B. Jackson, S. R. Alin, P. Anthoni, N. R. Bates, M. Becker, N. Bellouin, L. Bopp, T. T. T. Chau, F. Chevallier, L. P. Chini, M. Cronin, K. I. Currie, B. Decharme, L. M. Djeutchouang, X. Dou, W. Evans, R. A. Feely, L. Feng, T. Gasser, D. Gilfillan, T. Gkritzalis, G. Grassi, L. Gregor, N. Gruber, Ö. Gürses, I. Harris, R. A. Houghton, G. C. Hurtt, Y. Iida, T. Ilyina, I. T. Lujckx, A. Jain, S. D. Jones, E. Kato, D. Kennedy, K. Klein Goldewijk, J. Knauer, J. I. Korsbakken, A. Körtzinger, P. Landschützer, S. K. Lauvset, N. Lefèvre, S. Lienert, J. Liu, G. Marland, P. C. McGuire, J. R. Melton, D. R. Munro, J. E. M. S. Nabel, S.-I. Nakaoka, Y. Niwa, T. Ono, D. Pierrot, B. Poulter, G. Rehder, L. Resplandy, E. Robertson, C. Rödenbeck, T. M. Rosan, J. Schwinger, C. Schwingshackl, R. Séférian, A. J. Sutton, C. Sweeney, T. Tanhua, P. P. Tans, H. Tian, B. Tilbrook, F. Tubiello, G. R. van der Werf, N. Vuichard, C. Wada, R. Wanninkhof, A. J. Watson, D. Willis, A. J. Wiltshire, W. Yuan, C. Yue, X. Yue, S. Zaehle, and J. Zeng. Global carbon budget 2021. *Earth Syst. Sci. Data*, 14:1917–2005, 2022a. doi: 10.5194/essd-14-1917-2022.
- Pierre Friedlingstein, Laurent Bopp, Philippe Ciais, Jean-Louis Dufresne, Laurent Fairhead, Hervé Le Treut, Patrick Monfray, and James Orr. Positive feedback between future climate change and the carbon cycle. *Geophysical Research Letters*, 28(8):1543–1546, 2001. ISSN 1944-8007. doi: 10.1029/2000GL012015. URL <https://onlinelibrary.wiley.com/doi/abs/10.1029/2000GL012015>. _eprint: <https://onlinelibrary.wiley.com/doi/pdf/10.1029/2000GL012015>.
- Pierre Friedlingstein, Michael O’Sullivan, Matthew W. Jones, Robbie M. Andrew, Judith Hauck, Are Olsen, Glen P. Peters, Wouter Peters, Julia Pongratz, Stephen Sitch, Corinne Le Quéré, Josep G. Canadell, Philippe Ciais, Robert B. Jackson, Simone Alin, Luiz E. O. C. Aragão, Almut Arneth, Vivek Arora, Nicholas R. Bates, Meike Becker, Alice Benoit-Cattin, Henry C. Bittig, Laurent Bopp, Selma Bultan, Naveen Chandra, Frédéric Chevallier, Louise P. Chini, Wiley Evans, Liesbeth Florentie, Piers M.

Forster, Thomas Gasser, Marion Gehlen, Dennis Gilfillan, Thanos Gkritzalis, Luke Gregor, Nicolas Gruber, Ian Harris, Kerstin Hartung, Vanessa Haverd, Richard A. Houghton, Tatiana Ilyina, Atul K. Jain, Emilie Joetzjer, Koji Kadono, Etsushi Kato, Vassilis Kitidis, Jan Ivar Korsbakken, Peter Landschützer, Nathalie Lefèvre, Andrew Lenton, Sebastian Lienert, Zhu Liu, Danica Lombardozzi, Gregg Marland, Nicolas Metzler, David R. Munro, Julia E. M. S. Nabel, Shin-Ichiro Nakaoka, Yosuke Niwa, Kevin O'Brien, Tsuneo Ono, Paul I. Palmer, Denis Pierrot, Benjamin Poulter, Laure Resplandy, Eddy Robertson, Christian Rödenbeck, Jörg Schwinger, Roland Séférian, Ingunn Skjelvan, Adam J. P. Smith, Adrienne J. Sutton, Toste Tanhua, Pieter P. Tans, Hanqin Tian, Bronte Tilbrook, Guido Van Der Werf, Nicolas Vuichard, Anthony P. Walker, Rik Wanninkhof, Andrew J. Watson, David Willis, Andrew J. Wiltshire, Wenping Yuan, Xu Yue, and Sönke Zaehle. Global Carbon Budget 2020. *Earth System Science Data*, 12(4):3269–3340, December 2020. ISSN 1866-3516. doi: 10.5194/essd-12-3269-2020. URL <https://essd.copernicus.org/articles/12/3269/2020/>.

Pierre Friedlingstein, Michael O'Sullivan, Matthew W. Jones, Robbie M. Andrew, Luke Gregor, Judith Hauck, Corinne Le Quéré, Ingrid T. Luijkx, Are Olsen, Glen P. Peters, Wouter Peters, Julia Pongratz, Clemens Schwingshackl, Stephen Sitch, Josep G. Canadell, Philippe Ciais, Robert B. Jackson, Simone R. Alin, Ramdane Alkama, Almut Arneth, Vivek K. Arora, Nicholas R. Bates, Meike Becker, Nicolas Bellouin, Henry C. Bittig, Laurent Bopp, Frédéric Chevallier, Louise P. Chini, Margot Cronin, Wiley Evans, Stefanie Falk, Richard A. Feely, Thomas Gasser, Marion Gehlen, Thanos Gkritzalis, Lucas Gloege, Giacomo Grassi, Nicolas Gruber, Özgür Gürses, Ian Harris, Matthew Hefner, Richard A. Houghton, George C. Hurtt, Yosuke Iida, Tatiana Ilyina, Atul K. Jain, Annika Jersild, Koji Kadono, Etsushi Kato, Daniel Kennedy, Kees Klein Goldeewijk, Jürgen Knauer, Jan Ivar Korsbakken, Peter Landschützer, Nathalie Lefèvre, Keith Lindsay, Junjie Liu, Zhu Liu, Gregg Marland, Nicolas Mayot, Matthew J. McGrath, Nicolas Metzler, Natalie M. Monacci, David R. Munro, Shin-Ichiro Nakaoka, Yosuke Niwa, Kevin O'Brien, Tsuneo Ono, Paul I. Palmer, Naiqing Pan, Denis Pierrot, Katie Pocock, Benjamin Poulter, Laure Resplandy, Eddy Robertson, Christian Rödenbeck, Carmen Rodriguez, Thais M. Rosan, Jörg Schwinger, Roland Séférian, Jamie D. Shutler, Ingunn Skjelvan, Tobias Steinhoff, Qing Sun, Adrienne J. Sutton, Colm Sweeney, Shintaro Takao, Toste Tanhua, Pieter P. Tans, Xiangjun Tian, Hanqin Tian, Bronte Tilbrook, Hiroyuki Tsujino, Francesco Tubiello, Guido R. Van Der Werf, Anthony P. Walker, Rik Wanninkhof, Chris Whitehead, Anna Willstrand Wranne, Rebecca Wright, Wenping Yuan, Chao Yue, Xu Yue, Sönke Zaehle, Jiye Zeng, and Bo Zheng. Global Carbon Budget 2022. *Earth System Science Data*, 14(11):4811–4900, November 2022b. ISSN 1866-3516. doi: 10.5194/essd-14-4811-2022. URL <https://essd.copernicus.org/articles/14/4811/2022/>.

Sabine Fuss, Josep G. Canadell, Philippe Ciais, Robert B. Jackson, Chris D. Jones, Anders Lyngfelt, Glen P. Peters, and Detlef P. Van Vuuren. Moving toward Net-Zero Emissions Requires New Alliances for Carbon Dioxide Removal. *One Earth*, 3(2):145–149, 8 2020. ISSN 25903322. doi: 10.1016/j.oneear.2020.08.002. URL <https://doi.org/10.1016/j.oneear.2020.08.002><https://linkinghub.elsevier.com/retrieve/pii/S2590332220303651>.

Kunshan Gao and Kelton R. McKinley. Use of macroalgae for marine biomass production and CO₂ remediation: a review. *Journal of Applied Phycology*, 6(1):45–60, 2 1994. ISSN 09218971. doi: 10.1007/BF02185904. URL <http://link.springer.com/10.1007/BF02185904>.

- Jean-Pierre Gattuso, Alexandre Magnan, Romain Billé, William W. L. Cheung, Ella L. Howes, Fortunat Joos, ..., and Carol Turley. Contrasting futures for ocean and society from different anthropogenic CO₂ emissions scenarios. *Science*, 349(6243):aac4722, 2015. doi: 10.1126/science.aac4722.
- Jean-Pierre Gattuso, Alexandre K Magnan, Laurent Bopp, William W. L. Cheung, Carlos M. Duarte, Jochen Hinkel, Elizabeth Mcleod, Fiorenza Micheli, Andreas Oschlies, Phillip Williamson, et al. Ocean solutions to address climate change and its effects on marine ecosystems. *Frontiers in Marine Science*, 5:337, 2018.
- Jean-Pierre Gattuso, Phillip Williamson, Carlos M. Duarte, and Alexandre K. Magnan. The Potential for Ocean-Based Climate Action: Negative Emissions Technologies and Beyond. *Frontiers in Climate*, 2: 575716, January 2021. ISSN 2624-9553. doi: 10.3389/fclim.2020.575716. URL <https://www.frontiersin.org/articles/10.3389/fclim.2020.575716/full>.
- Daniel S Goll, Philippe Ciais, Thorben Amann, Wolfgang Buermann, Jinfeng Chang, Sibel Eker, Jens Hartmann, Ivan Janssens, Wei Li, Michael Obersteiner, et al. Potential co₂ removal from enhanced weathering by ecosystem responses to powdered rock. *Nature Geoscience*, 14(8):545–549, 2021.
- Bronson W Griscom, Justin Adams, Peter W Ellis, Richard A Houghton, Guy Lomax, Daniela A Miteva, William H Schlesinger, David Shoch, Juha V Siikamäki, Pete Smith, et al. Natural climate solutions. *Proceedings of the National Academy of Sciences*, 114(44):11645–11650, 2017. doi: 10.1073/pnas.1710465114.
- Anke Günther, Alexandra Barthelmes, Vytas Huth, Hans Joosten, Gerald Jurasinski, Franziska Koebisch, and John Couwenberg. Prompt rewetting of drained peatlands reduces climate warming despite methane emissions. *Nature Communications*, 11(1):1644, April 2020. ISSN 2041-1723. doi: 10.1038/s41467-020-15499-z. URL <https://www.nature.com/articles/s41467-020-15499-z>.
- Dennis Hansell, Craig Carlson, Daniel Repeta, and Reiner Schlitzer. Dissolved Organic Matter in the Ocean: A Controversy Stimulates New Insights. *Oceanography*, 22(4):202–211, December 2009. ISSN 10428275. doi: 10.5670/oceanog.2009.109. URL <https://tos.org/oceanography/article/dissolved-organic-matter-in-the-ocean-a-controversy-stimulates-new-insights>.
- Dennis A. Hansell. Recalcitrant Dissolved Organic Carbon Fractions. *Annual Review of Marine Science*, 5(1):421–445, 2013. doi: 10.1146/annurev-marine-120710-100757. URL <https://doi.org/10.1146/annurev-marine-120710-100757>. [_eprint: https://doi.org/10.1146/annurev-marine-120710-100757](https://doi.org/10.1146/annurev-marine-120710-100757).
- S. V. Hanssen, V. Daioglou, Z. J. N. Steinmann, J. C. Doelman, D. P. Van Vuuren, and M. A. J. Huijbregts. The climate change mitigation potential of bioenergy with carbon capture and storage. *Nature Climate Change*, 10(11):1023–1029, November 2020. ISSN 1758-678X, 1758-6798. doi: 10.1038/s41558-020-0885-y. URL <https://www.nature.com/articles/s41558-020-0885-y>.
- Manoj Hari and Bhishma Tyagi. Terrestrial carbon cycle: tipping edge of climate change between the atmosphere and biosphere ecosystems. *Environmental Science: Atmospheres*, 2(5):867–890, 2022. doi: 10.1039/D1EA00102G. URL <https://pubs.rsc.org/en/content/articlelanding/2022/ea/d1ea00102g>. Publisher: Royal Society of Chemistry.

- Daniel P Harrison. Global negative emissions capacity of ocean macronutrient fertilization. *Environmental Research Letters*, 12(3):035001, March 2017. ISSN 1748-9326. doi: 10.1088/1748-9326/aa5ef5. URL <https://iopscience.iop.org/article/10.1088/1748-9326/aa5ef5>.
- Peter M. Haugan and Helge Drange. Sequestration of CO₂ in the deep ocean by shallow injection. *Nature*, 357(6376):318–320, May 1992. ISSN 1476-4687. doi: 10.1038/357318a0. URL <https://www.nature.com/articles/357318a0>. Number: 6376 Publisher: Nature Publishing Group.
- C. Heinze, S. Meyer, N. Goris, L. Anderson, R. Steinfeldt, N. Chang, C. Le Quéré, and D. C. E. Bakker. The ocean carbon sink –impacts, vulnerabilities and challenges. *Earth System Dynamics*, 6(1):327–358, June 2015. ISSN 2190-4987. doi: 10.5194/esd-6-327-2015. URL <https://esd.copernicus.org/articles/6/327/2015/>.
- Isaac M. Held and Brian J. Soden. Water vapor feedback and global warming. *Annual Review of Energy and the Environment*, 25:441–475, 2000. doi: 10.1146/annurev.energy.25.1.441.
- Cameron Hepburn, Ella Adlen, John Beddington, Emily A. Carter, Sabine Fuss, Niall Mac Dowell, Jan C. Minx, Pete Smith, and Charlotte K. Williams. The technological and economic prospects for CO₂ utilization and removal. *Nature*, 575(7781):87–97, November 2019. ISSN 0028-0836, 1476-4687. doi: 10.1038/s41586-019-1681-6. URL <https://www.nature.com/articles/s41586-019-1681-6>.
- Matthias Hofmann and Hans-Joachim Schellnhuber. Oceanic acidification affects marine carbon pump and triggers extended marine oxygen holes. *Proceedings of the National Academy of Sciences*, 106(9):3017–3022, March 2009. ISSN 0027-8424, 1091-6490. doi: 10.1073/pnas.0813384106. URL <https://pnas.org/doi/full/10.1073/pnas.0813384106>.
- Tatiana Ilyina, Dieter Wolf-Gladrow, Guy Munhoven, and Christoph Heinze. Assessing the potential of calcium-based artificial ocean alkalization to mitigate rising atmospheric CO₂ and ocean acidification. *Geophysical Research Letters*, 40(22):5909–5914, 2013. ISSN 00948276. doi: 10.1002/2013GL057981.
- IPCC. Climate change 2014: Synthesis report. Technical report, Intergovernmental Panel on Climate Change, 2014. URL https://www.ipcc.ch/site/assets/uploads/2018/05/SYR_AR5_FINAL_full_wcover.pdf.
- IPCC. *Global Warming of 1.5°C: An IPCC Special Report on the impacts of global warming of 1.5°C above pre-industrial levels and related global greenhouse gas emission pathways, in the context of strengthening the global response to the threat of climate change, sustainable development, and efforts to eradicate poverty*. World Meteorological Organization, Geneva, Switzerland, 2018. ISBN 978-92-9169-151-7. URL <https://www.ipcc.ch/sr15/>.
- IPCC. *Climate Change and Land: an IPCC special report on climate change, desertification, land degradation, sustainable land management, food security, and greenhouse gas fluxes in terrestrial ecosystems* [Shukla, P.R. and Skea, J. and Calvo Buendia, E. and Masson-Delmotte, V. and Pörtner, H.-O. and Roberts, D. C. and Zhai, P. and Slade, R. and Connors, S. and van Diemen, R. and Ferrat, M. and Haughey, E. and Luz, S. and Neogi, S. and Pathak, M. and Petzold, J. and Portugal Pereira, J. and Vyas, P. and Huntley, E. and Kissick, K. and Belkacemi, M. and Malley, J.J.]. IPCC, 2019. In press.

- IPCC. Summary for policymakers. In H. O. Pörtner, D. C. Roberts, M. Tignor, E. S. Poloczanska, K. Mintenbeck, A. Alegría, M. Craig, S. Langsdorf, S. Löschke, V. Möller, A. Okem, and B. Rama, editors, *Climate Change 2022: Impacts, Adaptation and Vulnerability. Contribution of Working Group II to the Sixth Assessment Report of the Intergovernmental Panel on Climate Change*. Cambridge University Press, Cambridge, UK and New York, NY, USA, 2022. doi: 10.1017/9781009325844.001. URL https://www.ipcc.ch/report/ar6/wg2/downloads/report/IPCC_AR6_WGII_SummaryForPolicymakers.pdf.
- I. A. Janssens, W. Dieleman, S. Luyssaert, J.-A. Subke, M. Reichstein, R. Ceulemans, P. Ciais, A. J. Dolman, J. Grace, G. Matteucci, D. Papale, S. L. Piao, E.-D. Schulze, J. Tang, and B. E. Law. Reduction of forest soil respiration in response to nitrogen deposition. *Nature Geoscience*, 3(5):315–322, May 2010. ISSN 1752-0908. doi: 10.1038/ngeo844. URL <https://www.nature.com/articles/ngeo844>. Number: 5 Publisher: Nature Publishing Group.
- Li-Qing Jiang, Brendan R. Carter, Richard A. Feely, Siv K. Lauvset, and Are Olsen. Surface ocean pH and buffer capacity: past, present and future. *Scientific Reports*, 9(1):18624, December 2019. ISSN 2045-2322. doi: 10.1038/s41598-019-55039-4. URL <https://www.nature.com/articles/s41598-019-55039-4>. Number: 1 Publisher: Nature Publishing Group.
- Zhibing Jiang, Jingjing Liu, Shanglu Li, Yue Chen, Ping Du, Yuanli Zhu, Yibo Liao, Quanzhen Chen, Lu Shou, Xiaojun Yan, Jiangning Zeng, and Jianfang Chen. Kelp cultivation effectively improves water quality and regulates phytoplankton community in a turbid, highly eutrophic bay. *Science of The Total Environment*, 707:135561, March 2020. ISSN 00489697. doi: 10.1016/j.scitotenv.2019.135561. URL <https://linkinghub.elsevier.com/retrieve/pii/S0048969719355561>.
- Nianzhi Jiao, Gerhard J. Herndl, Dennis A. Hansell, Ronald Benner, Gerhard Kattner, Steven W. Wilhelm, David L. Kirchman, Markus G. Weinbauer, Tingwei Luo, Feng Chen, and Farooq Azam. Microbial production of recalcitrant dissolved organic matter: long-term carbon storage in the global ocean. *Nature Reviews Microbiology*, 8(8):593–599, August 2010. ISSN 1740-1526, 1740-1534. doi: 10.1038/nrmicro2386. URL <http://www.nature.com/articles/nrmicro2386>.
- Fortunat Joos, I. Colin Prentice, Stephen Sitch, Robert Meyer, Georg Hooss, Gian-Kasper Plattner, Stefan Gerber, and Klaus Hasselmann. Global warming feedbacks on terrestrial carbon uptake under the Intergovernmental Panel on Climate Change (IPCC) Emission Scenarios. *Global Biogeochemical Cycles*, 15(4):891–907, 2001. ISSN 1944-9224. doi: 10.1029/2000GB001375. URL <https://onlinelibrary.wiley.com/doi/abs/10.1029/2000GB001375>. _eprint: <https://onlinelibrary.wiley.com/doi/pdf/10.1029/2000GB001375>.
- Kyung A Jung, Seong-Rin Lim, Yoori Kim, and Jong Moon Park. Potentials of macroalgae as feedstocks for biorefinery. *Bioresource Technology*, 135:182–190, May 2013. ISSN 09608524. doi: 10.1016/j.biortech.2012.10.025. URL <https://linkinghub.elsevier.com/retrieve/pii/S0960852412015271>.
- M. Jürchott, A. Oschlies, and W. Koeve. Artificial Upwelling—A Refined Narrative. *Geophysical Research Letters*, 50(4), February 2023. ISSN 0094-8276, 1944-8007. doi: 10.1029/2022GL101870. URL <https://onlinelibrary.wiley.com/doi/10.1029/2022GL101870>.

- Charles David Keeling. The concentration and distribution of carbon dioxide in the atmosphere. *Journal of Geophysical Research*, 63(4):346–351, 1958.
- Ralph F. Keeling, Arne Körtzinger, and Nicolas Gruber. Ocean Deoxygenation in a Warming World. *Annual Review of Marine Science*, 2(1):199–229, January 2010. ISSN 1941-1405, 1941-0611. doi: 10.1146/annurev.marine.010908.163855. URL <https://www.annualreviews.org/doi/10.1146/annurev.marine.010908.163855>.
- T.F. Keenan and C.A. Williams. The Terrestrial Carbon Sink. *Annual Review of Environment and Resources*, 43(1):219–243, October 2018. ISSN 1543-5938, 1545-2050. doi: 10.1146/annurev-environ-102017-030204. URL <https://www.annualreviews.org/doi/10.1146/annurev-environ-102017-030204>.
- David W. Keith, Geoffrey Holmes, David St Angelo, and Kenton Heidel. A Process for Capturing CO₂ from the Atmosphere. *Joule*, 2(8):1573–1594, August 2018. ISSN 2542-4785, 2542-4351. doi: 10.1016/j.joule.2018.05.006. URL [https://www.cell.com/joule/abstract/S2542-4351\(18\)30225-3](https://www.cell.com/joule/abstract/S2542-4351(18)30225-3). Publisher: Elsevier.
- D. P. Keller, A. Oschlies, and M. Eby. A new marine ecosystem model for the University of Victoria Earth System Climate Model. *Geoscientific Model Development*, 5(5):1195–1220, September 2012. ISSN 1991-9603. doi: 10.5194/gmd-5-1195-2012. URL <https://gmd.copernicus.org/articles/5/1195/2012/>.
- David P. Keller, Ellias Y. Feng, and Andreas Oschlies. Potential climate engineering effectiveness and side effects during a high carbon dioxide-emission scenario. *Nature Communications*, 5(1):3304, 5 2014a. ISSN 20411723. doi: 10.1038/ncomms4304. URL <http://dx.doi.org/10.1038/ncomms4304><http://www.nature.com/articles/ncomms4304>.
- David P. Keller, Ellias Y. Feng, and Andreas Oschlies. Potential climate engineering effectiveness and side effects during a high carbon dioxide-emission scenario. *Nature Communications*, 5(1):3304, February 2014b. ISSN 2041-1723. doi: 10.1038/ncomms4304. URL <https://www.nature.com/articles/ncomms4304>.
- David P. Keller, Andrew Lenton, Vivian Scott, Naomi E. Vaughan, Nico Bauer, Duoying Ji, Chris D. Jones, Ben Kravitz, Helene Muri, and Kirsten Zickfeld. The Carbon Dioxide Removal Model Intercomparison Project (CDRMIP): rationale and experimental protocol for CMIP6. *Geoscientific Model Development*, 11(3):1133–1160, March 2018. ISSN 1991-9603. doi: 10.5194/gmd-11-1133-2018. URL <https://gmd.copernicus.org/articles/11/1133/2018/>.
- David P. Keller, Kerryn Brent, Lennart T. Bach, and Wilfried Rickels. Editorial: The Role of Ocean-Based Negative Emission Technologies for Climate Mitigation. *Frontiers in Climate*, 3:743816, August 2021. ISSN 2624-9553. doi: 10.3389/fclim.2021.743816. URL <https://www.frontiersin.org/articles/10.3389/fclim.2021.743816/full>.
- Haroon S. Kheshgi. Sequestering atmospheric carbon dioxide by increasing ocean alkalinity. *Energy*, 20(9): 915–922, 1995. ISSN 03605442. doi: 10.1016/0360-5442(95)00035-F.

- Jang K. Kim, Charles Yarish, Eun Kyoung Hwang, Miseon Park, and Youngdae Kim. Seaweed aquaculture: cultivation technologies, challenges and its ecosystem services. *ALGAE*, 32(1):1–13, March 2017. ISSN 1226-2617, 2093-0860. doi: 10.4490/algae.2017.32.3.3. URL <http://www.e-algae.org/journal/view.php?doi=10.4490/algae.2017.32.3.3>.
- Jang K. Kim, George Kraemer, and Charles Yarish. Evaluation of the metal content of farm grown *Gracilaria tikvahiae* and *Saccharina latissima* from Long Island Sound and New York Estuaries. *Algal Research*, 40: 101484, June 2019. ISSN 22119264. doi: 10.1016/j.algal.2019.101484. URL <https://linkinghub.elsevier.com/retrieve/pii/S2211926419300554>.
- Christine Klaas and David E. Archer. Association of sinking organic matter with various types of mineral ballast in the deep sea: Implications for the rain ratio: OCEAN CARBON-MINERAL FLUX ASSOCIATION. *Global Biogeochemical Cycles*, 16(4):63–1–63–14, December 2002. ISSN 08866236. doi: 10.1029/2001GB001765. URL <http://doi.wiley.com/10.1029/2001GB001765>.
- Peter Köhler, Jens Hartmann, and Dieter A. Wolf-Gladrow. Geoengineering potential of artificially enhanced silicate weathering of olivine. *Proceedings of the National Academy of Sciences*, 107(47):20228–20233, 11 2010. ISSN 0027-8424. doi: 10.1073/pnas.1000545107. URL <http://www.pnas.org/cgi/doi/10.1073/pnas.1000545107https://pnas.org/doi/full/10.1073/pnas.1000545107>.
- Dorte Krause-Jensen and Carlos M. Duarte. Substantial role of macroalgae in marine carbon sequestration. *Nature Geoscience*, 9(10):737–742, 2016. ISSN 17520908. doi: 10.1038/ngeo2790. URL <http://dx.doi.org/10.1038/ngeo2790>.
- Amrit Kumar, David G. Madden, Matteo Lusi, Kai-Jie Chen, Emma A. Daniels, Teresa Curtin, John J. Perry IV, and Michael J. Zaworotko. Direct air capture of co2 by physisorbent materials. *Angewandte Chemie International Edition*, 54(48):14372–14377, 2015. doi: <https://doi.org/10.1002/anie.201506952>. URL <https://onlinelibrary.wiley.com/doi/abs/10.1002/anie.201506952>.
- Lee R. Kump, Susan L. Brantley, and Michael A. Arthur. Chemical Weathering, Atmospheric CO₂, and Climate. *Annual Review of Earth and Planetary Sciences*, 28(1):611–667, May 2000. ISSN 0084-6597, 1545-4495. doi: 10.1146/annurev.earth.28.1.611. URL <https://www.annualreviews.org/doi/10.1146/annurev.earth.28.1.611>.
- Rattan Lal. Soil carbon sequestration impacts on global climate change and food security. *Science*, 304 (5677):1623–1627, 2004.
- John Latham, Keith Bower, Tom Choullarton, Hugh Coe, Paul Connolly, Gary Cooper, Tim Craft, Jack Foster, Alan Gadian, Lee Galbraith, Hector Iacovides, David Johnston, Brian Launder, Brian Leslie, John Meyer, Armand Neukermans, Bob Ormond, Ben Parkes, Phillip Rasch, John Rush, Stephen Salter, Tom Stevenson, Hailong Wang, Qin Wang, and Rob Wood. Marine cloud brightening. *Philosophical Transactions of the Royal Society A: Mathematical, Physical and Engineering Sciences*, 370(1974):4217–4262, 2012. doi: 10.1098/rsta.2012.0086. URL <https://royalsocietypublishing.org/doi/abs/10.1098/rsta.2012.0086>.

Louis Legendre, Richard B. Rivkin, Markus G. Weinbauer, Lionel Guidi, and Julia Uitz. The microbial carbon pump concept: Potential biogeochemical significance in the globally changing ocean. *Progress in Oceanography*, 134:432–450, May 2015. ISSN 0079-6611. doi: 10.1016/j.pocean.2015.01.008. URL <https://www.sciencedirect.com/science/article/pii/S0079661115000105>.

Johannes Lehmann, Annette Cowie, Caroline A. Masiello, Claudia Kammann, Dominic Woolf, James E. Amonette, Maria L. Cayuela, Marta Camps-Arbestain, and Thea Whitman. Biochar in climate change mitigation. *Nature Geoscience*, 14(12):883–892, December 2021. ISSN 1752-0908. doi: 10.1038/s41561-021-00852-8. URL <https://www.nature.com/articles/s41561-021-00852-8>. Number: 12 Publisher: Nature Publishing Group.

Andrew Lenton, Richard J. Matear, David P. Keller, Vivian Scott, and Naomi E. Vaughan. Assessing carbon dioxide removal through global and regional ocean alkalization under high and low emission pathways. *Earth System Dynamics*, 9(2):339–357, 2018a. ISSN 21904987. doi: 10.5194/esd-9-339-2018.

Andrew Lenton, Richard J. Matear, David P. Keller, Vivian Scott, and Naomi E. Vaughan. Assessing carbon dioxide removal through global and regional ocean alkalization under high and low emission pathways. *Earth System Dynamics*, 9(2):339–357, April 2018b. ISSN 2190-4987. doi: 10.5194/esd-9-339-2018. URL <https://esd.copernicus.org/articles/9/339/2018/>.

Timothy M Lenton. The potential for land-based biological CO₂ removal to lower future atmospheric CO₂ concentration. *Carbon Management*, 1(1):145–160, October 2010. ISSN 1758-3004, 1758-3012. doi: 10.4155/cmt.10.12. URL <http://www.tandfonline.com/doi/abs/10.4155/cmt.10.12>.

Sydney Levitus, John I. Antonov, Timothy P. Boyer, and Cathy Stephens. Warming of the World Ocean. *Science*, 287(5461):2225–2229, March 2000. doi: 10.1126/science.287.5461.2225. URL <https://www.science.org/doi/full/10.1126/science.287.5461.2225>. Publisher: American Association for the Advancement of Science.

Min Luo, Joris Gieskes, Linying Chen, Jan Scholten, Binbin Pan, Gang Lin, and Duofu Chen. Sources, Degradation, and Transport of Organic Matter in the New Britain Shelf-Trench Continuum, Papua New Guinea. *Journal of Geophysical Research: Biogeosciences*, 124(6):1680–1695, 2019. ISSN 21698961. doi: 10.1029/2018JG004691. URL <https://onlinelibrary.wiley.com/doi/abs/10.1029/2018JG004691>.

Yiqi Luo. Terrestrial Carbon–Cycle Feedback to Climate Warming. *Annual Review of Ecology, Evolution, and Systematics*, 38(1):683–712, 2007. doi: 10.1146/annurev.ecolsys.38.091206.095808. URL <https://doi.org/10.1146/annurev.ecolsys.38.091206.095808>. [_eprint: https://doi.org/10.1146/annurev.ecolsys.38.091206.095808](https://doi.org/10.1146/annurev.ecolsys.38.091206.095808).

Fred T Mackenzie and Abraham Lerman. *Carbon in the Geobiosphere:-Earth’s Outer Shell*, volume 25. Springer Science & Business Media, 2006.

Peter I. Macreadie, Andrea Anton, John A. Raven, Nicola Beaumont, Rod M. Connolly, Daniel A. Friess, Jeffrey J. Kelleway, Hilary Kennedy, Tomohiro Kuwae, Paul S. Lavery, Catherine E. Lovelock, Dan A.

- Smale, Eugenia T. Apostolaki, Trisha B. Atwood, Jeff Baldock, Thomas S. Bianchi, Gail L. Chmura, Bradley D. Eyre, James W. Fourqurean, Jason M. Hall-Spencer, Mark Huxham, Iris E. Hendriks, Dorte Krause-Jensen, Dan Laffoley, Tiziana Luisetti, Núria Marbà, Pere Masque, Karen J. McGlathery, J. Patrick Megonigal, Daniel Murdiyarso, Bayden D. Russell, Rui Santos, Oscar Serrano, Brian R. Silliman, Kenta Watanabe, and Carlos M. Duarte. The future of Blue Carbon science. *Nature Communications*, 10(1):3998, 9 2019. ISSN 20411723. doi: 10.1038/s41467-019-11693-w. URL <https://www.nature.com/articles/s41467-019-11693-w>.
- Peter I. Macreadie, Micheli D.P. Costa, Trisha B. Atwood, Daniel A. Friess, Jeffrey J. Kelleway, Hilary Kennedy, Catherine E. Lovelock, Oscar Serrano, and Carlos M. Duarte. Blue carbon as a natural climate solution. *Nature Reviews Earth and Environment*, 2(12):826–839, 11 2021. ISSN 2662138X. doi: 10.1038/s43017-021-00224-1. URL <https://www.nature.com/articles/s43017-021-00224-1>.
- Margarida R. G. Maia, António J. M. Fonseca, Paulo P. Cortez, and Ana R. J. Cabrita. In vitro evaluation of macroalgae as unconventional ingredients in ruminant animal feeds. *Algal Research*, 40:101481, June 2019. ISSN 2211-9264. doi: 10.1016/j.algal.2019.101481. URL <https://www.sciencedirect.com/science/article/pii/S2211926418309822>.
- Ernst Maier-Reimer, Uwe Mikolajewicz, and Arne Winguth. Future ocean uptake of co₂: interaction between ocean circulation and biology. *Climate Dynamics*, 12:711–722, 1996.
- Cesare Marchetti. On geoengineering and the co₂ problem. *Climatic change*, 1(1):59–68, 1977.
- H. Damon Matthews, Nathan P. Gillett, Peter A. Stott, and Kirsten Zickfeld. The proportionality of global warming to cumulative carbon emissions. *Nature*, 459(7248):829–832, June 2009. ISSN 0028-0836, 1476-4687. doi: 10.1038/nature08047. URL <http://www.nature.com/articles/nature08047>.
- Elizabeth McLeod, Gail L. Chmura, Steven Bouillon, Rodney Salm, Mats Björk, Carlos M. Duarte, Catherine E. Lovelock, William H. Schlesinger, and Brian R. Silliman. A blueprint for blue carbon: Toward an improved understanding of the role of vegetated coastal habitats in sequestering CO₂. *Frontiers in Ecology and the Environment*, 9(10):552–560, 2011. ISSN 15409295. doi: 10.1890/110004.
- Figen Mekik, Paul Loubere, and Mathieu Richaud. Rain ratio variation in the Tropical Ocean: Tests with surface sediments in the eastern equatorial Pacific. *Deep Sea Research Part II: Topical Studies in Oceanography*, 54(5-7):706–721, March 2007. ISSN 09670645. doi: 10.1016/j.dsr2.2007.01.010. URL <https://linkinghub.elsevier.com/retrieve/pii/S0967064507000434>.
- N. Mengis, T. Martin, D. P. Keller, and A. Oschlies. Assessing climate impacts and risks of ocean albedo modification in the Arctic. *Journal of Geophysical Research: Oceans*, 121(5):3044–3057, 2016. ISSN 21699291. doi: 10.1002/2015JC011433.
- Surabi Menon, Kenneth L. Denman, Guy Brasseur, Amnat Chidthaisong, Philippe Ciais, Peter M. Cox, Robert E. Dickinson, Didier Hauglustaine, Christoph Heinze, Elisabeth Holland, Daniel Jacob, Ulrike Lohmann, Srikanthan Ramachandran, Steven C. Wofsy, and Xiaoye Zhang. Couplings between changes

- in the climate system and biogeochemistry. Technical Report LBNL-464E, Lawrence Berkeley National Lab. (LBNL), Berkeley, CA (United States), October 2007. URL <https://www.osti.gov/biblio/934721>.
- G. Myhre, D. Shindell, F.-M. Bréon, W. Collins, J. Fuglestvedt, J. Huang, D. Koch, J.-F. Lamarque, D. Lee, B. Mendoza, T. Nakajima, A. Robock, G. Stephens, T. Takemura, and H. Zhang. *Anthropogenic and natural radiative forcing*, pages 659–740. Cambridge University Press, Cambridge, UK, 2013. doi: 10.1017/CBO9781107415324.018.
- National Academies of Sciences, Engineering, and Medicine. *A Research Strategy for Ocean-based Carbon Dioxide Removal and Sequestration*. National Academies Press, Washington, D.C., April 2022. ISBN 978-0-309-08761-2. doi: 10.17226/26278. URL <https://www.nap.edu/catalog/26278>. Pages: 26278.
- National Aeronautics and Space Administration. Water vapor confirmed as major player in climate change, 2008. URL https://www.nasa.gov/topics/earth/features/vapor_warming.html. Accessed: 2023-04-05.
- National Aeronautics and Space Administration. The greenhouse effect, 2023. URL <https://climate.nasa.gov/resources/global-warming-vs-climate-change/>. Accessed: 2023-04-05.
- Ignacio A. Navarrete, Diane Y. Kim, Cindy Wilcox, Daniel C. Reed, David W. Ginsburg, Jessica M. Dutton, John Heidelberg, Yubin Raut, and Brian Howard Wilcox. Effects of depth-cycling on nutrient uptake and biomass production in the giant kelp *Macrocystis pyrifera*. *Renewable and Sustainable Energy Reviews*, 141:110747, May 2021. ISSN 13640321. doi: 10.1016/j.rser.2021.110747. URL <https://linkinghub.elsevier.com/retrieve/pii/S1364032121000423>.
- Loïc Nazaries, J. Colin Murrell, Pete Millard, Liz Baggs, and Brajesh K. Singh. Methane, microbes and models: fundamental understanding of the soil methane cycle for future predictions. *Environmental Microbiology*, 15(9):2395–2417, 2013. ISSN 1462-2920. doi: 10.1111/1462-2920.12149. URL <https://onlinelibrary.wiley.com/doi/abs/10.1111/1462-2920.12149>. _eprint: <https://onlinelibrary.wiley.com/doi/pdf/10.1111/1462-2920.12149>.
- C Nellemann, E Corcoran, C M Duarte, L Valdes, C De Young, L Fonseca, and G Grimsditch. *Blue carbon: A Rapid Response Assessment*. UNEP/Earthprint, 2009. ISBN 9788277010601. URL http://www.grida.no/files/publications/blue-carbon/BlueCarbon_screen.pdf.
- Michael Nowicki, Tim DeVries, and David A. Siegel. Quantifying the Carbon Export and Sequestration Pathways of the Ocean’s Biological Carbon Pump. *Global Biogeochemical Cycles*, 36(3):e2021GB007083, 2022. ISSN 1944-9224. doi: 10.1029/2021GB007083. URL <https://onlinelibrary.wiley.com/doi/abs/10.1029/2021GB007083>. _eprint: <https://onlinelibrary.wiley.com/doi/pdf/10.1029/2021GB007083>.
- Beth N. Orcutt, Isabelle Daniel, and Rajdeep Dasgupta, editors. *Deep Carbon: Past to Present*. Cambridge University Press, 1 edition, October 2019. ISBN 978-1-108-67795-0 978-1-108-47749-9 978-1-108-73360-1. doi: 10.1017/9781108677950. URL <https://www.cambridge.org/core/product/identifier/9781108677950/type/book>.

- James C Orr, Olivier Aumont, Andrew Yool, KASPER Plattner, Fortunat Joos, Ernst Maier-Reimer, M-F Weirig, Reiner Schlitzer, Ken Caldeira, MICHAEL Wickett, et al. Ocean CO₂ sequestration efficiency from 3-d ocean model comparison. In *Greenhouse Gas Control Technologies*, edited by D. Williams, B. Durie, P. McMullan, C. Paulson, and A. Smith, CSIRO, pages 469–474. 2001.
- James C. Orr, Victoria J. Fabry, Olivier Aumont, Laurent Bopp, Scott C. Doney, Richard A. Feely, ..., and Andrew Yool. Anthropogenic ocean acidification over the twenty-first century and its impact on calcifying organisms. *Nature*, 437(7059):681–686, 2005. doi: 10.1038/nature04095.
- A. Oschlies, W. Koeve, W. Rickels, and K. Rehdanz. Side effects and accounting aspects of hypothetical large-scale Southern Ocean iron fertilization. *Biogeosciences*, 7(12):4017–4035, December 2010a. ISSN 1726-4189. doi: 10.5194/bg-7-4017-2010. URL <https://bg.copernicus.org/articles/7/4017/2010/>.
- A. Oschlies, M. Pahlow, A. Yool, and R. J. Matear. Climate engineering by artificial ocean upwelling: Channelling the sorcerer’s apprentice. *Geophysical Research Letters*, 37(4):1–5, 2 2010b. ISSN 00948276. doi: 10.1029/2009GL041961. URL <http://doi.wiley.com/10.1029/2009GL041961>.
- A. Oschlies, M. Pahlow, A. Yool, and R. J. Matear. Climate engineering by artificial ocean upwelling: Channelling the sorcerer’s apprentice: OCEAN PIPE IMPACTS. *Geophysical Research Letters*, 37(4), February 2010c. ISSN 00948276. doi: 10.1029/2009GL041961. URL <http://doi.wiley.com/10.1029/2009GL041961>.
- Andreas Oschlies, Peter Brandt, Lothar Stramma, and Sunke Schmidt. Drivers and mechanisms of ocean deoxygenation. *Nature Geoscience*, 11(7):467–473, July 2018. ISSN 1752-0894, 1752-0908. doi: 10.1038/s41561-018-0152-2. URL <http://www.nature.com/articles/s41561-018-0152-2>.
- Uta Passow and Craig A. Carlson. The biological pump in a high CO world. *Marine Ecology Progress Series*, 470:249–272, 2012. ISSN 0171-8630. URL <https://www.jstor.org/stable/24876215>. Publisher: Inter-Research Science Center.
- M. Pathak, R. Slade, P.R. Shukla, J. Skea, R. Pichs-Madruga, and D. Ürge-Vorsatz. Technical Summary. In P.R. Shukla, J. Skea, R. Slade, A. Al Khourdajie, R. van Diemen, D. McCollum, M. Pathak, S. Some, P. Vyas, R. Fradera, M. Belkacemi, A. Hasija, G. Lisboa, S. Luz, and J. Malley, editors, *Climate Change 2022: Mitigation of Climate Change. Contribution of Working Group III to the Sixth Assessment Report of the Intergovernmental Panel on Climate Change*. Cambridge University Press, Cambridge, UK and New York, NY, USA, 2022. doi: 10.1017/9781009157926.002.
- Donald E. Penman, Jeremy K. Caves Rügenstein, Daniel E. Ibarra, and Matthew J. Winnick. Silicate weathering as a feedback and forcing in Earth’s climate and carbon cycle. *Earth-Science Reviews*, 209:103298, October 2020. ISSN 0012-8252. doi: 10.1016/j.earscirev.2020.103298. URL <https://www.sciencedirect.com/science/article/pii/S0012825220303445>.
- Albert Pessarrodona, Karen Filbee-Dexter, Kira A. Krumhansl, Morten F. Pedersen, Pippa J. Moore, and Thomas Wernberg. A global dataset of seaweed net primary productivity. *Scientific Data*, 9(1):484,

8 2022. ISSN 20524463. doi: 10.1038/s41597-022-01554-5. URL <https://www.nature.com/articles/s41597-022-01554-5>.

I.C. Prentice, G.D. Farquhar, M.J.R. Fasham, M.L. Goulden, M. Heimann, V.J. Jaramillo, H.S. Khesghi, C. Le Quéré, R.J. Scholes, D.W.R. Wallace, D. Archer, M.R. Ashmore, Olivier Aumont, D. Baker, M. Battle, M. Bender, L.P. Bopp, P. Bousquet, K. Caldeira, P. Ciais, P.M. Cox, W. Cramer, F. Dentener, I.G. Enting, C.B. Field, P. Friedlingstein, E.A. Holland, R.A. Houghton, J.I. House, A. Ishida, A.K. Jain, I.A. Janssens, F. Joos, T. Kaminski, C.D. Keeling, R.F. Keeling, D.W. Kicklighter, K.E. Kohfeld, W. Knorr, R. Law, T. Lenton, K. Lindsay, E. Maier-Reimer, A.C. Manning, R.J. Matear, A.D. McGuire, J.M. Melillo, R. Meyer, M. Mund, J.C. Orr, S. Piper, K. Plattner, P.J. Rayner, S. Sitch, R. Slater, S. Taguchi, P.P. Tans, H.Q. Tian, M.F. Weirig, T. Whorf, and A. Yool. The carbon cycle and atmospheric carbon dioxide. In *Climate change 2001: the scientific basis, Intergovernmental panel on climate change*. IPCC, 2001. URL <https://hal.science/hal-03333974>.

H Pörtner. Ecosystem effects of ocean acidification in times of ocean warming: a physiologist's view. *Marine Ecology Progress Series*, 373:203–217, December 2008. ISSN 0171-8630, 1616-1599. doi: 10.3354/meps07768. URL <http://www.int-res.com/abstracts/meps/v373/p203-217/>.

H.-O. Pörtner, D.C. Roberts, V. Masson-Delmotte, P. Zhai, E. Poloczanska, K. Mintenbeck, M. Tignor, A. Alegría, M. Nicolai, A. Okem, J. Petzold, B. Rama, and N.M. Weyer, editors. *IPCC Special Report on the Ocean and Cryosphere in a Changing Climate*, pages 447–587. Cambridge University Press, Cambridge, UK and New York, NY, USA, 2019. URL <https://doi.org/10.1017/9781009157964.007>.

H.-O. Pörtner, D.C. Roberts, H. Adams, I. Adelekan, C. Adler, R. Adrian, P. Aldunce, E. Ali, R. Ara Begum, B. Bednar-Friedl, R. Bezner Kerr, R. Biesbroek, J. Birkmann, K. Bowen, M.A. Caretta, J. Carnicer, E. Castellanos, T.S. Cheong, W. Chow, G. Cissé, S. Clayton, A. Constable, S. Cooley, M.J. Costello, M. Craig, W. Cramer, R. Dawson, D. Dodman, J. Efitre, M. Garschagen, E.A. Gilmore, B. Glavovic, D. Gutzler, M. Haasnoot, S. Harper, T. Hasegawa, B. Hayward, J.A. Hicke, Y. Hirabayashi, C. Huang, K. Kalaba, W. Kiessling, A. Kitoh, R. Lasco, J. Lawrence, M.F. Lemos, R. Lempert, C. Lennard, D. Ley, T. Lissner, Q. Liu, E. Liwenga, S. Lluch-Cota, S. Löschke, S. Lucatello, Y. Luo, B. Mackey, K. Mintenbeck, A. Mirzabaev, V. Möller, M. Moncassim Vale, M.D. Morecroft, L. Mortsch, A. Mukherji, T. Munstonen, M. Mycoo, J. Nalau, M. New, A. Okem (South Africa), J.P. Ometto, B. O' Neill, R. Pandey, C. Parmesan, M. Pelling, P.F. Pinho, J. Pinnegar, E.S. Poloczanska, A. Prakash, B. Preston, M.-F. Racault, D. Reckien, A. Revi, S.K. Rose, E.L.F. Schipper, D.N. Schmidt, D. Schoeman, R. Shaw, N.P. Simpson, C. Singh, W. Solecki, L. Stringer, E. Totin, C.H. Trisos, Y. Trisurat, M. van Aalst, D. Viner, M. Wairu, R. Warren, P. Wester, . Wrathall, D. and, and Z. Zaiton Ibrahim. Technical summary. In H. O. Pörtner, D. C. Roberts, M. Tignor, E. S. Poloczanska, K. Mintenbeck, A. Alegría, M. Craig, S. Langsdorf, S. Löschke, V. Möller, A. Okem, and B. Rama, editors, *Climate Change 2022: Impacts, Adaptation and Vulnerability. Contribution of Working Group II to the Sixth Assessment Report of the Intergovernmental Panel on Climate Change*. Cambridge University Press, Cambridge, UK and New York, NY, USA, 2022. doi: 10.1017/9781009325844.002. URL https://www.ipcc.ch/report/ar6/wg2/downloads/report/IPCC_AR6_WGII_TechnicalSummary.pdf.

- Song Qin, Peng Jiang, and Chengkui Tseng. Transforming kelp into a marine bioreactor. *Trends in Biotechnology*, 23(5):264–268, May 2005. ISSN 0167-7799, 1879-3096. doi: 10.1016/j.tibtech.2005.03.010. URL [https://www.cell.com/trends/biotechnology/abstract/S0167-7799\(05\)00082-X](https://www.cell.com/trends/biotechnology/abstract/S0167-7799(05)00082-X). Publisher: Elsevier.
- J. A. Raven and P. G. Falkowski. Oceanic sinks for atmospheric CO₂. *Plant, Cell & Environment*, 22(6):741–755, 1999. ISSN 1365-3040. doi: 10.1046/j.1365-3040.1999.00419.x. URL <https://onlinelibrary.wiley.com/doi/abs/10.1046/j.1365-3040.1999.00419.x>. _eprint: <https://onlinelibrary.wiley.com/doi/pdf/10.1046/j.1365-3040.1999.00419.x>.
- Ja Raven and K Crawford. Environmental controls on coccolithophore calcification. *Marine Ecology Progress Series*, 470:137–166, December 2012. ISSN 0171-8630, 1616-1599. doi: 10.3354/meps09993. URL <http://www.int-res.com/abstracts/meps/v470/p137-166/>.
- Peter B. Reich, Sarah E. Hobbie, and Tali D. Lee. Plant growth enhancement by elevated CO₂ eliminated by joint water and nitrogen limitation. *Nature Geoscience*, 7(12):920–924, December 2014. ISSN 1752-0908. doi: 10.1038/ngeo2284. URL <https://www.nature.com/articles/ngeo2284>. Number: 12 Publisher: Nature Publishing Group.
- Fabian Reith, David P. Keller, and Andreas Oschlies. Revisiting ocean carbon sequestration by direct injection: A global carbon budget perspective. *Earth System Dynamics*, 7(4):797–812, 11 2016a. ISSN 21904987. doi: 10.5194/esd-7-797-2016. URL <https://esd.copernicus.org/articles/7/797/2016/>.
- Fabian Reith, David P. Keller, and Andreas Oschlies. Revisiting ocean carbon sequestration by direct injection: a global carbon budget perspective. *Earth System Dynamics*, 7(4):797–812, November 2016b. ISSN 2190-4987. doi: 10.5194/esd-7-797-2016. URL <https://esd.copernicus.org/articles/7/797/2016/>.
- REN21. Renewables 2021 global status report, 2022. URL https://www.ren21.net/wp-content/uploads/2019/05/GSR2022_Full_Report.pdf.
- Aurora M Ricart, Dorte Krause-Jensen, Kasper Hancke, Nichole N Price, Pere Masqué, and Carlos M Duarte. Sinking seaweed in the deep ocean for carbon neutrality is ahead of science and beyond the ethics. *Environmental Research Letters*, 17(8):081003, August 2022. ISSN 1748-9326. doi: 10.1088/1748-9326/ac82ff. URL <https://iopscience.iop.org/article/10.1088/1748-9326/ac82ff>.
- W. Rickels, F. Reith, D. Keller, A. Oschlies, and M. F. Quaas. Integrated Assessment of Carbon Dioxide Removal. *Earth's Future*, 6(3):565–582, 2018. ISSN 2328-4277. doi: 10.1002/2017EF000724. URL <https://onlinelibrary.wiley.com/doi/abs/10.1002/2017EF000724>. _eprint: <https://onlinelibrary.wiley.com/doi/pdf/10.1002/2017EF000724>.
- U. Riebesell, K. G. Schulz, R. G. J. Bellerby, M. Botros, P. Fritsche, M. Meyerhöfer, C. Neill, G. Nondal, A. Oschlies, J. Wohlers, and E. Zöllner. Enhanced biological carbon consumption in a high CO₂ ocean. *Nature*, 450(7169):545–548, November 2007. ISSN 0028-0836, 1476-4687. doi: 10.1038/nature06267. URL <http://www.nature.com/articles/nature06267>.

Ulf Riebesell, Ingrid Zondervan, Björn Rost, Philippe D Tortell, Richard E Zeebe, and François MM Morel. Reduced calcification of marine plankton in response to increased atmospheric CO₂. *Nature*, 407(6802): 364–367, 2000.

Ulf Riebesell, Arne Körtzinger, and Andreas Oschlies. Sensitivities of marine carbon fluxes to ocean change. *Proceedings of the National Academy of Sciences of the United States of America*, 106(49):20602–20609, 12 2009. ISSN 00278424. doi: 10.1073/pnas.0813291106. URL <http://www.pnas.org/cgi/doi/10.1073/pnas.0813291106>.

Joeri Rogelj, Alexander Popp, Katherine V. Calvin, Gunnar Luderer, Johannes Emmerling, David Ger-
naat, Shinichiro Fujimori, Jessica Strefler, Tomoko Hasegawa, Giacomo Marangoni, Volker Krey, El-
mar Kriegler, Keywan Riahi, Detlef P. Van Vuuren, Jonathan Doelman, Laurent Drouet, Jae Ed-
monds, Oliver Fricko, Mathijs Harmsen, Petr Havlík, Florian Humpenöder, Elke Stehfest, and Mas-
simo Tavoni. Scenarios towards limiting global mean temperature increase below 1.5 °C. *Nature
Climate Change*, 8(4):325–332, 4 2018. ISSN 17586798. doi: 10.1038/s41558-018-0091-3. URL
<http://www.nature.com/articles/s41558-018-0091-3>.

Jorge L. Sarmiento and Nicolas Gruber. Sinks for Anthropogenic Carbon. *Physics Today*, 55(8):30–36,
August 2002. ISSN 0031-9228, 1945-0699. doi: 10.1063/1.1510279. URL <http://physicstoday.scitation.org/doi/10.1063/1.1510279>.

Felix Schenuit, Rebecca Colvin, Mathias Fridahl, Barry McMullin, Andy Reisinger, Daniel L. Sanchez,
Stephen M. Smith, Asbjørn Torvanger, Anita Wreford, and Oliver Geden. Carbon Dioxide Removal
Policy in the Making: Assessing Developments in 9 OECD Cases. *Frontiers in Climate*, 3:638805, March
2021. ISSN 2624-9553. doi: 10.3389/fclim.2021.638805. URL <https://www.frontiersin.org/articles/10.3389/fclim.2021.638805/full>.

David Schimel, Britton B. Stephens, and Joshua B. Fisher. Effect of increasing CO₂ on the terrestrial carbon
cycle. *Proceedings of the National Academy of Sciences*, 112(2):436–441, January 2015. doi: 10.1073/
pnas.1407302112. URL <https://www.pnas.org/doi/10.1073/pnas.1407302112>. Publisher: Proceedings of
the National Academy of Sciences.

B. Schlamadinger, N. Bird, T. Johns, S. Brown, J. Canadell, L. Ciccarese, M. Dutschke, J. Fiedler, A. Fis-
chlin, P. Fearnside, C. Forner, A. Freibauer, P. Frumhoff, N. Hoehne, M. U. F. Kirschbaum, A. La-
bat, G. Marland, A. Michaelowa, L. Montanarella, P. Moutinho, D. Murdiyarsa, N. Pena, K. Pingoud,
Z. Rakonczay, E. Rametsteiner, J. Rock, M. J. Sanz, U. A. Schneider, A. Shvidenko, M. Skutsch,
P. Smith, Z. Somogyi, E. Trines, M. Ward, and Y. Yamagata. A synopsis of land use, land-use change
and forestry (LULUCF) under the Kyoto Protocol and Marrakech Accords. *Environmental Science
& Policy*, 10(4):271–282, June 2007. ISSN 1462-9011. doi: 10.1016/j.envsci.2006.11.002. URL
<https://www.sciencedirect.com/science/article/pii/S1462901107000184>.

E.-D. Schulze. Biological control of the terrestrial carbon sink. *Biogeosciences*, 3(2):147–166, March 2006.
ISSN 1726-4170. doi: 10.5194/bg-3-147-2006. URL <https://bg.copernicus.org/articles/3/147/2006/>. Pub-
lisher: Copernicus GmbH.

- Vivian Scott, R. Stuart Haszeldine, Simon F. B. Tett, and Andreas Oschlies. Fossil fuels in a trillion tonne world. *Nature Climate Change*, 5(5):419–423, May 2015. ISSN 1758-678X, 1758-6798. doi: 10.1038/nclimate2578. URL <http://www.nature.com/articles/nclimate2578>.
- Brad A. Seibel and Patrick J. Walsh. Potential Impacts of CO₂ Injection on Deep-Sea Biota. *Science*, 294(5541):319–320, October 2001. doi: 10.1126/science.1065301. URL <https://www.science.org/doi/full/10.1126/science.1065301>. Publisher: American Association for the Advancement of Science.
- Zongyao Sha, Yongfei Bai, Ruren Li, Hai Lan, Xueliang Zhang, Jonathon Li, Xuefeng Liu, Shujuan Chang, and Yichun Xie. The global carbon sink potential of terrestrial vegetation can be increased substantially by optimal land management. *Communications Earth & Environment*, 3(1):1–10, January 2022. ISSN 2662-4435. doi: 10.1038/s43247-021-00333-1. URL <https://www.nature.com/articles/s43247-021-00333-1>. Number: 1 Publisher: Nature Publishing Group.
- John G Shepherd. *Geoengineering the climate: science, governance and uncertainty*. Royal Society, 2009.
- Drew T. Shindell, Greg Faluvegi, Dorothy M. Koch, Gavin A. Schmidt, Nadine Unger, and Susanne E. Bauer. Improved Attribution of Climate Forcing to Emissions. *Science*, 326(5953):716–718, October 2009. doi: 10.1126/science.1174760. URL <https://www.science.org/doi/full/10.1126/science.1174760>. Publisher: American Association for the Advancement of Science.
- Andreas Sichert, Christopher H. Corzett, Matthew S. Schechter, Frank Unfried, Stephanie Markert, Dörte Becher, Antonio Fernandez-Guerra, Manuel Liebeke, Thomas Schweder, Martin F. Polz, and Jan Hendrik Hehemann. Verrucomicrobia use hundreds of enzymes to digest the algal polysaccharide fucoidan. *Nature Microbiology*, 5(8):1026–1039, 2020. ISSN 20585276. doi: 10.1038/s41564-020-0720-2. URL <http://dx.doi.org/10.1038/s41564-020-0720-2>.
- D A Siegel, T DeVries, S C Doney, and T Bell. Assessing the sequestration time scales of some ocean-based carbon dioxide reduction strategies. *Environmental Research Letters*, 16(10):104003, October 2021. ISSN 1748-9326. doi: 10.1088/1748-9326/ac0be0. URL <https://iopscience.iop.org/article/10.1088/1748-9326/ac0be0>.
- Norman H. Sleep and Kevin Zahnle. Carbon dioxide cycling and implications for climate on ancient Earth. *Journal of Geophysical Research: Planets*, 106(E1):1373–1399, January 2001. ISSN 01480227. doi: 10.1029/2000JE001247. URL <http://doi.wiley.com/10.1029/2000JE001247>.
- Pete Smith. Soil carbon sequestration and biochar as negative emission technologies. *Global Change Biology*, 22(3):1315–1324, 2016. ISSN 13652486. doi: 10.1111/gcb.13178.
- T. M. Smith and H. H. Shugart. The transient response of terrestrial carbon storage to a perturbed climate. *Nature*, 361(6412):523–526, February 1993. ISSN 1476-4687. doi: 10.1038/361523a0. URL <https://www.nature.com/articles/361523a0>. Number: 6412 Publisher: Nature Publishing Group.
- Wake Smith and Gernot Wagner. Stratospheric aerosol injection tactics and costs in the first 15 years of deployment. *Environmental Research Letters*, 13(12):124001, nov 2018. doi: 10.1088/1748-9326/aae98d. URL <https://dx.doi.org/10.1088/1748-9326/aae98d>.

- T.F. Stocker, D. Qin, G.-K. Plattner, M. Tignor, S.K. Allen, J. Boschung, A. Nauels, Y. Xia, V. Bex, and P.M. Midgley, editors. *Climate Change 2013: The Physical Science Basis. Contribution of Working Group I to the Fifth Assessment Report of the Intergovernmental Panel on Climate Change*. Cambridge University Press, 2013. URL <https://www.ipcc.ch/report/ar5/wg1/>.
- Lyla L. Taylor, Joe Quirk, Rachel M.S. Thorley, Pushker A. Kharecha, James Hansen, Andy Ridgwell, Mark R. Lomas, Steve A. Banwart, and David J. Beerling. Enhanced weathering strategies for stabilizing climate and averting ocean acidification. *Nature Climate Change*, 6(4):402–406, 2016a. ISSN 17586798. doi: 10.1038/nclimate2882.
- Lyla L Taylor, Joe Quirk, Rachel MS Thorley, Pushker A Kharecha, James Hansen, Andy Ridgwell, Mark R Lomas, Steve A Banwart, and David J Beerling. Enhanced weathering strategies for stabilizing climate and averting ocean acidification. *Nature Climate Change*, 6(4):402–406, 2016b.
- Lina Teckentrup, Martin G. De Kauwe, Andrew J. Pitman, and Benjamin Smith. Examining the sensitivity of the terrestrial carbon cycle to the expression of El Niño. *Biogeosciences*, 18(6):2181–2203, March 2021. ISSN 1726-4170. doi: 10.5194/bg-18-2181-2021. URL <https://bg.copernicus.org/articles/18/2181/2021/>. Publisher: Copernicus GmbH.
- Thejna Tharammal, Govindasamy Bala, Narayanappa Devaraju, and Ramakrishna Nemani. A review of the major drivers of the terrestrial carbon uptake: model-based assessments, consensus, and uncertainties. *Environmental Research Letters*, 14(9):093005, September 2019. ISSN 1748-9326. doi: 10.1088/1748-9326/ab3012. URL <https://dx.doi.org/10.1088/1748-9326/ab3012>. Publisher: IOP Publishing.
- CK Tseng. Laminaria mariculture in china. *Case studies of seven commercial seaweed resources. FAO Fisheries Technical Paper*, 281:239–263, 1987.
- Jefferson T. Turner. Zooplankton fecal pellets, marine snow, phytodetritus and the ocean’s biological pump. *Progress in Oceanography*, 130:205–248, January 2015. ISSN 00796611. doi: 10.1016/j.pocean.2014.08.005. URL <https://linkinghub.elsevier.com/retrieve/pii/S0079661114001281>.
- Bla Gasparini Ulrike Lohmann. A cirrus cloud climate dial? *Science*, 357(6348):248–249, 2017. doi: 10.1126/science.aan3325. URL <https://www.science.org/doi/abs/10.1126/science.aan3325>.
- UNFCCC. Adoption of the paris agreement. *United Nations Office at Geneva, Geneva Google Scholar*, 2015.
- United States Environmental Protection Agency. Overview of greenhouse gases, 2023. URL <https://www.epa.gov/ghgemissions/overview-greenhouse-gases>. Accessed: 2023-04-05.
- Tyler Volk and Martin I Hoffert. Ocean carbon pumps: Analysis of relative strengths and efficiencies in ocean-driven atmospheric co2 changes. *The carbon cycle and atmospheric CO2: natural variations Archean to present*, 32:99–110, 1985.

- Anthony P. Walker, Martin G. De Kauwe, Ana Bastos, Soumaya Belmecheri, Katerina Georgiou, Ralph F. Keeling, Sean M. McMahon, Belinda E. Medlyn, David J. P. Moore, Richard J. Norby, Sönke Zaehle, Kristina J. Anderson-Teixeira, Giovanna Battipaglia, Roel J. W. Brienen, Kristine G. Cabugao, Maxime Cailleret, Elliott Campbell, Josep G. Canadell, Philippe Ciais, Matthew E. Craig, David S. Ellsworth, Graham D. Farquhar, Simone Fatichi, Joshua B. Fisher, David C. Frank, Heather Graven, Lianhong Gu, Vanessa Haverd, Kelly Heilman, Martin Heimann, Bruce A. Hungate, Colleen M. Iversen, Fortunat Joos, Mingkai Jiang, Trevor F. Keenan, Jürgen Knauer, Christian Körner, Victor O. Leshyk, Sebastian Leuzinger, Yao Liu, Natasha MacBean, Yadvinder Malhi, Tim R. McVicar, Josep Penuelas, Julia Pongratz, A. Shafer Powell, Terhi Riutta, Manon E. B. Sabot, Juergen Schleucher, Stephen Sitch, William K. Smith, Benjamin Sulman, Benton Taylor, César Terrer, Margaret S. Torn, Kathleen K. Treseder, Anna T. Trugman, Susan E. Trumbore, Phillip J. van Mantgem, Steve L. Voelker, Mary E. Whelan, and Pieter A. Zuidema. Integrating the evidence for a terrestrial carbon sink caused by increasing atmospheric CO₂. *New Phytologist*, 229(5):2413–2445, 2021. ISSN 1469-8137. doi: 10.1111/nph.16866. URL <https://onlinelibrary.wiley.com/doi/abs/10.1111/nph.16866>. _eprint: <https://onlinelibrary.wiley.com/doi/pdf/10.1111/nph.16866>.
- Michelle A. Walvoord and Barret L. Kurylyk. Hydrologic Impacts of Thawing Permafrost-A Review. *Vadose Zone Journal*, 15(6):vzj2016.01.0010, June 2016. ISSN 15391663. doi: 10.2136/vzj2016.01.0010. URL <http://doi.wiley.com/10.2136/vzj2016.01.0010>.
- Rong Wang, Daniel Goll, Yves Balkanski, Didier Hauglustaine, Olivier Boucher, Philippe Ciais, Ivan Janssens, Josep Penuelas, Bertrand Guenet, Jordi Sardans, Laurent Bopp, Nicolas Vuichard, Feng Zhou, Bengang Li, Shilong Piao, Shushi Peng, Ye Huang, and Shu Tao. Global forest carbon uptake due to nitrogen and phosphorus deposition from 1850 to 2100. *Global Change Biology*, 23(11):4854–4872, 2017. ISSN 1365-2486. doi: 10.1111/gcb.13766. URL <https://onlinelibrary.wiley.com/doi/abs/10.1111/gcb.13766>. _eprint: <https://onlinelibrary.wiley.com/doi/pdf/10.1111/gcb.13766>.
- A. J. Weaver, C. M. Bitz, A. F. Fanning, and M. M. Holland. THERMOHALINE CIRCULATION: High-Latitude Phenomena and the Difference Between the Pacific and Atlantic. *Annual Review of Earth and Planetary Sciences*, 27(1):231–285, May 1999. ISSN 0084-6597, 1545-4495. doi: 10.1146/annurev.earth.27.1.231. URL <https://www.annualreviews.org/doi/10.1146/annurev.earth.27.1.231>.
- Andrew White, Melvin G. R. Cannell, and Andrew D. Friend. Climate change impacts on ecosystems and the terrestrial carbon sink: a new assessment. *Global Environmental Change*, 9:S21–S30, October 1999. ISSN 0959-3780. doi: 10.1016/S0959-3780(99)00016-3. URL <https://www.sciencedirect.com/science/article/pii/S0959378099000163>.
- Richard G. Williams and Michael J. Follows. *Ocean Dynamics and the Carbon Cycle: Principles and Mechanisms*. Cambridge University Press, 1 edition, July 2011. ISBN 978-0-521-84369-0 978-0-511-97781-7. doi: 10.1017/CBO9780511977817. URL <https://www.cambridge.org/core/product/identifier/9780511977817/type/book>.
- Stanley N Williams, Stephen J Schaefer, V Marta Lucia Calvache, and Dina Lopez. Global carbon dioxide emission to the atmosphere by volcanoes. *Geochimica et Cosmochimica Acta*, 56(4):1765–1770, April

1992. ISSN 00167037. doi: 10.1016/0016-7037(92)90243-C. URL <https://linkinghub.elsevier.com/retrieve/pii/001670379290243C>.

Matthew J. Winnick and Kate Maher. Relationships between CO₂, thermodynamic limits on silicate weathering, and the strength of the silicate weathering feedback. *Earth and Planetary Science Letters*, 485:111–120, March 2018. ISSN 0012-821X. doi: 10.1016/j.epsl.2018.01.005. URL <https://www.sciencedirect.com/science/article/pii/S0012821X18300098>.

Jiajun Wu, David P. Keller, and Andreas Oschlies. Carbon dioxide removal via macroalgae open-ocean mariculture and sinking: an Earth system modeling study. *Earth System Dynamics*, 14(1):185–221, February 2023. ISSN 2190-4987. doi: 10.5194/esd-14-185-2023. URL <https://esd.copernicus.org/articles/14/185/2023/>.

Xi Xiao, Susana Agusti, Fang Lin, Ke Li, Yaoru Pan, Yan Yu, Yuhan Zheng, Jiaping Wu, and Carlos M. Duarte. Nutrient removal from Chinese coastal waters by large-scale seaweed aquaculture. *Scientific Reports*, 7(1):46613, April 2017. ISSN 2045-2322. doi: 10.1038/srep46613. URL <https://www.nature.com/articles/srep46613>.

Jing Zhang, Tao Liu, Dapeng Bian, Lei Zhang, Xiaobo Li, Detong Liu, Cui Liu, Jingjin Cui, and Luyang Xiao. Breeding and genetic stability evaluation of the new *Saccharina* variety “Ailunwan” with high yield. *Journal of Applied Phycology*, 28(6):3413–3421, December 2016. ISSN 0921-8971, 1573-5176. doi: 10.1007/s10811-016-0810-y. URL <http://link.springer.com/10.1007/s10811-016-0810-y>.

Robert J. Zomer, Antonio Trabucco, Deborah A. Bossio, and Louis V. Verchot. Climate change mitigation: A spatial analysis of global land suitability for clean development mechanism afforestation and reforestation. *Agriculture, Ecosystems & Environment*, 126(1):67–80, June 2008. ISSN 0167-8809. doi: 10.1016/j.agee.2008.01.014. URL <https://www.sciencedirect.com/science/article/pii/S0167880908000169>.

Ingrid Zondervan, Björn Rost, and Ulf Riebesell. Effect of CO₂ concentration on the PIC/POC ratio in the coccolithophore *Emiliania huxleyi* grown under light-limiting conditions and different daylengths. *Journal of Experimental Marine Biology and Ecology*, 272(1):55–70, June 2002. ISSN 00220981. doi: 10.1016/S0022-0981(02)00037-0. URL <https://linkinghub.elsevier.com/retrieve/pii/S0022098102000370>.

Chapter 2

Carbon dioxide removal via macroalgae open-ocean mariculture and sinking: an Earth system modeling study

This chapter is based on the paper 'Carbon dioxide removal via macroalgae open-ocean mariculture and sinking: an Earth system modeling study' published in the journal Earth System Dynamics.

Citation: Wu, J., Keller, D. P., & Oschlies, A. (2023). Carbon dioxide removal via macroalgae open-ocean mariculture and sinking: an Earth system modeling study. Earth System Dynamics, 14(1), 185-221. doi:10.5194/esd-14-185-2023

Abstract

In this study, we investigate the maximum physical and biogeochemical potential of macroalgae open-ocean mariculture and sinking (MOS) as an ocean-based carbon dioxide removal (CDR) method. Embedding a macroalgae model into an Earth system model, we simulate macroalgae mariculture in the open-ocean surface layer followed by fast sinking of the carbon-rich macroalgal biomass to the deep seafloor (depth > 3000m), which assumes no remineralization of the harvested biomass during the quick sinking. We also test the combination of MOS with artificial upwelling (AU), which fertilizes the macroalgae by pumping nutrient-rich deeper water to the surface. The simulations are done under RCP 4.5, a moderate-emissions pathway. When deployed globally between years 2020 and 2100, the carbon captured and exported by MOS is 270 PgC, which is further boosted by AU of 447 PgC. Because of feedbacks in the Earth system, the oceanic carbon inventory only increases by 171.8 PgC (283.9 PgC with AU) in the idealized simulations. More than half of this carbon remains in the ocean after cessation at year 2100 until year 3000. The major side effect of MOS on pelagic ecosystems is the reduction of phytoplankton net primary production (PNPP) due to the competition for nutrients with macroalgae and due to canopy shading. MOS shrinks the mid-layer oxygen-minimum zones (OMZs) by reducing the organic matter export to, and remineralization in, subsurface and intermediate waters, while it creates new OMZs on the seafloor by oxygen consumption from remineralization of sunken biomass. MOS also impacts the global carbon cycle by reducing the atmospheric and terrestrial carbon reservoirs when enhancing the ocean carbon reservoir. MOS also enriches dissolved inorganic carbon in the deep ocean. Effects are mostly reversible after cessation of MOS, though recovery is not complete by year 3000. In a sensitivity experiment without remineralization of sunken MOS biomass, the whole of the MOS-captured carbon is permanently stored in the ocean, but the lack of remineralized nutrients causes a long-term nutrient decline in the surface layers and thus reduces PNPP. Our results suggest that MOS has, theoretically, considerable CDR potential as an ocean-based CDR method. However, our simulations also suggest that such large-scale deployment of MOS would have substantial side effects on marine ecosystems and biogeochemistry, up to a reorganization of food webs over large parts of the ocean.

2.1 Introduction

Anthropogenic emissions are rapidly increasing the global atmospheric CO₂ concentration. In the last decade (2011 to 2020), global fossil CO₂ emissions averaged ~ 9.49 PgC yr⁻¹ (equivalent ~ 34.8 Pg CO₂ yr⁻¹) with a growth rate of 0.4 % yr⁻¹ (Friedlingstein et al., 2022). In 2019, CO₂ emissions reached a record high of 9.71 ± 0.49 PgC yr⁻¹ (equivalent 35.6 ± 1.8 Pg CO₂ yr⁻¹), and there is no sign of a peak (Edo et al., 2022; Friedlingstein et al., 2022). The slow speed of emission reductions until now makes it difficult to reach the promised climate goals to keep global warming within the guardrail of 2 °C (Peters et al., 2013), much less the recent agreement to seriously consider an even more ambitious 1.5 °C goal (UNFCCC, 2015).

In addition to mitigation efforts to reduce greenhouse gas (GHG) emissions, it is increasingly realized that carbon dioxide removal (CDR), sometimes also called negative emissions technologies (NETs), will likely be a necessary step to achieve the targets of the Paris Agreement (Minx et al., 2017; Rogelj et al., 2018). CDR aims to remove CO₂ from the atmosphere and to store it, ideally permanently, in either the terrestrial, marine or geological carbon reservoirs, thereby mitigating global warming (Glaser, 2010). Due to the limited remaining emission budget (650 ± 130 Pg CO₂ to 1.5 °C and 1300 ± 130 Pg CO₂ to 2 °C), deployment of CDR is required in most pathways studied in the scientific literature to achieve these ambitious targets (Lawrence et al., 2018; Masson-Delmotte et al., 2018). As the second-largest inorganic carbon reservoir on the planet, the ocean plays a pivotal role in naturally regulating the atmospheric CO₂ concentration. Since the beginning of the industrial era, the ocean has taken up more than 560 Pg CO₂, about 25 % of the anthropogenic CO₂ emissions (~ 2030 Pg CO₂; Gruber et al., 2019; Ciais et al., 2013; Heinze et al., 2015). Its high carbon storage capacity could theoretically match or exceed fossil fuel resources (Scott et al., 2015). Thus, a variety of ocean-based CDR methods have been proposed to take advantage of this potential storage capacity. The proposed ocean-based CDR approaches aim to increase the rate of oceanic CO₂ uptake and storage by either enhancing abiotic processes (i.e., chemical or physical, e.g., ocean alkalization; Keller et al., 2014; Taylor et al., 2016; Köhler et al., 2013; Albright et al., 2016) or biotic processes (e.g., ocean fertilization; Keller et al., 2014; Smetacek et al., 2012; Oschlies et al., 2010b; Matear and Elliott, 2004; Robinson et al., 2014). Some technologies also seek to remove CO₂ directly from seawater and to store it in some other reservoir, e.g., a geological one (Eisaman et al., 2012).

Macroalgae species (also known as “seaweed” or “kelp”) are highly efficient carbon

fixers with a high C:N ratio (Atkinson and Smith, 1983; Fernand et al., 2017) and observed net primary production (NPP) rates of 91–522 gC m² yr⁻¹. In the 1970's, the concept of ocean farming using macroalgae for marine carbon sink and bioenergy production was studied with an actual small test farm established off the coast of southern California. These research activities were abandoned due to the damage of the test farm by winter storms and for several technical and economic reasons (Ritschard, 1992). Utilizing macroalgae for biological ocean-based CDR has recently received renewed interest (Duarte et al., 2017; Chung et al., 2011; Gao et al., 2020; Fernand et al., 2017; Raven, 2018). The macroalgae aquaculture industry is well established globally, with an annual harvest of over 30 million t wet weight (WW, FAO, 2018). Thus, some proposals have focused on using harvested macroalgae for producing biochar (Roberts et al., 2015; Bird et al., 2011) or bio-energy combined with carbon capture and storage (BECCS, Chung et al., 2011; Buschmann et al., 2017; Gao and McKinley, 1994; Chen et al., 2015; Fernand et al., 2017). However, as current macroalgae aquaculture facilities are mainly located in coastal regions, the scope to expand macroalgae aquaculture is limited by the shortage of suitable coastal areas due to nutrient availability and shifting temperature regimes (Duarte et al., 2017; Oyinlola et al., 2020). To address these issues, several offshore macroalgae aquaculture facilities have been designed and evaluated (e.g., the SeaweedPaddock by Sherman et al. (2019), the offshore ring by Buck and Buchholz (2004) and the depth-cycling strategy by Navarrete et al. (2021), in which macroalgae are physically towed into the deep nutrient-rich water at night). Moreover, the Advanced Research Projects Agency–Energy (ARPA-E) of the US Department of Energy (DOE) has committed more than 60 million dollars on the Macroalgae Research Inspiring Novel Energy Resources (MARINER) program to develop the technologies for macroalgal biomass production, including integrated ocean cultivation and harvesting systems (APAR-e, 2021). Thus, the ideas of expanding macroalgae cultivation to the open oceans (mariculture) are ambitious but no longer fictional, and they provide a theoretical possibility to expand macroalgae aquaculture to the open ocean for CDR.

In this study, we evaluate “macroalgae open-ocean mariculture and sinking (MOS)” as an ocean-based CDR method that is designed to artificially enhance the macroalgae-based carbon dioxide removal. The aim of this study is to investigate (1) the maximum physical and biogeochemical CDR potential of MOS, (2) the side effects of such large-scale deployment, and (3) to understand where offshore macroalgae farming would be viable if done at a large scale. This information is needed to help prioritize further research into CDR, to understand if there are potential MOS side effects that become evident only at a large scale and to provide information on the viability of large-scale offshore macroalgae farming in

different regions over time by accounting for the implications of nutrient utilization and climate change.

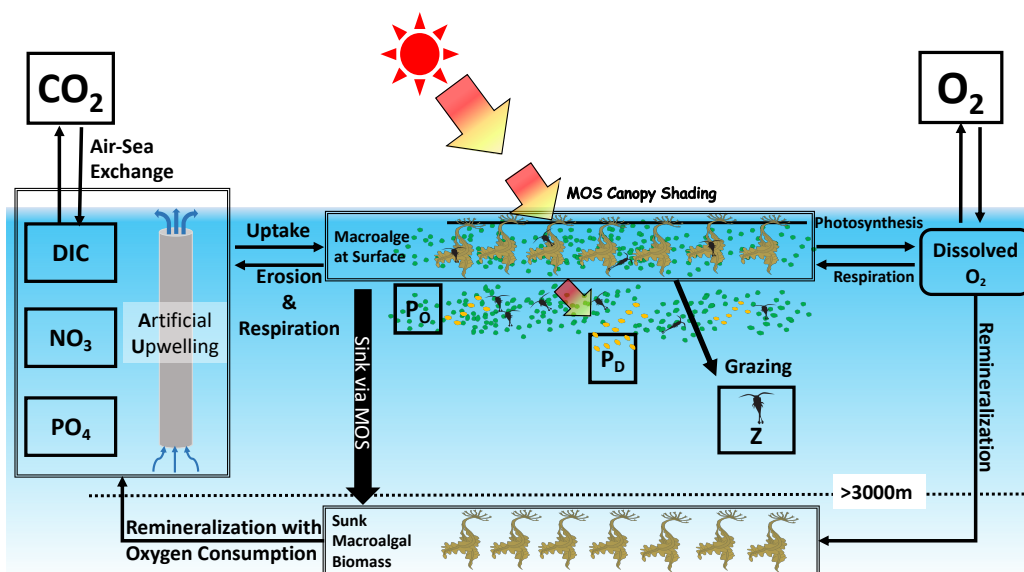


Figure 2.1: Schematic illustrating the biogeochemical fluxes and physical impacts of MOS on nutrients (NO_3 and PO_4), oxygen, dissolved inorganic carbon (DIC), ordinary phytoplankton (P_O in green), diazotrophs (P_D in pale brown) and zooplankton (Z).

To do this, simulated macroalgae are seeded and cultivated on offshore floating platforms that are moored to the seabed (e.g., see platform designs in Buck and Buchholz, 2004). The platforms are also assumed to float below the open-ocean surface (at 5 m depth) to avoid storm damages. At the end of an annual cycle, platforms with matured macroalgae are rapidly sunk to the seafloor and unload the biomass there. This can be thought of as a short circuiting of the biological pump by bringing marine biomass directly to the seafloor without having it remineralized along the way. Afterwards, the sunken biomass is assumed to continue remineralization at the seafloor, consuming oxygen and releasing dissolved inorganic carbon (C), nitrogen (N) and phosphate (P) into the deep ocean where it ideally remains for centuries to millennia (Fig. 2.1). The macroalgae used here is an idealized genus. The assumed constant C:N:P ratio is 400:20:1, which is higher than the stoichiometric ratio of the general phytoplankton in the University of Victoria Earth system climate model (UVic ESCM; C:N:P = 106:16:1, the Redfield ratio). In practice, some of the biomass may also be permanently buried in sediments (Luo et al., 2019; Sichert et al., 2020), and we will explore the extreme case of zero remineralization in the water column in a sensitivity experiment. In another sensitivity experiment, we investigate combining MOS with artificial upwelling (AU) to alleviate nutrient limitation in the open-ocean sur-

face (Duarte et al., 2017; Kim et al., 2019; Laurens et al., 2020).

To investigate the biogeochemical and climatic implications of MOS, we use an Earth system model of intermediate complexity. Though the idea of massive macroalgae cultivation and biomass offsetting for CDR has been assessed in some earlier publications (Orr and Sarmiento, 1992; Gao and McKinley, 1994; Froehlich et al., 2019; Lehahn et al., 2016), as far as we are aware it has not been evaluated using an Earth system model (ESM). ESM-based assessments are required for studying the response of the global carbon cycle to such perturbations and for estimating the efficacy of such methods in a global carbon cycle context (with regards to atmospheric CO₂ removal). Furthermore, such models can dynamically simulate macroalgae growth and the permanence of carbon storage (i.e., the fate of sunken biomass on the seafloor), as well as their interactions with global marine biogeochemistry. It is essential to clarify these issues before any decisions about eventual implementation of MOS can be made.

2.2 Methods

2.2.1 Model description

In this study, we employ the University of Victoria Earth system climate model (UVic ESCM) version 2.9 (Weaver et al., 2001; Eby et al., 2009; Keller et al., 2012), which consists of three dynamically coupled components: a three-dimensional ocean circulation model (Pacanowski, 1996) including a dynamic–thermodynamic sea-ice model (Bitz and Lipscomb, 1999), a terrestrial model (Meissner et al., 2003; Weaver et al., 2001) and a simple one-layer atmospheric energy–moisture balance model (Fanning and Weaver, 1996). The model has a fully coupled carbon cycle including dynamic terrestrial, atmospheric and oceanic carbon inventories. The horizontal resolution of all components is 3.6° longitude × 1.8° latitude, and the ocean component has 19 vertical layers. The descriptions of air–sea gas exchange and seawater carbonate chemistry are based on the Ocean Carbon Cycle Model Intercomparison Project (OCMIP) abiotic protocol (Orr et al., 1999). The ocean biogeochemistry is presented with a nutrients–phytoplankton–zooplankton–detritus (NPZD) model that includes one general phytoplankton, diazotrophs, and one zooplankton type (Keller et al., 2012; Eby et al., 2013). The UVic ESCM has been evaluated in several recent studies (e.g., Keller et al., 2014; Mengis et al., 2016; Reith et al., 2016; Kvale et al., 2021).

2.2.2 Modeling MOS in the UVic ESCM

In this study, the modeling of macroalgae is done with a macroalgae growth model coupled into the UVic ESCM. The aim of the macroalgae model is to investigate the carbon sequestration capacity of MOS and the potential impacts on marine biogeochemistry. In the macroalgae model, the net growth rate is affected by several limiting factors, including nutrients, temperature and solar radiation intensity. The cellular C:N:P ratio of macroalgae is fixed. The loss of macroalgal biomass includes erosion and grazing by zooplankton. The deployment of MOS is done with an algorithm that considers spatial and temporal conditions.

The macroalgae model is also connected to global marine biogeochemical processes, including the inorganic carbon and nutrient pools. In the surface layers, it impacts phytoplankton via nutrients competition and canopy shading. The single, aggregated zooplankton compartment of the biogeochemical model, which represents higher trophic levels, is also designed to graze on macroalgae. In the bottom layers, the remineralization of sunken macroalgal biomass will consume the dissolved oxygen, which in turn limits the rate of remineralization.

Macroalgae model

The macroalgae model is an idealized generic model of genus *Laminaria* and *Saccharina*, mainly based on Martins and Marques (2002) and Zhang et al. (2016). The rate of biomass change is governed by Eq. (2.1) as the imbalance of NGR (net growth rate, d^{-1}) and LR (loss rate, fraction of daily biomass loss due to mortality, erosion and grazing by zooplankton, d^{-1}).

Modeled macroalgae is seeded 5 m below sea surface, considering the light requirement and reduction of damaging risks by surface wave activity (Eq. 2.11). The deployment of macroalgae considers ambient nutrients availability and avoidance of winter periods (Sect. 2.3.1).

$$\frac{\text{dBiomass}}{\text{dt}} = (\text{NGR} - \text{LR}) \times \text{Biomass} \quad (2.1)$$

The NGR is regulated by

$$\text{NGR} = R_{\text{growth}} - R_{\text{resp}}, \quad (2.2)$$

where R_{growth} is the gross growth rate (d^{-1}), and R_{resp} is the respiration rate (d^{-1}). The growth rate of macroalgae (R_{growth}) is given by Eq. (2.3), regulated by water temperature

(T), solar irradiance (I) and dissolved nutrient concentrations (NO_3 and PO_4 , NP).

$$R_{\text{growth}} = \mu_{\text{max}} \times f(T_w) \times f(\text{NP}) \times f(I_{\text{ma}}) \quad (2.3)$$

In the current model, the macroalgal growth rates are controlled by external concentrations of available nutrients via assumed Michaelis–Menten kinetics with half-saturation constants K_N and K_P for NO_3 and PO_4 , respectively:

$$f(\text{N}) = \frac{\text{NO}_3}{K_N + \text{NO}_3}, \quad (2.4)$$

$$f(\text{P}) = \frac{\text{PO}_4}{K_P + \text{PO}_4}, \quad (2.5)$$

$$f(\text{NP}) = \text{Min}\{f(\text{N}), f(\text{P})\}. \quad (2.6)$$

The need for iron is not considered in our macroalgae growth model. Although iron is utilized during macroalgae growth (e.g., Suzuki et al., 1995; Kuffner and Paul, 2001), iron limitation on macroalgae is not widely discussed, especially for the genus *Saccharina*. Besides, as iron is a micronutrient needed in low quantities, the MOS platform could be designed with an iron supply for the macroalgae, in which case MOS could be considered to include a targeted variant of the ocean iron fertilization concept.

The temperature limiting factor used here is an optimum curve following Bowie et al. (1985). T_{opt} is the species-specific optimum temperature at which the growth rate is maximized. T_{max} and T_{min} define the upper and lower temperature limits above and below which macroalgae growth ceases. The temperature optimum curve of the macroalgae is shown in Fig. A.3.

$$f(T_w) = e^{-2.3 \times X_T^2} \quad (2.7)$$

$$X_T = \frac{T_w - T_{\text{opt}}}{T_x - T_{\text{opt}}} \quad (2.8)$$

$$T_x = \begin{cases} T_{\text{min}} & \text{if } T_w \leq T_{\text{opt}} \\ T_{\text{max}} & \text{if } T_w > T_{\text{opt}} \end{cases} \quad (2.9)$$

Respiration is described by an Arrhenius function considering water temperature T_w in degrees Celsius (Duarte and Ferreira, 1997; Martins and Marques, 2002):

$$R_{\text{resp}} = R_{\text{max20}} \times r^{(T_w - 20)}, \quad (2.10)$$

where $R_{\max 20}$ is the maximum respiration rate of the simulated macroalgae species at 20 °C, and r stands for the empirical coefficient for macroalgae respiration (Table 2.1).

The limiting factor of solar irradiance density for macroalgae photosynthesis ($f(I_{\text{ma}})$) is given in Eq. (2.11) (Steele's photo-inhibition relationship – Kirk, 1994):

$$f(I_{\text{ma}}) = \frac{I_{\text{ma}}}{I_{\text{opt}}} \times e^{(1 - \frac{I_{\text{ma}}}{I_{\text{opt}}})}, \quad (2.11)$$

where I_{ma} stands for the shortwave radiation intensity reaching the depth Z (given by Eq. 2.12), and I_{opt} stands for the optimum light intensity for macroalgae growth (constant, Table 2.1).

$$I_{\text{ma}} = I_s \times e^{(-k_w Z_m - \int_0^{Z_m} (P_o + P_D) k_c \times dZ_m)} \times df \quad (2.12)$$

Equation (2.12) calculates the shortwave radiation (I_{ma}) reaching the depth Z_m . This is modified from Keller et al. (2012) and Schmittner et al. (2005), with Z_m denoting the depth of MOS macroalgae platforms beneath the water surface. Z_m is assumed to be 5 m, compromising the empirical depth with sufficient light for macroalgae photosynthesis (1 to 2 m for cultivation (Buck and Buchholz, 2004), 0 to 10 m for wild communities (Eriksson and Bergström, 2005)) and the depth to reduce the risks of damage by stressful turbulence or severe weather events (e.g., hurricanes). df denotes the day length as a fraction of 24 h. I_s stands for the shortwave radiation density at the top of the layer. P_o and P_D are the biomass of ordinary phytoplankton and diazotrophs, respectively, in the layers above the macroalgae. k_w is the light attenuation coefficient for water. I_{opt} is the optimum light intensity for macroalgae growth. k_c is the light attenuation coefficient of phytoplankton and also accounts for co-varying particulate and dissolved inorganic and organic materials (Kvale and Meissner, 2017). As described in Sect. 2.2.2, the morphology of the frond will not be considered, and the self-shading effects by fronds are not considered here (Duarte and Ferreira, 1997; Brush and Nixon, 2010).

The loss rate LR is regulated by the following:

$$\text{LR} = \text{ER} + \text{Graze}_{\text{ma}}, \quad (2.13)$$

$$\text{ER} = \text{Biomass} \times R_{\text{erosion}}, \quad (2.14)$$

$$\text{Graze}_{\text{ma}} = \mu_Z^{\max} Z \times \psi_{\text{ma}} \times \text{Biomass}, \quad (2.15)$$

where the erosion of biomass (ER) is controlled by the individual erosion rate R_{erosion} . As the frond morphology of macroalgae is not modeled here, we set the R_{erosion} as a constant

independent of physical impacts (Trancoso et al., 2005; Zhang et al., 2016). The eroded macroalgal biomass will be directly converted back to nutrients and DIC (dissolved inorganic carbon) according to the macroalgae stoichiometry ratios without remineralization or further degradation by zooplankton. We set this parameterization of erosion, a small biomass loss of 0.01 % per day, pragmatically as instantaneous remineralization rather than introducing another finite remineralization and finite sinking parameterization with difficult-to-constrain parameters. It was used to minimize the computational expense of the model and to avoid having to add another state variable that is subjected to physical transport.

Graze_{ma} is the biomass loss due to grazing by zooplankton. Z is the zooplankton biomass which is calculated by the NPZD model. μ_Z^{max} stands for the maximum potential growth rate of zooplankton, defined in Keller et al. (2012, Eq. 28). The zooplankton grazing preference on macroalgae (ψ_{ma}) is defined in Sect. 2.2.2.

For simplicity and to limit the number of state variables, we made the following modifications to the macroalgae model:

1. We did not include a dynamic C:N:P ratio or a representation of luxury nutrient uptake and storage (Broch and Slagstad, 2012; Hadley et al., 2015). Instead, the C:N:P ratio of the macroalgae biomass was set as a constant (Table 2.1), which is based on seasonally averaged measurements of the biomass composition of these genera (Zhang et al., 2016; Martins and Marques, 2002).
2. The macroalgae life cycle processes (e.g., alternations of generations) are also not considered in our model (Brush and Nixon, 2010; Trancoso et al., 2005; Duarte and Ferreira, 1997). We thus assumed that the plantlet (e.g., sporophytes for *Saccharina*) will be reseeded annually on the MOS infrastructure. The assumed deployment strategy, i.e., timing of seeding and sinking, of MOS is latitude dependent according to the seasonality of solar irradiance (see Sect. 2.3.1). Whenever conditions are unfavorable for macroalgae and no growth occurs during an annual cycle, no re-seeding of macroalgae will occur in these regions.

The parameterization of DOC release by macroalgae could not be included because of the lack of enough information. Few studies exist, and the uncertainties about the release of DOC are large. For example, Barrón et al. (2014) reported a release of DOC by macroalgae from a few species of $23.2 \pm 12.6 \text{ mmol C m}^{-2} \text{ d}^{-1}$ with no information on bioavailability. Meanwhile, refractory DOC dynamics are difficult to include in a global Earth system

model and are beyond the scope of this study (Anderson et al., 2015; Mentges et al., 2019; Zakem et al., 2021). Thus, the DOC release from macroalgae is not included in this study.

Remineralization of sunken macroalgal biomass

Biomass sinking is simulated by instantly transferring the macroalgal biomass from the surface grid cell to the deepest grid cell at the respective location at the end of each cultivating period. This assumes that the harvested biomass could be engineered to sink to the seafloor in a rapid and efficient manner with no remineralization along the way. Afterwards, the next macroalgae generation will start to grow in the surface layer. Equation (2.16) calculates the temperature-dependent remineralization rate of sunken macroalgal biomass (μ_{ma}) following the function of remineralization of detritus in the UVic ESCM (described in Schmittner et al., 2008, Eq. A16). Remineralization consumes oxygen and returns DIC, PO_4 and NO_3 from the sunken macroalgal biomass to the sea water and is described as

$$\mu_{\text{ma}} = \mu_{\text{ma}0} \exp(T_w/T_b) [0.65 + 0.35 \tanh(O_2 - 6)], \quad (2.16)$$

where $\mu_{\text{ma}0}$ is the remineralization rate of sunken macroalgal biomass at 0 °C. T_w and T_b represent the sea water temperature and e -folding temperature of biological rates, and O_2 is the dissolved-oxygen concentration in mmol m^{-3} . When the dissolved oxygen is insufficient ($< 5 \text{ mmol m}^{-3}$), aerobic remineralization will be replaced by oxygen-equivalent, but slower, denitrification via reduction of NO_3 (Keller et al., 2012). Note that remineralization will cease when NO_3 is also completely consumed.

There are considerable uncertainties concerning the fate of sunken macroalgae (Sichert et al., 2020; Krause-Jensen and Duarte, 2016; Luo et al., 2019). A sensitivity simulation explores the situation where $\mu_{\text{ma}0}$ is set to zero, which would assume permanent deposition of the sunken biomass on (or in) the seafloor without decaying (Sect. 2.3.2).

Interactions with pelagic microbial ecosystems

Besides the competition for nutrient resources, the macroalgae canopies may also reduce solar irradiance downward (“canopy shading”) and thus limit phytoplankton photosynthesis beneath the macroalgae (Jiang et al., 2020). Equation (2.17) (modified from Eq. 14, Keller et al., 2012) describes the shortwave radiation attenuation (I_{phyt}) through the macroalgae layer, as well as through phytoplankton and water (MOS is not deployed in

areas covered by sea ice):

$$I_{\text{phyt}} = I_s \times e^{-k_w Z - \int_0^Z (P_O + P_D) k_c \times dZ - k_{\text{ma}} \times h_{\text{ma}} \times \text{Biomass}}, \quad (2.17)$$

where k_{ma} , the macroalgae light extinction coefficient (m^{-1}), is calculated based on the biomass of macroalgae in carbon as follows:

$$k_{\text{ma}} = a_{\text{ma}} \times \text{Biomass} \times \text{MR}_{\text{C:N}}. \quad (2.18)$$

Here, a_{ma} is the macroalgae carbon-specific shading area ($\text{m}^2 \text{kgC}^{-1}$; Trancoso et al., 2005), h_{ma} is the thickness of macroalgae layer, and $\text{MR}_{\text{C:N}}$ stands for the molar C:N ratio of macroalgal biomass.

The original NPZD model in Keller et al. (2012) is extended by allowing zooplankton to graze on macroalgae. Our assumption that zooplankton can graze on macroalgae is based on the notion that the marine biogeochemical component of “zooplankton” in UVic ESCM represents all higher trophic levels, including known macroalgae grazers such as amphipods (Jacobucci et al., 2008), gastropods (Chikaraishi et al., 2007; Krumhansl and Scheibling, 2011), sea urchins (e.g., Yatsuya et al., 2020) and fishes (e.g., Peteiro et al., 2014). Thus, we included this food web pathway to assess the sensitivity of macroalgae to potential grazers in the ocean, assuming that with large macroalgae farms the pelagic larvae of some grazing organisms like fish or urchins would settle within the farms.

The grazing preference for macroalgae (ψ_{ma}) is set to 1×10^{-4} according to observational studies (Trancoso et al., 2005). Macroalgae thus provide a grazing option for zooplankton in addition to the traditional NPZD-type model food sources (phytoplankton, diazotrophs, detritus and zooplankton via self-grazing). Therefore, the four original grazing preferences (0.3 on phytoplankton, 0.1 on diazotrophs, 0.3 on detritus and 0.3 on zooplankton; Keller et al., 2012, Table 1) are reduced by $\frac{1}{4} \psi_{\text{ma}}$ each. In the areas where MOS is absent (i.e, in the ice-covered ocean surface), the zooplankton grazing will follow the original description in Keller et al. (2012, Table 1) without the preference for macroalgae. No CaCO_3 formation by macroalgae is simulated here (Bach et al., 2021; Macreadie et al., 2017, 2019), as calcareous macroalgae species and epibiont calcifiers are not considered. Therefore, the only alkalinity impact of growing and remineralizing macroalgae comes via changes in nitrate and phosphate.

Mass conversions

In order to parameterize and validate the model, it is necessary to convert from commonly measured macroalgae variables (often in wet- and dry-weight units) to the model units. These conversions include the calculation of carbon and CO₂ sequestered in macroalgal biomass (C_{ma} , gram carbon), as well as the conversions of dry weight (DW, gram) and wet weight (WW, gram):

$$C_{\text{ma}} = \text{Biomass} \times \text{MR}_{\text{C:N}} \times 12.011, \quad (2.19)$$

$$\text{CO}_{2\text{ma}} = C_{\text{ma}} \times 3.67, \quad (2.20)$$

$$\text{DW} = C_{\text{ma}} \div \text{MR}_{\text{C:DW}}, \quad (2.21)$$

$$\text{WW} = \text{DW} \times \text{MR}_{\text{DW:WW}}, \quad (2.22)$$

where 3.67 is the ratio between the atomic mass of CO₂ (44 g mol⁻¹) and carbon (12 g mol⁻¹), Biomass is in moles of nitrogen, and 12.011 is the relative molecular weight of carbon (g mol⁻¹).

MOS carbon retained in the ocean and outgassing

The DIC from remineralization of sunken biomass will eventually be conveyed back to the ocean surface and may leak back to the atmosphere. Equation (2.23) calculates the ocean-retained fraction (FR, %) of MOS-captured carbon (MOS-C), where the C_{captured} is carbon in the cumulative sunken biomass, $C_{\text{Sunken Biomass}}$ is the carbon in sunken macroalgal biomass that still remains on the seafloor.

$$\text{FR} = \frac{C_{\text{retained}}}{C_{\text{captured}}} = \frac{(\text{DIC}_{\text{remineralized}} + C_{\text{Sunken Biomass}})}{C_{\text{captured}}} \quad (2.23)$$

In order to track the leakage of MOS-C after remineralization, a tracer of remineralized MOS-C (MOS_DIC) is added to the UVic ESCM in addition to the original DIC tracer. MOS_DIC participates in the inorganic ocean carbon cycle (Weaver et al., 2001, Sect. 3e). When reaching the surface, the outgassing of MOS_DIC will follow the air–sea gas exchange process in UVic ESCM, which is given in Weaver et al. (2001, Sect. 3e). The air–sea exchange flux of MOS-C is also calculated for analyzing the location and quantity of outgassing. The results of MOS-C outgassing are shown in Sect. 2.4.6.

Table 2.1: Model parameters.

Symbol	Parameter	Unit	Value	Reference
a_{ma}	Macroalgae carbon specific shading area	$m^2 kgC^{-1}$	11.1	Trancoso et al. (2005)
d	Distance between the cultivating ropes	m	10	Van Der Molen et al. (2018)
$R_{erosion}$	Individual erosion rate	$\% d^{-1}$	0.01	Zhang et al. (2016)
I_{opt}	Optimum light intensity for macroalgae growth	$W m^{-2}$	180	Zhang et al. (2016)
NO_3	Nitrate concentration	$\mu mol l^{-1}$	Model calculation	Keller et al. (2012)
PO_4	Phosphate concentration	$\mu mol l^{-1}$	Model calculation	Keller et al. (2012)
K_N	Half-saturation constant for nitrogen uptake	$\mu mol l^{-1}$	2	Zhang et al. (2016)
K_P	Half-saturation constant for phosphorus uptake	$\mu mol l^{-1}$	0.1	Zhang et al. (2016)
k_w	Coefficient of light attenuation through water	m^{-1}	0.04	Keller et al. (2012)
k_c	Coefficient of light attenuation through phytoplankton	$m^{-1} (mmol m^{-3})$	0.047	Keller et al. (2012)
A_{ma}	Thickness of MOS macroalgae canopy	m	10	Trevathan-Tackett et al. (2015)
$MR_{C:N}$	Molar C:N ratio of macroalgal biomass	-	20	Atkinson and Smith (1983)
$MR_{P:N}$	Molar P:N ratio of macroalgal biomass	-	0.05	Atkinson and Smith (1983)
$MR_{C:P}$	Molar C:P ratio of macroalgal biomass	-	400	Calculated
$MR_{DW:WW}$	Ratio of DW to WW of macroalgal biomass	-	0.1 (values reported: 0.05~0.2)	Aldridge and Trimmer (2009); Conover et al. (2016); Van Der Molen et al. (2018)
$MR_{C:DW}$	Carbon content of dried macroalgal biomass	%	30	Chung et al. (2011)
$MR_{N:DW}$	Nitrogen content of dried macroalgal biomass	%	0.16	Duarte et al. (2003)
$R_{minar20}$	Maximum respiration rate at 20 °C	$\% d^{-1}$	1.5	Martins and Marques (2002); Zhang et al. (2016)
r	Empirical coefficient for macroalgae respiration	d^{-1}	1.047	Martins and Marques (2002)
Seed	Initial macroalgal biomass (per kilometer cultivating line)	$kgC km^{-1}$	2.5	Van Der Molen et al. (2018)
	Initial macroalgal biomass (concentration of N)	$mmol N m^{-3}$	0.02	Calculated
T_b	e -folding temperature of biological rates	°C	15.56	Schmittner et al. (2008)
T_{opt}	Optimum temperature for growth	°C	20 (values reported: 13–30)	Zhang et al. (2016); Martins and Marques (2002)
T_{max}	Upper temperature limit above which growth ceases	°C	35	Breenan (1988)
T_{min}	Bottom temperature limit below which growth ceases	°C	0	Martins and Marques (2002)
u_{max}	Maximum growth rate	d^{-1}	0.2	Zhang et al. (2016)
w	Areal mean artificial upwelling rate	$cm d^{-1}$	1	Oschlies et al. (2010b)
Y_{max}	Maximum yield of macroalgal biomass on MOS	$DW km^{-2}$	3300	Trancoso et al. (2005)
ψ_{ma}	Zooplankton grazing preference on macroalgae	-	1×10^{-4}	Partanen et al. (2016)
μ_{min0}	Remineralization rate of sunk macroalgal biomass at 0 °C	$\% d^{-1}$	7	

2.3 Experiment design

The UVic ESCM is spun up for > 10000 years to an equilibrium state under pre-industrial (year 1765) atmospheric and astronomical boundary conditions and is then integrated for another 250 years without prescribing atmospheric CO_2 concentrations to allow the carbon cycle to equilibrate. Afterwards, the model is run from 1765 until 2005 and forced with historical fossil fuel emissions and land-use changes (crop and pastureland; Keller et al., 2014). From year 2005 to 2100, simulations are forced with CO_2 emissions represented as a direct adjustment to radiative forcing, land-use change by agriculture, volcanic radiative forcing and sulfate aerosols which are prescribed according to the Representative Concentration Pathway 4.5 (RCP 4.5; Meinshausen et al., 2011; Thomas, 2014; Keller et al., 2014; Partanen et al., 2016). Solar insolation at the top of the atmosphere, wind stress and wind fields are varied seasonally. After the year 2300, CO_2 emissions are assumed to decrease linearly until the end of year 3000 with other forcing held constant to zero.

The full list of simulations is given in Table 2.3. To test the maximum potential, as well as the global carbon cycle and biogeochemical responses, we simulate MOS for 1000 years, beginning in year 2020 (MOS_Conti). Additionally, termination experiments (MOS_Stop) are performed to analyze the response of the ocean and climate to an abrupt termination of MOS at year 2100.

2.3.1 Deployment strategies of MOS

The current study focuses on estimating the maximum carbon sequestration potential of MOS and assumes instantaneous seeding on floating infrastructure in the open ocean. The macroalgae is represented as a biogeochemical tracer (Eq. 2.1) that is not subject to physical transports and remains fixed in the top (first) ocean layer of the UVic ESCM, which is assumed to be well mixed. In our idealized experiments, MOS deployment must fulfill the following requirements:

- The water depth must be ≥ 3000 m; according to the assessment by Reith et al. (2016), leakage of dissolved inorganic carbon added to deep waters (in this case from remineralization of sunken macroalgal biomass) is small at such depths compared to shallower ones.
- The ambient surface NO_3 concentration is greater than *Seed* plus K_N (Table 2.1); this ensures sufficient nutrients for initial growth, as *Seed* is directly transferred from

dissolved NO_3 , and K_N is the half-saturation constant for NO_3 uptake. Note that in this calculation, *Seed* has been converted from the unit of kgC km^{-1} in Table 2.1, the unit of concentration of nitrogen (mmol N m^{-3}).

- It must be spatially located between 57° N and 72° S to remain in sea-ice-free waters.

Note that the DIC, N and P components of the initial *Seed* are directly removed from the inorganic-matter pool of the respective grid box in order to maintain model mass balance and to avoid adding extra nutrients and/or carbon to the ocean at the time of seeding.

During the MOS simulations, the seasonality of temperature and of solar radiation is an essential limiting factor of the primary productivity of MOS in various latitudinal regions. In order to avoid the unnecessary loss of macroalgal biomass during winter periods when solar radiation is insufficient and when the ambient water temperature is low, we partitioned the global ocean surface into three belts (N, M and S) and pragmatically applied farming strategies according to Table 2.2. The period between the seeding and sinking of macroalgae is set as 6 months, from May to October in belt N and from November to the next April in belt S. In belt M, the macroalgae is seeded at the beginning of the year, and sinking occurs after 12 months. The geographical locations of the three belts are shown in Fig. 2.2.

Table 2.2: Latitudinal division of MOS deployment regions.

Belt	Latitudinal range	Date for	
		seeding	sinking
N	51.3° N to 17.1° N	1 May	31 Oct
M	17.1° N to 18.9° S	1 Jan	31 Dec
S	18.9° S to 56.7° S	1 Nov	30 Apr*

* In the following year.

The maximum yield of *Biomass* is set to a constant value of Y_{\max} (Table 2.1). When the biomass reaches Y_{\max} in a grid cell, macroalgae will stop growing and wait for sinking. After an annual cultivation cycle, the macroalgal biomass is instantaneously delivered to the seafloor, except for a small fraction (equivalent to *Seed*) that remains at the surface for re-seeding. In some regions where conditions are unfavorable and no net macroalgae growth had occurred during the last cultivation period, the total *Biomass* will be sunk once without any further re-seeding. In order to prevent MOS from removing too much atmospheric CO_2 in long-term simulations where emissions eventually reach zero, MOS deployment will be terminated once atmospheric CO_2 concentration hits 280 ppm, assuming that there is no need for more CDR once pre-industrial CO_2 values have been reached.

2.3.2 Sensitivity studies

As test simulations indicated that the CDR potential of MOS is, in many ocean regions, limited by the availability of nutrients in the surface layer, sensitivity simulations were performed with MOS combined with artificial upwelling (AU) that pumps up nutrient-rich deeper waters to the surface and thereby relaxes nutrient stress and enhances the macroalgae growth.

The simulated MOS-AU system is based on Oschlies et al. (2010b) and Keller et al. (2014). We placed modeled “pipes” that pump deeper water to the ocean surface in areas where MOS is deployed. The simulated upwelling works by transferring water adiabatically from the grid box at the lower end of the pipe to the surface grid box at a rate of 1 cm d^{-1} . These pipes will function continuously until the termination of MOS (in year 2100 or 3000). However, because these earlier studies have revealed a dominant effect associated with the low temperatures of the upwelled colder waters, we here concentrate on the nutrient aspect and simulate a hypothetical MOS-AU system that keeps temperatures at ambient levels (e.g., via heat exchangers).

In the simulated AU system, water, together with dissolved tracers, is transferred from the grid box at the lower end of the pipes to the surface grid box, resulting in a model grid box-average upwelling rate (w , set to 1 cm d^{-1} ; Table 2.1). The lower end of the pipes is fixed at a depth of 1000 m. Similarly to the normal MOS simulations without AU, the MOS-AU simulations are deployed from year 2020 and then terminated at either year 2100 in a discontinuous run or at year 3000 in a continuous one (Table 2.3).

The MOS-AU joint system is deployed using the following strategies: AU pipes will be deployed everywhere with depth $\geq 3000 \text{ m}$ and start upwelling immediately. If surface nutrient concentrations are raised to the initial seeding condition (Sect. 2.3.1) in any grid box, MOS will be deployed, thereby expanding the range where MOS can grow.

Another model parameter selected for sensitivity studies is the remineralization rate of sunken macroalgal biomass (μ_{ma} , Eq. 2.16). μ_{ma} is a critical factor impacting the residence time of MOS-captured carbon in the ocean and associated benthic oxygen consumption by remineralization. Macroalgal biomass has been reported to be recalcitrant to microbial degradation; however, the fate of macroalgal biomass in the deep sea is uncertain (Krause-Jensen and Duarte, 2016; Luo et al., 2019; Sichert et al., 2020). Thus, an extreme and idealized situation with μ_{ma} set to zero is tested in sensitivity simulations (MOS-NoRe, MOS with zero mineralization of sunk macroalgal biomass). This can be thought of as a case where all biomass is permanently buried upon reaching the seafloor. This sensitivity

study can also simulate an extreme case of infinitely slow remineralization, which can help in estimating the range of possible fates of remineralized organic matter. Meanwhile, this sensitivity study also represents a different macroalgae farming approach – that of harvesting the biomass to create bioenergy with carbon capture or storage (BECCS) or biochar (e.g., Kerrison et al., 2015; Laurens et al., 2020; Roberts et al., 2015), with the assumption that all harvested biomass was permanently removed from the ocean. While this is a very idealized case, it serves the useful purpose of providing information on how marine biogeochemistry is impacted by the permanent removal of fixed C, N and P.

The stoichiometric C:N ratio of macroalgal biomass ($MR_{C:N}$) may also influence the CDR capacity of MOS. In the current study, the $MR_{C:N}$ (400 : 20, Table 2.1) is set as 20, nearly 2 times higher than the phytoplankton stoichiometric biomass C:N ratio in the UVic ESCM (C:N= $_{106:16}$, the Redfield ratio). However, the difference between the macroalgae and phytoplankton stoichiometric C:N ratio may have strong influences on the CDR potential of MOS. For instance, Bach et al. (2021) have indicated that the CDR potential of a floating-macroalgae (*Sargassum*) belt may be reduced by 7 % to 50 % due to the nutrient reallocation caused by the variation of gaps of C:N between macroalgae and phytoplankton. Thus, sensitivity experiments of macroalgal C:N ratios (MOS_Conti_CN_{High} and MOS_Conti_CN_{Low}) have been performed to investigate the impacts of $MR_{C:N}$ on the MOS CDR capacity.

Table 2.3: Description of the model experiments. “Stop” represents the termination of the simulation in year 2100; “Conti” represents the continuous MOS deployment till year 3000; “AU” represents artificial upwelling; NoRe represents zero remineralization of sunken macroalgal biomass; CN represents the molar C:N ratio of macroalgal biomass ($MR_{C:N}$ in Table 2.1).

Category	Experiment	Description
Normal MOS simulations	Control_RCP 4.5	Control simulation under RCP 4.5
	MOS_Conti	As Control_RCP 4.5 but MOS deployed from year 2020 to year 3000
	MOS_Stop	As Control_RCP 4.5 but MOS implemented from year 2020 to year 2100
Sensitivity simulations	MOS_Conti_NoRe	As MOS_Conti but with zero-remineralization rate
	MOS_Stop_NoRe	As MOS_Stop but with zero-remineralization rate
	MOS_AU_Conti	MOS synergy with AU; area-averaged upwelling velocity(w) is 1 cm d ⁻¹
	MOS_AU_Stop	As MOS_AU_Conti, but MOS implemented until year 2100
	MOS_Conti_CN _{High}	As MOS_Conti, but the $MR_{C:N}$ increases by 20 % from 20 to 24
	MOS_Conti_CN _{Low}	As MOS_Conti, but the $MR_{C:N}$ decreases by 20 % from 20 to 16

2.4 Results

2.4.1 Evaluation of MOS

To evaluate if the simulated MOS systems have plausible macroalgae growth characteristics, we evaluate the seasonal dynamics of the simulated MOS system for a 30 d averaged time slice from 2020 to 2024 under the RCP 4.5 emission scenario and without artificial upwelling.

Distribution of MOS

The red contours in Fig. 2.2a delineate the occupied area that basically follows the pattern of the simulated NO_3 -rich ocean surface (Keller et al., 2012, Fig. 9; Garcia et al., 2010, WOA2009 Dataset) in the northern and the equatorial Eastern Pacific, as well as in the Southern Ocean. Except for the coastal regions and Arctic areas, which are not considered for MOS here, the distribution pattern of MOS agrees with the other estimation of potential open-ocean macroalgae farming locations (e.g., Lehahn et al., 2016, Fig. 2a; Froehlich et al., 2019, Fig. 1). Another powerful limiting factor is the ocean surface temperature (Garcia et al., 2010, WOA2009 Dataset) which is too warm for our idealized species in many places, i.e., temperatures are above the T_{opt} (20 °C) and nearly reach T_{max} (35 °C).

At the beginning of year 2020, a surface area S_{MOS} of $72 \times 10^6 \text{ km}^2$ was selected by the MOS algorithm according to the requirements described in Sect. 2.3. This is equivalent to a total cultivated rope length (L_{MOS}) of $7.2 \times 10^6 \text{ km}$ (Eq. A.1, Sect. A.1.1). When the macroalgae start to grow and to consume nutrients, regions with nutrient levels insufficient for further growth are gradually abandoned. By the end of year 2024, the MOS coverage has declined by about 3 % to $69.6 \times 10^6 \text{ km}^2$ (Table 2.4).

Despite the similar distribution patterns, MOS-occupied area ($69.6 \times 10^6 \text{ km}^2$, ~ 19.7 % of the world ocean) is larger than the assessments of ~ 10 % of the world ocean by Lehahn et al. (2016) and $\sim 48 \times 10^6 \text{ km}^2$ by Froehlich et al. (2019). Compared to the static estimation based on historical nutrient levels and temperature suitability (Lehahn et al., 2016, Fig. 2a), the dynamic processes redistributing nutrients, as well as the explicit macroalgae growth module in our simulations, contribute to the simulated larger potential area for MOS, especially in the equatorial Eastern Pacific and the Southern Ocean (Table 2.3). Besides, the adequate area for macroalgae cultivation was limited to the Economic Zones (EEZs) delineated by Froehlich et al. (2019) due to limitations of cost and political feasibility. This constraint has been ignored in the current study. Thus, our simulated

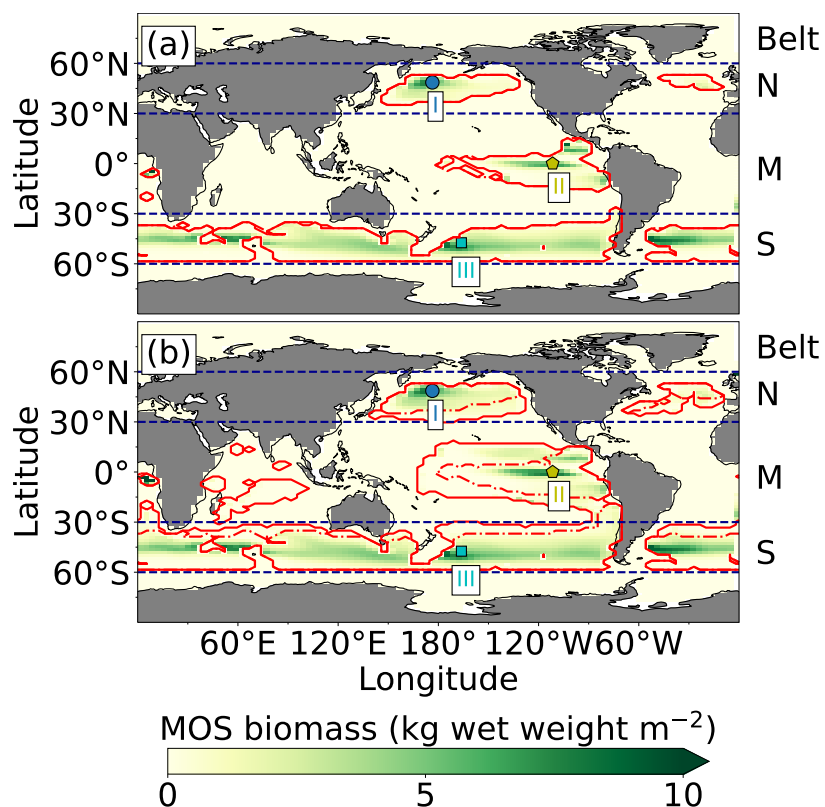


Figure 2.2: Annual vertically integrated macroalgae biomass of MOS (a) and MOS-AU (b) in year 2024. Solid red lines outline the MOS-occupied area at year 2024 in both, while dashed red lines outline the initial MOS seeding area at year 2020 in (a). The simulated MOS area generally covers the NO_3 -rich ocean surface (a) and can be expanded with nutrients supplemented by AU (b), making it larger than the estimated adequate area for macroalgae in previous studies Lehahn et al., 2016; Froehlich et al., 2019). Results for Areas I (blue circle), II (yellowish pentagon) and III (cyan rectangle) are discussed in the text and displayed in Fig. 2.3. Braces indicate the belts of N, M and S with various seeding strategies of macroalgae (Table 2.2), which are designed to avoid winter periods.

MOS-adequate area is 45 % larger than the estimation by Froehlich et al. (2019).

Macroalgae model validation

Validation of the macroalgae model is crucial, as the productivity and macroalgal biomass yield are vital for CO_2 sequestration. Here, we examine the simulated seasonality, NPP rate and biomass yield of MOS in comparison with available observations and assessments. Simulated NPP is high in the first year of deployment in many regions because nutrients are abundant, and then it sharply declines in the following years as a new local biogeochemical state is reached. Thereafter, NPP gradually reaches a relatively steady state by 2024 (Fig. A.2). To provide some validation of the macroalgae model, we select three

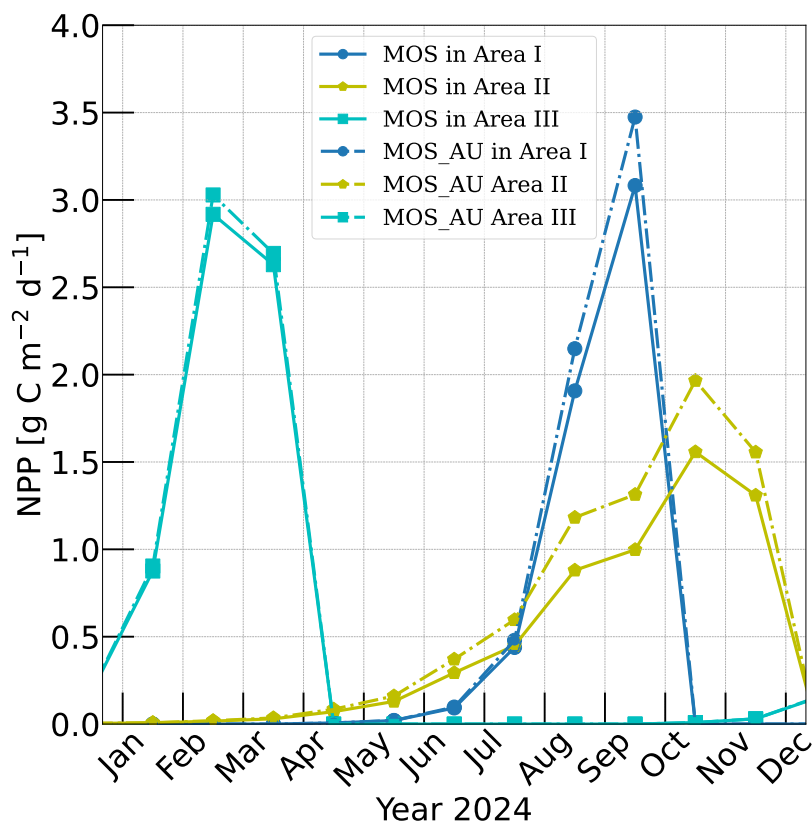


Figure 2.3: Vertically integrated macroalgae NPP simulated by experiment MOS (solid lines) for year 2024 and with representative Areas I (dark blue circle), II (yellow pentagon) and III (cyan rectangle) highlighted by rectangles with corresponding colors in Fig. 2.2. The NPP of macroalgae of experiment MOS_AU (dashed) shows an enhancement of NPP as expected.

areas named Area I, II and III from Belt N, M and S and analyze their performance in year 2024 (Fig. 2.3). Each area covers four grid boxes in the uppermost ocean layer of the UVic ESCM.

According to Sect. 2.3.1 and Table 2.2, the seeding date for MOS is 1 May in Area I, 1 January in Area II and 1 November in Area III, while the sinking dates are 31 October, 31 December and 30 April the next year, correspondingly. As a result, shown in Fig. 2.3, the macroalgae NPP in Area I peaks around September with the accumulation of macroalgae biomass in that area. In Area II, due to the nutrient limitation and nutrient competition with ambient phytoplankton, macroalgae biomass grows slower than in the other two areas, leading to a later peak of NPP around October. In Area III, which is located in the Southern Ocean where the nutrients are rich, the macroalgae NPP peaks in February. These results indicates a plausible seasonality of our macroalgae model.

In our simulations, simulated macroalgae NPP rates are comparable to the observed ranges in the productive areas that we selected here. Observed wild macroalgae NPP varies

widely, ranging from 91 to 750 gC m⁻² yr⁻¹ (Krause-Jensen and Duarte, 2016). Our model reproduces the macroalgae NPP of 159.2–199.3 gC m⁻² yr⁻¹ in the selected areas (Table 2.4). Simulated biomass yields in these areas are in the previously reported range as well. Reports of the biomass yield of aqua-cultured *Laminaria saccharina* (now regarded as a synonym of *Saccharina latissima*) range from 40 t DW km⁻² yr⁻¹ in an offshore cultivation experiment by Buck and Buchholz (2004) to 456 t DW km⁻² in a coastal cultivation experiment by Peteiro et al. (2014). In our simulations, the yield of selected areas ranges from 492.4 to 648.2 t DW km⁻² yr⁻¹. The selected Area I yields 648.2 DW km⁻² yr⁻¹. In regions with similar latitudes to that of Area I, the biomass yield of aqua-cultured *Saccharina japonica* (formerly classified as *Laminaria japonica*) was ~ 300 t DW km⁻² yr⁻¹ in China (Zhang et al., 2016) and reached 7280 t DW km⁻² yr⁻¹ in Japan (Yokoyama et al., 2007). Nevertheless, some simulated low values from the globally averaged and latitudinal belt-averaged results are not surprising considering that the open ocean tends to be more nutrient limited than coastal or near-shore regions where the aforesaid observed macroalgae NPP was measured. Our results provide some confidence that our idealized model can simulate macroalgae well enough with respect to typical biomass yield, seasonality and geographical distribution.

Table 2.4: Properties of globally implemented MOS. Selected areas are from data of year 2024, whereas belt areas are values averaged from 2020 to 2024. Areal NPP rates and “Biomass yield” refer to the respective MOS area. The observational data come from the references.

Property	Unit	Observations	Selected area (10 ³ km ²)			Belt (10 ⁶ km ²)				
			Exp.	Area I	Area II	Area III	N	M	S	Global
MOS occupied area (S _{MOS})	km ²	–	MOS	218.8	320.3	204.2	9.1	15.7	44.8	69.6
			MOS_AU				17.4	44.3	64.6	126.3
NPP	gC m ⁻² yr ⁻¹	91–750 ¹	MOS	159.2	176.9	199.3	50.8	52.0	67.5	61.8
			MOS_AU	202.2	231.1	217.7	45.5	32.2	56.9	46.7
Biomass yield	t DW km ⁻² yr ⁻¹	40–456 ² Area I: 300–7280 ³	MOS	648.2	492.4	579.7	173.2	160.3	206	191.4
			MOS_AU	715.3	615.4	597.0	142.2	85.4	169	136
Total CO ₂ captured in biomass	Pg CO ₂ yr ⁻¹	–	MOS	0.14	0.16	0.12	1.6	2.5	9.2	13.3
			MOS_AU	0.15	0.20	0.12	2.5	3.8	10.9	17.2

a: Krause-Jensen and Duarte (2016); b: Buck and Buchholz (2004); Peteiro et al. (2014); c: Zhang et al. (2016); Yokoyama et al. (2007)

2.4.2 Evaluation of MOS with artificial upwelling (AU)

As expected, AU increases the area occupied by MOS from 69.6×10^6 km² in the run without AU to 129.6×10^6 km² in the run with AU (Fig. 2.2). Obvious expansions of areas with suitable growing conditions are found in the eastern tropical Pacific and the North Atlantic. AU also expands S_{MOS} to the Indian Ocean, which was almost abandoned

in regular MOS simulations. In Areas I, II and III, both NPP rate and biomass yield are enhanced due to the upwelled nutrients (belt column, Table 2.4 and Fig. 2.3). A closer look into the belt N, M and S areas shows that both the NPP rate and biomass yield per square meter of the deployment area decrease in simulation MOS_AU when compared to the standard MOS simulation (belt column, Table 2.4). This is related to a “dilution effect”: in the new adequate areas made accessible for MOS by AU, the available nutrients are limited, thus the MOS NPP is relatively low compared to the original nutrient-rich NPP areas. Despite of this, the expanded MOS area in MOS_AU increases the total CO₂ captured by about ~ 30 % (Table 2.4).

2.4.3 MOS deployment until year 2100

This section showcases the CDR and climate change mitigation capacities of MOS within the 21st century. Impacts of MOS on marine biogeochemistry (nutrients, dissolved oxygen and pelagic ecosystem) and global carbon cycles will also be examined.

CDR & climate change mitigation capacities

Over the 80 years between year 2020 and year 2100, MOS will mainly be deployed in nutrient-rich regions such as the Southern Ocean and the northern and eastern equatorial Pacific (Fig. A.4a), although some contraction of initially occupied areas occurred due to the removal of nutrients.

By the year 2100, MOS (MOS_Stop and MOS_Conti) has sequestered 270 PgC (990 Pg CO₂; Table 2.5), representing ~ 37 % of the cumulative CO₂ emissions in the RCP 4.5 pathway. Essentially all of MOS-captured carbon is retained in the ocean over this period as either remineralized dissolved inorganic carbon or organic carbon in the sunken biomass.

The CDR capacity of MOS is sensitive to the MR_{C:N} (molar C:N ratio of macroalgal biomass; Table 2.1). Compared to MOS_Conti, the carbon captured by MOS (MOS-C) in MOS_Conti_CN_{High} is raised by 22 % (by the year 2100) and by 19 % (by the year 3000) when the MR_{C:N} is increased by 20 %, to 24. When the MR_{C:N} is 20 % lower than the original value, MOS-C decreases by 13 % (by the year 2100) and by 18 % (by the year 3000). Our results agree with the range of CDR potential reduction by nutrient reallocation (7 %–50 %) reported in Bach et al. (2021).

In the model, MOS thus gradually reduces atmospheric CO₂ and thereby also limits global warming with respect to the pre-industrial period (Δ SAT; Fig. 2.4); i.e., the temperature increase of 2.14 °C by the year 2100 is 0.38 °C lower than Δ SAT of Control_RCP 4.5

Table 2.5: Model simulations under the RCP 4.5 emission scenario. MOS-C represents the carbon sequestered via MOS. C_{atm} , C_{oc} and C_{ter} stand for atmospheric, oceanic and terrestrial carbon reservoirs respectively. ΔSAT stands for surface-averaged temperature relative to 13.18°C, the pre-industrial.

Experiment	pCO ₂ (ppm)		Cumulative CO ₂ emission (PgC)		MOS-C (PgC)		FR (%)	C_{atm} (PgC)	C_{oc} (PgC)	C_{ter} (PgC)	ΔSAT (°C)	Phyt NPP (PgC/yr)							
	2100	3000	2020–2100	2020–3000	2020–2100	2020–3000													
Year	2100	3000	2020–2100	2020–3000	2020–2100	2020–3000	2100	3000	2100	3000	2100	3000							
Control_RCP 4.5	573.1	615.5	718.1	1392	–	–	–	–	1217	1307	37611	38180	1854	1935	2.52	4.32	47.6	56.8	
Normal MOS experiments minus Control_RCP 4.5																			
MOS_Conti	–67.2	–297.0	718.1	1392	270.0	2533	100	75.3	–142.6	–630.5	171.8	901.9	–29.7	–278.8	–0.38	–2.87	–9.5	–22.2	
MOS_Stop	–67.2	–28.5	718.1	1392	270.0	270.0	100	58.6	–142.6	–60.5	171.8	77.4	–29.7	–16.8	–0.38	–0.23	–9.5	–1.8	
Sensitivity MOS experiments minus Control_RCP 4.5																			
MOS_AU_Conti	–108.7	–225.3	718.1	1392	446.8	1970	99.9	72.9	–230.7	–452.3	283.9	665.3	–53.2	–186.8	–0.63	–2.49	–5.1	–13.0	
MOS_AU_Stop	–108.7	–52.3	718.1	1392	446.8	446.8	99.9	64.4	–230.7	–111.1	283.9	143.5	–53.2	–32.4	–0.63	–0.43	–5.1	–3.2	
MOS_Conti_NoRe	–67.3	–310.5	718.1	1392	269.9	2008	100	100	–142.9	–659.2	171.8	964.3	–29.8	–305.0	–0.38	–3.27	–9.5	–15.1	
MOS_Stop_NoRe	–67.3	–54.34	718.1	1392	269.9	269.9	100	100	–142.9	–115.4	171.8	145.0	–29.8	–29.6	–0.38	–0.40	–9.5	–2.9	
MOS_Conti_CN ^{High}	–79.5	–335.1	718.1	1392	329.5	3011	100	75.0	–168.8	–711.4	204.5	1059	–36.3	–347.4	–0.46	–3.61	–9.2	–19.1	
MOS_Conti_CN ^{Low}	–53.6	–270.7	718.1	1392	235.1	2078	100	79.3	–113.7	–574.6	136.1	817.7	–22.7	–229.1	–0.30	–2.67	–9.4	–22.9	

but is still missing the 2 °C target.

When AU is deployed in conjunction with MOS, the CDR capacity and mitigation effects of MOS are enhanced (Figs. 2.4a, c, 2.5). By the end of year 2100, 446.8 Pg carbon is sequestered by MOS_AU, an increase of 39.5 % relative to normal MOS. Correspondingly, MOS_AU successfully achieves the 2 °C target of the Paris Agreement by maintaining a Δ SAT at 1.89 °C relative to pre-industrial (Fig. 2.4c and Table 2.5). As in the run without AU, essentially all of the carbon captured via MOS is stored in the ocean until the end of the 21st century (FR, Table 2.5).

Global carbon cycle impacts

The net effect of the MOS-induced climate–carbon cycle perturbation is an increase of the oceanic carbon reservoir (C_{oc}) and a decrease of the atmospheric and terrestrial carbon reservoirs (C_{atm} , C_{ter}). MOS enhances oceanic carbon uptake by increasing the atmosphere to ocean carbon flux (Fig. A.14), which is driven by the DIC removal by MOS in the oceans' surface layers. However, the terrestrial carbon reservoir declines (relative to Control_RCP 4.5) in all MOS simulations (Table 2.5). The atmosphere-to-land carbon flux is reduced in MOS simulations (Fig. A.13). One cause is the photosynthesis that is reduced by lower CO₂ fertilization of land biota (Keller et al., 2018). This result is in line with other studies showing that CDR can lead to a weakening and even reversal of natural carbon sinks (Keller et al., 2018). For instance, by the year 2100 (Table 2.5), due to the declined terrestrial carbon pool (C_{ter} , –29.7 PgC), the reduction in atmospheric carbon pool (C_{oc} , –142.6 PgC) is less than the gain in the ocean (C_{oc} , 171.8 PgC). Besides, it is also worth noting that the increment of C_{oc} in MOS and MOS_AU is 171.8 and 283.9 PgC, which is less than the cumulative amount of carbon sunk out of the surface layer via MOS by year 2100 (Table 2.5). One reason is that the reduced oceanic carbon uptake by declined PNPP (phytoplankton net primary production; Sect. 2.4.3) offsets the MOS-induced carbon sequestration. As shown in Fig. 2.9, by the year 2100, global PNPP has been reduced by 20 %, while POC export has been reduced by 30 % in MOS_Stop.

MOS also impacts the distribution of DIC in the ocean. The DIC profiles in Fig. 2.6 illustrate that the general effect of MOS is to move more DIC to a greater depth ($z \geq 3000$ m). By the end of year 2100, MOS simulations show an increased total DIC concentration in the deeper oceans when compared to Control_RCP 4.5 (except for the zero-remineralization sensitivity runs discussed below). For instance, in the deep Southern Ocean, the DIC concentration is, on average, nearly 80 $\mu\text{mol kg}^{-1}$ higher than the Con-

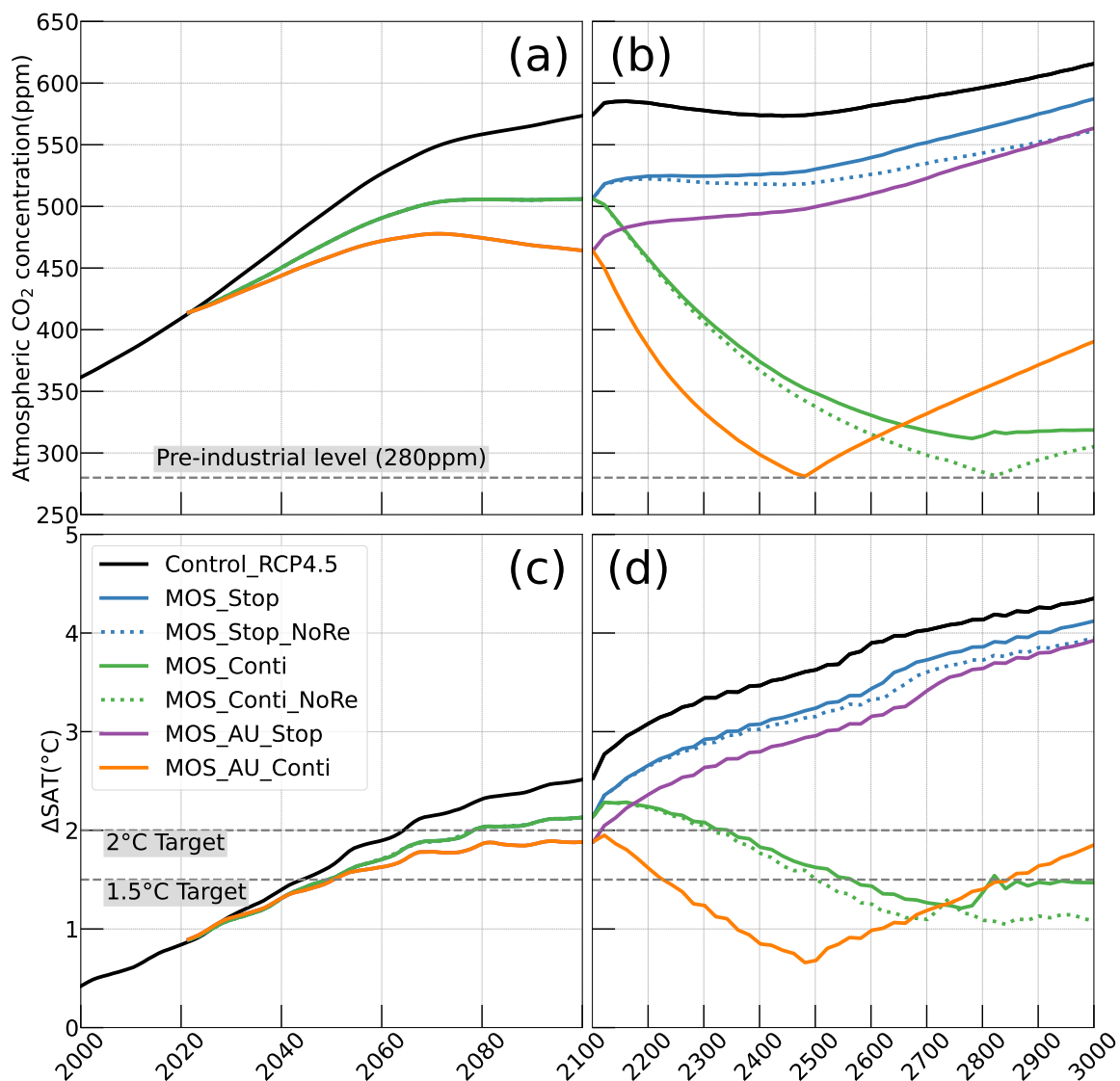


Figure 2.4: Simulations of (a, b) annual global mean atmospheric CO₂ concentration and (c, d) surface-averaged temperature relative to the pre-industrial (average of year 1850 to year 1900) level of 13.18 °C (Δ SAT). Under RCP 4.5 scenario, MOS reaches the 2 °C target in conjunction with AU, while the 1.5 °C cannot be met in all MOS simulations. Note that MOS is terminated whenever pre-industrial concentrations of atmospheric CO₂ are reached, as seen for MOS_AU_Conti (solid orange) and MOS_Conti_NoRe (dotted blue) in (b, d). Both atmospheric CO₂ and Δ SAT remain lower than control after MOS termination.

rol_RCP 4.5 in year 2100 (Fig. 2.6). The conjunction of MOS with AU increases average deep-ocean DIC even more. An example is the simulated increase of DIC in the deep Pacific Ocean and Atlantic Ocean basins by MOS_AU in year 2100 (orange line in Fig. 2.6, DIC panel). In contrast, DIC concentrations are reduced in shallower waters (depth < 1000m), as the air–sea carbon flux is unable to fully compensate for the carbon removal

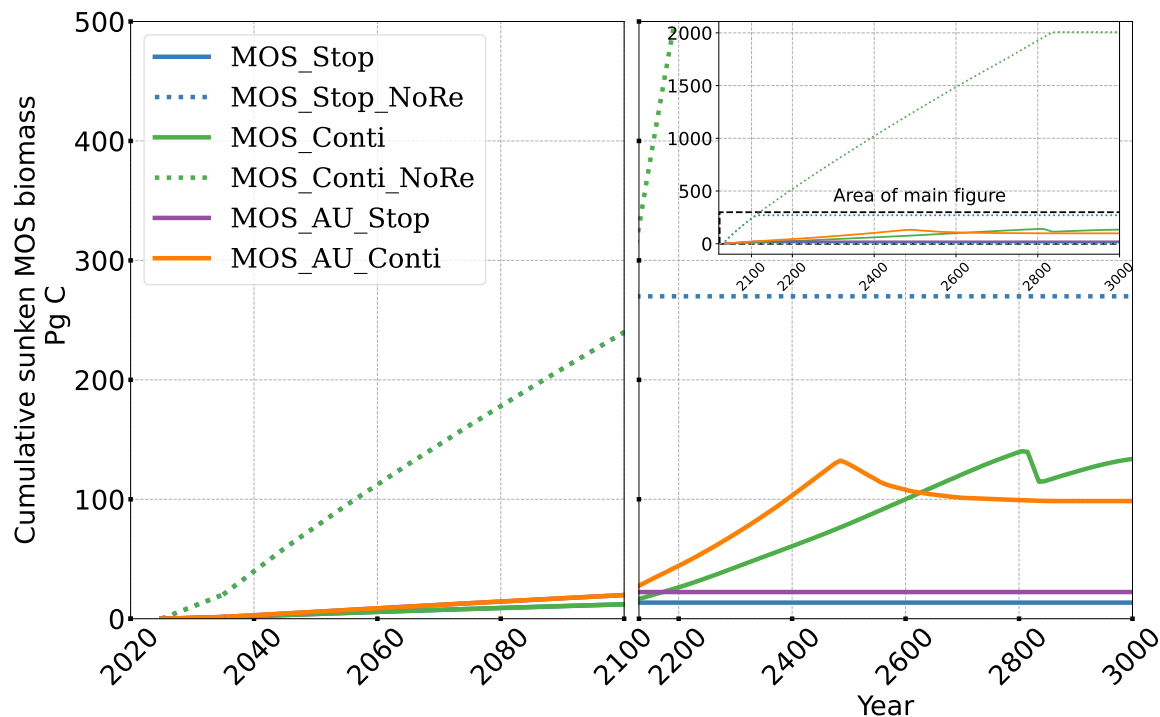


Figure 2.5: Temporal evolution of globally integrated sunken macroalgal biomass on the seafloor. Biomass generally increases with fertilization by AU. In the idealized zero-remineralization simulations, all sunken macroalgal biomass remains on the seafloor, and globally integrated sunken macroalgal biomass shows a monotonous increase.

by MOS. The current model results provide additional evidence that the CDR potential of MOS is partly offset by its negative impacts on the pelagic biological production and the biological carbon pump. In an additional model run (not shown) without MOS but with CO_2 emissions reduced by the annual equivalents of the MOS-induced carbon exports, yielding a total amount of 270 PgC by year 2100, the 270 PgC emissions removal yields a reduction of atmospheric CO_2 by 171.5 GtC by year 2100. This reduction is 20 % higher than the atmospheric CO_2 reduction of 142.6 PgC realized in the original MOS simulation where the MOS-induced shading and removal of nutrients from the surface layers reduce the biological carbon pump and the associated carbon storage in the ocean. When CO_2 emissions are instead cut by an amount corresponding to 80 % of the MOS-induced carbon export, atmospheric CO_2 concentrations simulated by the MOS-free emission-cut runs agree closely with those of the respective MOS experiments. That is, each tonne of CO_2 sequestered in the ocean by MOS is, in our model and on a 100-year timescale, equivalent to an emission cut of about 0.8 t of CO_2 .

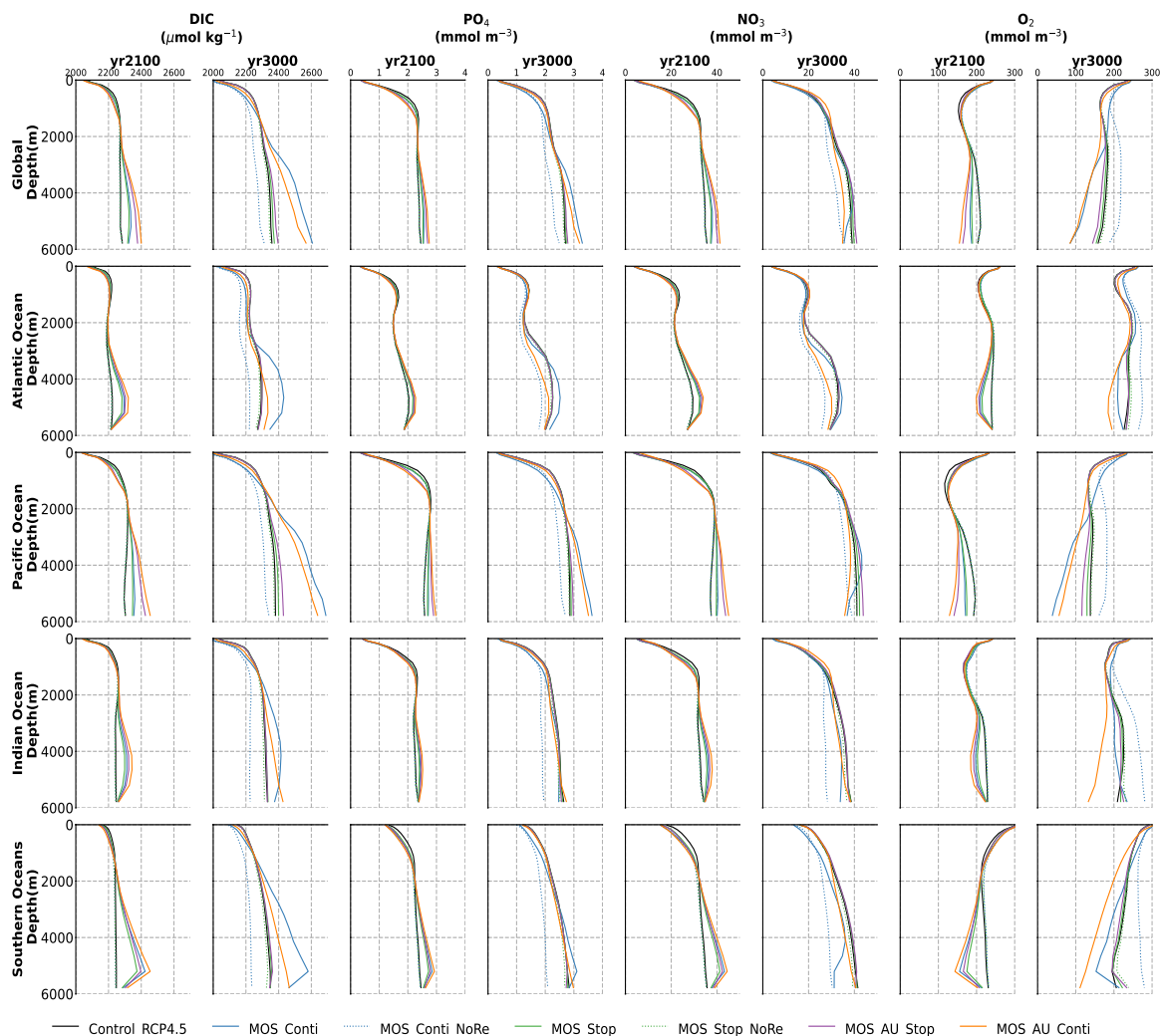


Figure 2.6: Global and basin-wide averaged vertical profiles of various model tracers in year 2100 and year 3000 under the RCP 4.5 emission scenario. In general, MOS (except for the zero-rem mineralization one) transports DIC and nutrients in the surface layer to the deep ocean. The oxygen levels are increased in the mid layers due to the declined downward organic-particle flux (Sect. 2.4.3), but they are decreased in the deep ocean as a result of the remineralization of sunken biomass. These impacts are strengthened when MOS is deployed continuously and/or in conjunction with AU.

Impacts on global nutrients distributions

By the year 2100, the deployment of MOS has changed the global patterns of NO_3 and PO_4 . At the surface, NO_3 and PO_4 concentrations decrease due to MOS nutrient consumption. In the deep ocean (depth ≥ 3000 m), PO_4 and NO_3 increase due to the remineralization of sunken macroalgal biomass (except for in the MOS_NoRe simulations). The largest increase in deep-ocean PO_4 appears in the Southern Ocean, while the smallest increase is found in the Indian Ocean (PO_4 yr2100 groups in Fig. 2.6). This is caused by

the distribution of MOS in the surface layer, which, in our simulations, occupies large areas in the Southern Ocean but only a relatively small region in the Indian Ocean (Fig. 2.2).

The remineralization of sunken biomass consumes dissolved oxygen and releases NO_3 and PO_4 . However, low-oxygen environments and the associated switch from aerobic remineralization to denitrification occupy relatively small areas so that this impact is not easily detectable in global nutrient profiles.

In addition to the localized depletion of nutrients by MOS, the MOS-induced Southern Ocean uptake and transport of N and P to the deep ocean act as a type of “nutrient trapping” (Fig. A.5). These dynamics thereby reduce nutrients and productivity in middle to low latitudes because less N and P are available to be transported out of the Southern Ocean. A similar dynamic has been seen in modeling studies of ocean iron fertilization (Oschlies et al., 2010a; Keller et al., 2014).

Impacts on simulated pelagic ecosystems and the organic particle export

In our simulations, large-scale deployment of MOS has an impact on pelagic ecosystems, mainly on phytoplankton NPP (PNPP) and biomass.

In the MOS simulations (MOS_Conti/Stop), globally integrated annual PNPP decreases by 20 % (9.5 PgC yr^{-1}) by year 2100 (Table 2.5). One reason is the canopy shading effect of the floating macroalgae farms, which reduces downward solar radiation available for the phytoplankton community below. In addition, there is nutrient competition between macroalgae and phytoplankton. As shown in Fig. 2.7a, by the end of the 21st century, PNPP will decline in MOS areas, e.g., the northern and eastern equatorial Pacific and the Southern Ocean. Intriguingly, in a few regions outside the MOS deployment region, PNPP has increased instead. For instance, a “halo” of enhanced PNPP can be observed surrounding the eastern equatorial Pacific MOS region (Fig. 2.7a). Similar circumstances are simulated in the North Pacific, in the Southern Ocean (60° E : 120° E , 30° S) and off the equatorial west coast of Africa. This PNPP enhancement is sustained by the outflow of residual nutrients from MOS deployment regions (see Fig. A.12). One reason is that the macroalgae growth is constrained by the maximum biomass yield, as described in Sect. 2.2.2. Macroalgae nutrient uptake thus cannot compensate for the loss of nutrient consumption by light-limited PNPP within the MOS region, which results in enhanced surface nutrients compared to the simulation without MOS, especially when AU supplies additional nutrients to the surface.

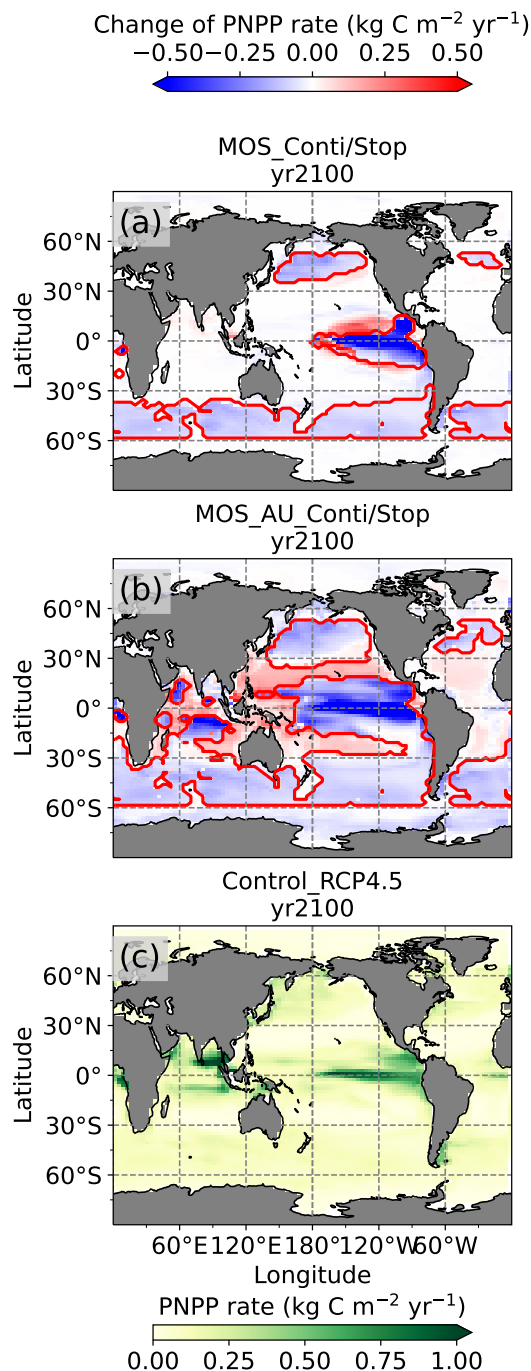


Figure 2.7: Vertically integrated annual PNPP in year 2100. (a, b) MOS minus Control_RCP 4.5, with red boundaries contouring the MOS-occupied area; (c) Control_RCP 4.5; (a) illustrates a decline in PNPP in MOS-occupied areas accompanied by a “halo” of enhanced PNPP surrounding MOS areas, particularly in the ETP caused by the leakage of residual nutrients (Sect. 2.4.3). These impacts on PNPP are amplified in MOS_AU (b).

In the MOS_AU simulations, the PNPP “halo” can be seen in almost the entire MOS-free ocean surface (Fig. 2.7b). The AU fertilization effect enhances the nutrient leakage

from the MOS area. This leads to a higher PNPP in MOS_AU than in the normal MOS simulations (Fig. 2.7c), but one that is still lower than in the Control_RCP 4.5 run (Fig. 2.9a1).

Changes in the global particulate organic carbon (POC) export flux generally follow the pattern of PNPP changes (Fig. 2.9b1). Thus, when MOS is present, the PNPP reduction results in a weakened POC flux.

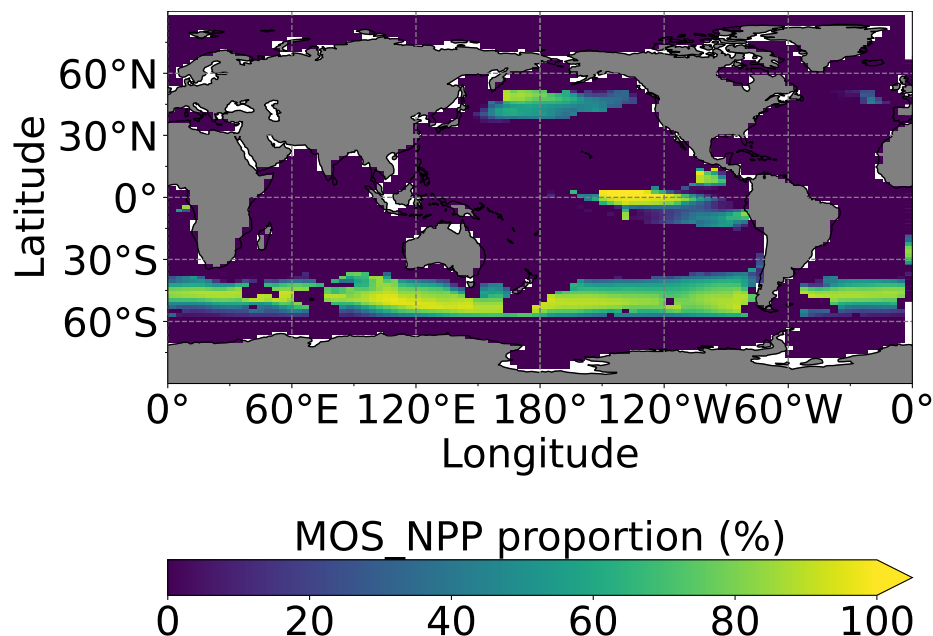


Figure 2.8: Proportion of MOS NPP in the global oceanic NPP by year 2100 ($\text{MOS_NPP}/(\text{MOS_NPP} + \text{PNPP}) \times 100$). Note that the NPP values are converted to carbon using the respective C:N ratio. The MOS_NPP generally amounts to more than 70 % of total oceanic NPP where MOS is deployed, indicating an obvious NPP shift from phytoplankton PNPP to MOS_NPP.

Figure 2.8 illustrates the shift of oceanic NPP from PNPP to MOS_NPP. In regions where MOS is deployed, 70 % of the total NPP is macroalgae NPP. The macroalgal NPP is thus nearly twice as high as PNPP. This may lead to additional ecological and biogeochemical issues. One of them is the decline of zooplankton led by the reduced PNPP in this study. We performed an additional simulation, in which the zooplankton grazing on MOS is turned off, and the grazing preferences follow the original settings in Keller et al. (2012). As shown in Fig. A.15, the grazing by zooplankton on MOS has no significant effect on either the zooplankton biomass or the MOS_NPP. As the zooplankton grazing preference for macroalgae is lower than for phytoplankton, the zooplankton community is still mainly fed by phytoplankton. Therefore, the decline in zooplankton biomass (Fig. A.7) follows the declining phytoplankton biomass trend (Fig. A.9).

Impacts on dissolved oxygen

The two major impacts of MOS on oceanic dissolved oxygen are as follows: (1) increased deoxygenation at the seafloor by the remineralization of sunken macroalgal biomass (except for in MOS_NoRe) and (2) increased dissolved oxygen at middle depths (e.g., 300 m depth) caused by the reduction of the downward POC flux and the associated decline in

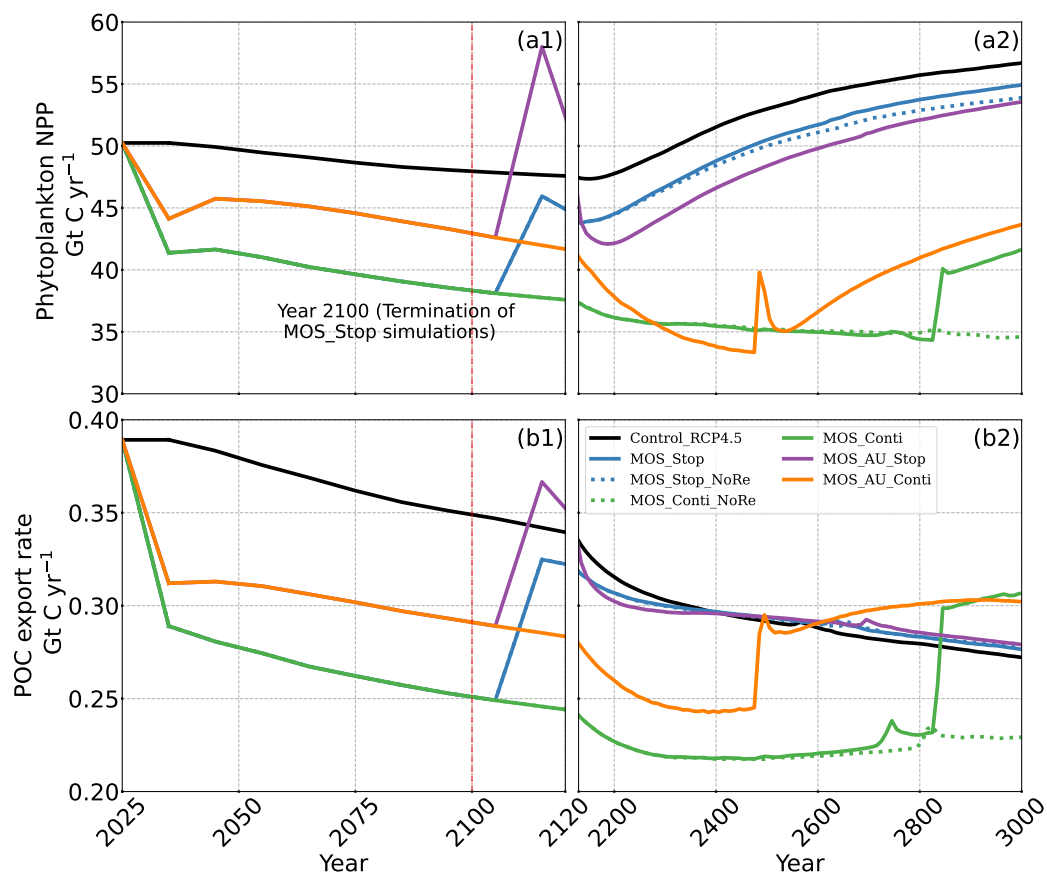


Figure 2.9: Temporal evolution of globally integrated PNPP (**a1**, **a2**); downward POC flux at 2 km depth (**b1**, **b2**). The termination runs branch off of the continuous ones in year 2100 and are identical up to that point. Through the 21st century, MOS reduces PNPP and POC export due to canopy shading and competition for nutrients. Obvious rebounds followed by quick decline can be observed right after terminations of MOS.

oxygen consumption by POC remineralization.

In Control_RCP 4.5, the global oceanic dissolved oxygen inventory decreases throughout the simulation. The two main driving mechanisms are the reduced solubility in the warming ocean and the decelerating overturning circulation. The long-term decline of oxygen is especially obvious at depth (1200 m), which is induced by increasing deep-water residence times and the accumulation of respiratory oxygen deficits under global warming (Oschlies et al., 2019; Oschlies, 2021).

As a result of reduced respiration in the upper water column, the size of the oxygen-minimum zone (OMZ) in the eastern tropical Pacific (ETP) shrinks substantially, and the volume of water with $O_2 < 80 \text{ mmol m}^{-3}$ in the North Pacific even disappears. In the Southern Ocean, dissolved oxygen increases as well (Fig. 2.10c). This is more pronounced when AU is applied (Fig. 2.10e). The increase in dissolved oxygen is caused by decreased micro-

bial remineralization of POC, a consequence of the reduced downward POC flux resulting from the inhibition of PNPP in the surface layer (Sect. 2.4.3). Some decrease in oxygen concentrations occurs in the western Pacific and the Indian Ocean (Fig. 2.10g), where the surface PNPP is enhanced by the surplus nutrients that leaked out from the MOS-occupied area (see Sect. 2.4.3 and Fig. 2.7c).

Figure 2.10d, f and the O_2 yr2100 panel of Fig. 2.6 illustrate how MOS changes dissolved oxygen in the deep ocean. Within the normal MOS simulations, the decline of benthic dissolved oxygen has mainly happened in the Southern Ocean by year 2100, with the appearance of a few new areas with oxygen concentrations of less than 80 mmol m^{-3} (Fig. 2.10d). However, when AU is also deployed, the increased macroalgal biomass sinking and remineralization creates even more benthic low-oxygen zones (Fig. 2.10f) in the ETP and North Pacific Ocean. These new locations correspond to MOS-occupied surface areas.

2.4.4 Long-term effects of MOS

Here, we will analyze the long-term effects of hypothetical massive MOS deployment beyond the Paris Agreement timeframe on a millennial timescale.

Even after a simulated continuous millennial-scale deployment, the distribution of MOS in year 3000 is nearly identical to the one in year 2100 with only a minimal decrease in biomass (Fig. A.4b). When deployed beyond the year 2100 (MOS_Conti), MOS will continue to sequester carbon and reduce atmospheric CO_2 on millennial timescales or, in our setup, until atmospheric CO_2 falls back to the pre-industrial level of 280 ppm. The MOS_Conti simulation ultimately sequesters 2533 PgC and decreases atmospheric CO_2 to 318.5 ppm CO_2 by the year 3000 but never achieves the pre-industrial CO_2 level. Notably, atmospheric CO_2 stops decreasing by year 2780 and rebounds afterwards even though MOS continues to sequester carbon. This can be explained by a recurrent deep convection in the Southern Ocean around year 2800 that accelerates oceanic carbon leakage back to the atmosphere (Martin et al., 2013; Reith et al., 2016; Oschlies, 2021). Meanwhile, the leakage of MOS-captured carbon eventually offsets the MOS carbon sequestration (Sect. 2.4.6).

In the sensitivity simulations MOS_Conti_NoRe and MOS_AU_Conti, atmospheric CO_2 reaches 280 ppm by the years 2820 and 2475, respectively. After reaching 280 ppm, MOS is stopped, and atmospheric CO_2 increases again as remineralized carbon leaks out of the ocean and as the surface ocean adjusts to the no-MOS situation. The largest increase in CO_2 is found in MOS_AU_Conti. Meanwhile, when MOS is deployed (uninterrupt-

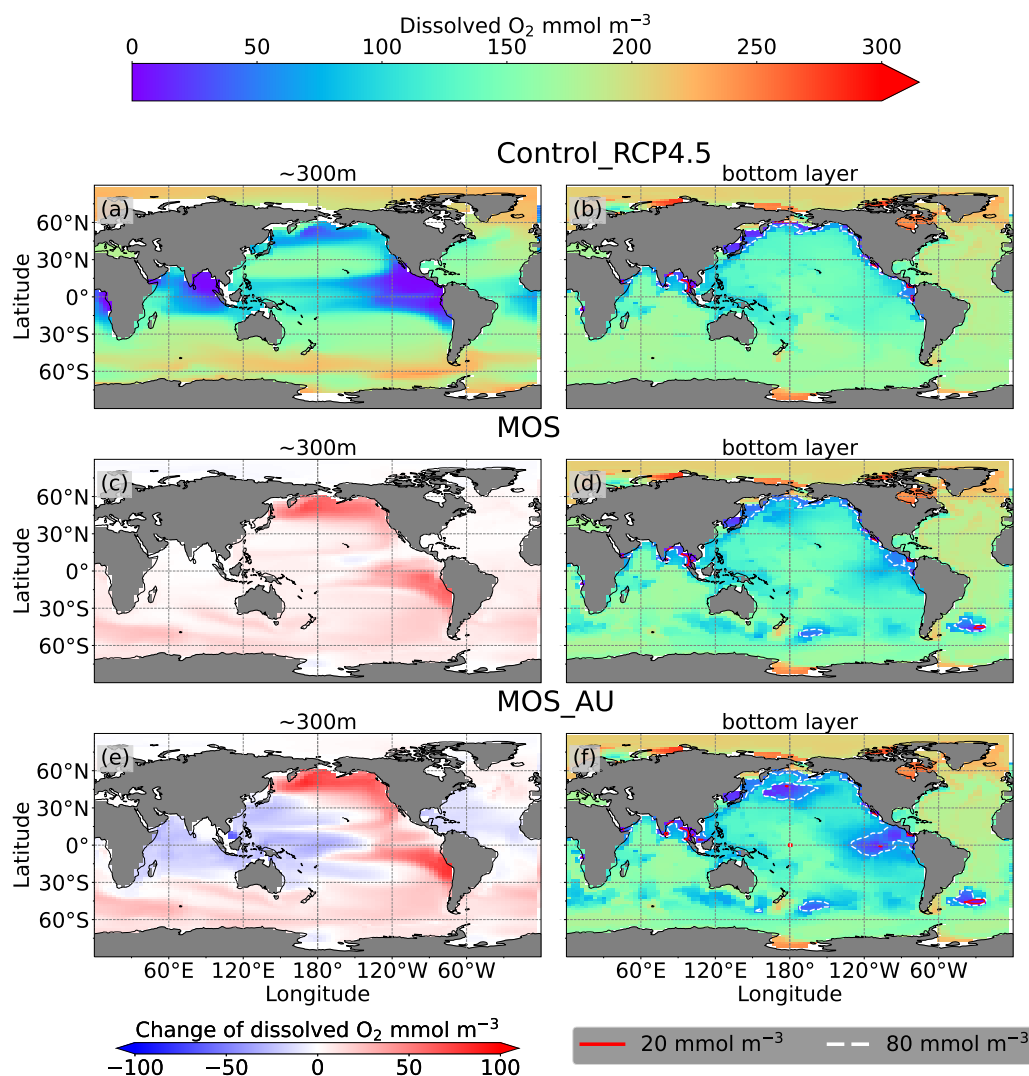


Figure 2.10: Dissolved O_2 concentration distribution in year 2100 at 300 m depth (**a**, **c**, **e**) and at the seafloor (**b**, **d**, **f**); lines delineate boundaries of OMZs at any location within the water column with less than 80 mmol m^{-3} oxygen (dashed white) and less than 20 mmol m^{-3} oxygen (solid red). At 300 m depth, elevated dissolved-oxygen levels in MOS simulations are caused by the decline in POC export (**c**); exceptions are the reduced oxygen concentrations in regions outside the MOS_AU deployment (**e**). On the seafloor, remineralization of sunken biomass creates several new low-oxygen areas (**d**, **f**).

edly or till the CO_2 280 ppm trigger), the land carbon uptake is constantly lower than the control level owing to the reduced CO_2 fertilization effect. Due to the permanent storage of MOS-C in sunken biomass, rebounds of atmospheric CO_2 are relatively gentle in MOS_Conti_NoRe (Fig. A.14). Nevertheless, the atmospheric CO_2 levels in continuous MOS simulations are significantly lower (35 % to 50 % of Control_RCP 4.5) by the end of year 3000.

The side effects of MOS also persist and often grow in magnitude with continuous deployment. Though PNPP is enhanced around MOS areas by means of nutrient leakage (PNPP “halo”; see Sect. 2.4.3), the global reduction of surface nutrients and local canopy shading by MOS leads to continuous but gentle lowering of global PNPP after the sharp decreases in the initial 20 years (Fig. 2.9a2). For instance, in MOS_Conti, PNPP drops by $\sim 60\%$ by the end of year 3000 (Table 2.5). Correspondingly, in MOS_Conti POC export eventually declines by 50% relative to Control_RCP 4.5 (Fig. 2.9b2). In sensitivity run MOS_AU_Conti, the nutrient supply by AU, which initially maintains a higher phytoplankton biomass and NPP than in MOS without AU (Sect. 2.4.3), declines with time as source waters of the upwelling become reduced in nutrients. Therefore, PNPP and the POC export levels drop after year 2200 (Fig. 2.9a2, b2).

The redistribution of DIC and nutrients is intensified in the continuous simulations. As shown in Fig. 2.6, when remineralization of MOS sunken biomass is turned on, the Pacific deep ocean and the Southern deep ocean show the highest DIC and PO_4 enrichment by year 3000. The accumulations depend on ocean circulation (e.g., thermohaline circulation) and the distribution of MOS at the surface. In MOS_Conti_NoRe, the ocean DIC decreases globally relative to Control_RCP 4.5. This results from the continuous DIC removal into biomass via MOS with no remineralization. Another cause of the declined global DIC is the declining downward POC flux owing to the PNPP reduction caused by the declining nutrient levels in the surface layer (see Sect. 2.4.3). NO_3 enrichment in the deep ocean is considerably smaller than that of DIC and PO_4 because of enhanced denitrification in the developing benthic low-oxygen regions (Sect. 2.4.3, Fig. A.6). In the zero-remineralization situations, deep-ocean PO_4 and NO_3 concentrations decrease compared to the control levels due to the reduced remineralization of POM resulting from the weakened downward flux of POM.

As shown in Fig. 2.11 and the O_2 yr3000 panel of Fig. 2.6, dissolved oxygen concentrations at middle depth (e.g., 300 m) increased during millennial MOS deployment due to reduced PNPP and associated downward flux and remineralization of POM in the water column. In benthic waters, regions with very low dissolved oxygen are shown in Fig. 2.11f, j in the Pacific and Southern oceans. In contrast, increased oxygen concentrations are found in MOS_Conti_NoRe (Fig. 2.11h), especially in the Atlantic, the Indian and the Southern oceans. Besides the absence of oxygen consumption by macroalgal biomass remineralization, another reason for these oxygen increases lies in the reduction of POC downward flux described in Sect. 2.4.3.

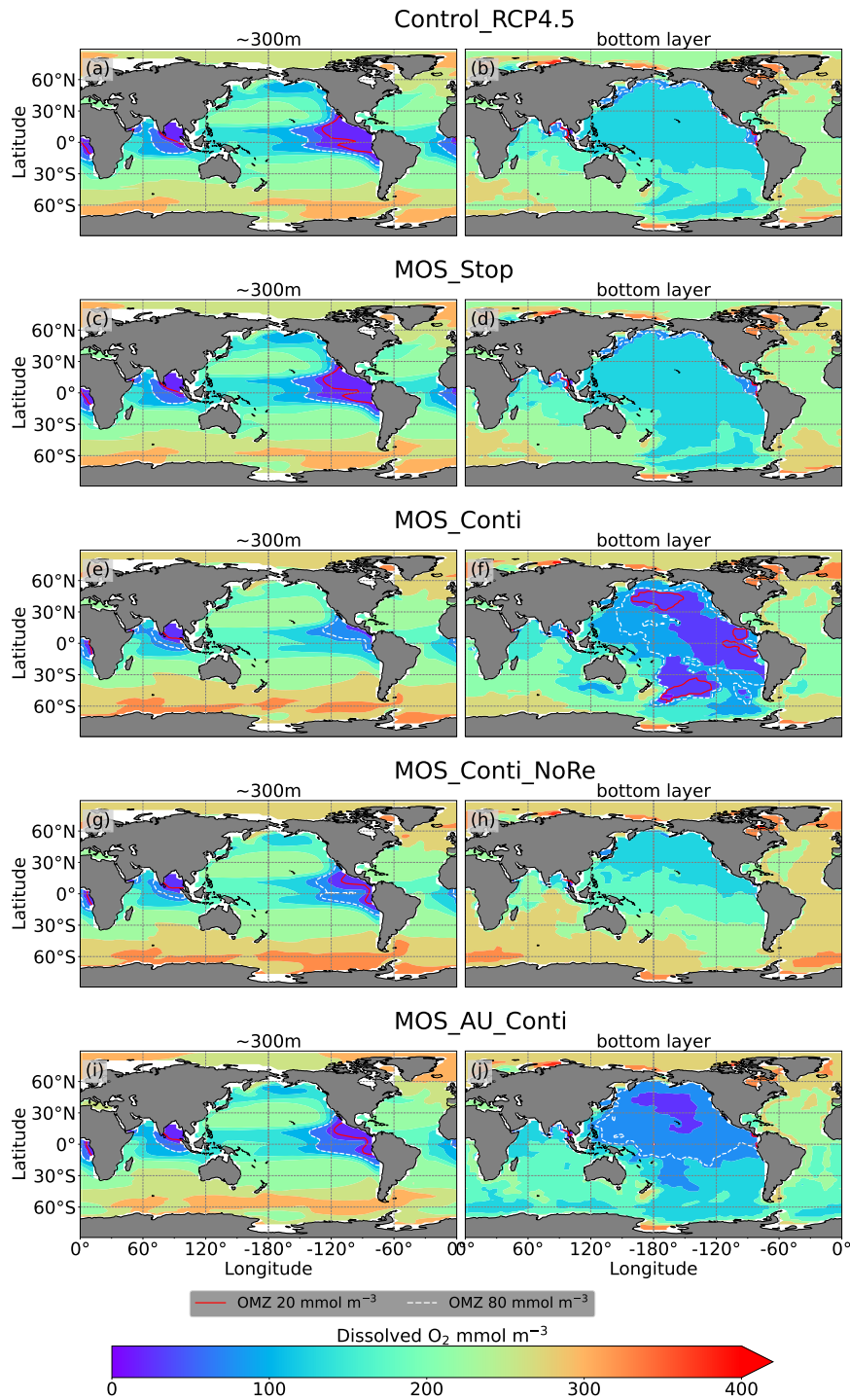


Figure 2.11: Dissolved O_2 concentrations at depth $\sim 300\text{m}$ (left panel) and the ocean bottom (right panel) in year 3000: contour lines indicate boundaries of OMZs with less than 80 mmol m^{-3} oxygen (dashed white) and less than 20 mmol m^{-3} oxygen (solid red). Continuous MOS deployment further shrinks the OMZ at 300m depth (**e**, **g**, **i**) but expands them at the bottom (**f**, **j**), except for the zero-remineralization one in (**h**).

2.4.5 Termination effects

After termination of MOS_Stop in year 2100, the atmospheric CO₂ concentrations and SAT (surface-averaged temperature) both rise but generally remain lower than those of the Control_RCP 4.5 simulation (Fig. 2.4b, d). More than half (FR ranges from 58.6 % to 64.4 %, Table 2.5, calculated by Eq. 2.23) of MOS-captured carbon is still stored in the ocean by the end of year 3000. As shown in Fig. 2.4b, d, in the termination simulations MOS_Stop and MOS_AU_Stop, CO₂ concentration and SAT gradually converge against the Control_RCP 4.5 run as a result of DIC from remineralized macroalgal biomass being transported to the ocean surface and into the atmosphere (see subsequent Sect. 2.4.6). By year 3000, the atmospheric CO₂ in MOS_Stop is only 28.5 PgC less than in Control_RCP 4.5, while Δ SAT rebounds slightly from -0.38 to -0.23 °C. In MOS_AU_Stop, the differences between pCO₂ and Δ SAT are smaller than the normal MOS, as AU has augmented MOS carbon sequestration, and 64.4 % of it is retained in the ocean. As expected, the idealized non-remineralization condition (MOS_Stop_NoRe) is able to permanently store the sequestered carbon; thus, the rebounds of CO₂ and Δ SAT are less than the normal MOS_Stop.

In all MOS termination simulations, PNPP and POC export rebound abruptly following the cessation of MOS, but they sharply drop over the subsequent decades (Fig. 2.7a1). The sharp increase in PNPP and POC export results from the sudden absence of macroalgae as a main competitor for nutrients and light. The subsequent decline in PNPP and POC export results from the consumption of the surface nutrients and the lack of subsurface nutrients that had previously been exported directly to the seafloor with the sinking of macroalgae biomass (Fig. A.10). Afterwards, PNPP recovers gradually due to the slow returning of remineralized nutrients to the upper ocean. By the year 3000, PNPP in MOS_Stop recovers to 97 % of the control level (Table 2.5), with the only differences being attributable to the slightly different climate state. In the MOS_NoRe simulation, the PNPP recovery is slower due to the permanent nutrient removal from the upper water column. In the MOS_AU_Stop simulation, PNPP rebounds to higher levels than the normal MOS but drops to lower levels afterwards. The amplified oscillation of PNPP results from the simultaneous termination of AU and MOS: when MOS_AU_Stop is suddenly terminated, the canopy shading and nutrient competition by MOS are removed. Meanwhile, the surplus of nutrients from AU still remains. This boosts PNPP rapidly. However, once these nutrients are consumed, the natural nutrient supply to surface waters is insufficient to maintain the high PNPP.

After the termination of MOS, the rate of oceanic carbon uptake falls abruptly (Fig. A.14). After a short peak caused by the abrupt rebound of PNPP, it remains slightly lower than the control level due to the declined PNPP rates and lower atmospheric CO₂ levels. Oppositely, the MOS-induced reduction in terrestrial carbon uptake starts to rebound after MOS cessation (Fig. A.13) due to the rise of atmospheric CO₂, which tends to enhance the terrestrial photosynthesis.

When MOS deployment is stopped, the elevated (compared to Control_RCP 4.5) dissolved-oxygen concentrations at middle depth generally decline as the downward POC flux recovers (O₂ yr3000 panel in Fig. 2.6). The lowered oxygen concentrations in the deep ocean are also reversible after cessation of MOS. For instance, by year 3000, the benthic dissolved oxygen of MOS_Stop (Fig. 2.10d) is similar to that of Control_RCP 4.5 (Fig. 2.10b).

2.4.6 Leakage of MOS-sequestered carbon

The leakage of MOS-sequestered carbon (MOS-C) occurs mostly in the Southern Ocean (Fig. 2.12, A.8). The explanation lies in the dynamics of Southern Ocean upwelling, where Pacific deep water (PDW), Indian deep water (IDW) and Antarctic deep water (AADW), laden with DIC of remineralized MOS biomass, reach the subantarctic ocean surface (Talley, 2013; Weber and Bianchi, 2020; Anderson and Peters, 2016). Moreover, the recurrent deep convection (see Sect. 2.4.4) in the Southern Ocean around year 2600 accelerates the carbon leakage, which can be observed in Fig. 2.12 as an enhanced outgassing around year 2600.

The outgassing of MOS-C in discontinuous simulations (e.g., MOS_Stop) starts from year 2100, while the continuous ones starts from year 2300 (Fig. 2.12). Thus, by the end of the 21st century, nearly all the MOS-C in all MOS simulations is retained in the ocean. However, by the year 3000, even in the continuous MOS simulation, only about 75 % of MOS-C remains in the ocean, while the accelerated vertical water transport by AU slightly reduces this portion to 73 %. In run MOS_Stop, 59 % of MOS-C remains in the ocean by year 3000, whereas the additional sunken macroalgal biomass in MOS_AU_Stop results in more MOS-C (64 %) being retained (Table 2.5). When sunken biomass is free from remineralization (NoRe runs), the contained carbon is permanently isolated from the atmosphere and stored in the ocean.

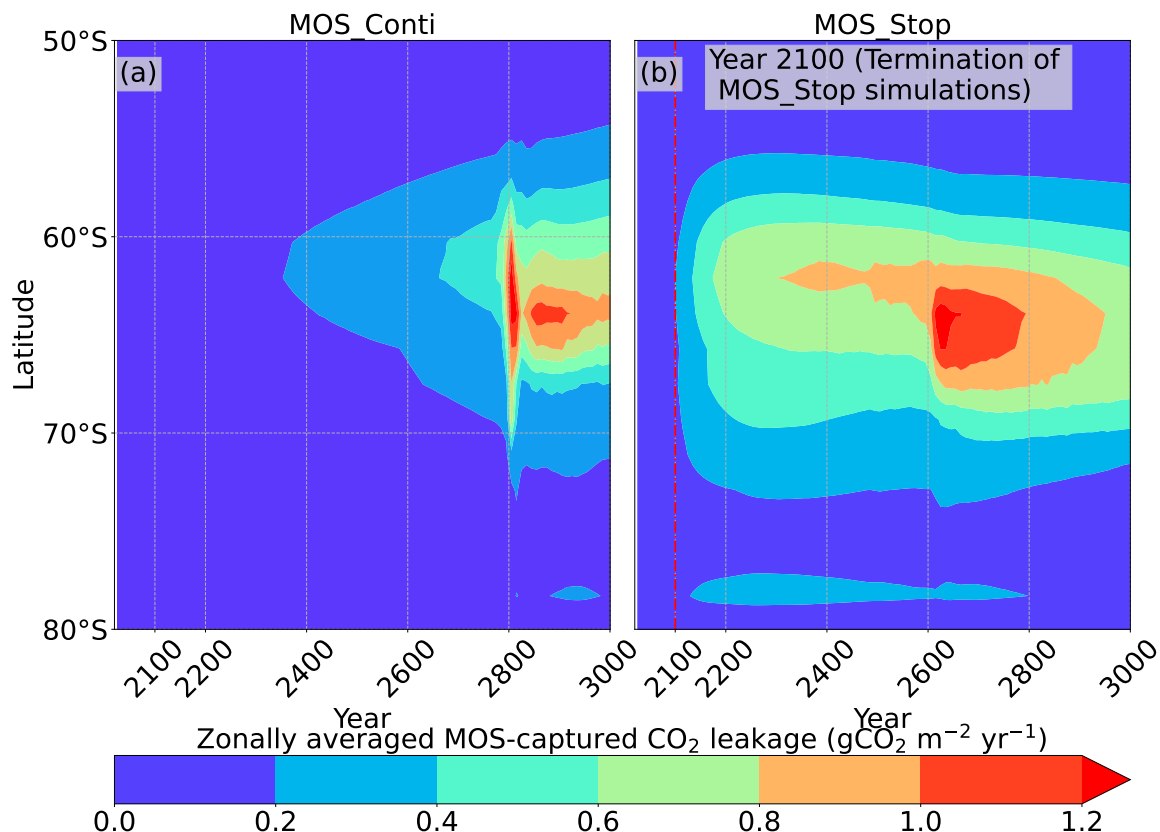


Figure 2.12: Zonally averaged MOS-captured carbon outgassing in the simulation (a) MOS_Conti and (b) MOS_Stop. When conveyed back to the surface, the DIC from MOS remineralization participates in the air–sea exchange (Sect. 2.2.2). MOS-C outgassing starts in year 2100 when MOS is terminated (a) or after year 2300 when MOS is continuously deployed. The outgassing mainly happens in the Southern Ocean. The outgassing is strengthened around year 2800 when a Southern Ocean deep-convection event accelerates the upwelling of deep waters with high concentrations of remineralized DIC (Sect. 2.4.4).

2.5 Concluding discussions

In this study, we have tested the potential of the “macroalgae open-ocean mariculture and sinking (MOS)” as a carbon dioxide removal method. Although environmental conditions (e.g., nutrients, temperature) in the open oceans differ considerably from the coastal and/or near-shore regions where macroalgae aquaculture is currently applied in reality, our simulations suggest that, in certain open-ocean regions, macroalgae may successfully grow and sequester carbon (if engineering constraints can be overcome).

Even for continuous deployment at a maximum scale currently deemed possible, MOS alone is not able to reduce the warming to the 2 °C target by the end of the 21st century under the RCP 4.5 moderate-mitigation scenario. This finding is consistent with conclusions from previous studies that no single carbon dioxide removal (CDR) method alone can

ensure that the current climate goals are reached (Keller et al., 2014; Anderson and Peters, 2016; Fuss et al., 2020; Masson-Delmotte et al., 2018). Clearly, emissions reductions must be the primary means of mitigation; a portfolio of CDR options can only complement these other efforts.

In order to estimate the maximum CO₂ removal potential, the possible synergy of MOS with artificial upwelling (AU) has been investigated. The employed AU concept aims at piping nutrient-rich deep water to the surface to enhance the growth of macroalgae in MOS. As expected, AU is found to have the potential to successfully enlarge the growing area of MOS and to enhance the CDR capacity of MOS.

In the first 80 years of deployment, the maximum MOS carbon sequestration potential is 3.38 PgC yr⁻¹ for regular MOS, but it can be boosted up to 5.56 PgC yr⁻¹ with assistance from AU. If deployment is discontinued from year 2100, about 58.6 % to 70.2 % (normal MOS and MOS_AU, respectively) of MOS-sequestered carbon would be retained in the ocean by year 3000.

Several potential side effects have also been revealed and analyzed. One side effect is the reduction in phytoplankton NPP (PNPP) due to canopy shading and nutrient removal from the sea surface to the bottom by MOS. The declined PNPP in turn offsets ~ 37 % of the MOS CDR. Intriguingly, some areas with enhanced PNPP (PNPP “halo”, Sect. 2.4.3) are found surrounding the major areas occupied by MOS, fueled by the residual NO₃ that leaks from MOS areas.

Another strong side effect of large-scaled MOS is the impact on oxygen distributions. Dissolved-oxygen concentrations increase in near-surface and intermediate waters, as MOS reduces the downward flux of plankton-derived organic matter by restraining the surface PNPP. On the other hand, the massive amount of sunken biomass from MOS at the ocean bottom and its subsequent remineralization consumes oxygen and can create large benthic OMZs.

An uncertain factor is the fate of the sunken biomass. It will affect the benthic fauna by depositing large amounts of organic matter, as well as by expanding low-oxygen regions on the seafloor upon oxygen consumption by remineralization. Therefore, we performed additional sensitivity simulations focusing on the macroalgal biomass remineralization rate. When macroalgal biomass does not undergo microbial remineralization, the captured CO₂ can be permanently stored without leakage. This increases the CDR potential of MOS. The benthic OMZs created by remineralization of sunken biomass would also be avoided, while the shrinking of intermediate water OMZs persists. However, other side effects cannot be neglected: in zero-remineralization simulations, the constant removal of nutrients

in the surface will impede the recovery of PNPP. This may eventually affect the marine surface ecology and ocean services such as food provision. These potential side effects are also noteworthy for another macroalgae farming approach, i.e., harvesting the macroalgae biomass for bioenergy with carbon capture or storage (BECCS) or biochar (Sect. 2.3.2).

The impacts of MOS on oxygen distributions may also influence the oceanic sources of N_2O , an atmospheric GHG gas and a major ozone-depleting compound (Ravishankara et al., 2009). The increased and decreased oxygen levels in the middle and bottom layers impact denitrification and may weaken the N_2O sources in the subsurface but increase those in the deep waters (Bange et al., 2019).

Moreover, attention should also be paid to the calcification by calcareous macroalgae (if cultivated) and/or associated epibionts that grow on macroalgae. Bach et al. (2021) have suggested that epibionts living on *Sargassum* offset 16.5 % of the POC fixed by *Sargassum* and therefore decrease its natural carbon sequestration potential if the biomass was intentionally sunk for CDR purposes. These calcification rates and the response to ocean acidification of macroalgae are also species specific (Koch et al., 2013). These factors need to be investigated with further research if macroalgae are to be considered for ocean-based CDR methods.

The production and export of DOC is also an area of further study for large-scale farmed macroalgae for carbon sequestration. Macroalgae have been reported to release considerable amounts of DOC and to contribute to the global DOC export from coastal to open-ocean waters. The estimated global DOC release of macroalgae habitats is 355 Tg C yr^{-1} (Krause-Jensen and Duarte, 2016). The averaged DOC release rate by macroalgae is of 23.2 ± 12.6 mmol C $m^{-2} d^{-1}$ (equivalent to 8.5 ± 4.6 mol C $m^{-2} yr^{-1}$) but with a wide range of 8.4 to 71.9 mmol C $m^{-2} yr^{-1}$ (Barrón et al., 2014). If we simply multiply this annual-averaged DOC release rate with the MOS-occupied area (S_{MOS} , Table 2.5), the estimated annual DOC release by MOS would be 7.1 ± 3.8 PgC (MOS) or 12.9 ± 7.0 PgC (MOS_AU). Although the refractory DOC released by macroalgae could potentially be an additional contribution of carbon sinking by MOS, the available information on the generation and composition of the macroalgae DOC is not enough to parameterize a model of this process, and more research on the topic is needed (Krause-Jensen and Duarte, 2016; Barrón et al., 2014; Barrón and Duarte, 2015).

Another side effect not investigated here is the production and emission of halocarbons from macroalgae farms. Macroalgae species have been reported to generate halocarbons in polar, temperate and tropical coastal regions, with a highest producing rate of 6000 pmol $CHBr_3$ $gFW^{-1} h^{-1}$ (Leedham et al., 2013; Baker et al., 2001; Carpenter and Liss, 2000;

Latumus, 1995). These volatile low-molecular-weight halocarbon compounds (e.g., CH_3I , CHBr_3 and CHCl_3) are potent greenhouse gases (Meinshausen et al., 2011). They also influence stratospheric ozone destruction when transported by deep atmospheric convection into the stratosphere (Ziska et al., 2013; Tegtmeier et al., 2012, 2013), therefore enhancing radiative forcing (Ramaswamy et al., 1992; Daniel et al., 1995). Large-scale MOS cultivation might release a significant quantity of halocarbons. However, as MOS also reduces global phytoplankton NPP, it is likely that the production of halocarbons by phytoplankton decreases. Further studies are needed to investigate the possible effects of halocarbon emissions from large-scale macroalgae cultivation and how this is offset by a potential decrease in phytoplankton halocarbon production.

Meanwhile, here, we only discuss the CDR potential of the MOS-AU combination under an idealized situation, where the artificial upwelling (AU) upwells nutrients without changing the ambient water temperature on the surface. The aim of deploying akin AU to MOS is to assess the maximum potential of CDR, as AU can upwell nutrient-rich deeper water. However, it can be expected that the NPP of MOS will be slower if the ambient water temperature is reduced by the upwelled cold water, which will further limit the CDR potential of MOS_AU. Moreover, several dominant side effects due to the upwelled cold water in ordinary AU have been revealed, such as the quick rebound or even surpassing of CO_2 concentrations and surface temperatures after the termination of AU (Oschlies et al., 2010b). If the cold-water upwelling was included, there would be extra analysis on the associated impacts on planetary radiation budget imbalance, marine biogeochemistry and global carbon pool (e.g., the enhanced terrestrial carbon sequestration due to the cold effects by AU), which are beyond the scope of this study. Thus, we used the hypothetical AU systems excluding thermal exchange to address the nutrients supplementation of AU to MOS and to avoid the unnecessary complexities and side effects in the meantime. However, further studies are required if ordinary AU should be considered in association with macroalgae farming.

Besides the CDR effect of MOS, in the case of large-scale deployment, the macroalgae farms are likely to increase the albedo of the oceans' surfaces, especially when they occur near the sea surface (Fogarty et al., 2018; Bach et al., 2021). Meanwhile, we have not considered possible hydrodynamic impacts on ocean circulation, as the thick macroalgae layers and the farming infrastructures may influence the momentum and mixing of the ambient flow fields (Liu and Huguenard, 2020; Nepf, 2012; Thomas and McLelland, 2015). The MOS model analysis presented here clearly has some limitations that future studies might improve on. One of the most critical issues is to improve the realism of the model

design by including more representative macroalgae species for various regions. Another aspect is the consideration of dynamic cellular stoichiometry of macroalgae. With a better simulation of the cellular quota, we could improve our understanding of the relation of nutrient and carbon fluxes to MOS and the environment. Explicit consideration of the variable morphology of the macroalgae, as well as of the impacts of currents on frond erosion (Broch and Slagstad, 2012), would also improve the representation of macroalgae loss rates in the model. Further optimization of deployment timing and location for MOS are achievable by evaluating data from field tests or implementations of macroalgae mariculture in the open oceans. Another aspect that needs improvement is the modeling of benthic macroalgal biomass remineralization. Here, we treated macroalgal biomass homogeneously as particulate organic matter. Though the degradation of macroalgal fragments under deep-sea conditions (e.g., low temperature and unique microbial colonies) remains unclear, it might be different from POC in terms of remineralization rate and oxygen consumption. Tracking of macroalgae-sequestered carbon will be required to record its fate and possible carbon leakage after sinking (e.g., by an eDNA method to trace macroalgae carbon in marine sediments, such as that by Anglès d'Auriac et al., 2021). The economic perspectives of developing and deploying MOS also need to be investigated. Furthermore, more research on how large-scale macroalgae mariculture will impact human activities (e.g., ocean shipping, fisheries) needs to be undertaken. Associated legal and political issues regarding the usage of international waters for MOS deployment should be considered as well.

Overall, this study adds to the rapidly expanding field of considering macroalgae cultivation for CO₂ removal. The evidence from this study suggests that macroalgae mariculture and sinking has a considerable CDR potential under these idealized conditions, but it brings about substantial side effects on marine ecosystems and marine biogeochemistry. Given this, the concept requires further research with less idealized experimental settings to determine if its CDR benefits outweigh the side effects (Dean et al., 2021).

2.6 References

Rebecca Albright, Lilian Caldeira, Jessica Hosfelt, Lester Kwiatkowski, Jana K. Maclaren, Benjamin M. Mason, Yana Nebuchina, Aaron Ninokawa, Julia Pongratz, Katharine L. Ricke, Tanya Rivlin, Kenneth Schneider, Marine Sesboüé, Kathryn Shamberger, Jacob Silverman, Kennedy Wolfe, Kai Zhu, and Ken

- Caldeira. Reversal of ocean acidification enhances net coral reef calcification. *Nature*, 531(7594):362–365, 2016. ISSN 14764687. doi: 10.1038/nature17155. URL <http://dx.doi.org/10.1038/nature17155>.
- J. N. Aldridge and M. Trimmer. Modelling the distribution and growth of 'problem' green seaweed in the Medway estuary, UK. *Hydrobiologia*, 629(1):107–122, 8 2009. ISSN 00188158. doi: 10.1007/s10750-009-9760-6. URL <http://link.springer.com/10.1007/s10750-009-9760-6>.
- Kevin Anderson and Glen Peters. The trouble with negative emissions. *Science*, 354(6309):182–183, 2016. ISSN 10959203. doi: 10.1126/science.aah4567.
- Thomas R. Anderson, James R. Christian, and Kevin J. Flynn. Modeling DOM Biogeochemistry. In *Biogeochemistry of Marine Dissolved Organic Matter*, pages 635–667. Elsevier, 2015. ISBN 978-0-12-405940-5. doi: 10.1016/B978-0-12-405940-5.00015-7. URL <https://linkinghub.elsevier.com/retrieve/pii/B9780124059405000157>.
- Marc Anglès d'Auriac, Kasper Hancke, Hege Gundersen, Helene Frigstad, and Gunhild Borgersen. Blue Carbon eDNA –A novel eDNA method to trace macroalgae carbon in marine sediments. Technical report, Norwegian Institute for Water Research, 2021. URL <https://niva.brage.unit.no/niva-xmlui/handle/11250/2772376>.
- APAR-e. Macroalgae research inspiring novel energy resources. <https://arpa-e.energy.gov/technologies/programs/mariner>, 2021. last access: 13 February 2023.
- M. J. Atkinson and S. V. Smith. C:N:P ratios of benthic marine plants. *Limnology and Oceanography*, 28(3): 568–574, 1983. ISSN 19395590. doi: 10.4319/lo.1983.28.3.0568. URL <http://onlinelibrary.wiley.com/doi/10.4319/lo.1983.28.3.0568/abstract>.
- Lennart T. Bach, Veronica Tamsitt, Jim Gower, Catriona L. Hurd, John A. Raven, and Philip W. Boyd. Testing the climate intervention potential of ocean afforestation using the Great Atlantic Sargassum Belt. *Nature Communications*, 12(1):2556, 5 2021. ISSN 20411723. doi: 10.1038/s41467-021-22837-2. URL <http://dx.doi.org/10.1038/s41467-021-22837-2><http://www.nature.com/articles/s41467-021-22837-2><https://www.nature.com/articles/s41467-021-22837-2>.
- J. M. Baker, W. T. Sturges, J. Sugier, G. Sunnenberg, A. A. Lovett, C. E. Reeves, P. D. Nightingale, and S. A. Penkett. Emissions of CH₃Br, organochlorines, and organoiodines from temperate macroalgae. *Chemosphere - Global Change Science*, 3(1):93–106, 1 2001. ISSN 14659972. doi: 10.1016/S1465-9972(00)00021-0. URL <https://linkinghub.elsevier.com/retrieve/pii/S1465997200000210>.
- Hermann W. Bange, Damian L. Arévalo-Martínez, Mercedes de la Paz, Laura Farías, Jan Kaiser, Annette Kock, Cliff S. Law, Andrew P. Rees, Gregor Rehder, Philippe D. Tortell, Robert C. Upstill-Goddard, and Samuel T. Wilson. A harmonized nitrous oxide (N₂O) ocean observation network for the 21st century. *Frontiers in Marine Science*, 6(APR):1–10, 2019. ISSN 22967745. doi: 10.3389/fmars.2019.00157.

- Cristina Barrón, Eugenia T. Apostolaki, and Carlos M. Duarte. Dissolved organic carbon fluxes by seagrass meadows and macroalgal beds. *Frontiers in Marine Science*, 1(OCT):1–11, 10 2014. ISSN 22967745. doi: 10.3389/fmars.2014.00042. URL <http://journal.frontiersin.org/article/10.3389/fmars.2014.00042/abstract>.
- Cristina Barrón and Carlos M. Duarte. Dissolved organic carbon pools and export from the coastal ocean. *Global Biogeochemical Cycles*, 29(10):1725–1738, 10 2015. ISSN 19449224. doi: 10.1002/2014GB005056. URL <http://doi.wiley.com/10.1002/2014GB005056>.
- Michael I. Bird, Christopher M. Wurster, Pedro H. de Paula Silva, Adrian M. Bass, and Rocky de Nys. Algal biochar - production and properties. *Bioresource Technology*, 102(2):1886–1891, 1 2011. ISSN 09608524. doi: 10.1016/j.biortech.2010.07.106. URL <http://dx.doi.org/10.1016/j.biortech.2010.07.106><https://linkinghub.elsevier.com/retrieve/pii/S0960852410013179>.
- C. M. Bitz and William H. Lipscomb. An energy-conserving thermodynamic model of sea ice. *Journal of Geophysical Research: Oceans*, 104(C7):15669–15677, 7 1999. ISSN 01480227. doi: 10.1029/1999JC900100. URL <http://doi.wiley.com/10.1029/1999JC900100>.
- George L. Bowie, William B. Mills, Donald B. Porcella, Carrie L. Campbell, R Pagenkopf, James, Gretchen L. Rupp, Kay M Johnson, Peter W.H. Chan, and Steven A. Gherini. Rates, Constants, and Kinetics Formulation in Surface Water Quality Modeling (Second Edition). *Tetra Tech, Inc for USEPA*, 600(January 1978):3–85, 1985.
- A. M. Breeman. Relative importance of temperature and other factors in determining geographic boundaries of seaweeds: Experimental and phenological evidence. *Helgoländer Meeresuntersuchungen*, 42(2):199–241, 1988. ISSN 01743597. doi: 10.1007/BF02366043.
- Ole Jacob Broch and Dag Slagstad. Modelling seasonal growth and composition of the kelp *Saccharina latissima*. *Journal of Applied Phycology*, 24(4):759–776, August 2012. ISSN 0921-8971, 1573-5176. doi: 10.1007/s10811-011-9695-y. URL <http://link.springer.com/10.1007/s10811-011-9695-y>.
- Mark J. Brush and Scott W. Nixon. Modeling the role of macroalgae in a shallow sub-estuary of Narragansett Bay, RI (USA). *Ecological Modelling*, 221(7):1065–1079, 4 2010. ISSN 03043800. doi: 10.1016/j.ecolmodel.2009.11.002. URL <https://linkinghub.elsevier.com/retrieve/pii/S0304380009007480>.
- Bela Hieronymus Buck and Cornelia Maria Buchholz. The offshore-ring: A new system design for the open ocean aquaculture of macroalgae. *Journal of Applied Phycology*, 16(5):355–368, 2004. ISSN 09218971. doi: 10.1023/B:JAPH.0000047947.96231.ea.
- Alejandro H. Buschmann, Carolina Camus, Javier Infante, Amir Neori, Álvaro Israel, María C. Hernández-González, Sandra V. Pereda, Juan Luis Gomez-Pinchetti, Alexander Golberg, Niva Tadmor-Shalev, and Alan T. Critchley. Seaweed production: overview of the global state of exploitation, farming and emerging research activity. *European Journal of Phycology*, 52(4):391–406, 10 2017. ISSN 14694433. doi: 10.1080/09670262.2017.1365175. URL <https://doi.org/10.1080/09670262.2017.1365175><https://www.tandfonline.com/doi/full/10.1080/09670262.2017.1365175>.

- L. J. Carpenter and P. S. Liss. On temperate sources of bromoform and other reactive organic bromine gases. *Journal of Geophysical Research Atmospheres*, 105(D16):20539–20547, 2000. ISSN 01480227. doi: 10.1029/2000JD900242.
- Huihui Chen, Dong Zhou, Gang Luo, Shicheng Zhang, and Jianmin Chen. Macroalgae for biofuels production: Progress and perspectives. *Renewable and Sustainable Energy Reviews*, 47:427–437, 7 2015. ISSN 18790690. doi: 10.1016/j.rser.2015.03.086. URL <https://linkinghub.elsevier.com/retrieve/pii/S1364032115002397>.
- Yoshito Chikaraishi, Yuichiro Kashiyama, Nanako O. Ogawa, Hiroshi Kitazato, and Naohiko Ohkouchi. Metabolic control of nitrogen isotope composition of amino acids in macroalgae and gastropods: Implications for aquatic food web studies. *Marine Ecology Progress Series*, 342(2003):85–90, 2007. ISSN 01718630. doi: 10.3354/meps342085.
- Ik Kyo Chung, John Beardall, Smita Mehta, Dinabandhu Sahoo, and Slobodanka Stojkovic. Using marine macroalgae for carbon sequestration: a critical appraisal. *Journal of Applied Phycology*, 23(5):877–886, October 2011. ISSN 0921-8971, 1573-5176. doi: 10.1007/s10811-010-9604-9. URL <http://link.springer.com/10.1007/s10811-010-9604-9>.
- Philippe Ciais, Christopher Sabine, G Bala, Laurent Bopp, Victor Brovkin, J. Canadell, A Chhabra, R DeFries, J. Galloway, Martin Heimann, C Jones, C. Le Quéré, R.B. Myneni, S Piao, and P Thornton. Carbon and other biogeochemical cycles. In Intergovernmental Panel on Climate Change, editor, *Climate Change 2013 the Physical Science Basis: Working Group I Contribution to the Fifth Assessment Report of the Intergovernmental Panel on Climate Change*, volume 9781107057, pages 465–570. Cambridge University Press, Cambridge, 2013. ISBN 9781107415324. doi: 10.1017/CBO9781107415324.015. URL http://www.ipcc.ch/report/ar5/wg1/docs/review/WG1AR5_SOD_Ch06_All_Final.pdf%5Cnhttp://ebooks.cambridge.org/ref/id/CBO9781107415324A023https://www.cambridge.org/core/product/identifier/CBO9781107415324A023/type/book_part.
- Jessie Conover, Lindsay A. Green, and Carol S. Thornber. Biomass decay rates and tissue nutrient loss in bloom and non-bloom-forming macroalgal species. *Estuarine, Coastal and Shelf Science*, 178:58–64, September 2016. ISSN 02727714. doi: 10.1016/j.ecss.2016.05.018. URL <https://linkinghub.elsevier.com/retrieve/pii/S0272771416301627>.
- J. S. Daniel, S. Solomon, and D. L. Albritton. On the evaluation of halocarbon radiative forcing and global warming potentials. *Journal of Geophysical Research*, 100(D1):1271–1285, 1 1995. ISSN 01480227. doi: 10.1029/94JD02516. URL <http://doi.wiley.com/10.1029/94JD02516>.
- Joshua Dean, Astrid Kiendler-Scharr, Nadine Mengis, Yinon Rudich, Kerstin Schepanski, and Ralf Zimmermann. Above us only sky. *Communications Earth and Environment*, 2(1):179, 12 2021. ISSN 26624435. doi: 10.1038/s43247-021-00245-0. URL <http://dx.doi.org/10.1038/s43247-021-00245-0https://www.nature.com/articles/s43247-021-00245-0>.

- Carlos M. Duarte, Jiaping Wu, Xi Xiao, Annette Bruhn, and Dorte Krause-Jensen. Can seaweed farming play a role in climate change mitigation and adaptation? *Frontiers in Marine Science*, 4(APR), 4 2017. ISSN 22967745. doi: 10.3389/fmars.2017.00100. URL <http://journal.frontiersin.org/article/10.3389/fmars.2017.00100/full>.
- P. Duarte and J. G. Ferreira. A model for the simulation of macroalgal population dynamics and productivity. *Ecological Modelling*, 98(2-3):199–214, 5 1997. ISSN 03043800. doi: 10.1016/S0304-3800(96)01915-1. URL <https://linkinghub.elsevier.com/retrieve/pii/S0304380096019151>.
- P. Duarte, R. Meneses, A. J.S. Hawkins, M. Zhu, J. Fang, and J. Grant. Mathematical modelling to assess the carrying capacity for multi-species culture within coastal waters. *Ecological Modelling*, 168(1-2): 109–143, 2003. ISSN 03043800. doi: 10.1016/S0304-3800(03)00205-9.
- M. Eby, K. Zickfeld, A. Montenegro, D. Archer, K. J. Meissner, and A. J. Weaver. Lifetime of anthropogenic climate change: Millennial time scales of potential CO₂ and surface temperature perturbations. *Journal of Climate*, 22(10):2501–2511, 2009. ISSN 08948755. doi: 10.1175/2008JCLI2554.1.
- M. Eby, A. J. Weaver, K. Alexander, K. Zickfeld, A. Abe-Ouchi, A. A. Cimatoribus, E. Cressin, S. S. Drijfhout, N. R. Edwards, A. V. Eliseev, G. Feulner, T. Fichefet, C. E. Forest, H. Goosse, P. B. Holden, F. Joos, M. Kawamiya, D. Kicklighter, H. Kienert, K. Matsumoto, I. I. Mokhov, E. Monier, S. M. Olsen, J. O. P. Pedersen, M. Perrette, G. Philippon-Berthier, A. Ridgwell, A. Schlosser, T. Schneider von Deimling, G. Shaffer, R. S. Smith, R. Spahni, A. P. Sokolov, M. Steinacher, K. Tachiiri, K. Tokos, M. Yoshimori, N. Zeng, and F. Zhao. Historical and idealized climate model experiments: an intercomparison of Earth system models of intermediate complexity. *Climate of the Past*, 9(3):1111–1140, 5 2013. ISSN 1814-9332. doi: 10.5194/cp-9-1111-2013. URL <https://cp.copernicus.org/articles/9/1111/2013/>.
- Abraham Edo, Edgar Hertwich, and Niko Heeren. *Bridging the gap: Enhancing mitigation ambition and action at G20 level and globally*. UNEP/Earthprint, Nairobi, 2022. ISBN 9789280737660. doi: 10.18356/9789210022262c008. URL <http://www.unenvironment.org/emissionsgap>.
- Matthew D. Eisaman, Keshav Parajuly, Alexander Tuganov, Craig Eldershaw, Norine Chang, and Karl A. Littau. CO₂ extraction from seawater using bipolar membrane electro dialysis. *Energy and Environmental Science*, 5(6):7346–7352, 2012. ISSN 17545706. doi: 10.1039/c2ee03393c.
- Britas Klemens Eriksson and Lena Bergström. Local distribution patterns of macroalgae in relation to environmental variables in the northern Baltic Proper. *Estuarine, Coastal and Shelf Science*, 62(1-2):109–117, 2005. ISSN 02727714. doi: 10.1016/j.ecss.2004.08.009.
- Augustus F. Fanning and Andrew J. Weaver. An atmospheric energy-moisture balance model: Climatology, interpentadal climate change, and coupling to an ocean general circulation model. *Journal of Geophysical Research Atmospheres*, 101(10):15111–15128, 6 1996. ISSN 01480227. doi: 10.1029/96jd01017. URL <http://doi.wiley.com/10.1029/96JD01017>.
- FAO. The state of world fisheries and aquaculture 2018-meeting the sustainable development goals, 2018.

- Francois Fernand, Alvaro Israel, Jorunn Skjermo, Thomas Wichard, Klaas R. Timmermans, and Alexander Golberg. Offshore macroalgae biomass for bioenergy production: Environmental aspects, technological achievements and challenges. *Renewable and Sustainable Energy Reviews*, 75(November 2016):35–45, 8 2017. ISSN 18790690. doi: 10.1016/j.rser.2016.10.046. URL <https://linkinghub.elsevier.com/retrieve/pii/S1364032116307018>.
- M. C. Fogarty, M. R. Fewings, A. C. Paget, and H. M. Dierssen. The Influence of a Sandy Substrate, Seagrass, or Highly Turbid Water on Albedo and Surface Heat Flux. *Journal of Geophysical Research: Oceans*, 123(1):53–73, 2018. ISSN 21699291. doi: 10.1002/2017JC013378.
- P. Friedlingstein, M. W. Jones, M. O’Sullivan, R. M. Andrew, D. C. E. Bakker, J. Hauck, C. Le Quéré, G. P. Peters, W. Peters, J. Pongratz, S. Sitch, J. G. Canadell, P. Ciais, R. B. Jackson, S. R. Alin, P. Anthoni, N. R. Bates, M. Becker, N. Bellouin, L. Bopp, T. T. T. Chau, F. Chevallier, L. P. Chini, M. Cronin, K. I. Currie, B. Decharme, L. M. Djeutchouang, X. Dou, W. Evans, R. A. Feely, L. Feng, T. Gasser, D. Gilfillan, T. Gkritzalis, G. Grassi, L. Gregor, N. Gruber, Ö. Gürses, I. Harris, R. A. Houghton, G. C. Hurtt, Y. Iida, T. Ilyina, I. T. Lujckx, A. Jain, S. D. Jones, E. Kato, D. Kennedy, K. Klein Goldewijk, J. Knauer, J. I. Korsbakken, A. Körtzinger, P. Landschützer, S. K. Lauvset, N. Lefèvre, S. Lienert, J. Liu, G. Marland, P. C. McGuire, J. R. Melton, D. R. Munro, J. E. M. S. Nabel, S.-I. Nakaoka, Y. Niwa, T. Ono, D. Pierrot, B. Poulter, G. Rehder, L. Resplandy, E. Robertson, C. Rödenbeck, T. M. Rosan, J. Schwinger, C. Schwingshackl, R. Séférian, A. J. Sutton, C. Sweeney, T. Tanhua, P. P. Tans, H. Tian, B. Tilbrook, F. Tubiello, G. R. van der Werf, N. Vuichard, C. Wada, R. Wanninkhof, A. J. Watson, D. Willis, A. J. Wiltshire, W. Yuan, C. Yue, X. Yue, S. Zaehle, and J. Zeng. Global carbon budget 2021. *Earth Syst. Sci. Data*, 14:1917–2005, 2022. doi: 10.5194/essd-14-1917-2022.
- Halley E. Froehlich, Jamie C. Afflerbach, Melanie Frazier, and Benjamin S. Halpern. Blue Growth Potential to Mitigate Climate Change through Seaweed Offsetting. *Current Biology*, 29(18):3087–3093, 8 2019. ISSN 09609822. doi: 10.1016/j.cub.2019.07.041. URL <https://doi.org/10.1016/j.cub.2019.07.041><https://linkinghub.elsevier.com/retrieve/pii/S0960982219308863>.
- Sabine Fuss, Josep G. Canadell, Philippe Ciais, Robert B. Jackson, Chris D. Jones, Anders Lyngfelt, Glen P. Peters, and Detlef P. Van Vuuren. Moving toward Net-Zero Emissions Requires New Alliances for Carbon Dioxide Removal. *One Earth*, 3(2):145–149, 8 2020. ISSN 25903322. doi: 10.1016/j.oneear.2020.08.002. URL <https://doi.org/10.1016/j.oneear.2020.08.002><https://linkinghub.elsevier.com/retrieve/pii/S2590332220303651>.
- Guang Gao, James Grant Burgess, Min Wu, Shujun Wang, and Kunshan Gao. Using macroalgae as biofuel: Current opportunities and challenges. *Botanica Marina*, 63(4):355–370, 8 2020. ISSN 14374323. doi: 10.1515/bot-2019-0065. URL <https://www.degruyter.com/document/doi/10.1515/bot-2019-0065/html>.
- Kunshan Gao and Kelton R. McKinley. Use of macroalgae for marine biomass production and CO₂ remediation: a review. *Journal of Applied Phycology*, 6(1):45–60, 2 1994. ISSN 09218971. doi: 10.1007/BF02185904. URL <http://link.springer.com/10.1007/BF02185904>.

- H. E. Garcia, R. A. Locarnini, T. P. Boyer, J. I. Antonov, M. M. Zweng, O. K. Baranova, and D. R. Johnson. World Ocean Atlas 2009, Volume 4: Nutrients (phosphate, nitrate, and silicate). *NOAA World Ocean Atlas*, 71(March):398, 2010. URL <http://www.nodc.noaa.gov/OC5/indprod.html>.
- John A. Glaser. Climate geoengineering. *Clean Technologies and Environmental Policy*, 12(2):91–95, 4 2010. ISSN 1618-954X. doi: 10.1007/s10098-010-0287-3. URL <http://scholar.google.com/scholar?hl=en&btnG=Search&q=intitle:Geoengineering+the+climate#0http://link.springer.com/10.1007/s10098-010-0287-3>.
- Nicolas Gruber, Dominic Clement, Brendan R. Carter, Richard A. Feely, Steven van Heuven, Mario Hoppema, Masao Ishii, Robert M. Key, Alex Kozyr, Siv K. Lauvset, Claire Lo Monaco, Jeremy T. Mathis, Akihiko Murata, Are Olsen, Fiz F. Perez, Christopher L. Sabine, Toste Tanhua, and Rik Wanninkhof. The oceanic sink for anthropogenic CO₂ from 1994 to 2007. *Science*, 363(6432):1193–1199, 3 2019. ISSN 10959203. doi: 10.1126/science.aau5153. URL <https://www.sciencemag.org/lookup/doi/10.1126/science.aau5153>.
- Scott Hadley, Karen Wild-Allen, Craig Johnson, and Catriona Macleod. Modeling macroalgae growth and nutrient dynamics for integrated multi-trophic aquaculture. *Journal of Applied Phycology*, 27(2):901–916, 2015. ISSN 09218971. doi: 10.1007/s10811-014-0370-y.
- C. Heinze, S. Meyer, N. Goris, L. Anderson, R. Steinfeldt, N. Chang, C. Le Quéré, and D. C.E. Bakker. The ocean carbon sink - Impacts, vulnerabilities and challenges. *Earth System Dynamics*, 6(1):327–358, 2015. ISSN 21904987. doi: 10.5194/esd-6-327-2015.
- Giuliano Buzá Jacobucci, Arthur Ziggianti Güth, and Fosca Pedini Pereira Leite. Experimental evaluation of amphipod grazing over biomass of *Sargassum filipendula* (Phaeophyta) and its dominant epiphyte. *Nauplius*, 16(2):65–71, 2008.
- Zhibing Jiang, Jingjing Liu, Shanglu Li, Yue Chen, Ping Du, Yuanli Zhu, Yibo Liao, Quanzhen Chen, Lu Shou, Xiaojun Yan, Jiangning Zeng, and Jianfang Chen. Kelp cultivation effectively improves water quality and regulates phytoplankton community in a turbid, highly eutrophic bay. *Science of the Total Environment*, 707:135561, 3 2020. ISSN 18791026. doi: 10.1016/j.scitotenv.2019.135561. URL <https://doi.org/10.1016/j.scitotenv.2019.135561https://linkinghub.elsevier.com/retrieve/pii/S0048969719355561>.
- D. P. Keller, A. Oschlies, and M. Eby. A new marine ecosystem model for the University of Victoria earth system climate model. *Geoscientific Model Development*, 5(5):1195–1220, 9 2012. ISSN 1991959X. doi: 10.5194/gmd-5-1195-2012. URL <https://gmd.copernicus.org/articles/5/1195/2012/>.
- David P. Keller, Ellias Y. Feng, and Andreas Oschlies. Potential climate engineering effectiveness and side effects during a high carbon dioxide-emission scenario. *Nature Communications*, 5(1):3304, 5 2014. ISSN 20411723. doi: 10.1038/ncomms4304. URL <http://dx.doi.org/10.1038/ncomms4304http://www.nature.com/articles/ncomms4304>.

- David P. Keller, Andrew Lenton, Emma W. Littleton, Andreas Oschlies, Vivian Scott, and Naomi E. Vaughan. The Effects of Carbon Dioxide Removal on the Carbon Cycle. *Current Climate Change Reports*, 4(3): 250–265, 9 2018. ISSN 21986061. doi: 10.1007/s40641-018-0104-3. URL <http://link.springer.com/10.1007/s40641-018-0104-3>.
- Philip D. Kerrison, Michele S. Stanley, Maeve D. Edwards, Kenneth D. Black, and Adam D. Hughes. The cultivation of European kelp for bioenergy: Site and species selection. *Biomass and Bioenergy*, 80(0): 229–242, 2015. ISSN 1873-2909. doi: 10.1016/j.biombioe.2015.04.035. URL <http://dx.doi.org/10.1016/j.biombioe.2015.04.035>.
- Jang Kyun Kim, Michael Stekoll, and Charles Yarish. Opportunities, challenges and future directions of open-water seaweed aquaculture in the United States. *Phycologia*, 58(5):446–461, 2019. ISSN 23302968. doi: 10.1080/00318884.2019.1625611. URL <https://doi.org/10.1080/00318884.2019.1625611>.
- John T. O. Kirk. *Light and Photosynthesis in Aquatic Ecosystems*. Cambridge University Press, 2 edition, 1994. doi: 10.1017/CBO9780511623370.
- Marguerite Koch, George Bowes, Cliff Ross, and Xing Hai Zhang. Climate change and ocean acidification effects on seagrasses and marine macroalgae. *Global Change Biology*, 19(1):103–132, 2013. ISSN 13541013. doi: 10.1111/j.1365-2486.2012.02791.x.
- Peter Köhler, Jesse F. Abrams, Christoph Völker, Judith Hauck, and Dieter A. Wolf-Gladrow. Geoengineering impact of open ocean dissolution of olivine on atmospheric CO₂, surface ocean pH and marine biology. *Environmental Research Letters*, 8(1), 2013. ISSN 17489326. doi: 10.1088/1748-9326/8/1/014009.
- Dorte Krause-Jensen and Carlos M. Duarte. Substantial role of macroalgae in marine carbon sequestration. *Nature Geoscience*, 9(10):737–742, 2016. ISSN 17520908. doi: 10.1038/ngeo2790. URL <http://dx.doi.org/10.1038/ngeo2790>.
- Kira A. Krumhansl and Robert E. Scheibling. Spatial and temporal variation in grazing damage by the gastropod *Lacuna vincta* in Nova scotian kelp beds. *Aquatic Biology*, 13(2):163–173, 9 2011. ISSN 18647782. doi: 10.3354/ab00366. URL <http://www.int-res.com/abstracts/ab/v13/n2/p163-173/>.
- I. B. Kuffner and Valerie J. Paul. Effects of nitrate, phosphate and iron on the growth of macroalgae and benthic cyanobacteria from cocos lagoon, guam. *Marine Ecology Progress Series*, 222(Noviembre):63–72, 2001. ISSN 01718630. doi: 10.3354/meps222063. URL <http://www.int-res.com/abstracts/meps/v222/p63-72/>.
- K. Kvale, A. E.F. Prowe, C. T. Chien, A. Landolfi, and A. Oschlies. Zooplankton grazing of microplastic can accelerate global loss of ocean oxygen. *Nature Communications*, 12(1), 2021. ISSN 20411723. doi: 10.1038/s41467-021-22554-w.
- Karin F. Kvale and Katrin J. Meissner. Primary production sensitivity to phytoplankton light attenuation parameter increases with transient forcing. *Biogeosciences*, 14(20):4767–4780, 10 2017. ISSN 17264189. doi: 10.5194/bg-14-4767-2017. URL <https://bg.copernicus.org/articles/14/4767/2017/>.

- Frank Latumus. Release of volatile halogenated organic compounds by unialgal cultures of polar macroalgae. *Chemosphere*, 31(6):3387–3395, 9 1995. ISSN 00456535. doi: 10.1016/0045-6535(95)00190-J. URL <https://linkinghub.elsevier.com/retrieve/pii/004565359500190J>.
- Lieve M.L. Laurens, Madeline Lane, and Robert S. Nelson. Sustainable Seaweed Biotechnology Solutions for Carbon Capture, Composition, and Deconstruction. *Trends in Biotechnology*, 38(11):1232–1244, 2020. ISSN 18793096. doi: 10.1016/j.tibtech.2020.03.015. URL <https://doi.org/10.1016/j.tibtech.2020.03.015>.
- Mark G. Lawrence, Stefan Schäfer, Helene Muri, Vivian Scott, Andreas Oschlies, Naomi E. Vaughan, Olivier Boucher, Hauke Schmidt, Jim Haywood, and Jürgen Scheffran. Evaluating climate geoengineering proposals in the context of the Paris Agreement temperature goals. *Nature Communications*, 9(1), 2018. ISSN 20411723. doi: 10.1038/s41467-018-05938-3. URL <http://dx.doi.org/10.1038/s41467-018-05938-3>.
- E. C. Leedham, C. Hughes, F. S.L. Keng, S. M. Phang, G. Malin, and W. T. Sturges. Emission of atmospherically significant halocarbons by naturally occurring and farmed tropical macroalgae. *Biogeosciences*, 10(6):3615–3633, 6 2013. ISSN 17264170. doi: 10.5194/bg-10-3615-2013. URL <https://bg.copernicus.org/articles/10/3615/2013/>.
- Yoav Lehahn, Kapilkumar Nivrutti Ingle, and Alexander Golberg. Global potential of offshore and shallow waters macroalgal biorefineries to provide for food, chemicals and energy: Feasibility and sustainability. *Algal Research*, 17:150–160, 7 2016. ISSN 22119264. doi: 10.1016/j.algal.2016.03.031. URL <http://dx.doi.org/10.1016/j.algal.2016.03.031><https://linkinghub.elsevier.com/retrieve/pii/S2211926416301151>.
- Zhilong Liu and Kimberly Huguenard. Hydrodynamic Response of a Floating Aquaculture Farm in a Low Inflow Estuary. *Journal of Geophysical Research: Oceans*, 125(5):0–3, 5 2020. ISSN 21699291. doi: 10.1029/2019JC015625. URL <https://onlinelibrary.wiley.com/doi/10.1029/2019JC015625>.
- Min Luo, Joris Gieskes, Linying Chen, Jan Scholten, Binbin Pan, Gang Lin, and Duofu Chen. Sources, Degradation, and Transport of Organic Matter in the New Britain Shelf-Trench Continuum, Papua New Guinea. *Journal of Geophysical Research: Biogeosciences*, 124(6):1680–1695, 2019. ISSN 21698961. doi: 10.1029/2018JG004691. URL <https://onlinelibrary.wiley.com/doi/abs/10.1029/2018JG004691>.
- Peter I. Macreadie, Oscar Serrano, Damien T. Maher, Carlos M. Duarte, and John Beardall. Addressing calcium carbonate cycling in blue carbon accounting. *Limnology and Oceanography Letters*, 2(6):195–201, December 2017. ISSN 2378-2242, 2378-2242. doi: 10.1002/lol2.10052. URL <https://onlinelibrary.wiley.com/doi/10.1002/lol2.10052>.
- Peter I. Macreadie, Andrea Anton, John A. Raven, Nicola Beaumont, Rod M. Connolly, Daniel A. Friess, Jeffrey J. Kelleway, Hilary Kennedy, Tomohiro Kuwae, Paul S. Lavery, Catherine E. Lovelock, Dan A. Smale, Eugenia T. Apostolaki, Trisha B. Atwood, Jeff Baldock, Thomas S. Bianchi, Gail L. Chmura, Bradley D. Eyre, James W. Fourqurean, Jason M. Hall-Spencer, Mark Huxham, Iris E. Hendriks, Dorte Krause-Jensen, Dan Laffoley, Tiziana Luisetti, Núria Marbà, Pere Masque, Karen J. McGlathery, J. Patrick Megonigal, Daniel Murdiyarso, Bayden D. Russell, Rui Santos, Oscar Serrano, Brian R.

- Silliman, Kenta Watanabe, and Carlos M. Duarte. The future of Blue Carbon science. *Nature Communications*, 10(1):3998, 9 2019. ISSN 20411723. doi: 10.1038/s41467-019-11693-w. URL <https://www.nature.com/articles/s41467-019-11693-w>.
- Torge Martin, Wonsun Park, and Mojib Latif. Multi-centennial variability controlled by Southern Ocean convection in the Kiel Climate Model. *Climate Dynamics*, 40(7-8):2005–2022, 4 2013. ISSN 14320894. doi: 10.1007/s00382-012-1586-7. URL <http://link.springer.com/10.1007/s00382-012-1586-7>.
- I. Martins and J. C. Marques. A model for the growth of opportunistic macroalgae (*Enteromorpha* sp.) in tidal estuaries. *Estuarine, Coastal and Shelf Science*, 55(2):247–257, 2002. ISSN 02727714. doi: 10.1006/ecss.2001.0900.
- Valérie Masson-Delmotte, Panmao Zhai, Hans-Otto Pörtner, Debra Roberts, Jim Skea, Priyadarshi R Shukla, Anna Pirani, Wilfran Moufouma-Okia, Clotilde Péan, Roz Pidcock, Sarah Connors, J B Robin Matthews, Yang Chen, Xiao Zhou, Melissa I Gomis, Elisabeth Lonnoy, Tom Maycock, Melinda Tignor, Tim Waterfield, Anna Pirani, Wilfran Moufouma-Okia, Clotilde Péan, Roz Pidcock, Sarah Connors, J B Robin Matthews, Yang Chen, Xiao Zhou, Melissa I Gomis, Elisabeth Lonnoy, Tom Maycock, Melinda Tignor, and Tim Waterfield, editors. *Global Warming of 1.5°C: An IPCC Special Report on the impacts of global warming of 1.5°C above pre-industrial levels and related global greenhouse gas emission pathways, in the context of strengthening the global response to the threat of climate change, sustainable development, and efforts to eradicate poverty*. World Meteorological Organization, Geneva, Switzerland, 2018. ISBN 978-92-9169-151-7. URL <https://www.ipcc.ch/sr15/>.
- Richard J. Matear and Bronwyn Elliott. Enhancement of oceanic uptake of anthropogenic CO₂ by macronutrient fertilization. *Journal of Geophysical Research: Oceans*, 109(4):1–14, 2004. ISSN 21699291. doi: 10.1029/2000JC000321.
- Malte Meinshausen, S. J. Smith, K. Calvin, J. S. Daniel, M. L.T. Kainuma, J. Lamarque, K. Matsumoto, S. A. Montzka, S. C.B. Raper, K. Riahi, A. Thomson, G. J.M. Velders, and D. P.P. van Vuuren. The RCP greenhouse gas concentrations and their extensions from 1765 to 2300. *Climatic Change*, 109(1): 213–241, 11 2011. ISSN 01650009. doi: 10.1007/s10584-011-0156-z. URL <http://link.springer.com/10.1007/s10584-011-0156-z>.
- K. J. Meissner, A. J. Weaver, H. D. Matthews, and P. M. Cox. The role of land surface dynamics in glacial inception: A study with the UVic Earth System Model. *Climate Dynamics*, 21(7-8):515–537, 12 2003. ISSN 09307575. doi: 10.1007/s00382-003-0352-2. URL <http://link.springer.com/10.1007/s00382-003-0352-2>.
- N. Mengis, T. Martin, D. P. Keller, and A. Oschlies. Assessing climate impacts and risks of ocean albedo modification in the Arctic. *Journal of Geophysical Research: Oceans*, 121(5):3044–3057, 2016. ISSN 21699291. doi: 10.1002/2015JC011433.
- A. Mentges, C. Feenders, C. Deutsch, B. Blasius, and T. Dittmar. Long-term stability of marine dissolved organic carbon emerges from a neutral network of compounds and microbes. *Scientific Reports*, 9(1):

- 17780, 12 2019. ISSN 20452322. doi: 10.1038/s41598-019-54290-z. URL <http://www.nature.com/articles/s41598-019-54290-z>.
- Jan C. Minx, William F. Lamb, Max W. Callaghan, Lutz Bornmann, and Sabine Fuss. Fast growing research on negative emissions. *Environmental Research Letters*, 12(3), 2017. ISSN 17489326. doi: 10.1088/1748-9326/aa5ee5.
- Ignacio A. Navarrete, Diane Y. Kim, Cindy Wilcox, Daniel C. Reed, David W. Ginsburg, Jessica M. Dutton, John Heidelberg, Yubin Raut, and Brian Howard Wilcox. Effects of depth-cycling on nutrient uptake and biomass production in the giant kelp *Macrocystis pyrifera*. *Renewable and Sustainable Energy Reviews*, 141(May 2020):110747, 5 2021. ISSN 18790690. doi: 10.1016/j.rser.2021.110747. URL <https://doi.org/10.1016/j.rser.2021.110747><https://linkinghub.elsevier.com/retrieve/pii/S1364032121000423>.
- Heidi M. Nepf. Hydrodynamics of vegetated channels. *Journal of Hydraulic Research*, 50(3):262–279, 6 2012. ISSN 00221686. doi: 10.1080/00221686.2012.696559. URL <https://www.tandfonline.com/doi/full/10.1080/00221686.2012.696559>.
- J Orr, R Najjar, CL Sabine, and F Joos. Abiotic-howto. *Internal OCMIP Report, LSCE/CEA Saclay, Gifsur-Yvette, France*, 1999:1–29, 1999. URL <http://www.cgd.ucar.edu/oce/klindsay/OCMIP/HOWTO-Abiotic.pdf>.
- James C. Orr and Jorge L. Sarmiento. Potential of marine macroalgae as a sink for CO₂: Constraints from a 3-D general circulation model of the global ocean. *Water, Air, & Soil Pollution*, 64(1-2):405–421, 8 1992. ISSN 00496979. doi: 10.1007/BF00477113. URL <http://link.springer.com/10.1007/BF00477113>http://link.springer.com/chapter/10.1007/978-94-011-2793-6_22http://link.springer.com/10.1007/978-94-011-2793-6_22.
- A. Oschlies, W. Koeve, W. Rickels, and K. Rehdanz. Side effects and accounting aspects of hypothetical large-scale Southern Ocean iron fertilization. *Biogeosciences*, 7(12):4014–4035, 2010a. ISSN 17264170. doi: 10.5194/bg-7-4017-2010.
- A. Oschlies, M. Pahlow, A. Yool, and R. J. Matear. Climate engineering by artificial ocean upwelling: Channeling the sorcerer’s apprentice. *Geophysical Research Letters*, 37(4):1–5, 2 2010b. ISSN 00948276. doi: 10.1029/2009GL041961. URL <http://doi.wiley.com/10.1029/2009GL041961>.
- Andreas Oschlies. A committed fourfold increase in ocean oxygen loss. *Nature Communications*, 12(1): 2307, 12 2021. ISSN 20411723. doi: 10.1038/s41467-021-22584-4. URL <http://dx.doi.org/10.1038/s41467-021-22584-4><http://www.nature.com/articles/s41467-021-22584-4>.
- Andreas Oschlies, Wolfgang Koeve, Angela Landolfi, and Paul Kähler. Loss of fixed nitrogen causes net oxygen gain in a warmer future ocean. *Nature Communications*, 10(1):1–7, 2019. ISSN 20411723. doi: 10.1038/s41467-019-10813-w.
- Muhammed A. Oyinlola, Gabriel Reygondeau, Colette C.C. Wabnitz, and William W.L. Cheung. Projecting global mariculture diversity under climate change. *Global Change Biology*, 26(4):2134–2148, 2020. ISSN 13652486. doi: 10.1111/gcb.14974.

- Ronald Pacanowski. MOM 2 Version 2.0 (beta) Documentation User's Guide and Reference Manual. *Model Manual*, 0, 1996.
- Antti Ilari Partanen, David P. Keller, Hannele Korhonen, and H. Damon Matthews. Impacts of sea spray geoengineering on ocean biogeochemistry. *Geophysical Research Letters*, 43(14):7600–7608, 7 2016. ISSN 19448007. doi: 10.1002/2016GL070111. URL <http://doi.wiley.com/10.1002/2016GL070111>.
- César Peteiro, Noemí Sánchez, Clara Dueñas-Liaño, and Brezo Martínez. Open-sea cultivation by transplanting young fronds of the kelp *Saccharina latissima*. *Journal of Applied Phycology*, 26(1):519–528, 2 2014. ISSN 09218971. doi: 10.1007/s10811-013-0096-2. URL <http://link.springer.com/10.1007/s10811-013-0096-2>.
- Glen P. Peters, Robbie M. Andrew, Tom Boden, Josep G. Canadell, Philippe Ciais, Corinne Le Quéré, Gregg Marland, Michael R. Raupach, and Charlie Wilson. The challenge to keep global warming below 2C. *Nature Climate Change*, 3(1):4–6, 2013. ISSN 1758678X. doi: 10.1038/nclimate1783. URL <http://dx.doi.org/10.1038/nclimate1783>.
- V. Ramaswamy, M. D. Schwarzkopf, and K. P. Shine. Radiative forcing of climate from halocarbon-induced global stratospheric ozone loss. *Nature*, 355(6363):810–812, 2 1992. ISSN 00280836. doi: 10.1038/355810a0. URL <https://doi.org/10.1038/355810a0><http://www.nature.com/articles/355810a0>.
- John Raven. Blue carbon: Past, present and future, with emphasis on macroalgae. *Biology Letters*, 14(10), 2018. ISSN 1744957X. doi: 10.1098/rsbl.2018.0336.
- A. R. Ravishankara, John S. Daniel, and Robert W. Portmann. Nitrous oxide (N₂O): The dominant ozone-depleting substance emitted in the 21st century. *Science*, 326(5949):123–125, 10 2009. ISSN 00368075. doi: 10.1126/science.1176985. URL <https://www.science.org/doi/10.1126/science.1176985>.
- Fabian Reith, David P. Keller, and Andreas Oeschlies. Revisiting ocean carbon sequestration by direct injection: A global carbon budget perspective. *Earth System Dynamics*, 7(4):797–812, 11 2016. ISSN 21904987. doi: 10.5194/esd-7-797-2016. URL <https://esd.copernicus.org/articles/7/797/2016/>.
- R. L. Ritschard. Marine algae as a CO₂ sink. *Water, Air, & Soil Pollution*, 64(1-2):289–303, 8 1992. ISSN 00496979. doi: 10.1007/BF00477107. URL <http://link.springer.com/10.1007/BF00477107>.
- David A. Roberts, Nicholas A. Paul, Symon A. Dworjanyn, Michael I. Bird, and Rocky De Nys. Biochar from commercially cultivated seaweed for soil amelioration. *Scientific Reports*, 5(1):9665, 4 2015. ISSN 20452322. doi: 10.1038/srep09665. URL <https://www.nature.com/articles/srep09665>.
- J. Robinson, E. E. Popova, A. Yool, M. Srokosz, R. S. Lampitt, and J. R. Blundell. How deep is deep enough? Ocean iron fertilization and carbon sequestration in the Southern Ocean. *Geophysical Research Letters*, 41(7):2489–2495, 4 2014. ISSN 19448007. doi: 10.1002/2013GL058799. URL <http://doi.wiley.com/10.1002/2013GL058799>.

- Joeri Rogelj, Alexander Popp, Katherine V. Calvin, Gunnar Luderer, Johannes Emmerling, David Ger-
naat, Shinichiro Fujimori, Jessica Strefler, Tomoko Hasegawa, Giacomo Marangoni, Volker Krey, El-
mar Kriegler, Keywan Riahi, Detlef P. Van Vuuren, Jonathan Doelman, Laurent Drouet, Jae Ed-
monds, Oliver Fricko, Mathijs Harmsen, Petr Havlík, Florian Humpenöder, Elke Stehfest, and Mas-
simo Tavoni. Scenarios towards limiting global mean temperature increase below 1.5 °C. *Nature
Climate Change*, 8(4):325–332, 4 2018. ISSN 17586798. doi: 10.1038/s41558-018-0091-3. URL
<http://www.nature.com/articles/s41558-018-0091-3>.
- A. Schmittner, Andreas Oschlies, X. Giraud, M. Eby, and H. L. Simmons. A global model of the marine
ecosystem for long-term simulations: Sensitivity to ocean mixing, buoyancy forcing, particle sinking,
and dissolved organic matter cycling. *Global Biogeochemical Cycles*, 19(3):1–17, 2005. ISSN 08866236.
doi: 10.1029/2004GB002283.
- Andreas Schmittner, Andreas Oschlies, H. Damon Matthews, and Eric D. Galbraith. Future changes in
climate, ocean circulation, ecosystems, and biogeochemical cycling simulated for a business-as-usual
CO₂ emission scenario until year 4000 AD. *Global Biogeochemical Cycles*, 22(1):1–21, 2008. ISSN
08866236. doi: 10.1029/2007GB002953.
- Vivian Scott, R. Stuart Haszeldine, Simon F.B. Tett, and Andreas Oschlies. Fossil fuels in a trillion tonne
world. *Nature Climate Change*, 5(5):419–423, 5 2015. ISSN 17586798. doi: 10.1038/nclimate2578.
URL <http://www.nature.com/articles/nclimate2578>.
- Martin T. Sherman, Reginald Blaylock, Kelly Lucas, Mark E. Capron, Jim R. Stewart, Steven F. DiMarco,
Kristen Thyng, Robert Hetland, Mh Kim, Corey Sullivan, Zach Moscicki, Igor Tsukrov, M. Robinson
Swift, Michael D. Chambers, Scott C. James, Maureen Brooks, Brian Von Herzen, Anthony Jones, and
Don Piper. SeaweedPaddock: Initial Modeling and Design for a Sargassum Ranch. In *OCEANS 2018
MTS/IEEE Charleston, OCEAN 2018*, pages 1–6. IEEE, 10 2019. ISBN 9781538648148. doi: 10.1109/
OCEANS.2018.8604848. URL <https://ieeexplore.ieee.org/document/8604848/>.
- Andreas Sichert, Christopher H. Corzett, Matthew S. Schechter, Frank Unfried, Stephanie Markert, Dörte
Becher, Antonio Fernandez-Guerra, Manuel Liebeke, Thomas Schweder, Martin F. Polz, and Jan Hendrik
Hehemann. Verrucomicrobia use hundreds of enzymes to digest the algal polysaccharide fucoidan. *Nature
Microbiology*, 5(8):1026–1039, 2020. ISSN 20585276. doi: 10.1038/s41564-020-0720-2. URL <http://dx.doi.org/10.1038/s41564-020-0720-2>.
- Victor Smetacek, Christine Klaas, Volker H. Strass, Philipp Assmy, Marina Montresor, Boris Cisewski, Nico-
las Savoye, Adrian Webb, Francesco D’Ovidio, Jesús M. Arrieta, Ulrich Bathmann, Richard Bellerby,
Gry Mine Berg, Peter Croot, Santiago Gonzalez, Joachim Henjes, Gerhard J. Herndl, Linn J. Hoffmann,
Harry Leach, Martin Losch, Matthew M. Mills, Craig Neill, Ilka Peeken, Rüdiger Röttgers, Oliver Sachs,
Eberhard Sauter, Maike M. Schmidt, Jill Schwarz, Anja Terbrüggen, and Dieter Wolf-Gladrow. Deep
carbon export from a Southern Ocean iron-fertilized diatom bloom. *Nature*, 487(7407):313–319, 7 2012.
ISSN 00280836. doi: 10.1038/nature11229. URL <http://www.nature.com/articles/nature11229>.

- Y. Suzuki, K. Kuma, I. Kudo, and K. Matsunaga. Iron requirement of the brown macroalgae *Laminaria japonica*, *Undaria pinnatifida* (Phaeophyta) and the crustose coralline alga *Lithophyllum yessoense* (Rhodophyta), and their competition in the northern Japan Sea. *Phycologia*, 34(3):201–205, 5 1995. ISSN 00318884. doi: 10.2216/i0031-8884-34-3-201.1. URL <https://www.tandfonline.com/doi/full/10.2216/i0031-8884-34-3-201.1>.
- Lynne D. Talley. Closure of the global overturning circulation through the Indian, Pacific, and southern oceans. *Oceanography*, 26(1):80–97, 3 2013. ISSN 10428275. doi: 10.5670/oceanog.2013.07. URL <https://tos.org/oceanography/article/closure-of-the-global-overturning-circulation-through-the-indian-pacific-an>.
- Lyla L. Taylor, Joe Quirk, Rachel M.S. Thorley, Pushker A. Kharecha, James Hansen, Andy Ridgwell, Mark R. Lomas, Steve A. Banwart, and David J. Beerling. Enhanced weathering strategies for stabilizing climate and averting ocean acidification. *Nature Climate Change*, 6(4):402–406, 2016. ISSN 17586798. doi: 10.1038/nclimate2882.
- S. Tegtmeier, K. Krüger, B. Quack, E. L. Atlas, I. Pisso, A. Stohl, and X. Yang. Emission and transport of bromocarbons: From the West Pacific ocean into the stratosphere. *Atmospheric Chemistry and Physics*, 12(22):10633–10648, 11 2012. ISSN 16807316. doi: 10.5194/acp-12-10633-2012. URL <https://acp.copernicus.org/articles/12/10633/2012/>.
- S. Tegtmeier, K. Krüger, B. Quack, E. Atlas, D. R. Blake, H. Boenisch, A. Engel, H. Hepach, R. Hossaini, M. A. Navarro, S. Raimund, S. Sala, Q. Shi, and F. Ziska. The contribution of oceanic methyl iodide to stratospheric iodine. *Atmospheric Chemistry and Physics*, 13(23):11869–11886, 2013. ISSN 16807316. doi: 10.5194/acp-13-11869-2013.
- Robert E. Thomas and Stuart J. Mcllelland. The impact of macroalgae on mean and turbulent flow fields. *Journal of Hydrodynamics*, 27(3):427–435, 6 2015. ISSN 18780342. doi: 10.1016/S1001-6058(15)60500-5. URL [http://dx.doi.org/10.1016/S1001-6058\(15\)60500-5](http://dx.doi.org/10.1016/S1001-6058(15)60500-5)[http://link.springer.com/10.1016/S1001-6058\(15\)60500-5](http://link.springer.com/10.1016/S1001-6058(15)60500-5).
- Sebastian Thomas. Blue carbon: Knowledge gaps, critical issues, and novel approaches. *Ecological Economics*, 107:22–38, 2014. ISSN 09218009. doi: 10.1016/j.ecolecon.2014.07.028. URL <http://dx.doi.org/10.1016/j.ecolecon.2014.07.028>.
- A.R. Trancoso, S. Saraiva, L. Fernandes, P. Pina, P. Leitão, and R. Neves. Modelling macroalgae using a 3d hydrodynamic-ecological model in a shallow, temperate estuary. *Ecol. Modell.*, 187(2-3):232–246, 9 2005. ISSN 03043800. doi: 10.1016/j.ecolmodel.2005.01.054. URL <https://linkinghub.elsevier.com/retrieve/pii/S0304380005000918>.
- Stacey M. Trevathan-Tackett, Jeffrey Kelleway, Peter I. Macreadie, John Beardall, Peter Ralph, and Alecia Bellgrove. Comparison of marine macrophytes for their contributions to blue carbon sequestration. *Ecology*, 96(11):3043–3057, 2015. ISSN 00129658. doi: 10.1890/15-0149.1.
- UNFCCC. Adoption of the paris agreement. *United Nations Office at Geneva, Geneva Google Scholar*, 2015.

- Johan Van Der Molen, Piet Ruardij, Karen Mooney, Philip Kerrison, Nessa E. O'Connor, Emma Gorman, Klaas Timmermans, Serena Wright, Maeve Kelly, Adam D. Hughes, and Elisa Capuzzo. Modelling potential production of macroalgae farms in UK and Dutch coastal waters. *Biogeosciences*, 15(4):1123–1147, 2 2018. ISSN 17264189. doi: 10.5194/bg-15-1123-2018. URL <https://www.biogeosciences-discuss.net/bg-2017-195/https://www.biogeosciences.net/15/1123/2018/https://bg.copernicus.org/articles/15/1123/2018/>.
- Andrew J. Weaver, Michael Eby, Edward C. Wiebe, Tracy L. Ewen, Augustus F. Fanning, Amy MacFadyen, H. Damon Matthews, Katrin J. Meissner, Oleg Saenko, Andreas Schmittner, Masakazu Yoshimori, Cecilia M. Bitz, Marika M. Holland, Phil B. Duffy, and Huaxiao Wang. The UVic earth system climate model: Model description, climatology, and applications to past, present and future climates. *Atmosphere - Ocean*, 39(4):361–428, 12 2001. ISSN 14809214. doi: 10.1080/07055900.2001.9649686. URL <https://www.tandfonline.com/doi/full/10.1080/07055900.2001.9649686>.
- Thomas Weber and Daniele Bianchi. Efficient Particle Transfer to Depth in Oxygen Minimum Zones of the Pacific and Indian Oceans. *Frontiers in Earth Science*, 8(September):1–11, 9 2020. ISSN 22966463. doi: 10.3389/feart.2020.00376. URL <https://www.frontiersin.org/article/10.3389/feart.2020.00376/full>.
- Kousuke Yatsuya, Yukio Matsumoto, Kei Sasaki, Norio Shirafuji, and Daisuke Muraoka. Reduced biomass of the kelp *Saccharina japonica* cumulatively affects gonad production of sea urchins over ensuing years off northeastern Japan. *Journal of Applied Phycology*, 32(4):2599–2604, 8 2020. ISSN 15735176. doi: 10.1007/s10811-019-02030-1. URL <http://link.springer.com/10.1007/s10811-019-02030-1>.
- Shinya Yokoyama, Katsunari Jonouchi, and Kenji Imou. Energy Production from Marine Biomass : Fuel Cell Power Generation Driven by Methane Produced from Seaweed. *Engineering and Technology*, 22(4): 320–323, 2007. URL <http://www.waset.org/journals/waset/v28.php>.
- Emily J. Zakem, B. B. Cael, and Naomi M. Levine. A unified theory for organic matter accumulation. *Proceedings of the National Academy of Sciences of the United States of America*, 118(6), 2021. ISSN 10916490. doi: 10.1073/pnas.2016896118.
- Jihong Zhang, Wenguang Wu, Jeffrey S. Ren, and Fan Lin. A model for the growth of mariculture kelp *Saccharina japonica* in Sanggou Bay, China. *Aquaculture Environment Interactions*, 8:273–283, 4 2016. ISSN 18697534. doi: 10.3354/aei00171. URL <http://www.int-res.com/abstracts/aei/v8/p273-283/>.
- F. Ziska, B. Quack, K. Abrahamsson, S. D. Archer, E. Atlas, T. Bell, J. H. Butler, L. J. Carpenter, C. E. Jones, N. R.P. Harris, H. Hepach, K. G. Heumann, C. Hughes, J. Kuss, K. Krüger, P. Liss, R. M. Moore, A. Orlikowska, S. Raimund, C. E. Reeves, W. Reifenhäuser, A. D. Robinson, C. Schall, T. Tanhua, S. Tegtmeier, S. Turner, L. Wang, D. Wallace, J. Williams, H. Yamamoto, S. Yvon-Lewis, and Y. Yokouchi. Global sea-to-air flux climatology for bromoform, dibromomethane and methyl iodide. *Atmospheric Chemistry and Physics*, 13(17):8915–8934, 9 2013. ISSN 16807316. doi: 10.5194/acp-13-8915-2013. URL <https://acp.copernicus.org/articles/13/8915/2013/>.

Chapter 3

Nearshore macroalgae cultivation for carbon sequestration by biomass harvesting: evaluating potential and impacts with an Earth system model

This chapter is based on the paper 'Nearshore Macroalgae Cultivation for Carbon Sequestration by Biomass Harvesting: Evaluating Potential and Impacts with An Earth System Model' submitted to the journal Geophysical Research Letters.

Abstract

This study introduces an ocean-based carbon dioxide removal (CDR) approach: Nearshore Macroalgae Aquaculture for Carbon Sequestration (N-MACS) by biomass harvesting. By cultivating macroalgae in nearshore ocean surface areas, N-MACS aims to sequester CO₂ with subsequent carbon storage. Utilizing an Earth System Model with intermediate complexity (EMIC), we explore the CDR potential of N-MACS alongside its impacts on the global carbon cycle, marine biogeochemistry and marine ecosystems. Our investigations unveil that coastal N-MACS could potentially sequester 0.7 to 1.1 GtC yr⁻¹. However, it also significantly suppresses marine phytoplankton net primary productivity because of nutrient removal and canopy shading, counteracting approximately 30% of the N-MACS CDR capacity. This suppression of surface NPP, in turn, reduces carbon export out of the euphotic zone to the ocean interior, leading to elevated dissolved oxygen levels and diminished denitrification in present-day oxygen minimum zones. Effects due to harvesting-induced phosphorus removal continue for centuries even beyond the cessation of N-MACS.

3.1 Introduction

The IPCC's Sixth Assessment Report ((IPCC, 2022)) stipulates global net-zero CO₂ emissions by the early 2050s to restrict global warming to 1.5°C, recognizing Carbon Dioxide Removal (CDR) as essential to counterbalance residual emissions. Ocean-based CDR approaches are gaining traction due to the ocean's inherent carbon sequestration capacity (IPCC (2022); Keller et al. (2021); GESAMP (2019)). As the Earth's largest dynamic carbon reservoir (Falkowski et al. (2000); Sarmiento and Gruber (2013)), the ocean's expanse and natural carbon absorption capacity, combined with measures like ocean fertilization, ocean alkalinity enhancement, can substantially augment carbon sequestration efforts (Buesseler et al. (2004); Bach et al. (2019)).

Macroalgae offer an avenue for ocean-based CDR due to their notable net primary production rates and high carbon-to-nutrient ratios, facilitating effective carbon sequestration (Yeurt et al. (2012); Fernand et al. (2017); Gao et al. (2022)). The global potential carbon export by macroalgae has been estimated as 1.4 GtC per year (Krause-Jensen and Duarte (2016); Ortega et al. (2019); Barrón and Duarte (2015)). Cultivation technologies for macroalgae are well-established (e.g., (Buck and Buchholz, 2004; Goecke et al., 2020; Zhang et al., 2016)), with a global harvest reaching 34.7 million tonnes wet weight (WW) in 2019 (FAO (2018); Cai et al. (2021)). Macroalgae cultivation for ocean-CDR has been

considered recently Wu et al. (2023); Fernand et al. (2017). Based on geographic location, macroalgae-based CDR can be categorized into two categories: open-ocean cultivation with deep-ocean carbon storage Wu et al. (2023); Bach et al. (2021), and nearshore cultivation for harvesting, followed by subsequent carbon storage achieved outside of the ocean such as biochar and Bioenergy with Carbon Capture and Storage (BECCS, (Roberts et al., 2015; Bird et al., 2011; Fernand et al., 2017; Gattuso et al., 2021; Capron et al., 2020; Borchers et al., 2022; Chen et al., 2015)).

Prior to the large-scale implementation of ocean-based CDR strategies, comprehensive evaluations are essential to understand their potential and impacts on the marine environment IPCC (2022); Gattuso et al. (2021). Particularly, numerical simulations with Earth system models are pivotal as they, in contrast to field experiments pose, have no direct environmental impact Oeschle et al. (2010); Keller et al. (2014, 2018b); Siegel et al. (2021). Several modelling studies have examined macroalgae-based CDR strategies, revealing CDR capacities ranging from Mega (10^6) to Giga (10^9) tonnes depending on location and species. These studies, referenced as (Wu et al., 2023; Bach et al., 2019) for open-ocean and (Arzeno-Soltero et al., 2023; Berger et al., 2023) for nearshore areas, also underscore the constraints posed by marine physical and biogeochemical feedbacks on CDR capacity and efficiency. Furthermore, they highlight the potentially significant impacts on the global carbon cycle, marine biogeochemistry, and ecosystems through the alteration of ocean nutrient distributions and primary production patterns.

Here we evaluate ‘Nearshore Macroalgae Aquaculture for Carbon Sequestration’ (hereinafter N-MACS), operating under the assumption that the harvested carbon content will be sequestered from atmosphere and hence achieving CDR. The evaluation employs an Earth System Model of intermediate complexity, encompassing an explicit macroalgae component, to rigorously assess implications and carbon sequestration efficacy of N-MACS from 2020 to 3000, with N-MACS deployment from 2020 to 2100. Our objectives are to: a) examine the idealised large-scale CDR potential of N-MACS, and b) evaluate its effects on the global carbon cycle and marine biogeochemistry, including termination effects and millennial long-term effects.

3.2 Methods

We employ the University of Victoria Earth System Climate Model version 2.9 (UVic; (Keller et al., 2012; Weaver et al., 2001)), an intermediate complexity Earth system model coupling a three-dimensional ocean circulation model Pacanowski (1996) including a dy-

dynamic thermodynamic sea ice module Bitz and Lipscomb (1999), a terrestrial model Meissner et al. (2003); Weaver et al. (2001) and a one-layer atmospheric energy-moisture model Fanning and Weaver (1996). The horizontal resolution is 3.6° longitude \times 1.8° latitude, and the ocean component has 19 vertical layers with thicknesses ranging from 50 m near the surface to 500 m in the deep ocean. The ocean biogeochemistry module includes nutrients (nitrogen and phosphate), one general phytoplankton type, and one diazotrophic phytoplankton (i.e., nitrogen fixers), one general macroalgae (see below section), one type of zooplankton, dissolved inorganic carbon, oxygen, and total alkalinity Keller et al. (2012); Eby et al. (2013).

Upon spinning up the model under pre-industrial conditions, we employed CMIP5 forcing data for the historical period Eby et al. (2013). From 2005 to 2100, we aligned the inputs of CO₂ emissions, land-use changes, volcanic radiative forcing, and sulfate aerosols with the RCP4.5 scenario. For the period post-2300, CO₂ emissions are projected to decline linearly, reaching zero by 3000, with other forcings maintained at constant levels. RCP4.5 is a moderate emissions trajectory with a radiative forcing of 4.5 W/m^2 by 2100 Thomson et al. (2011); Meinshausen et al. (2011).

N-MACS is an extension of the Macroalgae Open-ocean Mariculture and Sinking (MOS) framework developed by Wu et al. (2023), featuring an idealized generic model of the Phaeophyceae (brown algae) *Sacharina* integrated with UVic. Macroalgae growth is controlled by multiple limiting factors (erosion, nutrient availability, light, and temperature) with a fixed C:N:P stoichiometric molar ratio of 400:20:1. Initial seed biomass is deployed in each surface ocean grid box with adequate nutrients to be converted into seed biomass. The initial plantlet biomass in each N-MACS grid cell is equivalent to $0.02 \text{ mmol N m}^{-3}$, sourced directly from the grid box's inorganic N, P, and C pools without extra nutrient or carbon input. A constant maximum biomass yield of $3,300 \text{ tDW km}^{-2}$ is set, focusing on large-scale impacts rather than optimizing farming strategies. Once biomass in a grid cell reaches this limit, macroalgae growth halts until end-of-season harvesting. In temperate zones, seeding starts on May 1st and harvesting occurs on October 31st in the northern hemisphere, while in the southern hemisphere, seeding begins on November 1 with harvesting on April 30, aligning with macroalgae growth phases. The model annually selects grid boxes with ample nutrients for reseeded, implying no further reseeded post-harvest in nutrient-depleted regions (detailed in Section 3.1, (Wu et al., 2023)). Additionally, surface layer macroalgae create canopy shading effects on phytoplankton communities. Potential grazers like amphipods and gastropods Jacobucci et al. (2008); Chikaraishi et al. (2007) are modeled within the UVic's zooplankton compartment Keller et al. (2012). Further

macroalgae model specifics, including parameters, functions, and cultivation strategies, are delineated in (Wu et al., 2023, Sect. 2).

3.2.1 Experimental design

Our study contains a control run (Ctrl_RCP4.5) and two N-MACS simulations: the standard N-MACS simulation with all growth constraints, and a sensitivity simulation (No_Temp) with temperature constraint removed to examine the uncertainty in temperature-dependant growth rate in the modeled macroalgae. In both N-MACS simulations, macroalgae farms are limited to ocean surface zones directly along coasts between 60°S and 60°N, with grid boxes 200 to 400 km wide, aligning with Exclusive Economic Zones (EEZs) extending to 200 nautical miles from sovereign state coasts Froehlich et al. (2019); Feng et al. (2017). It's presumed that all macroalgae production is promptly harvested post cultivation for biochar conversion or BECCS feedstock on land, indicating permanent carbon sequestration from the biomass with no nutrient return to the ocean. Meanwhile, natural macroalgae habitats are globally distributed along coastlines with species exhibiting varied temperature sensitivities Duarte et al. (2022). The No_Temp simulation investigates the theoretical maximum coastal macroalgae biomass production with species optimally adapted to local temperatures. N-MACS CDR capacity is defined as the total carbon in harvested biomass, while its CDR efficacy is defined by the changes in combined oceanic and macroalgae carbon reservoir relative to the harvested macroalgal biomass carbon content. Our focus is on the the cultivation process outcomes, excluding possible carbon leakages in post-harvest CDR applications like biochar or BECCS Chen et al. (2015); Fernand et al. (2017); Bird et al. (2011); Chen et al. (2022).

3.3 Results & Discussions

3.3.1 Macroalgae model validation

The employed macroalgae model was validated against literature data and used in idealized open-ocean cultivation simulations by (Wu et al., 2023). Given the notable nutrient availability differences between nearshore regions and open oceans, we compare the productivity of simulated nearshore macroalgae with relevant observational and modeling data.

Fig.3.1 illustrates the N-MACS distribution and its mean annual biomass yield from

2020 to 2100. Simulations indicate a total N-MACS footprint of about 24 million km², with 14 to 15 million km² yielding significant productivity (over 100 tonnes DW km⁻²yr⁻¹; Tab.3.1). These values are lower than other model-based estimates ranging from 48 to 100 million km² Froehlich et al. (2019); Lehahn et al. (2016); Berger et al. (2023), hence presenting a more conservative N-MACS productivity. The reduced macroalgae farming areas in our model result from several factors: suboptimal UVic simulation of nutrient concentrations in nearshore regions without land run-off Eby et al. (2009); Keller et al. (2012); Tivig et al. (2021), unique parameters for chosen brown algae species in our dynamic growth model Froehlich et al. (2019), consistent nutrient feedback consideration unlike earlier assessments Froehlich et al. (2019); Lehahn et al. (2016), and the assumption that farms are located within EEZs Lehahn et al. (2016). Despite these differences, the N-MACS distribution pattern aligns with those in (Lehahn et al., 2016, Fig. 3. A), (Berger et al., 2023, Figure 4), (Duarte et al., 2022, greenish pattern of Figure 1(a)), and (Froehlich et al., 2019, Figure 1). While the total N-MACS area remains steady over time, regions of significant productivity (significant N-MACS areas) expand during the initial deployment decade (Fig.A11), resulting from dynamic nutrient cycling. Here, N-MACS suppresses phytoplankton due to canopy shading (Fig.A3), creating a nutrient surplus within its habitat that fertilizes N-MACS (see Sect.3.3.3).

In productive N-MACS regions, simulated macroalgae productivity averages 165 tonnes DW km⁻² yr⁻¹, rising to 223 tonnes DW km⁻² yr⁻¹ in No_Temp (Tab.3.1). Farmed seaweed productivity, including the modeled *Saccharina* species, varies significantly depending on species, cultivation techniques, and environmental conditions. Reported *Saccharina* yields in Europe range from 4 to 450 tonnes DW km⁻² yr⁻¹ Peteiro et al. (2014); Buck and Buchholz (2004), while in northeast Asia, yields can reach 2,400-3,000 tonnes DW km⁻² yr⁻¹ Yokoyama et al. (2007); Zhang et al. (2011).

Although N-MACS farms were initially established in all ocean grid boxes adjacent to land between 60°S and 60°N in year 2020, sustainable biomass harvests are mainly found in four regions with high nutrient availability: the Eastern Boundary Upwelling Systems in the nearshore Pacific regions of South America and the Atlantic coasts of Africa Chavez and Messié (2009); Fréon et al. (2009), the northeast Pacific and the Southern Ocean. This is consistent with the findings of (Berger et al., 2023), (Arzeno-Soltero et al., 2023), and (Duarte et al., 2021).

In the sensitivity study (No_Temp), where temperature no longer affects macroalgae growth, the N-MACS distribution mirrors the base case, albeit with increased biomass productivity in mid to high latitudinal coastal regions (Tab.3.1, Fig.A2). By employing

local macroalgae species better adapted to specific temperature ranges, optimization of macroalgae cultivation and enhancement of the CDR potential of nearshore macroalgae-based strategies may be achievable.

Table 3.1: Summary table of N-MACS simulations. Significant N-MACS area is area with ≥ 100 tonnes DW per km² per year. The changes are N-MACS variations relative to Ctrl_RCP4.5.

	Unit	N-MACS	No_Temp
Total yield	Gt DW	188.96	293.40
N-MACS total area	10 ⁶ km ²	24.34	23.65
Significant N-MACS area		14.29	15.97
Total carbon fixation in N-MACS	GtC	56.7	88.0
Annual carbon fixation (avg. 2020 to 2100)	GtC yr ⁻¹	0.7	1.1
Annual unit area carbon fixation	tC km ⁻² yr ⁻¹	29.1	46.5
Change of global climate system in 2100 (3000 in parentheses)			
Surface averaged temperature (SAT)	°C	-0.07 (-0.08)	-0.12 (-0.13)
Atmospheric CO ₂ concentration	ppm	-14.2 (-12.0)	-22.6 (-18.3)
Change of global carbon reservoirs in 2100 (3000 in parentheses)			
Atmosphere		-30.1 (-25.5)	-47.9 (-38.9)
Ocean (including carbon fixation by N-MACS)	GtC	35.9 (31.4)	57.1 (48.8)
Land		-5.8 (-5.9)	-9.2 (-9.9)
Change of integrated marine biogeochemical parameters in 2100 (3000 in parentheses)			
POM export at 2km depth	GtC yr ⁻¹	-4.151 (0.37)	-7.245 (0.58)
PO ₄ (full depth)	Tmol	-11.64 (-11.91)	-18.10 (-18.49)
NO ₃ (full depth)	Tmol	7.68 (15.78)	-62.51 (-6.01)
Phytoplankton NPP	GtC yr ⁻¹	-0.36 (-0.52)	-0.50 (-0.82)

* DW: dry weight; POM: particle organic matter; tC: tonnes of carbon (10³ Kg);

GtC: Giga (10⁹) tonnes of carbon; Tmol: Tera moles (10¹² moles).

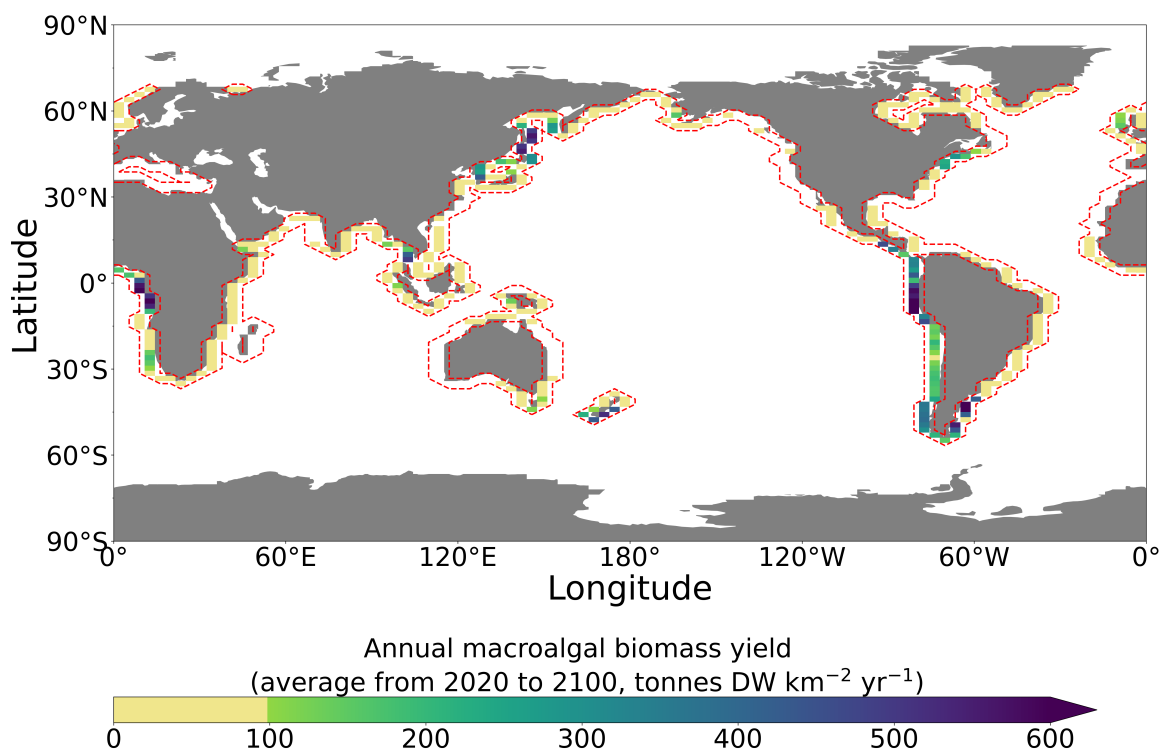


Figure 3.1: Annual macroalgae biomass yield (averaged from year 2020 to year 2100). Dashed red lines outline the initial seeding locations in year 2020. Regions with high macroalgae productivity include: Coasts of North Western Pacific (near northern China, Japan and Korean Peninsula), South Eastern Pacific (coasts of South America), South Eastern Atlantic (mid-south Africa coast), coast of New Zealand, and South Eastern of Australia. Yellowish areas indicate relatively lower yield (≤ 100 tonnes DW per km² per year).

3.3.2 CDR capacity and impacts on carbon cycle

The CDR capacity of the N-MACS approach can be quantified as the carbon contained (and securely stored) within the harvested macroalgae biomass. From 2020 to 2100, the N-MACS simulation demonstrates a total sequestration of 56.7 GtC (equivalent to 207.9 GtCO₂). In the No_Temp simulation, this capacity increases to 88 GtC due to elevated macroalgal productivity. The atmospheric CO₂ sequestration in N-MACS/No_Temp scenarios translates to a reduction in global-mean surface air temperature (SAT) by 0.07°C/0.12°C (Tab.3.1, Fig.A1). While this reduction in SAT alone does not enable the RCP 4.5 emission scenario to align with the Paris Agreement, the annual carbon removal (equivalent to 2.60/4.03 Gt CO₂eq) is, for example, on par with the 2022 annual CO₂ emissions from the global building sector (2.94 Gt CO₂, (IEA, 2023)).

The simulated global average unit-area CDR capacity is 29.1 to 46.5 tC km⁻² within N-MACS occupied regions (106.8 to 170.7 tCO₂ km⁻², Tab.3.1). Conversely, the global

dynamic seaweed growth model of (Arzeno-Soltero et al., 2023) suggested that macroalgae farming, particularly in the equatorial Pacific, could yield about 1 GtC for 1 million km² of EEZ waters, translating to 1,000 tC km⁻² yr⁻¹. These differences stem from model differences and experiment setups. Their model, incorporating four types of macroalgae species with high carbon content and yield, operates independently from dynamic nutrient changes, which we find often limits N-MACS growth, and runs for one year. Our estimation is also lower than the globally averaged per-unit-area CDR capacity of 57 tC km⁻² yr⁻¹ in (Wu et al., 2023), where the identical macroalgae model of N-MACS is applied to open-ocean regions. This difference primarily arises from the diverse distribution of macroalgae farms across varying nutrient fields, as depicted by (Wu et al., 2023) for open-ocean regions, contrasted with the current N-MACS in nearshore areas. The discrepancy is exacerbated by the coarse grid resolution in UVic, likely underestimating coastal productivity Keller et al. (2012); Tivig et al. (2021). Nevertheless, the annually averaged carbon sequestration of N-MACS is estimated at 0.7 to 1.1 GtC yr⁻¹ (2.6 to 4.0 GtCO₂ yr⁻¹), surpassing the 0.37 GtC yr⁻¹ reported by (Berger et al., 2023), something again attributable to the different dynamic macroalgae growth and Earth system modeling approaches.

The net increase in the oceanic carbon reservoir, consisting of water-column carbon content and the harvested macroalgae in the N-MACS (No_Temp) simulations, is 35.9 (57.1) GtC in 2100 (Tab.3.1), equivalent to the N-MACS induced air-sea carbon flux in the model (Fig.A6, Fig.A7). However, the increase in the oceanic plus macroalgae carbon reservoir is approximately two-thirds of the harvested macroalgae carbon, corresponding to 63.3% (64.9%) of the net carbon removed by harvesting the macroalgae. The disparity between the increase in the ocean plus macroalgae carbon pool and the carbon harvested in the form of macroalgal biomass is largely caused by backfluxes from the ocean into the atmosphere due to diminished atmospheric pCO₂ Oschlies (2009) and partially by the reduced phytoplankton net primary production (PNPP) from canopy shading and nutrient competition effects introduced by N-MACS (see Sect.3.3.3). This efficiency is somewhat higher than the CDR efficiency of 58% in (Berger et al., 2023), who employed a dynamic macroalgae growth model in conjunction with a high-resolution ocean biogeochemical model with prescribed atmospheric CO₂, i.e. without back-fluxes from the ocean into the atmosphere due to diminished atmospheric pCO₂, for 5-year simulations.

Meanwhile, the increase in the oceanic plus macroalgae carbon reservoir induced by N-MACS until 2100 leads to a corresponding decline in the terrestrial carbon reservoir of 5.8 to 9.2 GtC (see Tab. 3.1) via an atmospheric carbon climate feedback. This response illustrates the Earth system's endeavor to maintain equilibrium, with carbon cycling be-

tween terrestrial and oceanic reservoirs, primarily mediated by atmospheric interactions. This finding aligns with other studies, suggesting that ocean-based CDR could potentially weaken terrestrial carbon sinks, especially through the reduction of the CO₂ fertilization effect on terrestrial photosynthesis Keller et al. (2018a).

During the implementation phase, an enhancement of approximately 29% (37%) in the air-to-sea downward carbon flux was observed within the macroalgae-occupied areas in N-MACS (No_Temp)(Fig.A5), aligning with the 52% enhancement reported by (Berger et al., 2023). The lesser degree of carbon flux enhancement observed in our simulation within the macroalgae-occupied areas is attributed to 1) the canopy shading effect on phytoplankton in our model, reducing PNPP and subsequent carbon flux into the ocean (Fig.3.2d & Fig. A3); and 2) the dynamic atmospheric pCO₂ in our model compared to prescribed fixed pCO₂ in (Berger et al., 2023), as well as different biogeochemical properties of macroalgae and phytoplankton in the two models. Our results further highlight the potential challenges inherent in the measurement, reporting, and verification processes when assessing carbon flux enhancements. Additionally, a slight decrease in DIC in mid and deep waters is evident in Fig.A4a, stemming from reduced water column remineralization due to the diminished downward particulate organic carbon (POC) export (see Sect.3.3.3).

3.3.3 Impacts on global marine biogeochemistry

In our simulations, the 80-year implementation of N-MACS has significantly impacted global marine biogeochemistry. This includes ocean surface nutrient distributions, surface ocean alkalinity, and dissolved oxygen concentrations at mid-depth (Fig. 3.2). Additionally, simulated net primary production and the distributions of ordinary phytoplankton and diazotrophs are also affected by N-MACS deployment. Notably, some of these impacts persist until the year 3000, despite the cessation of N-MACS in 2100 (see below).

The N-MACS macroalgae model delineates two primary impacts of macroalgae on phytoplankton: nutrient competition and canopy shading (Wu et al., 2023, Sect.2.2.3). Harvesting macroalgae not only sequesters carbon but also extracts nutrients within the harvested biomass, leading to an immediate drop in global PNPP post N-MACS initiation in 2020, with a gradual reduction during N-MACS deployment till 2100 (Fig.3.3e). This PNPP decline predominantly occurs along coast-adjacent N-MACS areas (Fig.3.2d). Additionally, certain open-ocean regions beyond coastal farms exhibit a PNPP increase, notably in the Indian Ocean, eastern Atlantic near Africa, and eastern equatorial Pacific. This is attributed to nutrient leakage from N-MACS areas (see Fig.3.2d; further details in

the subsequent paragraph). N-MACS implementation suppresses oceanic nitrogen fixers, diazotrophs, due to canopy shading and phosphate competition by macroalgae (Fig.A9). Although certain regions exhibit heightened diazotroph biomass due to increased phosphate levels (Fig.A10a&c), the overall nitrogen fixation relative to DNPP diminishes during N-MACS deployment (Fig.3.3h). Zooplankton, assumed capable of grazing on macroalgae Wu et al. (2023), primarily feed on phytoplankton due to a lower macroalgae grazing preference, hence their biomass trends closely with those of phytoplankton (not shown).

Fig.3.3a illustrates a notable increase in surface ocean PO_4 concentrations (top 50m) following N-MACS initiation, followed by a decrease. Three primary factors underlie this PO_4 rise. Firstly, the suppression of phytoplankton by macroalgae leads to a decreased organic carbon export out of the euphotic zone. Secondly, macroalgae cannot fully utilize the *in-situ* PO_4 due to the limited growth rate and maximum macroalgae biomass Wu et al. (2023). Lastly, the higher stoichiometric N:P ratio of 20:1 in macroalgae, compared to the Redfield ratio of 16:1 in phytoplankton, entails less PO_4 consumption per nitrogen unit for growth. This explains the increases in surface PO_4 levels in N-MACS regions shown in Fig.3.2c (Fig.A8c for No_Temp). Nitrate concentrations in N-MACS regions also rise due to phytoplankton inhibition and unexhausted available nitrate from macroalgae growth (Fig.3.2a). These disparities consequently induce lateral nutrient leakage from N-MACS areas, fertilizing the aforementioned downstream area of coastal N-MACS farms. Here, augmented PNPP consumes the displaced nutrients, driving a regional PO_4 concentration reduction (Fig.3.2c).

A reduction in surface PNPP within N-MACS regions triggers a decline in particulate organic matter (POM) export to ocean depths, as observed at 2000 m in Fig. 3.3f and Tab.3.1. This decline subsequently diminishes oxygen consumption via aerobic remineralization of organic carbon, thus elevating the oxygen concentration across middle and bottom waters (Fig.A4d, Fig.A12d). Notable increases in dissolved oxygen concentrations at 300m depth are apparent in the northwestern Pacific, eastern equatorial Pacific, and southern Atlantic near the South American continent (Fig.3.2e & Fig.3.3). Specifically, oxygen minimum zones (OMZs) in the North Pacific and equatorial Atlantic Ocean have shrunk compared to Ctrl_RCP4.5. The increased oxygen levels inhibit denitrification in the subsurface and the upwelling system in the eastern equatorial Pacific (Fig.3.2f&i, (Bange et al., 2019; Ravishankara et al., 2009)), and diminished remineralization of organic carbon curtails nutrient regeneration, reducing nutrient upwelling (Fig.3.2g&h). This results in elevated NO_3 but reduced PO_4 compared to the Ctrl_RCP4.5 in the open ocean of the eastern equatorial Pacific (Fig.3.2a, c, d & f). Another factor contributing to the reduced PO_4

in the source waters of the upwelling regions is the decreased PNPP in the N-MACS areas, which lessens export and thereby reduces the PO_4 source from POM remineralization (Fig.3.2d, Fig.3.3f). Furthermore, the aforementioned decreased denitrification increases the NO_3 supply in the upwelling system to the surface, especially in oxygen-depleted regions off Peru where reduced POM remineralization leads to lesser denitrification and nitrogen loss. However, in the No_Temp simulation, amplified macroalgae growth utilizes upwelled NO_3 before export to the open ocean, mitigating the NO_3 increase in the eastern equatorial Pacific (Fig.A8a).

Despite the reduction in mid-depth denitrification (Fig.3.2i), which also diminishes alkalinity production, the surface alkalinity in N-MACS increases about 1% or 10 to 20 mmol m^{-3} by 2100 (Fig.3.2b), due to reduced CaCO_3 generation from the PNPP reduction induced by continuous phosphate removal by N-MACS (Fig.A12, (Schmittner et al., 2008, Eq.2)). Post N-MACS discontinuation in 2100, which effectively terminates canopy shading and nutrient competition effects, results in a marked resurgence in PNPP and thereby also a decrease in global surface nutrient concentrations (Fig3.3a, b&e). Additionally, diazotroph biomass, DNPP, and nitrogen fixation recover (Fig.A9, Fig3.3h). The export of PNPP and POC as well as the subsurface oxygen consumption via organic carbon remineralization also recovers (Fig3.3g). Additionally, the air-sea CO_2 flux reverts to baseline levels after cessation of the carbon sequestration by macroalgal harvest from the ocean (Fig.A6, A7).

By year 3000, the average surface temperature in the N-MACS/No_Temp simulations is slightly lower by $-0.08/-0.13$ °C, respectively, compared to Ctrl_RCP4.5, maintaining the temperature reduction achieved by N-MACS in 2100 (Tab.3.1). After N-MACS termination in year 2100 and until year 3000, both oceanic and terrestrial carbon reservoirs shrink, with oceanic plus macroalgae carbon storage decreasing by 4.5 GtC in N-MACS and 8.3 GtC in No_Temp, and terrestrial carbon storage declining by 0.1 GtC and 0.7 GtC in N-MACS and No_Temp scenarios respectively. This leads to a 4.6 / 9.0 GtC or 2.2 / 4.3 ppm atmospheric CO_2 increase (tab.3.1). Decreased global temperatures slow photosynthesis and soil respiration, in combination yielding a small reduction in the terrestrial carbon pool. The decrease in the oceanic carbon pool mainly arises from the PNPP reduction as a consequence of permanent phosphate removal during the operation of N-MACS. This enduring PO_4 removal leads to long-term alterations in marine biogeochemistry, as shown by extended simulations until year 3000 (Fig.3.3). Though only 0.4% of total oceanic phosphate is removed by 2100 (Fig.3.3c), it induces a persistent reduction in PNPP, DNPP, and nitrogen fixation (Fig.3.3a&h, A10b&d). This prevents PNPP and DNPP recovery to

RCP4.5 levels from 2100 to 3000 (Fig. 3.3 e), leading to increased oxygen due to overall POC export reduction (Fig.3.3d&g, Fig.A12).

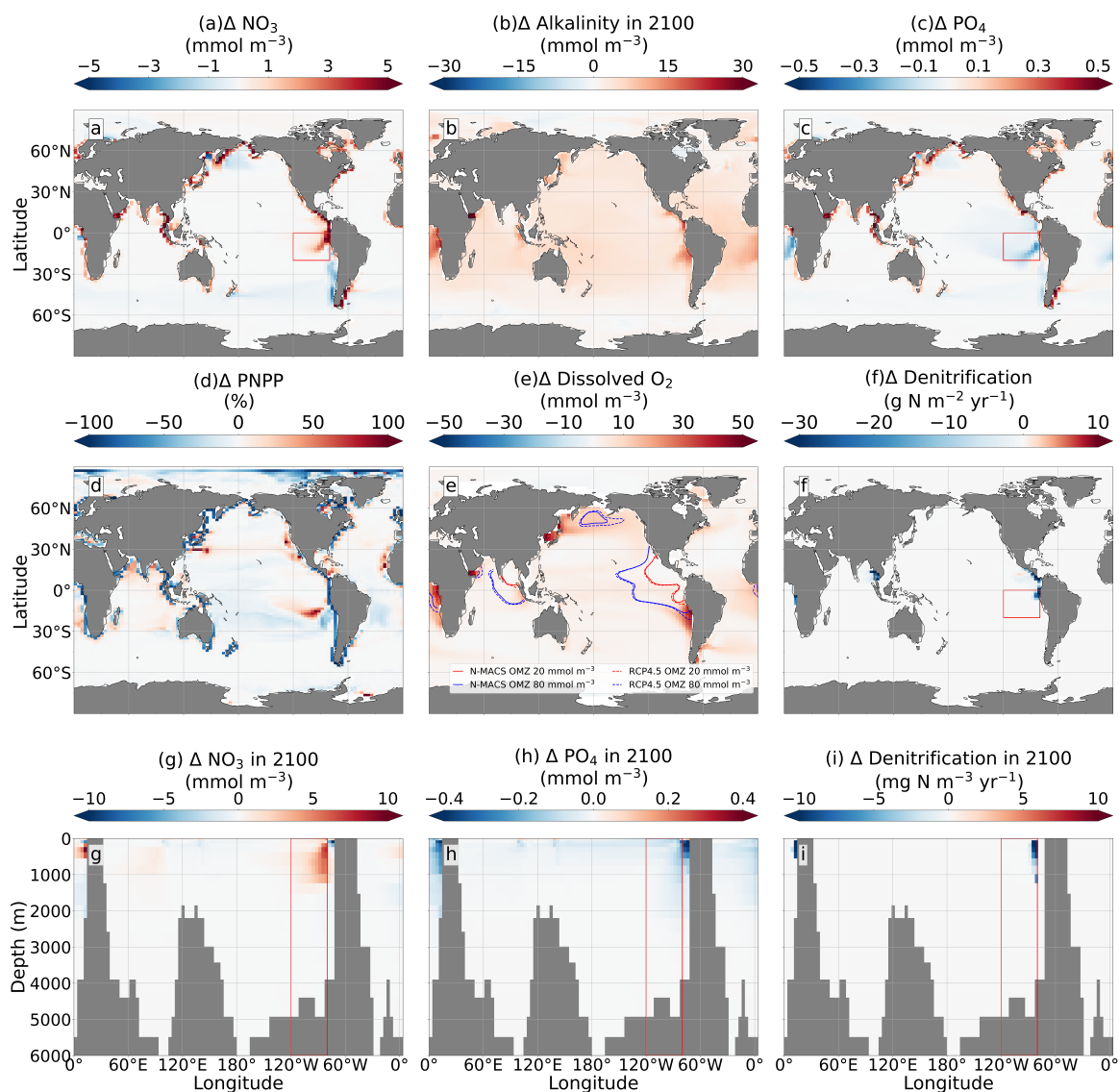


Figure 3.2: Differences in simulated oceanic properties in year 2100 after continuous N-MACS deployment from 2020 to 2100, with respect to Ctrl_RCP4.5 without N-MACS deployment (data averaged over this period, except for **d** and **e** representing data in 2100): **a**: Surface-layer nitrate (top 50m); **b**: Surface-layer alkalinity; **c**: Surface-layer phosphate; **d**: Phytoplankton net primary production (PNPP); **e**: Dissolved oxygen concentrations and oxygen minimum zones (OMZs) at a depth of 300m; **f**: Oceanic denitrification rates. Subfigures **g**, **h** & **i** represent latitudinally averaged data from 20°S to 0°, relative to the Ctrl_RCP4.5 scenario depicted in subfigures **a**, **c**, & **f** (highlighted by red rectangular regions between latitudes 20°S to 0° and longitudes 80°W to 120°W): **g**: Phosphate concentrations, **h**: Nitrate concentrations, **i**: Annual denitrification rates.

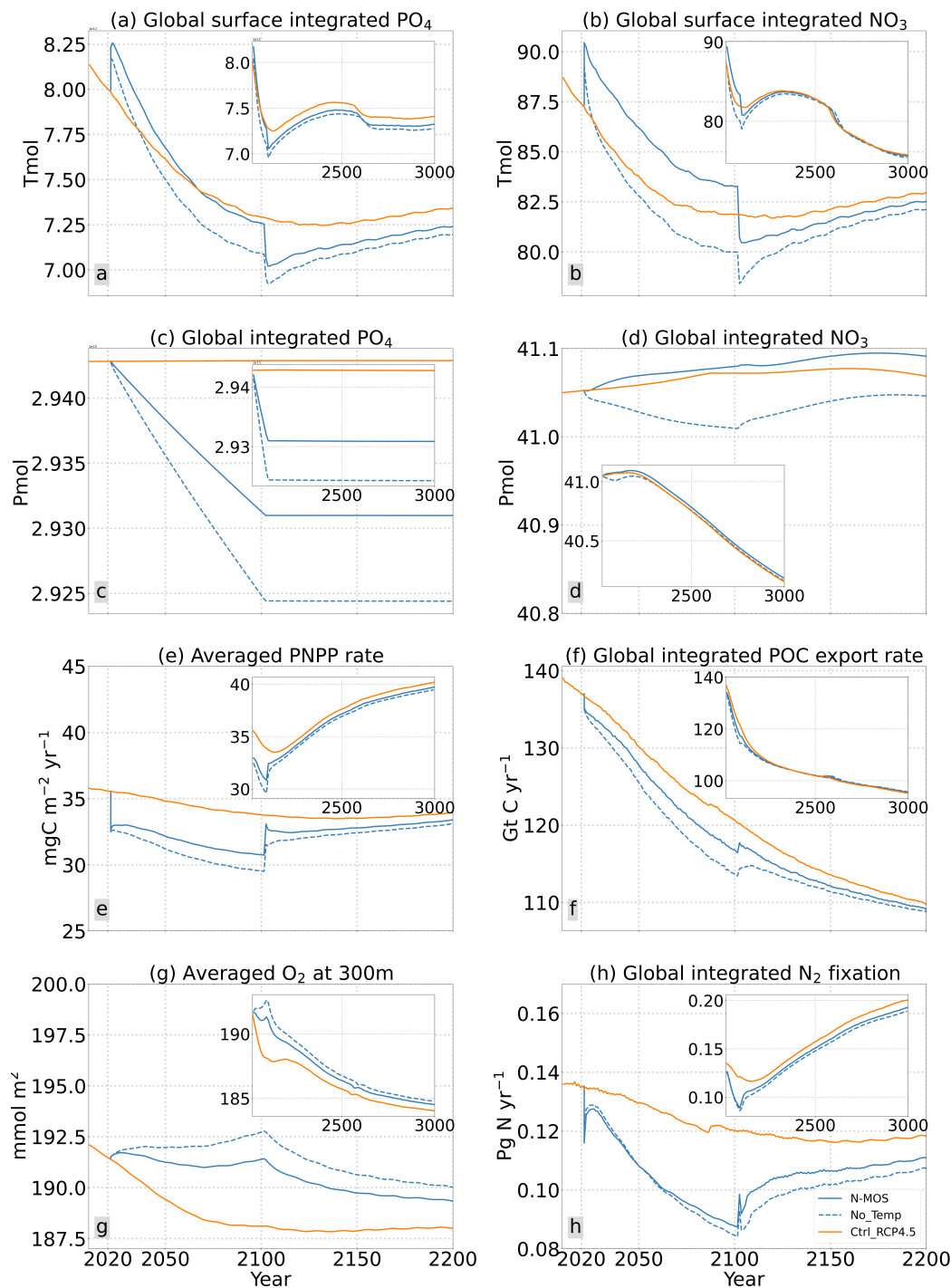


Figure 3.3: Temporal evolution of globally integrated nutrients, Phytoplankton Net Primary Production (PNPP), and Particulate Organic Carbon (POC) Export at 2,000m depth: Comparison of N-MACS (solid blue), No_Temp (dashed blue), and Ctrl_RCP4.5 Baseline Simulation (orange). Insets in each panel extend the timeline to the year 3000. **a & c**: Permanent removal of PO_4 from the surface, **b & d**: Surface NO_3 levels and global NO_3 trends (increase in N-MACS, decrease in No_Temp). **e**: Surface PNPP (see also Fig.3.2d). **f**: The export of POC at 2,000m depth. **g**: The averaged O_2 concentration at 300m depth. **h**: Globally integrated Nitrogen fixation.

3.4 Conclusion & Outlook

Our analysis highlights the substantial annual gigatonne-scale CO₂ sequestration potential of N-MACS, though with marine biogeochemical and global carbon cycle feedbacks reducing the additional air-sea CO₂ flux by 35% compared to carbon removal via harvesting. Large-scale N-MACS deployment considerably alters marine biogeochemistry and ecosystems, suppressing PNPP, elevating dissolved oxygen concentrations, reducing denitrification, and decreasing surface ocean alkalinity. Terminating N-MACS in 2100 triggers a transient rebound in surface PNPP and a decrease in the air-sea CO₂ flux, yet long-term effects like nutrient depletion and increased oxygen levels persist for centuries. Promising regions for macroalgae production include the upwelling systems in South America, Africa's Atlantic coasts, the Northeast Pacific, and the Southern Ocean.

Our simulations have certain limitations: Given that the UVic operates on a coarse grid resolution ($1.8^\circ \times 3.6^\circ$), it inadequately represents the physical and biogeochemical processes of the coastal ecosystem in the marine ecosystem model Keller et al. (2012). While not significantly impacting our current global and millennial scale simulations, it may affect coastal macroalgae farming simulations when considering nutrient fluxes in coastal areas (e.g., (Van Der Molen et al., 2018)). Possible improvements to our model include a consideration of a wider range of macroalgae species Arzeno-Soltero et al. (2023); Duarte et al. (2022), explicit accounting of iron limitation Paine et al. (2023); Anton et al. (2018), dynamic cellular stoichiometry, and current impacts on macroalgae frond erosion Frieder et al. (2022); Broch and Slagstad (2012). Acknowledging both remineralization-resistant particulate and dissolved organic carbon release from macroalgae and subsequent deep-water may be crucial for comprehending the CDR capacity Pedersen et al. (2021); Ortega et al. (2019); Duarte and Krause-Jensen (2017); Wada and Hama (2013). Further considerations include macroalgae halocarbon emissions Baker et al. (2001); Leedham et al. (2013); Jia et al. (2021) and alterations in ocean surface albedo and local ecosystem Bach et al. (2021); Boyd et al. (2022). Herein it's assumed that no nutrients from the harvested biomass are returned to the ocean, which significantly impacts the simulated biogeochemistry. Thus, evaluating nutrient extraction and return strategies is imperative if N-MACS is pursued as a sustainable CDR approach.

Governance and societal facets need consideration in macroalgae-based CDR, particularly due to potential spatial competition between macroalgae cultivation and fisheries, especially along the Peruvian coast Gattuso et al. (2021); Ricart et al. (2022); Merk et al. (2022). A Comprehensive Life Cycle Analysis (LCA) considering energy consumption

biomass conversion efficiency, and financial cost is pivotal Fernand et al. (2017); Melara et al. (2020); Capron et al. (2020); Hughes et al. (2012); Aitken et al. (2014).

3.5 References

- Douglas Aitken, Cristian Bulboa, Alex Godoy-Faundez, Juan L. Turrion-Gomez, and Blanca Antizar-Ladislao. Life cycle assessment of macroalgae cultivation and processing for biofuel production. *Journal of Cleaner Production*, 75:45–56, July 2014. ISSN 09596526. doi: 10.1016/j.jclepro.2014.03.080. URL <https://linkinghub.elsevier.com/retrieve/pii/S0959652614003138>.
- Andrea Anton, Iris E. Hendriks, Núria Marbà, Dorte Krause-Jensen, Neus Garcias-Bonet, and Carlos M. Duarte. Iron Deficiency in Seagrasses and Macroalgae in the Red Sea Is Unrelated to Latitude and Physiological Performance. *Frontiers in Marine Science*, 5, 2018. ISSN 2296-7745. URL <https://www.frontiersin.org/articles/10.3389/fmars.2018.00074>.
- Isabella B. Arzeno-Soltero, Benjamin T. Saenz, Christina A. Frieder, Matthew C. Long, Julianne DeAngelo, Steven J. Davis, and Kristen A. Davis. Large global variations in the carbon dioxide removal potential of seaweed farming due to biophysical constraints. *Communications Earth & Environment*, 4(1):1–12, June 2023. ISSN 2662-4435. doi: 10.1038/s43247-023-00833-2. URL <https://www.nature.com/articles/s43247-023-00833-2>. Number: 1 Publisher: Nature Publishing Group.
- Lennart T. Bach, Sophie J. Gill, Rosalind E. M. Rickaby, Sarah Gore, and Phil Renforth. CO₂ Removal With Enhanced Weathering and Ocean Alkalinity Enhancement: Potential Risks and Co-benefits for Marine Pelagic Ecosystems. *Frontiers in Climate*, 1:7, October 2019. ISSN 2624-9553. doi: 10.3389/fclim.2019.00007. URL <https://www.frontiersin.org/article/10.3389/fclim.2019.00007/full>.
- Lennart T. Bach, Veronica Tamsitt, Jim Gower, Catriona L. Hurd, John A. Raven, and Philip W. Boyd. Testing the climate intervention potential of ocean afforestation using the Great Atlantic Sargassum Belt. *Nature Communications*, 12(1):2556, May 2021. ISSN 2041-1723. doi: 10.1038/s41467-021-22837-2. URL <https://www.nature.com/articles/s41467-021-22837-2>.
- J.M. Baker, W.T. Sturges, J. Sugier, G. Sunnenberg, A.A. Lovett, C.E. Reeves, P.D. Nightingale, and S.A. Penkett. Emissions of CH₃Br, organochlorines, and organoiodines from temperate macroalgae. *Chemosphere - Global Change Science*, 3(1):93–106, January 2001. ISSN 14659972. doi: 10.1016/S1465-9972(00)00021-0. URL <https://linkinghub.elsevier.com/retrieve/pii/S1465997200000210>.
- Hermann W. Bange, Damian L. Arévalo-Martínez, Mercedes De La Paz, Laura Farías, Jan Kaiser, Annette Kock, Cliff S. Law, Andrew P. Rees, Gregor Rehder, Philippe D. Tortell, Robert C. Upstill-Goddard, and Samuel T. Wilson. A Harmonized Nitrous Oxide (N₂O) Ocean Observation Network for the 21st Century. *Frontiers in Marine Science*, 6:157, April 2019. ISSN 2296-7745. doi: 10.3389/fmars.2019.00157. URL <https://www.frontiersin.org/article/10.3389/fmars.2019.00157/full>.

- Cristina Barrón and Carlos M. Duarte. Dissolved organic carbon pools and export from the coastal ocean: DOC EXPORT COASTAL OCEAN. *Global Biogeochemical Cycles*, 29(10):1725–1738, October 2015. ISSN 08866236. doi: 10.1002/2014GB005056. URL <http://doi.wiley.com/10.1002/2014GB005056>.
- Manon Berger, Lester Kwiatkowski, David T Ho, and Laurent Bopp. Ocean dynamics and biological feedbacks limit the potential of macroalgae carbon dioxide removal. *Environmental Research Letters*, 18(2):024039, February 2023. ISSN 1748-9326. doi: 10.1088/1748-9326/acb06e. URL <https://iopscience.iop.org/article/10.1088/1748-9326/acb06e>.
- Michael I. Bird, Christopher M. Wurster, Pedro H. De Paula Silva, Adrian M. Bass, and Rocky De Nys. Algal biochar –production and properties. *Bioresource Technology*, 102(2):1886–1891, January 2011. ISSN 09608524. doi: 10.1016/j.biortech.2010.07.106. URL <https://linkinghub.elsevier.com/retrieve/pii/S0960852410013179>.
- C. M. Bitz and William H. Lipscomb. An energy-conserving thermodynamic model of sea ice. *Journal of Geophysical Research: Oceans*, 104(C7):15669–15677, July 1999. ISSN 01480227. doi: 10.1029/1999JC900100. URL <http://doi.wiley.com/10.1029/1999JC900100>.
- Malgorzata Borchers, Daniela Thrän, Yaxuan Chi, Nicolaus Dahmen, Roland Dittmeyer, Tobias Dolch, Christian Dold, Johannes Förster, Michael Herbst, Dominik HeSS, Aram Kalhori, Ketil Koop-Jakobsen, Zhan Li, Nadine Mengis, Thorsten B. H. Reusch, Imke Rhoden, Torsten Sachs, Cornelia Schmidt-Hattenberger, Angela Stevenson, Terese Thoni, Jiajun Wu, and Christopher Yeates. Scoping carbon dioxide removal options for Germany—What is their potential contribution to Net-Zero CO₂? *Frontiers in Climate*, 4:810343, October 2022. ISSN 2624-9553. doi: 10.3389/fclim.2022.810343. URL <https://www.frontiersin.org/articles/10.3389/fclim.2022.810343/full>.
- Philip W. Boyd, Lennart T. Bach, Catriona L. Hurd, Ellie Paine, John A. Raven, and Veronica Tamsitt. Potential negative effects of ocean afforestation on offshore ecosystems. *Nature Ecology & Evolution*, 6(6):675–683, April 2022. ISSN 2397-334X. doi: 10.1038/s41559-022-01722-1. URL <https://www.nature.com/articles/s41559-022-01722-1>.
- Ole Jacob Broch and Dag Slagstad. Modelling seasonal growth and composition of the kelp *Saccharina latissima*. *Journal of Applied Phycology*, 24(4):759–776, August 2012. ISSN 0921-8971, 1573-5176. doi: 10.1007/s10811-011-9695-y. URL <http://link.springer.com/10.1007/s10811-011-9695-y>.
- Bela Hieronymus Buck and Cornelia Maria Buchholz. The offshore-ring: A new system design for the open ocean aquaculture of macroalgae. *Journal of Applied Phycology*, 16(5):355–368, October 2004. ISSN 0921-8971. doi: 10.1023/B:JAPH.0000047947.96231.ea. URL <http://link.springer.com/10.1023/B:JAPH.0000047947.96231.ea>.
- Ken O. Buesseler, John E. Andrews, Steven M. Pike, and Matthew A. Charette. The Effects of Iron Fertilization on Carbon Sequestration in the Southern Ocean. *Science*, 304(5669):414–417, April 2004. doi: 10.1126/science.1086895. URL <https://www.science.org/doi/full/10.1126/science.1086895>. Publisher: American Association for the Advancement of Science.

- Junning Cai, Alessandro Lovatelli, José Aguilar-Manjarrez, Lynn Cornish, Lionel Dabbadie, Anne Desrochers, Simon Diffey, Esther Garrido Gamarro, James Geehan, Anicia Hurtado, et al. Seaweeds and microalgae: an overview for unlocking their potential in global aquaculture development. *FAO Fisheries and Aquaculture Circular*, 1229, 2021.
- Mark E. Capron, Jim R. Stewart, Antoine De Ramon N' Yeurt, Michael D. Chambers, Jang K. Kim, Charles Yarish, Anthony T. Jones, Reginald B. Blaylock, Scott C. James, Rae Fuhrman, Martin T. Sherman, Don Piper, Graham Harris, and Mohammed A. Hasan. Restoring Pre-Industrial CO₂ Levels While Achieving Sustainable Development Goals. *Energies*, 13(18):4972, September 2020. ISSN 1996-1073. doi: 10.3390/en13184972. URL <https://www.mdpi.com/1996-1073/13/18/4972>.
- Francisco P. Chavez and Monique Messié. A comparison of Eastern Boundary Upwelling Ecosystems. *Progress in Oceanography*, 83(1-4):80–96, December 2009. ISSN 00796611. doi: 10.1016/j.pocean.2009.07.032. URL <https://linkinghub.elsevier.com/retrieve/pii/S0079661109000998>.
- Binbin Chen, Zongrun Gu, Mingjiang Wu, Zengling Ma, Hooi Ren Lim, Kuan Shiong Khoo, and Pau Loke Show. Advancement pathway of biochar resources from macroalgae biomass: A review. *Biomass and Bioenergy*, 167:106650, December 2022. ISSN 0961-9534. doi: 10.1016/j.biombioe.2022.106650. URL <https://www.sciencedirect.com/science/article/pii/S0961953422003129>.
- Huihui Chen, Dong Zhou, Gang Luo, Shicheng Zhang, and Jianmin Chen. Macroalgae for biofuels production: Progress and perspectives. *Renewable and Sustainable Energy Reviews*, 47:427–437, July 2015. ISSN 13640321. doi: 10.1016/j.rser.2015.03.086. URL <https://linkinghub.elsevier.com/retrieve/pii/S1364032115002397>.
- Y Chikaraishi, Y Kashiyama, No Ogawa, H Kitazato, and N Ohkouchi. Metabolic control of nitrogen isotope composition of amino acids in macroalgae and gastropods: implications for aquatic food web studies. *Marine Ecology Progress Series*, 342:85–90, July 2007. ISSN 0171-8630, 1616-1599. doi: 10.3354/meps342085. URL <http://www.int-res.com/abstracts/meps/v342/p85-90/>.
- Carlos M. Duarte and Dorte Krause-Jensen. Export from Seagrass Meadows Contributes to Marine Carbon Sequestration. *Frontiers in Marine Science*, 4, January 2017. ISSN 2296-7745. doi: 10.3389/fmars.2017.00013. URL <http://journal.frontiersin.org/article/10.3389/fmars.2017.00013/full>.
- Carlos M. Duarte, Annette Bruhn, and Dorte Krause-Jensen. A seaweed aquaculture imperative to meet global sustainability targets. *Nature Sustainability*, 5(3):185–193, October 2021. ISSN 2398-9629. doi: 10.1038/s41893-021-00773-9. URL <https://www.nature.com/articles/s41893-021-00773-9>.
- Carlos M. Duarte, JeanPierre Gattuso, Kasper Hancke, Hege Gundersen, Karen FilbeeDexter, Morten F. Pedersen, Jack J. Middelburg, Michael T. Burrows, Kira A. Krumhansl, Thomas Wernberg, Pippa Moore, Albert Pessarrodona, Sarah B. Ørberg, Isabel S. Pinto, Jorge Assis, Ana M. Queirós, Dan A. Smale, Trine Bekkby, Ester A. Serrão, Dorte Krause-Jensen, and Richard Field. Global estimates of the extent and production of macroalgal forests. *Global Ecology and Biogeography*, 31(7):1422–1439, July 2022. ISSN 1466-822X, 1466-8238. doi: 10.1111/geb.13515. URL <https://onlinelibrary.wiley.com/doi/10.1111/geb.13515>.

- M. Eby, K. Zickfeld, A. Montenegro, D. Archer, K. J. Meissner, and A. J. Weaver. Lifetime of Anthropogenic Climate Change: Millennial Time Scales of Potential CO₂ and Surface Temperature Perturbations. *Journal of Climate*, 22(10):2501–2511, May 2009. ISSN 1520-0442, 0894-8755. doi: 10.1175/2008JCLI2554.1. URL <http://journals.ametsoc.org/doi/10.1175/2008JCLI2554.1>.
- M. Eby, A. J. Weaver, K. Alexander, K. Zickfeld, A. Abe-Ouchi, A. A. Cimadoribus, E. Crespin, S. S. Drijfhout, N. R. Edwards, A. V. Eliseev, G. Feulner, T. Fichet, C. E. Forest, H. Goosse, P. B. Holden, F. Joos, M. Kawamiya, D. Kicklighter, H. Kienert, K. Matsumoto, I. I. Mokhov, E. Monier, S. M. Olsen, J. O. P. Pedersen, M. Perrette, G. Philippon-Berthier, A. Ridgwell, A. Schlosser, T. Schneider Von Deimling, G. Shaffer, R. S. Smith, R. Spahni, A. P. Sokolov, M. Steinacher, K. Tachiiri, K. Tokos, M. Yoshimori, N. Zeng, and F. Zhao. Historical and idealized climate model experiments: an intercomparison of Earth system models of intermediate complexity. *Climate of the Past*, 9(3):1111–1140, May 2013. ISSN 1814-9332. doi: 10.5194/cp-9-1111-2013. URL <https://cp.copernicus.org/articles/9/1111/2013/>.
- P. Falkowski, R. J. Scholes, E. Boyle, J. Canadell, D. Canfield, J. Elser, N. Gruber, K. Hibbard, P. Högborg, S. Linder, F. T. Mackenzie, B. Moore Iii, T. Pedersen, Y. Rosenthal, S. Seitzinger, V. Smetacek, and W. Steffen. The Global Carbon Cycle: A Test of Our Knowledge of Earth as a System. *Science*, 290(5490):291–296, October 2000. ISSN 0036-8075, 1095-9203. doi: 10.1126/science.290.5490.291. URL <https://www.science.org/doi/10.1126/science.290.5490.291>.
- Augustus F. Fanning and Andrew J. Weaver. An atmospheric energy-moisture balance model: Climatology, interpentadal climate change, and coupling to an ocean general circulation model. *Journal of Geophysical Research: Atmospheres*, 101(D10):15111–15128, June 1996. ISSN 01480227. doi: 10.1029/96JD01017. URL <http://doi.wiley.com/10.1029/96JD01017>.
- FAO, editor. *Meeting the sustainable development goals*. Number 2018 in The state of world fisheries and aquaculture. Rome, 2018. ISBN 978-92-5-130562-1.
- E. Y. Feng, W. Koeve, D. P. Keller, and A. Oschlies. Model-Based Assessment of the CO₂ Sequestration Potential of Coastal Ocean Alkalinization. *Earth's Future*, 5(12):1252–1266, December 2017. ISSN 23284277. doi: 10.1002/2017EF000659. URL <http://doi.wiley.com/10.1002/2017EF000659>.
- Francois Fernand, Alvaro Israel, Jorunn Skjermo, Thomas Wichard, Klaas R. Timmermans, and Alexander Golberg. Offshore macroalgae biomass for bioenergy production: Environmental aspects, technological achievements and challenges. *Renewable and Sustainable Energy Reviews*, 75:35–45, August 2017. ISSN 13640321. doi: 10.1016/j.rser.2016.10.046. URL <https://linkinghub.elsevier.com/retrieve/pii/S1364032116307018>.
- Christina A. Frieder, Chao Yan, Marcelo Chamecki, Daniel Dauhajre, James C. McWilliams, Javier Infante, Meredith L. McPherson, Raphael M. Kudela, Fayçal Kessouri, Martha Sutula, Isabella B. Arzeno-Soltero, and Kristen A. Davis. A Macroalgal Cultivation Modeling System (MACMODS): Evaluating the Role of Physical-Biological Coupling on Nutrients and Farm Yield. *Frontiers in Marine Science*, 9:752951, March 2022. ISSN 2296-7745. doi: 10.3389/fmars.2022.752951. URL <https://www.frontiersin.org/articles/10.3389/fmars.2022.752951/full>.

- Halley E. Froehlich, Jamie C. Afflerbach, Melanie Frazier, and Benjamin S. Halpern. Blue Growth Potential to Mitigate Climate Change through Seaweed Offsetting. *Current Biology*, 29(18):3087–3093.e3, September 2019. ISSN 09609822. doi: 10.1016/j.cub.2019.07.041. URL <https://linkinghub.elsevier.com/retrieve/pii/S0960982219308863>.
- Pierre Fréon, Manuel Barange, and Javier Arístegui. Eastern Boundary Upwelling Ecosystems: Integrative and comparative approaches. *Progress in Oceanography*, 83(1-4):1–14, December 2009. ISSN 00796611. doi: 10.1016/j.pocean.2009.08.001. URL <https://linkinghub.elsevier.com/retrieve/pii/S0079661109001323>.
- Guang Gao, Lin Gao, Meijia Jiang, Ao Jian, and Linwen He. The potential of seaweed cultivation to achieve carbon neutrality and mitigate deoxygenation and eutrophication. *Environmental Research Letters*, 17(1): 014018, January 2022. ISSN 1748-9326. doi: 10.1088/1748-9326/ac3fd9. URL <https://iopscience.iop.org/article/10.1088/1748-9326/ac3fd9>.
- Jean-Pierre Gattuso, Phillip Williamson, Carlos M. Duarte, and Alexandre K. Magnan. The Potential for Ocean-Based Climate Action: Negative Emissions Technologies and Beyond. *Frontiers in Climate*, 2: 575716, January 2021. ISSN 2624-9553. doi: 10.3389/fclim.2020.575716. URL <https://www.frontiersin.org/articles/10.3389/fclim.2020.575716/full>.
- GESAMP. High level review of a wide range of proposed marine geoengineering techniques. In P. W. Boyd and C. M. G. Vivian, editors, *Rep. Stud. GESAMP No. 98*, page 144. International Maritime Organisation, 2019. (IMO/FAO/UNESCO-IOC/UNIDO/WMO/IAEA/UN/UN Environment/UNDP/ISA Joint Group of Experts on the Scientific Aspect of Marine Environmental Protection).
- Franz Goecke, Gunnar Klemetsdal, and Åshild Ergon. Cultivar Development of Kelps for Commercial Cultivation—Past Lessons and Future Prospects. *Frontiers in Marine Science*, 8:110, February 2020. ISSN 2296-7745. doi: 10.3389/fmars.2020.00110. URL <https://www.frontiersin.org/article/10.3389/fmars.2020.00110/full>.
- Adam D. Hughes, Kenny D. Black, Iona Campbell, Keith Davidson, Maeve S. Kelly, and Michael S. Stanley. Does seaweed offer a solution for bioenergy with biological carbon capture and storage? *Greenhouse Gases: Science and Technology*, 2(6):402–407, December 2012. ISSN 21523878. doi: 10.1002/ghg.1319. URL <https://onlinelibrary.wiley.com/doi/10.1002/ghg.1319>.
- IEA. Co2 emissions in 2022, 2023. URL <https://www.iea.org/reports/co2-emissions-in-2022>. License: CC BY 4.0.
- IPCC. Summary for Policymakers. In P.R. Shukla, J. Skea, R. Slade, A. Al Khouradajie, R. van Diemen, D. McCollum, M. Pathak, S. Some, P. Vyas, R. Fradera, M. Belkacemi, A. Hasija, G. Lisboa, S. Luz, and J. Malley, editors, *Climate Change 2022: Mitigation of Climate Change. Contribution of Working Group III to the Sixth Assessment Report of the Intergovernmental Panel on Climate Change*. Cambridge University Press, Cambridge, UK and New York, NY, USA, 2022. doi: 10.1017/9781009157926.001.

- Giuliano Buzá Jacobucci, Arthur Zigiatti Güth, and Fosca Pedini Pereira Leite. Experimental evaluation of amphipod grazing over biomass of *Sargassum filipendula* (Phaeophyta) and its dominant epiphyte. *Nauplius*, 2008.
- Yue Jia, Birgit Quack, Robert D. Kinley, Ignacio Pisso, and Susann Tegtmeier. Potential environmental impact of bromoform from Asparagopsis farming in Australia. preprint, Gases/Atmospheric Modelling/Troposphere/Chemistry (chemical composition and reactions), November 2021. URL <https://acp.copernicus.org/preprints/acp-2021-800/acp-2021-800.pdf>.
- D. P. Keller, A. Oschlies, and M. Eby. A new marine ecosystem model for the University of Victoria Earth System Climate Model. *Geoscientific Model Development*, 5(5):1195–1220, September 2012. ISSN 1991-9603. doi: 10.5194/gmd-5-1195-2012. URL <https://gmd.copernicus.org/articles/5/1195/2012/>.
- David P. Keller, Ellias Y. Feng, and Andreas Oschlies. Potential climate engineering effectiveness and side effects during a high carbon dioxide-emission scenario. *Nature Communications*, 5(1):3304, February 2014. ISSN 2041-1723. doi: 10.1038/ncomms4304. URL <https://www.nature.com/articles/ncomms4304>.
- David P. Keller, Andrew Lenton, Emma W. Littleton, Andreas Oschlies, Vivian Scott, and Naomi E. Vaughan. The Effects of Carbon Dioxide Removal on the Carbon Cycle. *Current Climate Change Reports*, 4(3):250–265, September 2018a. ISSN 2198-6061. doi: 10.1007/s40641-018-0104-3. URL <http://link.springer.com/10.1007/s40641-018-0104-3>.
- David P. Keller, Andrew Lenton, Vivian Scott, Naomi E. Vaughan, Nico Bauer, Duoying Ji, Chris D. Jones, Ben Kravitz, Helene Muri, and Kirsten Zickfeld. The Carbon Dioxide Removal Model Intercomparison Project (CDRMIP): rationale and experimental protocol for CMIP6. *Geoscientific Model Development*, 11(3):1133–1160, March 2018b. ISSN 1991-9603. doi: 10.5194/gmd-11-1133-2018. URL <https://gmd.copernicus.org/articles/11/1133/2018/>.
- David P. Keller, Kerryn Brent, Lennart T. Bach, and Wilfried Rickels. Editorial: The Role of Ocean-Based Negative Emission Technologies for Climate Mitigation. *Frontiers in Climate*, 3:743816, August 2021. ISSN 2624-9553. doi: 10.3389/fclim.2021.743816. URL <https://www.frontiersin.org/articles/10.3389/fclim.2021.743816/full>.
- Dorte Krause-Jensen and Carlos M. Duarte. Substantial role of macroalgae in marine carbon sequestration. *Nature Geoscience*, 9(10):737–742, October 2016. ISSN 1752-0894, 1752-0908. doi: 10.1038/ngeo2790. URL <https://www.nature.com/articles/ngeo2790>.
- E. C. Leedham, C. Hughes, F. S. L. Keng, S.-M. Phang, G. Malin, and W. T. Sturges. Emission of atmospherically significant halocarbons by naturally occurring and farmed tropical macroalgae. *Bio-geosciences*, 10(6):3615–3633, June 2013. ISSN 1726-4189. doi: 10.5194/bg-10-3615-2013. URL <https://bg.copernicus.org/articles/10/3615/2013/>.
- Yoav Lehahn, Kapilkumar Nivrutti Ingle, and Alexander Golberg. Global potential of offshore and shallow waters macroalgal biorefineries to provide for food, chemicals and energy: feasibility and sustainability.

- Algal Research*, 17:150–160, July 2016. ISSN 22119264. doi: 10.1016/j.algal.2016.03.031. URL <https://linkinghub.elsevier.com/retrieve/pii/S2211926416301151>.
- Malte Meinshausen, S. J. Smith, K. Calvin, J. S. Daniel, M. L. T. Kainuma, J-F. Lamarque, K. Matsumoto, S. A. Montzka, S. C. B. Raper, K. Riahi, A. Thomson, G. J. M. Velders, and D.P. P. Van Vuuren. The RCP greenhouse gas concentrations and their extensions from 1765 to 2300. *Climatic Change*, 109(1-2):213–241, November 2011. ISSN 0165-0009, 1573-1480. doi: 10.1007/s10584-011-0156-z. URL <http://link.springer.com/10.1007/s10584-011-0156-z>.
- K. J. Meissner, A. J. Weaver, H. D. Matthews, and P. M. Cox. The role of land surface dynamics in glacial inception: a study with the UVic Earth System Model. *Climate Dynamics*, 21(7-8):515–537, December 2003. ISSN 0930-7575, 1432-0894. doi: 10.1007/s00382-003-0352-2. URL <http://link.springer.com/10.1007/s00382-003-0352-2>.
- A. Jasmin Melara, Udayan Singh, and Lisa M. Colosi. Is aquatic bioenergy with carbon capture and storage a sustainable negative emission technology? Insights from a spatially explicit environmental life-cycle assessment. *Energy Conversion and Management*, 224:113300, November 2020. ISSN 01968904. doi: 10.1016/j.enconman.2020.113300. URL <https://linkinghub.elsevier.com/retrieve/pii/S0196890420308396>.
- Christine Merk, Jonas Grunau, Marie-Catherine Riekhof, and Wilfried Rickels. The need for local governance of global commons: The example of blue carbon ecosystems. *Ecological Economics*, 201:107581, November 2022. ISSN 0921-8009. doi: 10.1016/j.ecolecon.2022.107581. URL <https://www.sciencedirect.com/science/article/pii/S0921800922002439>.
- Antoine De Ramon N ‘Yeurt, David P. Chynoweth, Mark E. Capron, Jim R. Stewart, and Mohammed A. Hasan. Negative carbon via Ocean Afforestation. *Process Safety and Environmental Protection*, 90(6):467–474, November 2012. ISSN 09575820. doi: 10.1016/j.psep.2012.10.008. URL <https://linkinghub.elsevier.com/retrieve/pii/S0957582012001206>.
- Alejandra Ortega, Nathan R. Geraldi, Intikhab Alam, Allan A. Kamau, Silvia G. Acinas, Ramiro Logares, Josep M. Gasol, Ramon Massana, Dorte Krause-Jensen, and Carlos M. Duarte. Important contribution of macroalgae to oceanic carbon sequestration. *Nature Geoscience*, 12(9):748–754, September 2019. ISSN 1752-0894, 1752-0908. doi: 10.1038/s41561-019-0421-8. URL <http://www.nature.com/articles/s41561-019-0421-8>.
- A. Oschlies. Impact of atmospheric and terrestrial CO₂ feedbacks on fertilization-induced marine carbon uptake. *Biogeosciences*, 6(8):1603–1613, August 2009. ISSN 1726-4170. doi: 10.5194/bg-6-1603-2009. URL <https://bg.copernicus.org/articles/6/1603/2009/>. Publisher: Copernicus GmbH.
- A. Oschlies, M. Pahlow, A. Yool, and R. J. Matear. Climate engineering by artificial ocean upwelling: Channelling the sorcerer’s apprentice: OCEAN PIPE IMPACTS. *Geophysical Research Letters*, 37(4), February 2010. ISSN 00948276. doi: 10.1029/2009GL041961. URL <http://doi.wiley.com/10.1029/2009GL041961>.

- Ronald C Pacanowski. Documentation user's guide and reference manual (mom2, version 2). *GFDL Ocean Technical Report 3.2*, 329, 1996.
- Ellie R. Paine, Philip W. Boyd, Robert F. Strzepek, Michael Ellwood, Elizabeth A. Brewer, Guillermo Diaz-Pulido, Matthias Schmid, and Catriona L. Hurd. Iron limitation of kelp growth may prevent ocean afforestation. *Communications Biology*, 6(1):1–9, June 2023. ISSN 2399-3642. doi: 10.1038/s42003-023-04962-4. URL <https://www.nature.com/articles/s42003-023-04962-4>. Number: 1 Publisher: Nature Publishing Group.
- Mf Pedersen, K Filbee-Dexter, NI Frisk, Z Sárossy, and T Wernberg. Carbon sequestration potential increased by incomplete anaerobic decomposition of kelp detritus. *Marine Ecology Progress Series*, 660:53–67, February 2021. ISSN 0171-8630, 1616-1599. doi: 10.3354/meps13613. URL <https://www.int-res.com/abstracts/meps/v660/p53-67/>.
- César Peteiro, Noemí Sánchez, Clara Dueñas-Liaño, and Brezo Martínez. Open-sea cultivation by transplanting young fronds of the kelp *Saccharina latissima*. *Journal of Applied Phycology*, 26(1):519–528, February 2014. ISSN 0921-8971, 1573-5176. doi: 10.1007/s10811-013-0096-2. URL <http://link.springer.com/10.1007/s10811-013-0096-2>.
- A. R. Ravishankara, John S. Daniel, and Robert W. Portmann. Nitrous Oxide (N₂O): The Dominant Ozone-Depleting Substance Emitted in the 21st Century. *Science*, 326(5949):123–125, October 2009. ISSN 0036-8075, 1095-9203. doi: 10.1126/science.1176985. URL <https://www.science.org/doi/10.1126/science.1176985>.
- Aurora M Ricart, Dorte Krause-Jensen, Kasper Hancke, Nichole N Price, Pere Masqué, and Carlos M Duarte. Sinking seaweed in the deep ocean for carbon neutrality is ahead of science and beyond the ethics. *Environmental Research Letters*, 17(8):081003, August 2022. ISSN 1748-9326. doi: 10.1088/1748-9326/ac82ff. URL <https://iopscience.iop.org/article/10.1088/1748-9326/ac82ff>.
- David A. Roberts, Nicholas A. Paul, Symon A. Dworjanyn, Michael I. Bird, and Rocky De Nys. Biochar from commercially cultivated seaweed for soil amelioration. *Scientific Reports*, 5(1):9665, April 2015. ISSN 2045-2322. doi: 10.1038/srep09665. URL <https://www.nature.com/articles/srep09665>.
- Jorge L. Sarmiento and Nicolas Gruber. *Ocean Biogeochemical Dynamics*. Princeton University Press, July 2013. ISBN 978-1-4008-4907-9 978-0-691-01707-5. doi: 10.2307/j.ctt3fgxqx. URL <http://www.jstor.org/stable/10.2307/j.ctt3fgxqx>.
- Andreas Schmittner, Andreas Oschlies, H. Damon Matthews, and Eric D. Galbraith. Future changes in climate, ocean circulation, ecosystems, and biogeochemical cycling simulated for a business-as-usual CO₂ emission scenario until year 4000 AD. *Global Biogeochemical Cycles*, 22(1), 2008. ISSN 1944-9224. doi: 10.1029/2007GB002953. URL <https://onlinelibrary.wiley.com/doi/abs/10.1029/2007GB002953>. [_eprint: https://onlinelibrary.wiley.com/doi/pdf/10.1029/2007GB002953](https://onlinelibrary.wiley.com/doi/pdf/10.1029/2007GB002953).

- D A Siegel, T DeVries, S C Doney, and T Bell. Assessing the sequestration time scales of some ocean-based carbon dioxide reduction strategies. *Environmental Research Letters*, 16(10):104003, October 2021. ISSN 1748-9326. doi: 10.1088/1748-9326/ac0be0. URL <https://iopscience.iop.org/article/10.1088/1748-9326/ac0be0>.
- Allison M. Thomson, Katherine V. Calvin, Steven J. Smith, G. Page Kyle, April Volke, Pralit Patel, Sabrina Delgado-Arias, Ben Bond-Lamberty, Marshall A. Wise, Leon E. Clarke, and James A. Edmonds. RCP4.5: a pathway for stabilization of radiative forcing by 2100. *Climatic Change*, 109(1-2):77–94, November 2011. ISSN 0165-0009, 1573-1480. doi: 10.1007/s10584-011-0151-4. URL <http://link.springer.com/10.1007/s10584-011-0151-4>.
- Miriam Tivig, David P. Keller, and Andreas Oschlies. Riverine nitrogen supply to the global ocean and its limited impact on global marine primary production: a feedback study using an Earth system model. *Biogeosciences*, 18(19):5327–5350, October 2021. ISSN 1726-4170. doi: 10.5194/bg-18-5327-2021. URL <https://bg.copernicus.org/articles/18/5327/2021/>. Publisher: Copernicus GmbH.
- Johan Van Der Molen, Piet Ruardij, Karen Mooney, Philip Kerrison, Nessa E. O’Connor, Emma Gorman, Klaas Timmermans, Serena Wright, Maeve Kelly, Adam D. Hughes, and Elisa Capuzzo. Modelling potential production of macroalgae farms in UK and Dutch coastal waters. *Biogeosciences*, 15(4):1123–1147, February 2018. ISSN 1726-4189. doi: 10.5194/bg-15-1123-2018. URL <https://bg.copernicus.org/articles/15/1123/2018/>.
- Shigeki Wada and Takeo Hama. The contribution of macroalgae to the coastal dissolved organic matter pool. *Estuarine, Coastal and Shelf Science*, 129:77–85, September 2013. ISSN 02727714. doi: 10.1016/j.ecss.2013.06.007. URL <https://linkinghub.elsevier.com/retrieve/pii/S0272771413002722>.
- Andrew J. Weaver, Michael Eby, Edward C. Wiebe, Cecilia M. Bitz, Phil B. Duffy, Tracy L. Ewen, Augustus F. Fanning, Marika M. Holland, Amy MacFadyen, H. Damon Matthews, Katrin J. Meissner, Oleg Saenko, Andreas Schmittner, Huaxiao Wang, and Masakazu Yoshimori. The UVic earth system climate model: Model description, climatology, and applications to past, present and future climates. *Atmosphere-Ocean*, 39(4):361–428, December 2001. ISSN 0705-5900, 1480-9214. doi: 10.1080/07055900.2001.9649686. URL <https://www.tandfonline.com/doi/full/10.1080/07055900.2001.9649686>.
- Jiajun Wu, David P. Keller, and Andreas Oschlies. Carbon dioxide removal via macroalgae open-ocean mariculture and sinking: an Earth system modeling study. *Earth System Dynamics*, 14(1):185–221, February 2023. ISSN 2190-4987. doi: 10.5194/esd-14-185-2023. URL <https://esd.copernicus.org/articles/14/185/2023/>.
- Shinya Yokoyama, Katsunari Jonouchi, and Kenji Imou. Energy production from marine biomass: fuel cell power generation driven by methane produced from seaweed. *International Journal of Marine and Environmental Sciences*, 1(4):24–27, 2007.
- Jing Zhang, Yan Liu, Dan Yu, Hongze Song, Jingjin Cui, and Tao Liu. Study on high-temperature-resistant and high-yield Laminaria variety “Rongfu” . *Journal of Applied Phycology*, 23(2):165–171, April 2011.

ISSN 0921-8971, 1573-5176. doi: 10.1007/s10811-011-9650-y. URL <http://link.springer.com/10.1007/s10811-011-9650-y>.

Jing Zhang, Tao Liu, Dapeng Bian, Lei Zhang, Xiaobo Li, Detong Liu, Cui Liu, Jingjin Cui, and Luyang Xiao. Breeding and genetic stability evaluation of the new *Saccharina* variety “Ailunwan” with high yield. *Journal of Applied Phycology*, 28(6):3413–3421, December 2016. ISSN 0921-8971, 1573-5176. doi: 10.1007/s10811-016-0810-y. URL <http://link.springer.com/10.1007/s10811-016-0810-y>.

Chapter 4

Scoping carbon dioxide removal options for Germany What is their potential contribution to Net-Zero CO₂?

This chapter is based on the paper 'Scoping carbon dioxide removal options for Germany What is their potential contribution to Net-Zero CO₂?' published in the journal Frontiers in Climate.

*Citation: Borchers M, Thrän D, Chi Y, Dahmen N, Dittmeyer R, Dolch T, Dold C, Förster J, Herbst M, HeSS D, Kalhori A, Koop-Jakobsen K, Li Z, Mengis N, Reusch TBH, Rhoden I, Sachs T, Schmidt-Hattenberger C, Stevenson A, Thoni T, **Wu J** and Yeates C (2022) Scoping carbon dioxide removal options for Germany—What is their potential contribution to Net-Zero CO₂? *Front. Clim.* 4:810343. doi: 10.3389/fclim.2022.810343*

Abstract

In its latest assessment report the IPCC stresses the need for carbon dioxide removal (CDR) to counterbalance residual emissions to achieve net zero carbon dioxide or greenhouse gas emissions. There are currently a wide variety of CDR measures available. Their potential and feasibility, however, depends on context specific conditions, as among others biophysical site characteristics, or availability of infrastructure and resources. In our study, we selected thirteen CDR concepts which we present in the form of exemplary CDR units described in dedicated fact sheets. They cover technical CO₂ removal (two concepts of direct air carbon capture), hybrid solutions (six bioenergy with carbon capture technologies) and five options for natural sink enhancement. Our estimates for their CO₂ removal potentials in 2050 range from 0.06 to 30 million tonnes of CO₂, depending on the option. Ten of the thirteen CDR concepts provide technical removal potentials higher than 1 million tonnes of CO₂ per year. To better understand the potential contribution of analyzed CDR options to reaching net-zero CO₂ emissions, we compare our results with the current CO₂ emissions and potential residual CO₂ emissions in 2050 in Germany. To complement the necessary information on technology-based and hybrid options, we also provide an overview on possible solutions for CO₂ storage for Germany. Taking biophysical conditions and infrastructure into account, northern Germany seems a preferable area for deployment of many concepts. However, for their successful implementation further socio-economic analysis, clear regulations, and policy incentives are necessary.

4.1 Introduction

In order to meet the climate protection goals of the Paris Agreement (PA) and to keep global warming well below 2°C, global action to reduce greenhouse gas (GHG) emissions to zero (or net-zero) is needed (UNFCCC, 2015). To limit global warming to 1.5°C, the remaining carbon budget from 2020 onwards would allow us to emit another 440 (230, 670) gigatonnes (Gt) CO₂ globally (Matthews et al., 2021). The median amount of Carbon Dioxide Removal (CDR) included in the IPCC's 1.5° scenarios with limited overshoot amounts to 7 Gt CO₂ per year in 2050, high overshoot scenarios are at 9 Gt CO₂ per year in 2050 (Rogelj et al., 2018). The CDR measures in these scenarios have two functions: 1) they compensate for emissions up until the point net-zero is reached, potentially allowing more time to transition to a carbon neutral system, and 2) reaching substantial net-negative emissions (especially in overshoot scenarios) by removing previously emitted carbon diox-

ide. However, as stated by Zickfeld et al. (2021), one tonne emitted might not equate to one tonne removed.

Next to far-reaching mitigation actions, which would require systems transformation in the areas of energy, industry, land use, and transportation, CDR measures would compensate for remaining, hard-to-abate emissions to reach net-zero. However, the implementation of such CDR measures would require its very own infrastructure. To achieve the global goals of the PA, countries need to fulfill ambitious GHG reduction targets in line with their national carbon budgets. The revised Germany's Climate Change Act (KSG, 2021) pushes the climate neutrality goal to 2045 and strives for negative emissions after 2050. The permissible emission budget per sector for the years 2020-2030 has been set to 5.53 Gt CO₂-eq. For the years beyond 2030 the annual reduction targets will be announced in 2024 for the period 2031-2040, and no later than in 2032 for the period 2041-2045 (KSG, 2021).

Allocation of emission quota is a pivotal element of a country's emission reduction strategy. This distribution at the national level is a balance of many factors, including environmental effectiveness, equity, political feasibility, economic efficiency and technical requirements (Gignac and Matthews, 2015; Höhne et al., 2003; Höhne et al., 2014). Given Germany's capacities, abilities and responsibilities, a remaining CO₂ budget of 6.9 Gt (1st January 2021 until net-zero) seems to be a reasonable option (Mengis et al., 2021). It takes into account the infrastructural lock-in in Germany that needs to be overcome and reaches equal-per-capita emissions by 2035 (Mengis et al., 2021). Nevertheless, to stay within the assumed carbon budget of 6.9 Gt CO₂ for Germany, net-zero CO₂ emissions have to be achieved. This implies that supportive mitigation efforts such as the deployment of CDR measures are inevitable as some residual emissions sources, e.g. agriculture, industrial process, or aviation, will be hard to completely eliminate (cf. Geden and Schenuit, 2020). The amount of CDR required will depend on the progress in reducing emissions. In case we succeed in reducing fossil fuel and industry emissions by 85% in 2050, 1.9 Gt CO₂/year would need to be removed through CDR in Germany (Mengis et al., 2021). Other studies range between 36 to 63 megatonnes (Mt) of CO₂ per year for remaining, hard-to-abate emissions in Germany (Ariadne Report, 2021; Mengis and Kalhori et al., 2022), which in turn translates into the CDR needed for reaching net-zero. Pozo et al. (2020) allocate a cumulative CDR quota of 5-18 Gt CO₂ between 2018 and 2100 to Germany based on responsibility, capability and equality considerations.

In contrast to "conventional" mitigation where emissions from the use of fossil fuels or industrial processes are reduced or avoided, Carbon Dioxide Removal measures, some-

times referred to as “unconventional” climate change mitigation measures (Geden and Schenuit, 2020), take CO₂ directly out of the atmosphere. Such atmospheric CO₂ removal can occur by enhancing natural sinks of ecosystems or through technological processes. If anthropogenic carbon sinks exceed anthropogenic emissions to the atmosphere, so-called net negative CO₂ emissions can be achieved.

Natural sink enhancement (NSE), also called nature-based solutions or natural climate solutions, encompasses a variety of ecosystem-based options, which focus on ecosystem restoration or the increase of naturally occurring processes that sequester carbon. Those measures may relate to forests (re- and afforestation), wetlands (e.g. peatland rewetting), seas (seagrass meadows, salt marshes), or soils (restorative agriculture). Depending on the measure the captured CO₂ is then sequestered in above ground biomass, top-soils, peats or sediments, which influence the permanence of the CO₂ storage.

Technology-based solutions (or geochemical-based CDR (Schenuit et al., 2021)), like direct air carbon capture and storage (DACCS), remove CO₂ by using either chemical or physical processes to separate CO₂ from the ambient air. Unlike NSE (and bioenergy with carbon capture and storage - BECCS), DACCS requires large amounts of energy and is thus a costly CDR measure. While the plants are expected to become cheaper in the future due to economies of scale and mass fabrication, energy demand and associated costs may remain high. However, in case of DACCS, the area demand per tonne of CO₂ captured is smaller compared to other CDR options.

Bioenergy with carbon capture and storage is a hybrid approach of the two previously mentioned concepts (Bellamy and Osaka, 2020; UNEP, 2017). In this process, CO₂ is captured from the atmosphere by biological net primary production (nature-based capture) which is further used to generate bioenergy. The CO₂ which could be released in this conversion process, is captured (technology-based capture) and stored underground. If the biomass life cycle emissions are lower than the carbon captured, BECCS may provide negative emissions. BECCS is not a one-technology concept, it encompasses a wide portfolio of technological options, which follow the same principle: they convert biomass into energy (electricity, heat, fuels), capture CO₂ generated in this process, and store it under the ground or in long-lived products. The most common BECCS technology applied to date is bioethanol production with CCS, since it delivers high-purity fermentation CO₂ and thus provides a cost-competitive CDR solution with sequestration cost of \$60 or less per tonne of CO₂ (Sanchez et al., 2018). At such rate this option may compete with some natural sink enhancement solutions, such as afforestation, biochar, soil carbon sequestration or enhanced weathering (Minx et al., 2018). Other promising bioenergy technologies to

be coupled with CCS include direct combustion of biomass for generation of heat and/or power (CHP), biomass gasification or pyrolysis for biofuels production, or anaerobic digestion for biogas production with CHP or for upgrading to biomethane. Unlike DACCS, BECCS produces energy, but its land demand (and related impacts) is higher.

Although CDR provides a wide range of highly differentiated solutions, none of them can be treated like a silver bullet for addressing climate change (Minx et al., 2018). They need to become a part of national GHG removal strategies and be incorporated into existing national infrastructures, among further development of renewable energies or improvement of energy efficiency. Only in such combinations can they enable countries to achieve their national emission targets.

CDR options are at different stages of maturity, including both well researched and widely deployed options (e.g. afforestation) as well as options in a relatively early stage of development (e.g. ocean alkalinity enhancement). These differences between the various CDR option maturity levels lead to many uncertainties around the feasibility of their deployment, especially at larger scales (Low and Schäfer, 2020).

There is no “one-fits-all” solution. Thus, the deployment of CDR measures in each country or region needs to be tailor-made, both in terms of selecting best-fitting CDR options and defining their individual parameters and implementation aspects. This information needs to cover more than just techno-economic elements and be coherent among different CDR concepts. Therefore, in this study we present a portfolio of CDR options (technology-based, hybrid and NSE), which we embed specifically into the German context (e.g. biophysical and techno-economic). Each option is presented along a possible implementation example and assessed with regard to the following two analytical questions:

- How do experts envision and describe exemplary CDR concepts in Germany?
- What is the technical potential of the CDR concepts and their individual contribution to a net-zero carbon dioxide emission in Germany?

Our aim is to provide a harmonized dataset on different CDR options. These structured considerations can further serve as a basis for comparison and deeper evaluations of different CDR options as well as indicate pathways with the highest potential to support achieving net-zero CO₂ emissions in Germany.

4.2 Materials and Methods

In the following section we will describe how we selected CDR options that we identified for Germany, how we collected and checked the data for the CDR concepts, and how we finally calculated CO₂ removal potentials for Germany.

Our methodological approach is presented in the following steps:

- 1) Selection of CDR options available in Germany
- 2) CDR concepts development and description
- 3) Data collection review and quality control
- 4) Calculation of CO₂ removal potential

4.2.1 Selection of CDR options available in Germany

There are many CDR options already identified and described in the scientific literature (e.g. Oschlies and Klepper, 2017; Fuss et al., 2018; IPCC, 2018; IPCC, 2021). In this paper we selected and described options that are or likely will be available for deployment in Germany.

To provide a possibly wide portfolio of options, our selection was based on their general availability:

- Spatial availability –occurrence of geographical conditions which enable or facilitate their deployment, e.g., natural presence of seagrass meadows or areas suitable for peatlands, availability of biomass (type and amount), etc.
- Technology and market availability –maturity of CDR option in terms of its readiness to be deployed, e.g., state-of-the-art technologies.

However, our selection does not aim to provide an exhaustive list of options but rather is targeted to present possible examples.

4.2.2 CDR concepts development

There is vast information available on individual CDR options (Minx et al., 2018). Yet, it is scattered across many different research fields and levels of assessment (from laboratory to global scale). Putting this information into context by designing dedicated CDR concepts makes it not only more manageable but also increases the relevance of their

assessment for decision making since national (German) conditions (such as land availability, biomass potentials, existing infrastructure, or priorities in energy policy) shape and influence their prospective implementation.

On the basis of a literature review, experts' knowledge on CDR options and an analysis of German conditions, we prepared exemplary concepts of selected CDR options, which can be implemented in reality. For each CDR concept, we created a tabular fact sheet with a unified set of indicators (see Supplementary Materials) that serves as a tool for organizing the collected information. This allowed us to achieve a coherent description across selected CDR options.

In the fact sheets, information on the CDR concepts is further classified into eight categories which cover different aspects of the CDR systems:

- Concept characteristics - addresses general parameters of the concept
- Input - specifies the option's resources requirements
- Output - specifies expected CO₂ removal and co-products generated by the CDR
- Environmental parameters –address impacts on, among others, soils, water system and biodiversity
- Economic parameters - address the economic performance of the option
- Systemic parameters - consider potentials, permanence and verifiability
- Permission –addresses compliance with regulations
- Scalability - expresses reproducibility of the CDR unit

Each above mentioned category comprises a set of specific parameters which are listed and described in Table 1.

A limitation of the current study is that we have not considered socio-political parameters for the development of the CDR concepts. The main reasons behind this choice is that 1) there is relatively little socio-political information available on CDR options in Germany, 2) for this paper we focus on quantitative information whereas much of the available information about socio-political parameters comes from qualitative studies. Within the overarching research project (Cluster I of the Helmholtz Climate Initiative¹), broader assessments including socio-political parameters are carried out. In other words, the focus on quantitative information about the different CDR options is a delimitation of scope rather than

¹<https://www.netto-null.org/index.php.en> (accessed on: November 2, 2021)

a normative statement about what parameters are most important. Clearly, socio-political parameters matter for the deployment of CDR options (see e.g., Buck, 2016; Honegger et al., 2020; Morrow et al., 2020; Waller et al., 2020).

4.2.3 Data collection review and quality control

The data collection process has been conducted on each CDR option by dedicated assessment teams and CDR experts. Diverse data channels have been used by CDR experts including peer-reviewed literature, reports, results of simulation exercises and modeling and expert assessment for the data collection. For a literature review, a standard literature surveying (hand-selection process) as well as a systematic review using the search engine of Scopus has been carried out.

Since the data collected concerned different CDR options, it was essential to ensure a coherent integration of data into the fact sheets. Therefore, the units used in individual parameters have been standardized across all options and their integrity and quality has been checked with the respective experts.

4.2.4 Calculation of CO₂ removal potential

The ability of CDR options to avoid or remove CO₂ from the atmosphere is a key parameter which describes their CO₂ emission mitigation potential. In our study, we adopted the approach of Mengis and Kalhori et al. (2022), and focused on “(...) CO₂ rather than CO₂-equivalent emissions, following the scientific reasoning of (net) zero CO₂ targets based on the transient climate response to cumulative CO₂ emissions (Matthews et al., 2009; Rogelj et al., 2018).” as a necessary condition for temperature stabilization.

Avoided emissions express the amount of CO₂ that has not been emitted to the atmosphere as a result of actions which lower or prevent CO₂ emissions, i.e., shift to the renewable energies use, change in land-use practices or human behavior. Removed emissions express the amount of CO₂ removed from the atmosphere and durably stored in geological, terrestrial, or ocean reservoirs. These individual storage options provide a certain bandwidth for the storage durability as, e.g., for soil carbon sequestration a minimum 100 years is reached (Dynarski et al., 2020), whereas for geological CO₂ storage, several thousands of years may be achieved (Kempka et al., 2014). Such removal may be realized through enhancement of biological or biochemical sinks and DACCS. The natural CO₂ uptake, which is not caused by human intervention, is not regarded here as CO₂ removal (IPCC, 2018). If the overall process removes more emissions from the atmosphere than it emits, it can

be addressed as a negative emissions technology (NET). In this paper we quantify the CO₂ removal potential of selected CDR options by multiplying the emissions removed by one CDR unit by a number of possible units deployed by 2050 (Equation 1):

$$\begin{aligned} & \text{emissions removed through CDR option per unit} \\ & \frac{\text{Mt CO}_2}{\text{year}} \times \text{scalability [number of units]} \\ & = \text{CO}_2 \text{ removal potential of CDR option } \left[\frac{\text{Mt CO}_2}{\text{year}} \right] \end{aligned}$$

Apart from the option's emission reduction potential, we also estimate its technical implementation potential by taking into consideration the option's maturity level, availability of infrastructure, biophysical conditions, and scalability. Such a combination allows both the assessment of the possible dynamics of option implementation and the designation of the general readiness of the system for deployment.

The maturity level of a certain technology is often expressed as the Technology Readiness Level (TRL) (DOE, 2011). The TRL categorizes technologies into nine levels according to their maturity and scale of deployment: from being formulated (TRL1-2), through laboratory tests (TRL 3-4), demonstration (TRL 5-6), and pilots in a relevant environment (TRL 7-8) to market rollout (TRL 9). Progression to a higher TRL comes with an effort of further research, financial investment and/or policy support (Bui et al., 2018). Estimating a TRL of a CDR measure is not a straightforward task. First, not all concepts are strictly technology-based, and second, sometimes separate components of individual measures differ in their development stage (Hepburn et al., 2019). For this reason, in this study we do not adhere strictly to the common TRL classification (e.g. as defined by EC in HORIZON 2020 Work Programme²). Instead, we express the maturity of a certain concept by indicating the maturity of its components and level of their integration (see Annex 1 in Supplementary Materials).

Taking these factors into consideration, 13 CDR exemplary options were selected for this study as being prospective for deployment in Germany by 2050. The options are shortly described in Section 3, whereas the details are displayed in the fact sheets (see Supplementary Materials). Additionally, a fact sheet on CO₂ storage solutions has been created, complementing the information for the hybrid and technology-based options. This separation of the carbon storage component was dictated by the current legal situation in Germany, which does not allow underground storage of CO₂ and thus limits the full application of BECCS and DACCS in Germany (see Section 3.1.12). Because of this separation, we refer

²https://ec.europa.eu/research/participants/data/ref/h2020/other/wp/2016_2017/annexes/h2020-wp1617-annex-g-trl_en.pdf (accessed on: November 3, 2021)

to BECC and DACC when we talk about exemplary CDR concepts presented in our study, which do not have an integrated CO₂ storage component, and to BECCS and DACCS when we talk about the general concepts with the storage component. We use expert knowledge from different CDR fields to further identify some of the key characteristics of these options (e.g., concerning their economic parameters, permanence of storage, or scalability) and to develop the fact sheets and dedicated CDR concepts (see Section 3.1).

4.3 Results

4.3.1 CDR concepts portfolio

Following selection criteria (Section 2.1), our portfolio includes six technology options for BECC, two concepts of DACC, and five NSE options. Storage solutions were described as an additional concept (Figure 1).

BECC is considered as one of the most viable and cost-effective options to achieve negative emissions (Babin et al., 2021), but there are concerns related to its possible negative impacts on land use (competition for arable land and water) and biodiversity (IPBES-IPCC, 2021). To avoid negative interactions with the environment, only sustainable sources of biomass should be taken into account. This can include considerations such as favoring the usage of by-products, residues and waste, sourcing the biomass from sustainable agricultural and forestry practices, including novel approaches like paludiculture, or growing biomass in marine environments (e.g. macroalgae farming). In Germany, thanks to favorable geographical conditions and supporting funding programs for bioenergy provision (e.g., Renewable Energy Act (EEG, 2000 and later modifications), Biofuels Quota Act (BioKraftQuG 2006 and later modifications)), various types of biomass are already available and used for energy production (e.g., waste and residues, woody and agricultural biomass, energy crops). However, the German natural conditions also show a potential for growing new types of biomass, i.e., macroalgae or paludiculture biomass, and therefore, they have also been included in our portfolio. We also describe four terrestrial and one marine NSE (so-called “Blue Carbon” , Nellmann et al., 2009) options - all based on ecosystems that naturally occur in Germany. They include practices which either restore (e.g., peatland rewetting) or manage (e.g., soil carbon sequestration) existing ecosystems to increase their CO₂ capture and storage properties. Considering the coastal regions of Germany, we also examined coastal vegetation systems like seagrass meadows and salt marshes due to their ability to capture CO₂ from the air and store it as organic carbon

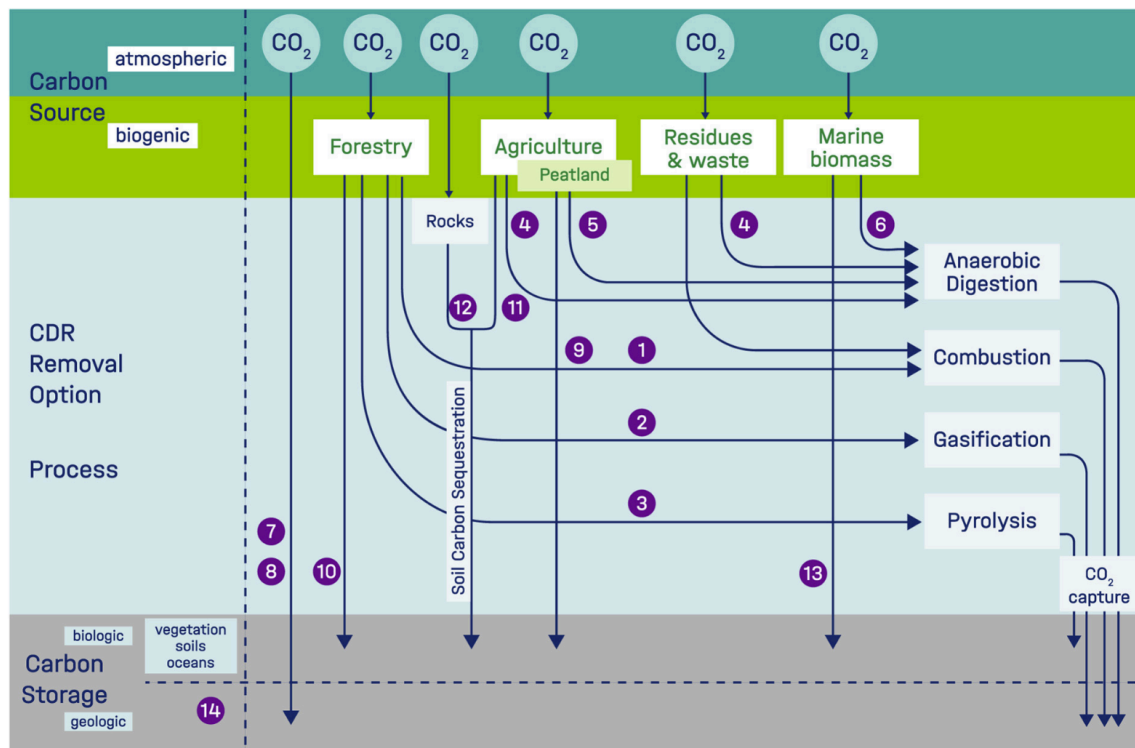


Figure 4.1: Overview of the selected CDR options. Circled numbers correspond to the numbering of CDR concepts in the paper and represent following options: 1 - BECC: biomass combustion CHP; 2 - BECC: biogas CHP; 3 - BECC: paludiculture for biogas CHP; 4 - BECC: macroalgae for biogas CHP; 5 - BECC: pyrolysis for biocoal production; 6 - BECC: gasification for biofuels production; 7 - DACC: centralized; 8 - DACC: decentralized; 9 - NSE: peatland rewetting; 10 - NSE: afforestation of cropland; 11 - NSE: SOC, cover crops; 12 - NSE: SOC, ERW; 13 - NSE: seagrass meadows Baltic Sea; 14 - geological storage solutions.

in biomass and below the ground. In our portfolio we also include DACC technologies, which are geographically independent with prerequisites being free space and access to energy sources.

Because climate mitigation requires immediate action, our portfolio consists exclusively of options whose maturity level is high enough to ensure possible implementation within a decade or sooner (assuming no social and legal constraints/barriers).

We shortly describe our CDR concepts below and enclose their details in the fact sheets provided in the supplementary materials.

BECC - Combustion of woody biomass for heat and power co-generation (Concept 1)

As Germany planned a coal phase-out by 2038 (KVBG, 2020), the conversion of coal-fired power plants to biomass may not only make a substantial contribution to the rapid re-

duction of CO₂ emissions but also support on multiple levels (e.g. economic, social) a system with largely existing infrastructure. Our concept assumes the use of a 500 megawatts electric (MWel) CHP plant fueled by wood pellets equipped with post-combustion, monoethanolamine (MEA)-based capture units, which could remove 2.99 Mt CO₂ per year. If 10 out of 18 currently operating coal-fired CHP plants (with minimum 500 MWel capacity) (BNetzA, 2021) would be converted to biomass and retrofitted with CCS units, approximately 30 Mt of CO₂ could be removed annually (Donnison et al., 2020). However, the use of woody biomass in large power plants is likely to significantly increase the overall demand for biomass including the need for biomass imports (Erlach et al., 2019). This is likely to cause direct and indirect land use impacts with negative environmental effects on forest ecosystems within and outside of Germany including additional carbon emissions resulting from land use change (Birdsey et al., 2018; Schlesinger et al., 2018).

BECC - Gasification of woody biomass for biofuels production (Concept 2)

Gasification is a well-developed technology for the conversion of fossil fuels and waste. Biomass as feedstock has been investigated intensively and large pilot and demonstration plants have been erected and operated worldwide (Rauch et al., 2014). The technology is mature for market implementation. Small scale facilities for CHP applications in the kilowatt (kW)-range are already commercialized (Patuzzi et al., 2021). Large scale conversion plants would aim at the production of several hundred thousand tonnes of synthetic hydrocarbon fuels per year. CO₂ is an inevitable by-product in autothermal gasification but can be separated by common means as already conducted in existing plants with fossil fuels. Our concept - a gasification plant of 100 megawatts thermal (MWth) capacity - could remove 60 kilotonnes (kt) CO₂ per year. If scaled up, it could provide removal of 3.72 Mt CO₂ by 2050. However, if this application leads to an increase in the use of woody biomass, it can also lead to direct and indirect land use impacts with negative environmental effects on ecosystems and additional carbon emissions from land use change (Birdsey et al., 2018, Schlesinger et al., 2018).

BECC - Pyrolysis of woody biomass for biocoal production (Concept 3)

Pyrolysis is well established for fossil fuels, but also for biomass feedstocks. Fast pyrolysis aims at the production of liquid fuels, which are used as heating oil today. CO₂ is a by-product here as well as in slow pyrolysis, which favors the production of biocoal (Tripathi et al., 2016). This product can be used energetically, but also for carbon storage

in soil applications. The impact of biocoal additions to soil have been investigated in a number of studies, considering a variety of soil-physical factors like dry density, water and nutrient exchange, pore volume and distribution and the like (e.g., Lehmann and Joseph, 2015). Naturally, long term investigations have not been finished so far. Also the number of studies investigating biocoal stability is constantly increasing (Lehmann et al., 2006; Leng et al., 2018). Biocoal stability can serve as an indicator to assess the carbon sequestration potential of biocoal. There are several methods for estimating the stability of biocoal, one of which is pyrolysis temperature (Leng et al., 2018). According to a rule of thumb, biocoal produced at higher temperature is expected to be more stable and thus persistent than low temperature char like hydrochar. While for the latter some decades have been derived as medium life time, for pyrochar average life times between 100 and over 1000 years have been estimated, depending on a number of parameters (environmental conditions, type of coal and feedstock used, soil use/treatment, investigation method). The presence of volatile, accessible organic molecules favors microbial attack, consequently leading to faster decomposition than mineralization by slow oxidation of the carbon by air. Derived from the existing studies, correlations for the mean residence times were suggested. As an example, Lehmann et al. (2009) estimated a carbon loss by around 20% in 500 years when 10 % of labile carbon was contained in the pyrochar. Other studies gave similar results (Kuzyakov, 2009, 2014) using biochar from grass pyrolysis (mean residence time > 400 yr). Interestingly it was found that incubation test in a laboratory environment led to higher biocoal degradation rates than open air tests. However, comparison and interpretation of the existing studies is difficult and for sure further investigations are required. Anyhow, in terms of carbon storage related to climate effects, biocoal stabilities of several hundred years can be reasonably assumed or need to be assured by appropriate processing and soil application.

Several technology providers entered the market already offering small to medium size conversion technologies. Our concept - a 50 MWth plant - could provide removal of 100 kt CO₂ per year. Assuming the use of 10 Mt of wood per year, which equals 15.5% of 66.8 Mt of wood used energetically today (FNR, 2018), 12.2 MtCO₂ could be removed annually if this technology would be implemented. Both the gasification and pyrolysis CDR numbers are based on the assumption that the around 10 Mt wood used energetically today in Germany are utilized. The lignocellulose feedstock potential is around twice as much, if non-woody biomass is included.

BECC - Biogas production for co-generation of heat and power (Concept 4)

With around 9 000 operating biogas plants (FNR, 2020), Germany has the biggest potential to explore this technology as a prospective option for bio-CCS in Europe. As estimated by Billig et al. (2019), in 2050 around 11.3 Mt of biogenic CO₂ could be captured from both biogas CHP and biogas upgrading plants based on wastes and residues. However, due to the upcoming termination of feed-in tariffs, limitations of support for “post-subsidy plants” and no long-term alternative support mechanisms (EEG, 2021), sustaining this potential can be possible only in a short term period (until approximately 2024-2027), and the future is highly uncertain (Scheftelowitz and Thrän, 2016). Our concept uses a medium sized, 500 kilowatts electric (kWel), biogas CHP plant which generates biogas from a mixture of feedstock, i.e., 50% wastes and residues, 20% cow manure and 30% energy crops, as described by Thrän (2019). CO₂ is separated in a post-combustion, MEA-based process. The annual removal per plant equals 3.15 kt CO₂. Assuming that until 2050 approximately 4,000 biogas plants with minimal capacity of 500 kWel would be retrofitted with carbon capture units, around 12.6 Mt CO₂ could be removed. The technical parameters of the biogas plant and capture unit described in this section have also been adapted for further two biogas-based concepts which differ in the type and amount of biomass used (concept 5 and 6, Sections 3.1.5 and 3.1.6, respectively).

BECC - Paludiculture-sourced biomass for biogas production for co-generation of heat and power (Concept 5)

Paludiculture is the use of wet ecosystems such as wetlands and peatlands for multiple purposes, including biomass and bioenergy production (Wichtmann et al., 2015). In our concept, we use it as a feedstock for biogas production with heat and power co-generation. Restored wetlands and peatlands can be used for paludiculture including the production of biomass for bioenergy, which is already practiced in a pilot site (Agrotherm GmbH³). Combining bioenergy production from paludiculture with CCS has not been done yet. However, using biomass from paludiculture could generate multiple benefits not only for generating negative emissions but also for CO₂ mitigation, climate change adaptation and biodiversity conservation. In Germany, large areas of wetlands and peatlands have been drained in the past for agricultural production. These drained areas are causing large carbon emissions - 43 Mt CO₂ per year in Germany alone (Tanneberger et al., 2021), and 2 Gt globally (Joosten, 2009; Joosten et al., 2016) - due to the ongoing degradation of the peat soils.

³<http://www.niedermoor-nutzen.de/> (accessed on: November 3, 2021)

Restoring these peatlands and wetlands by reversing the drainage and increasing the water table to the soil surface reduces carbon emissions substantially (Günther et al., 2020). In addition, establishing paludiculture on restored wetlands has considerable benefits for biodiversity by resembling more natural habitats, restoring the natural water cycle benefiting climate change adaptation (buffering impacts of droughts and floods) and retaining nutrients with benefits for water quality (Tanneberger et al., 2020; Tanneberger et al., 2022). Given the substantial benefits of paludiculture for addressing multiple challenges related to climate change, biodiversity and water quality, the use of paludiculture for BECCS could be considered a sustainable biomass source and a low-risk / low-regret option for CDR. In Germany paludiculture is estimated to be applicable on an area of at least 215,000 hectares (Scholwin and Siegert, 2020). Such an area could provide feedstock for approximately 156 biogas CHP plants with 500 kW_{el} capacity each, which would provide a removal of 0.49 Mt CO₂ per year.

BECC - Macroalgae farming for biogas production for co-generation of heat and power (Concept 6)

A BECC feedstock which could bypass the problem of competition for land is macroalgae (seaweed) biomass cultivated in the marine environment. Seaweeds have proved suitability for bioenergy production because of their notably high growth rates and high polysaccharide and negligible lignin content (Chung et al., 2013; Kim et al., 2017; Fernand et al., 2017). Thus, macroalgae biomass, together with microalgae biomass, are regarded as a feedstock for the third generation biofuels production (Montingelli et al., 2015). The macroalgae breeding and cultivation technologies have been well developed and matured with successful deployment, especially in Asian countries (e.g. China, Japan and South Korea). In Germany, a new structure for mariculture of brown macroalgae (*Saccharina latissima*) has been developed and tested off the North Sea coast (so-called ‘Offshore Ring’, e.g., Buck and Buchholz, 2004). A preference for offshore locations for macroalgae cultivation in Germany have also been suggested by Fernand et al. (2017). The German North Sea exclusive economic zone (EEZ) covers 20,600 km², which could potentially be utilized. Meanwhile, the increasing number of offshore wind farms in the German North Sea EEZ could expand the feasible area for anchoring cultivation infrastructures (Deutsche WindGuard GmbH, 2020). Cultivation of macroalgae does not require use of arable land or freshwater. Combined with ecological engineering aquaculture (e.g. the Integrated Multi-Trophic Aquaculture, IMTA), macroalgae cultivation can bring further ecological

and socioeconomic benefits by alleviating eutrophication and increasing bioremediation capability and aquaculture productivity (Wartenberg et al., 2017; Gao et al., 2020). There are approximately 250 biogas power plants with >400 kWel capacity each operating in the North Sea coast area in Germany (coastal districts in the states of Lower Saxony and Schleswig-Holstein). If those plants would be retrofitted with CCS units, it could provide removal of approximately 0.79 Mt CO₂/year.

DACC: centralized and decentralized options (Concepts 7 and 8)

Processes called Direct Air Carbon Capture, or short DACC, are technological solutions to filter CO₂ from the atmosphere. The systems use specific chemical interactions of the CO₂ with special materials to bind it and therefore remove the greenhouse gas from the air. DACC-processes generally function as a two-step process: capture and regeneration (HeSS et al., 2020). While captured, air is moved along the specialized material, called sorbent. This sorbent can be either a strong alkaline solution or a solid. Only the CO₂ reacts with the sorbent and forms covalent bonds, while most other components of the air are inert to the sorbent. Only water vapor also bonds to the sorbent. The CO₂-depleted air leaves the DACC-unit and the loaded sorbent is left behind. When sufficient loading is reached, the DACC changes to the regeneration step and the flow of air is shut down (Fasihi et al., 2019). To release the CO₂, the strong bonds must be broken by heating the sorbent. There are two different designs: on the one hand the Low Temperature (LT)-DACC uses solid amine sorbents, which are regenerated using steam at around 100°C (Deutz and Bardow, 2021), and on the other hand, High Temperature (HT)-DACC uses an alkaline solution, which must be regenerated at 900°C (Keith et al., 2018). While LT-DACC can use numerous heat sources, the high temperatures for HT-DACC can only be reached by combustion processes. The amount of heat needed is very similar for the two systems with roughly 1500 kilowatt-hour per tonne of CO₂ removed (HeSS et al., 2020). In addition, DACC needs to be supplied with 300 kilowatt-hour electric power per tonne of CO₂ removed, mainly for the fans, driving air through the absorber and the vacuum pumps in case of LT-DACC and the combined power demand of the process equipment at HT-DACC plants (such as pumps, fans, stirred tanks, etc.) (HeSS et al., 2020). The application of DACC units is, therefore, heavily dependent on external constraints like energy supply or available construction land. While HT-systems are usually only feasible at large scales (approximately 1 Mt of CO₂ per year), LT-DACC could potentially be fit into small scale systems and deployed in a decentralized application, e.g., into ventilation systems of buildings, reducing the required area

(Dittmeyer et al., 2019).

Since the deployment of DACC is heavily dependent on external factors, giving a potential is rather difficult. In the case of a decentralized implementation, an approximation via the current installed ventilation rate is possible (HI-CAM, 2020). For this parameter there are only numbers for the EU available (Kemna et al., 2014). If calculated per capita, it would be possible to filter up to 100 Mt of CO₂ per year in Germany (Eurostat Press Office, 2015; Kemna et al., 2014). If only large buildings would be equipped (over 2500 m² of floor space), the number would shrink to 15 Mt CO₂ a year (Stottrop and Flühöh, 2007). Other constraints such as space requirements or lower capture rates could further decrease the potential, yet, if compared to the DACC needed in Germany, it could play a significant role. Prognos et al. (2021) calculate the demand for DACC in Germany to be somewhere between 20 and 600 Mt CO₂ a year, depending on the decarbonisation scenario. The remaining DACC would have to be installed in big DACC farms, which are, large centralized DACC plants with several adsorber/absorber units and a large combined capture capacity in the Mt range. Considering the typical size of such a farm of approx. 1 Mt CO₂ captured per year and the associated energy demand, it is questionable if this technology is possible within the German territorial boundaries.

NSE - Peatland rewetting (Concept 9)

Peatlands are areas with naturally accumulated thick layers of dead organic material (peat) (Joosten and Clarke, 2002). Undrained peatlands, situated between upland and water as a subclass of wetlands, accumulate peat in soils owing to incomplete decomposition of plant material and animal remains under water-saturated conditions (Rydin and Jeglum, 2013). Degraded peatlands, largely caused by drainage for agriculture and forestry, are responsible for 5% of the total 2014 global anthropogenic CO₂ emissions despite their mere 0.4% coverage of global land surface (Joosten et al., 2016). In Germany, more than 5% (47 Mt CO₂-eq per year) of GHG emissions originate from drained organic soils. Across the globe, both public and private efforts to restore degraded peatlands are increasing as their benefits for providing multiple ecosystem services including carbon storage and the avoidance of CO₂ emissions are increasingly recognized and acknowledged to outweigh the needs for drainage-based agriculture and forestry on peatlands (Bonn et al., 2016). In Germany, more than 98% of the organic soils (about 1.8 Mha) are drained mainly for agricultural use (Trepel et al., 2017; Tanneberger et al., 2021). With appropriate planning to reconcile with the demands of agricultural land use and water use, rewetting these drained

peatlands offers cost-effective low-hanging fruits to avoid up to 43 Mt of CO₂ emissions in the agricultural sector along with additional multiple benefits for biodiversity and ecosystem services.

NSE - Afforestation of cropland (Concept 10)

Forests are land areas >0.5 ha with trees >5 m height and canopy cover >10% and without predominant agricultural or urban use (MacDicken, 2013). The anthropogenic land use change (LUC) of forests substantially affected carbon emissions over the last centuries. It was estimated that LUC from natural forests to cropland and pastures globally emitted on average 1,569 Gt CO₂-eq between 1765 and 2005 (Kim and Kirschbaum, 2015). Afforestation is the LUC to forest by active seeding/planting or natural rejuvenation of trees (MacDicken, 2013). The focus here is on afforestation of cropland because this LUC has reportedly the highest sequestration rates (Kim and Kirschbaum, 2015). The afforestation of cropland to secondary forests will sequester atmospheric carbon as soil organic carbon (SOC) and in biomass at rates of 2.2 and 2.8 tonnes of CO₂ per ha per year, respectively (Kim and Kirschbaum, 2015). The focus for afforestation measures should lie on marginal agricultural land, which has been subjected to land use change in the past years (Meyer and Früh-Müller, 2020). There is an estimated 3.3 Mha of marginal land in Germany suitable for plant production (Gerwin et al., 2018), of which a fraction may be also appropriate for afforestation. This estimate may also include non-cropland, however, this is outside the scope of this proposed concept. Winter cereals and winter rapeseed, apart from maize, are the most common field crops in Germany, covering 6.97 Mha of agricultural land (Griffiths et al., 2019). Winter crops can often not be combined with cover crops (see Section 3.1.10), and are considered here for afforestation. A proposed conversion of 10% of the area at a rate of 0.5% per year to secondary forests could sequester 72 Mt CO₂ between 2020 and 2050 in Germany.

NSE - Soil organic carbon sequestration - cover crops (Concept 11)

Soil organic carbon sequestration as a natural sink enhancement measure for atmospheric CO₂ capture has gained interest in the past years. Especially cropland soils have been of interest, because these soils (1) are highly managed, (2) are generally SOC depleted compared to natural ecosystems, and (3) cover vast areas on the planet. Including cover crops into the cropping cycle can reportedly increase SOC with a mean sequestration rate of 1.2 tonnes CO₂ ha/year (Poeplau and Don, 2015). In Germany, approximately

2.2 Mha cropland are already grown with cover crops (Griffiths et al., 2019; DESTATIS, 2018), meaning that growers have implemented this management option. Another 2 Mha of cropland (potato, sugar beet, summer cereals, and corn) may be suited for cover crops in crop rotations. Assuming that an additional 2 Mha of cropland are seeded with cover crops by 2050 with an annual 2% increase in cover crops, approximately 44 Mt CO₂ can be removed from the atmosphere.

NSE - Terrestrial enhanced weathering (Concept 12)

Increased weathering, both on land and on the seafloor, is one of the major natural responses of the Earth system to elevated atmospheric CO₂ concentrations or temperature (Archer, 2005). This naturally occurring weathering process is the main drawdown of anthropogenic CO₂ emissions over time scales of thousands to hundreds of thousands years (Archer and Brovkin, 2008). Enhanced rock weathering as a CDR measure accelerates this process to capture CO₂ by weathering carbonate and silicate minerals that are spread in powdered form on terrestrial surfaces like agricultural soils. In principle, a variety of natural or artificial sources of alkalinity can be used, but the focus here is on limestone or silicate rocks, like basalt. These rocks release positively charged magnesium or calcium ions when weathered. During this reaction, CO₂ is converted into carbonate and bicarbonate ions by consuming protons (i.e. "acid"), allowing the soils to absorb atmospheric CO₂ (Beerling et al., 2020). Basalt is mined mainly in the central part of Germany (BGR, 2017), with annual production rates per quarry of between 0.1 to 4.9 Mt rock with a maximum mining capacity of 32 Mt. There is substantial electric energy demand associated with this CDR option from extraction (18.8 MJ/t), crushing (510 MJ/t), and grinding (0.6-2 GJ/t) of silicate rocks. Taking one of the larger quarries as a reference, 4 Mt of basalt spread over cropland in Germany would allow for 0.727 Mt CO₂ to be removed from the atmosphere, at a cost of about 120-140 million \$US and an energy demand of 2.492 - 8.112*10⁶ GJ (calculations based on Moosdorf et al., 2014 and Beerling et al., 2020). If scaled up to maximum mining capacity (i.e., 32 Mt silicate rocks), approximately 5.82 Mt CO₂/year could be removed by enhanced rock weathering applied on 0.6 Mha of cropland by 2050.

NSE - Terrestrial enhanced weathering (Concept 12)

In addition to increasing associated biodiversity, seagrass meadows and salt marshes are already making an important contribution to mitigating man-made climate change. In Germany, these ecosystems absorb an estimated amount of around 132 kt of CO₂ annually.

As natural CO₂ sinks, the existing ecosystems are valuable resources for Germany. Salt marshes are among the most efficient carbon sequestering ecosystems in the world and occur naturally along the German Wadden Sea coast on an area of about 23,250 ha. Salt marsh sediments provide an environment that allows long-term storage of organic carbon derived either from autochthonous primary production in the salt marsh or from imported allochthonous organic material from adjacent ecosystems (Müller et al., 2019).

Similarly, seagrass can sequester significant amounts of carbon. Seagrasses are found in the southeastern North Sea (area about 18,000 ha), where they grow on tidal flats, and on the German Baltic coast, where sublittoral seagrasses occur (area about 28,500 ha). A large part of the CO₂ is absorbed by the seagrass during photosynthesis. Another part comes from organisms that live in these systems and absorb CO₂ via respiration. When seagrasses die, they sink to the sea floor where the CO₂ is stored as carbon. Still another portion comes from particles such as plankton that the dense seagrass canopy trap.

The expansion of natural CO₂ sinks is considered a carbon removal measure and can make an additional contribution to achieving climate goals. However, almost the entire Wadden Sea is under nature protection, and thus active measures aiming at the reestablishment or new establishment of seagrass beds or salt marshes are not allowed. By improving the general conditions, e.g., water quality through sewage treatment plants or adjustments to regulations of fertilizer use on agricultural land, the seagrass bed area can increase and the natural CO₂ uptake by seagrass could amount to a total 19.1 kt in the North Sea each year.

In the Baltic Sea, natural seagrass meadow expansion of up to 5672 ha is also possible through consistent implementation of EU-wide nutrient reduction targets (defined in the Baltic Sea Action Plan, BSAP) (Bobsien et al., 2021). In order to accelerate the slow recolonization, it is also possible to actively renaturalize such habitats in the Baltic Sea. The goal of these measures is also to increase the size of the existing seagrass meadows nearby, and essentially restore an area that once had seagrass. Already today one can implement such activities to increase the natural CO₂ sink. Assuming an additional 42,750 ha would be colonized with seagrass by 2050, doubling the existing area, about 103 kt of CO₂ could be sequestered from the atmosphere annually. However, these values are still subject to great uncertainty because there is little data on the rate of carbon sequestration, in stark contrast to information available on carbon pools. It is important to understand that seagrass beds reach their full potential after approximately 18 years (Marbà et al., 2015; Eriander et al., 2016; Infantes et al., 2016; Infantes and Moksnes, 2018; Moksnes et al., 2018). This means that the sooner we implement this measure, the sooner we can realize

the full potential of seagrasses.

Seagrass meadows and salt marshes in the North Sea and Baltic Sea hold the seafloor together because their complex roots and root stems prevent water movement from stirring it up. This creates fine-grained sediments that are virtually devoid of oxygen. These inhibit microorganisms from breaking down the carbon stored in the soil into its component parts, which would produce CO₂ that would be released into the ocean.

As a result, the carbon in the sediment and biomass is basically stored for several centuries to millennia. However, the actual storage capacity of seagrass beds depends on multiple factors. Temperature and depth are generally the most important limiting factors for seagrass beds. Thus, warming waters and sea level rise may affect their distribution and reduce their range. In addition, increased wave action and storm surges due to extreme weather events associated with climate change are detrimental to seagrass habitats. Strong movements due to storms also stir up the soil and expose buried carbon fixed in the sediment.

Assuming that by 2050 the entire area that can potentially sustain seagrass beds is vegetated (97,750 ha) and healthy seagrass beds absorb CO₂ according to their maximum, mature sequestration potential, approximately 122 kt of CO₂ could be removed from the atmosphere annually. As the development of salt marshes and their CO₂ uptake potential depend on many factors and as it is unknown whether erosion predominates or they increase in area, we assume that salt marshes absorb by 2050 as much CO₂ as they do today. Altogether, a total of 200 kt CO₂ could be removed from the atmosphere at the coasts of Germany every year.

Geological carbon dioxide storage solutions (Concept 14)

Geological storage at an industrial scale (i.e., captured CO₂ >400,000 tonnes/year) offers the capacity to lock CO₂ outside of the atmosphere within the vast porous space of the Earth's underground. Technological CDR solutions, such as BECCS and DACCS, are associated with this CO₂ storage option and enable large-scale removal of CO₂ from the atmosphere as a significant negative emission contribution to climate mitigation efforts. In this context, the chapter only deals with geological CO₂ storage.

Captured CO₂ can be permanently stored into a deep underground geological reservoir of porous rock (e.g., sandstone) overlaid by an impermeable layer of cap rocks, sealing the reservoir and preventing the CO₂ from upward migration out of the storage formation. Worldwide, there are several types of suitable CO₂ storage reservoirs available, e.g., deep

saline aquifer formations, depleted oil and gas reservoirs, unmineable coal beds and basalt rock formations (IPCC, 2005). Deep saline aquifer formations, offering the largest storage capacity, are layers of porous and permeable rocks saturated with saline formation water (brine). They are widely distributed across the globe in onshore and offshore sedimentary basins, and in Germany, the North East German Basin provides the major part of the country's saline aquifer assets. When CO₂ is injected into a reservoir, it flows through the rock pores, filling the pore space and displaces the saline formation water. Usually, the captured CO₂ is compressed into a liquid of increased density for efficient transport, ease of injection and reduced storage space requirement. The reservoir must be located at depths greater than 800 meters to retain the CO₂ in a dense liquid (supercritical) state (IPCC, 2005). The injected CO₂ is permanently trapped in the reservoir through several mechanisms: (i) structural trapping by the geological formation and its seal, (ii) solubility trapping in the formation water, (iii) residual trapping as gas in the rock pores, and (iv) mineral trapping by reacting with the reservoir rocks to form carbonate minerals. The shares of trapping mechanisms and their dominance depend on the individual storage site's characteristics and contribute to a safe, reliable and effective CO₂ storage over the years (Kempka et al., 2014). Environmental parameters are required to be controlled by a long-term monitoring program along the whole storage life-cycle, and energy and economic parameters depend on the location, size and site specific characterization of the storage project. Depending on the regional conditions and the technical parameters of the project, the resulting additional expenses for CO₂ conditioning and storage are indicated in the literature within cost bandwidths (Smith et al., 2021; Chen and Morosuk, 2021).

Until the end of 2019, a number of 19 large-scale CCS facilities with permanent CO₂ storage were in operation worldwide (GCCSI Report, 2019). The most prominent and longest running project is the Sleipner CCS facility with off-shore storage in the North Sea since 1996 and with about 20 Mt of CO₂ stored so far, offering a technology readiness level of TRL 9 (Kearns et al., 2021). A comparable on-shore CO₂ storage in a saline aquifer formation is presented by the Quest project, with a storage of about 4.8 Mt CO₂ since 2015 (Shell Canada Ltd. Report, 2019). In Kearns et al. (2017), a total global storage capacity has been estimated at between 8,000 Gt and 55,000 Gt, based on a methodology of estimated average CO₂ storage capacity per cubic kilometer of sedimentary rock. For Germany, Knopf and May (2017) used an updated volumetric CO₂ storage capacity approach which provided an estimate of about 40 Gt of regional aquifer based capacity assessment.

Due to the given constraints of the national act of carbon dioxide storage (KSpG, 2012) in Germany, the only currently available option to permanently store larger amounts

of CO₂ is seen in transportation to the North Sea fields, which is offered by the industrial-scale offshore projects, e.g., Northern Lights (Norway), Porthos (The Netherlands), and Net-Zero Teesside (UK) - also known as projects of common interest (PCI).

Table 4.1: Fact sheet design and description of individual parameters.

Category	Parameter	Description
Concept characteristics	Technology Readiness Level (TRL)	The technological maturity of a particular CDR option. An extent to which it is available on the market and can, therefore, be used.
	Energy concept	Describes whether a given CDR option produces and/or consumes energy.
	Infrastructure	The necessary infrastructure for a concept application, e.g., power grid, gas grid, CO ₂ -grid, other transportation pathways, etc.
	Siting conditions	Describes the necessary biophysical conditions of a concept (e.g., access to the sea, availability of certain biomass, etc.) and its possible location (Where in Germany can this CDR option be implemented? Where do favorable conditions occur and what are they?).
Input	Land	How much area is necessary for unit deployment? What kind of area is required? (e.g., agricultural area, forest area, urban area, marine area, etc.)
	Natural resources	Are there raw materials (e.g. biomass) necessary to run the concept? If yes, what kind and in what amount?
	Energy	What is the specific energy demand of the unit?
	Water	How much water is necessary to run the unit?
	Labor	How many jobs are expected to build and operate the unit
Output	CO ₂ removal potential	Expected yearly CO ₂ reduction (removal) of the unit (under the assumption that the system is fully established)
	Co-products	Additional products generated by the CDR option, including energy (electricity, heat, fuels).
Environmental parameters	Biodiversity	Impacts on species and ecosystems.
	Soils	Substances released into the soil and changes of soil physical state
	Water	Substances released into the groundwater, runoff water, seawater
	Air	Substances released into the air (including non-CO ₂ GHGs)
	Noise	Generation of noise (can impact air, water, soils)
Economic parameters	CO ₂ removal costs	Marginal removal cost (under the assumption that the system is fully established)
	Investment Capital expenditure (CAPEX)	Investment costs to build the unit (e.g., new machinery, real estate, administration).
	Operational expenditure (OPEX)	Elements: fixed and variable running costs, on-power costs, storage maintenance, monitoring costs.
	(Regional) Value added	Additional economic value generated, e.g. by increasing wages, taxes, land values, effects by attracting labor.
Systemic parameters	Long term CO ₂ emissions removal potential	Deployed net CO ₂ emissions removed (with assumption of permanent storage) in 2050
	Average CDR potential between 2020-2050	The average rate at which CO ₂ is removed/sequestered between 2020 and 2050
	Range and trend of CO ₂ removal rates	Temporal variability in annual CO ₂ removal rates (i.e., what is the min-max value?) and expected trend in CO ₂ removal rates from the CDR option between 2020 and 2050
	Permanence	In what form (gaseous, liquid, solid) is the CO ₂ stored and where (what kind of carbon reservoir, i.e., geological, terrestrial or marine biomass, terrestrial or marine soils/sediments?). What is the expected length of storage?
	Storage integration	Does the concept provide only removal or storage of CO ₂ or both? Ability to confirm the amount of CO ₂ removed
	Verifiability	Can fluxes, carbon stock changes or leakages be measured or estimated?
	Permission	Compliance with BImSchV* and/or other regulations
Scalability	What is a possible scale of deployment of the CDR option? How many such units could be deployed in Germany? What are the restrictions?	

*BImSchV - Ordinance for the Implementation of the Federal Immission Control Act (Verordnung zur Durchführung des Bundes-Immissionsschutzgesetzes), available at: https://www.gesetze-im-internet.de/bimschv_1_2010/

Another option would be an intermediate storage of CO₂ together with its subsequent usage as part of a decarburization cycle. For this application, the already injected CO₂ is back-produced on demand from the storage reservoir and returned into a chemical cycle as raw material for further chemical reactions, e.g., together with hydrogen for a methanation process towards synthetic fuels (Graves et al., 2011). In Germany the demonstration of efficient CO₂ back-production has been successfully conducted at the Ketzin CO₂ pilot storage site (Martens et al., 2015).

4.3.2 Data collection

The collected data for the 13 CDR and storage concepts is presented in tabular fact sheets included in supplementary materials.

4.3.3 Technical potential of options deployment

CDR options, whether technology- or ecosystem-based, come at different stages of development - some have been demonstrated as viable and are already widely deployed (e.g. afforestation), some may need more research and/or investment to advance and be put on the market (e.g. decentralized DACC).

In our portfolio, we present options which have been largely successfully demonstrated at different scales in deployment environments - e.g., from small projects to commercial-scale projects (Table 2). All selected ecosystem-based options are proven practices which could be implemented and/or expanded in Germany immediately. On the other hand, most technology-based options would require a few years to be successfully deployed (Table 2). This is related to the fact that some of their elements, even though they are mature, still need to be integrated (e.g. retrofitting bioenergy plants with CCS). Only DACC and ERW would require more time for implementation, due to a need for their further development. In case of DACC, a pilot application in real ventilation systems would be necessary, and ERW would need to be further tested to deliver conclusive results.

However, an option's implementation time is not only a function of their maturity, but is also influenced by societal factors such as public acceptance and/or political support. Those factors may either speed up or slow down their deployment (see Section 4).

Carbon dioxide removal potential of options for Germany

The amount of CDR that will be deployed in the next 30 years is highly uncertain. Estimates as to what would be the appropriate amount of CDR deployment in Germany range from 3 to 18 Gt CO₂ between today and 2100, depending on the historical responsibility, capability and global equity (Pozo et al., 2020). In addition, annual CO₂ removal demand to reach net-zero CO₂ emissions strongly depends on the actions to reduce and avoid emission in the coming years. In the following paragraph we will accordingly discuss the CDR options through the perspective of their respective system utility, i.e., how much CO₂ can they remove to achieve national net-zero targets. With regards to annual CO₂ removal potential,

our concepts differ widely, ranging from 34 tonnes to 2.9 million tonnes per year per concept (Figure 2). The by far highest specific removal potential of a single CDR concept can be realized with BECC, specifically with biomass combustion for CHP in former coal-fired power plants, followed by centralized DAC (1 Mt CO₂/year) assuming that effective CO₂ storage can be implemented. Other BECC and DAC options present smaller CO₂ capture potential which ranges between 3,150 and 100,000 tonnes CO₂ per unit. For NSE, the potential is expressed in the amount of CO₂ removed per hectare per year, and varies from 1.5 to 9.5 tCO₂/ha/year, with enhanced rock weathering having the highest removal potential per area. It is also important to consider the near-term deployment potentials of the different options. While NSE are partly already deployed today, and could potentially be expanded, most of the high-tech options would need 5-10 years to reach market readiness (see Section 3.3.1). This lower maturity level is an important characteristic considering the cumulative CDR potential between 2020 and 2050, as delays in the deployment of CDR options cause reduced cumulative CDR potential. Considering scalability of the CDR options, a more comprehensive picture of CDR potential can be drawn. Large-scale BECC deployment is limited by the amount of available biomass and number of bioenergy plants that would be available for retrofitting. DAC is mostly limited by its cost and access to renewable energy supply. Most of the NSE are limited by the available area. Taken each of these limiting factors into account, the BECC potentials range from 0.5, 0.8, 3.72, 12.6, 14, 29.9 Mt CO₂/year for paludi- and macroalgae-fed biogas CHP, gasification, mixed feedstock biogas CHP, pyrolysis and biomass combustion CHP, respectively. For the DAC options the potential ranges between 15 to 150 Mt CO₂/year, for the decentralized and centralized approach, respectively. The potential is based on the assumption that 15% of the largest 15% buildings in Germany can be equipped with DAC units and an area one hundredth as big as the agricultural area (115100 ha) can be utilized to install DAC farms. And finally, the projected CDR potentials for the NSE measures are found to be between 0.06, 2.3, 3.3, 3.5 and 5.8 Mt CO₂/year for seagrass restoration, cover crops, peatland rewetting, afforestation and enhanced rock weathering, respectively. In Figure 2 we present the efficiency of the different CDR concepts to remove CO₂ with regard to their potential to scale up, energy provision and demand (for the hybrid and technical solutions) and land/water area (for NSE).

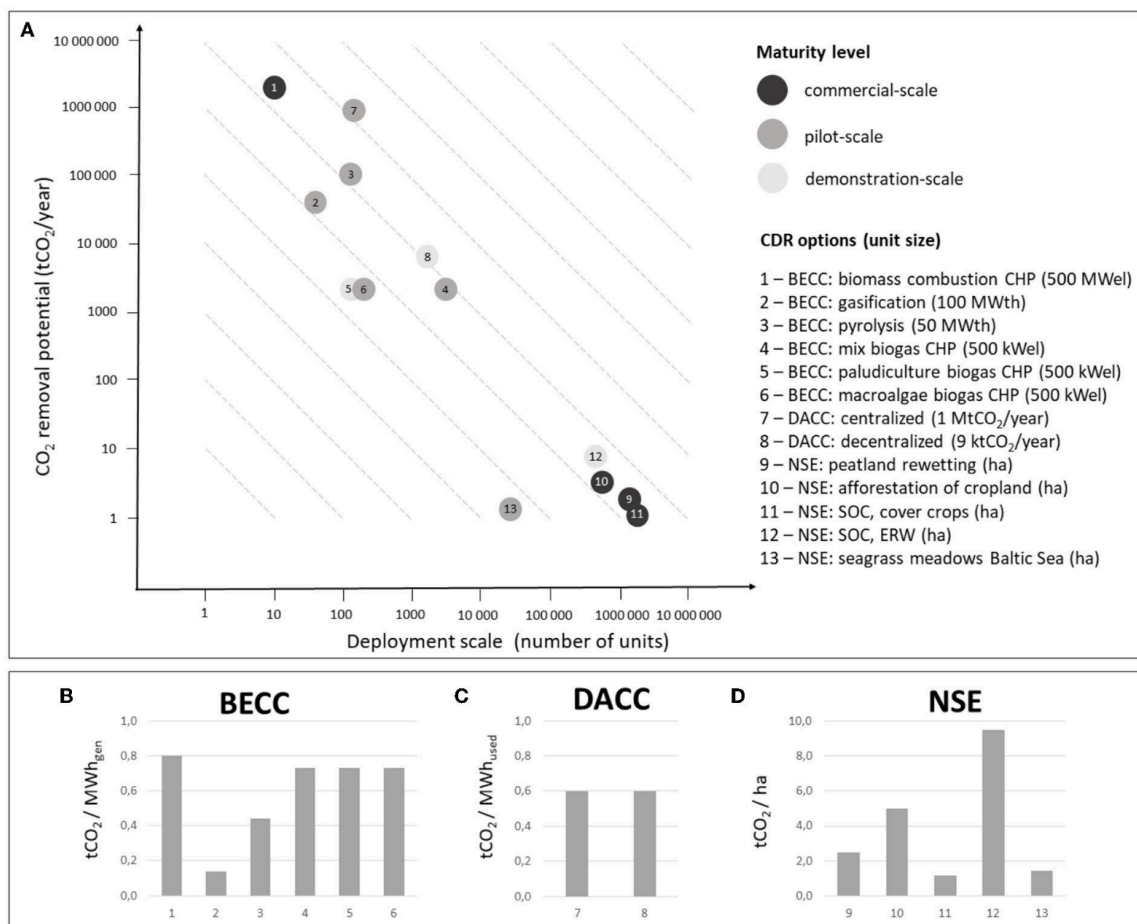


Figure 4.2: Overview of CO₂ removal potential of selected options. A: Scalability of options expressed as a number of units available for deployment by 2050 and CO₂ removal potential. B: Amount of CO₂ removed per unit of energy generated by BECC technologies. C: Amount of CO₂ removed per unit of energy used by DACC technologies. D: Amount of CO₂ removed per hectare by NSE options.

Table 4.2: Overview of the CDR concepts considered in the study with current scale and estimated time of deployment of CDR options. Estimation of implementation time for concepts 1-8 has been performed assuming allowance for CO₂ storage either on German territory under a German law (which currently is unfeasible due to restrictions in KSpG (2012)), or transportation of CO₂ for storage in other countries.

CDR option		Maturity		
Concept No.	Name	Size of the model unit	Deployment scale	Implementation time
1	BECC: biomass combustion CHP	500 MWel	commercial	possible deployment in a few years
2	BECC: gasification for biofuels production	100 MWth	pilot	possible deployment in a few years
3	BECC: pyrolysis for biocoal production	50 MWth	pilot	possible deployment in a few years
4	BECC: biogas CHP	500 kWel	pilot	possible deployment in a few years
5	BECC: paludiculture for biogas CHP	500 kWel	demonstration	possible deployment in a few years
6	BECC: macroalgae for biogas CHP	500 kWel	pilot	possible deployment in a few years
7	DACC: centralized	1 MtCO ₂ /year	pilot	possible deployment within a decade
8	DACC: decentralized	9 ktCO ₂ /year	demonstration	possible deployment within a decade or longer
9	NSE: peatland rewetting	650 ha	commercial	possible immediate deployment
10	NSE: afforestation of cropland	1 ha	commercial	possible immediate deployment
11	NSE: SOC, cover crops	1 ha	commercial	possible immediate deployment
12	NSE: SOC, ERW	76700 ha	demonstration	possible deployment within a decade or longer
13	NSE: seagrass meadows Baltic Sea	23.8 ha	commercial	possible immediate deployment

4.4 Discussion

4.4.1 Bringing CDR options closer to deployment - bottlenecks and open questions

There are many different options for CDR available today –from technological to hybrid and natural solutions. The principles of many options are already well researched. However, their real-life implementation is a process which cannot be based only on general assumptions. Our CDR concepts combine German framework conditions with their respective performance parameters to help bring CDR from the general conceptual level to the ground. They show not only the possible methods of CDR in Germany but also how they could look like in reality, in a more manageable, one-unit scale (i.e., easier to locate, run necessary calculations, evaluations and scaling).

In principle, German natural conditions and technology availability enable the implementation of diverse CDR options. While we are aware of the fact that some, if not all, of the CDR options discussed here will cause various side-effects, e.g., GHG generation in peatlands and short-lived halocarbons from macroalgae farming (Leedham et al., 2013; Ziska et al., 2013; Tanneberger et al., 2021), we wanted to concentrate on the technological readiness and potentials of these options within the German context. More comprehensive assessments will need to follow (see Thoni et al., 2020). Using our CDR concepts in combination with the analysis of German geophysical conditions, we determined an approximate area on which a given option could be applied and how much CO₂ per hectare it could remove. Such information represents a crucial first step to understanding the feasibility

of CDR deployment and can be understood as a measurement for maximum potential. To better understand the actual removal potential, social, political, and legal parameters need to be considered as well, as these may represent hurdles to deployment and thus reduce the actual removal potential (cf. Boysen et al., 2017; Geden et al., 2018; Wieding et al., 2020).

Economic viability of CDR options is also highly variable and dependent on the technologies and their characteristics. Regarding renewable energy-based options, the Budget Scenario by Simon et al. (2022), which aims at implementing a 100% renewable energy system by 2050 for Germany, requires considerable investment in technologies and infrastructure. In the short term, fuel costs determine overall costs to two thirds, whereas their share decreases from 2030, while power exchange costs increase. This is due to CO₂ emission costs being eliminated while phasing out fossil fuels. Considering energy security, increasing costs for energy imports also highlight that different energy systems are subject to dynamic changes of the economic circumstances. Future viability and reliability of CDR options are therefore sensitive and must be considered in a holistic approach, which, as a downside, increases the number of uncertainty parameters in modeling and for interpretation of feasible outcomes.

In this section, we highlight some of the most important bottlenecks and open questions that need further consideration, as highlighted in previous literature, focusing on the German context (Hahn et al., 2020). In other words, we see that the CDR potential of a single approach is limited under incremental implementation of the CDR concepts within an existing landscape and infrastructure. Hence, in addition to technological feasibility, a portfolio of concepts needs to be demonstrated and tested with regard to market implementation as well as socio-political acceptance. For example, the most mature option with an additionally high CDR potential is biomass combustion with CHP –an option which assumes retrofitting a coal-fired plant to burn biomass, which for certain industry actors can be attractive, especially in the light of the upcoming coal-phase out (KVBG, 2020). Such concepts can thus build on pre-existing infrastructure, as well as already tested technology, e.g., in the UK (Drax Group, 2018) or Denmark (Orsted Media Relations, 2016). However, if deployed at scale, their demand for resources (e.g., wooden pellets) may be a limiting factor, if no imports are taken into account (Thrän and Schindler, 2021). Moreover, previous research indicates that model assumptions for future biomass production for BECCS rely on optimistic views on increased agricultural efficiency, as well as land-use changes that may interfere with other societal goals such as food security, biodiversity, and cultural services, and could cause, inter alia, loss of ecosystems, replacement of natural ecosystems for monocultures, and pollution (Dooley et al., 2020; Dooley and Kartha,

2018; Daggash et al., 2019). These are all important factors that would need to be critically reviewed if BECCS options were to be moved closer to deployment in Germany. If such risks are deemed insurmountable and the impacts socially and ecologically unacceptable, they will, consequently, reduce the potential for BECCS. However, in comparison with the other CDR options, the integrated energy provision of BECCS is a significant advantage, especially in the light of ongoing energy transition and related strong need for renewables.

Scaling is not only an issue in sustainable biomass sourcing for large scale BECCS application. NSE are typically implemented in smaller units and therefore need different support and permission schemes than technical facilities. Some practices are already in use or tested in Germany, especially in urban areas (e.g. Kabisch et al., 2016) but the scale on which they could be implemented to maximize CO₂ capture has not been evaluated yet.

The CDR concept approach clarifies the options for CO₂ removal for Germany with regard to BECC, DACC and NSE under the consideration of technical, infrastructural and biophysical conditions. However, the relevant bottleneck for long term storage, which enables BECC to BECCS and DACC to DACCS is carbon storage, which is still not fully addressed in Germany. Theoretically, Germany has large potential for permanent CO₂ storage as well as multiple storage scenarios - local storage, offshore storage or a combination of these may all be envisaged. The choice of storage options is in turn closely tied to the organization of CO₂ emitters and CO₂ transportation networks around the storage sites. Indeed, the establishment of a CO₂ transportation network and CO₂ source clustering could represent a strategic opportunity for economic development. For instance, proximity to a storage site or even a CO₂ transportation network may offer an easy path to carbon neutrality for hard-to-abate industries such as cement or lime (Hills et al., 2017). Emitters may be clustered regionally, as spatial clusters in view of a local onshore storage site, or instead form a unique national network with a large unique storage location (or neighboring storage locations). While both scenarios are technically feasible, varying costs, political will and social acceptance will determine the chosen implementation. CO₂ storage is currently restricted to pilot-scale research endeavors and no new storage sites can currently be proposed (KSpG, 2012), although some emerging signs seem to indicate that politicians are reconsidering German CO₂ subsurface storage (Drucksache 19/25295, 2020; Drucksache 19/30724, 2021). Offshore storage in a select few, large North Sea storage sites may reduce geological prospection and storage costs but a significant CO₂ transport network will be required. On the other hand, onshore regional storage may require less infrastructure investment but storage availability is not uniform among German federal states and there is no legal support for CO₂ storage in Germany (KSpG, 2012). Moreover, public acceptance

of CO₂ storage in Germany is currently low (Tcvetkov et al., 2019) while acceptance for CCU is higher (Linzenich et al., 2019). In addition to low public support for CCS, the public's knowledge about CCS is also low (Merk et al., 2019). Hence, all options which rely on CCS may face a delay of unknown duration or insurmountable hurdles if acceptance is never generated. Early CCS projects generally faced limited public acceptance or outright public opposition for underground storage and transportation of CO₂ in pipelines, although research indicates that public acceptance is higher for Bio-CCS than CCS of fossil fuel emissions (Dütschke, 2011; Otto and Gross, 2021; Wallquist et al., 2012). Previous research suggests that reintroducing CO₂ storage firmly within the public debate may require a fine balancing of communication and lobbying to inform of the low risks and numerous opportunities associated with CO₂ storage, while avoiding association with the failed CCS impetus in Germany of the late 2000s (Linzenich et al., 2019).

When it comes to public acceptance of CDR in general, interfering with nature is often seen as problematic, and thus less technology heavy options could be more acceptable (Wallquist et al., 2012; Wolske et al., 2019, e.g. afforestation preferred over BECCS and DACCS). For instance, in addition to perceived risks of storage especially related to leakage, data from Germany shows that BECCS-options are also seen as problematic by the public because of concerns with regards to biodiversity impacts⁴. Similarly, data from the US and UK shows that for enhanced weathering people are generally concerned about downstream effects on oceans (Spence et al., 2020). That being said, also NSE like rewetting peatlands can be perceived as interfering with nature, if areas have been drained for a long time and thus perceived as naturally dry (Ziegler et al., 2021). In general, many CDR options could potentially cause trade-offs to other societal goals, such as energy- and food security, or cause health implications, or land-use conflicts (Honegger et al., 2020). This includes NSE like afforestation, which can have negative social and ecological impacts, such as loss of biodiversity, land-use conflicts, and high resource use, in particular, if forest plantations are established in previously non-forested areas, replace natural ecosystems and are established without the consent of local communities (e.g., Smith and Torn, 2013; Honegger et al., 2020). Societal impacts are, however, highly dependent on scale of implementation and need to be understood within their specific local context (Honegger et al., 2020). Acceptance is often associated with trust and seen as something that is built over time (e.g. Waller et al., 2020). Public participation in the decision making process has been highlighted as important for building trust and acceptance (e.g., Cox et al., 2021; Dütschke, 2011; Merk et al., 2019). According to Honegger et al. (2021), while Germany has well

⁴<https://www.spp-climate-engineering.de/index.php/buergerforum.htm> (accessed on: November 4, 2021)

developed participatory governance processes in general, not enough has been done for public engagement around CDR, which in turn makes it more challenging to build social acceptance around these measures.

Table 4.3: Distribution patterns of CDR options.

	Region of Germany					Type of area			
	N	E	S	W	C	urban	rural	marine	
BECC	BG_CHP					++ (bio-waste)	++ (agriculture)		
	BM_CHP	Depending on biomass availability (no clear priority regions)					++ (bio-MSW)	++ (forestry)	
	SP_BC								
	G_BtL						++ (forestry)		
	MA_BG	++						++	
	PC_BG	++			++		++		
DACC	centralized	Depending on renewable energy availability wind PV						++	
	decentralized	Depending on renewable energy availability wind PV					++	+	
Afforestation of cropland	++	+	++	+	+		++		
Peatland rewetting	++		++				++		
Soil Carbon Sequestration	Cover Crops	++	+	++	+	+	++		
	ERW						++		
Seagrass meadows	Baltic Sea	++						++	
Storage solutions		++	+		+	+	+	++	

the North: Schleswig-Holstein, Hamburg, Mecklenburg-West Pomerania, Lower Saxony, and Bremen; the East: Brandenburg, Berlin, and Saxony; the South: Bavaria and Baden-Württemberg; the West: North Rhine-Westphalia, Rhineland-Palatinate, and the Saarland; the Center - Saxony-Anhalt, Thuringia, and Hesse. BG_CHP - biogas for CHP; BM_CHP - biomass combustion for CHP; SP_BC - slow pyrolysis for biocoal production; G_BtL - gasification for fuels production; MA_BG - microalgae biogas for CHP; PC_BG - paludiculture for biogas with CHP; ERW - Enhanced Rock Weathering; N - north, E - east, S - south, W - west, C - central; PV - photovoltaics; MSW - Municipal Solid Waste; ++ particularly suitable, + moderately suitable

4.4.2 Distribution patterns

The location of different CDR options depends to a large extent on biophysical conditions occurring in the country of deployment. This parameter is inextricably linked to NSE, as these options are based directly on the occurrence of certain natural conditions and ecosystems. However, hybrid options like BECC and purely technology-driven options like DACC also rely to a different degree on natural conditions (e.g., proper conditions to grow different types of biomass in case of BECC, and intensity of insolation and wind for production of electricity for DACC).

Apart from biophysical conditions, some CDR options are accompanied by additional energy demand (especially DACC), and some generate energy (like BECC). Therefore, the

energy supply also plays an important role. The required transformation of the energy system on the path to achieve net zero CO₂ emissions by 2050 will further accelerate extensive societal and economic changes. The extension of the electrical grid, pipeline siting, various storage potential to be exploited and resistance against the phase out of coal-fired power plants affect different regions of Germany to varying degrees and scales. This, together with diverse levels of acceptance for decarbonization measures across Germany, could lead to strong regional differences in application potentials of technologies, which in turn could restrict a speedy transition. For instance, divergences can result from different resource allocation, which is especially important considering renewable energy. German photovoltaic (PV) power potential is allocated mostly in the South (The World Bank, 2019), whereas the northern regions can provide less of this resource. Contrastingly, the mean wind power density is located mostly in the North-West coastal regions and in few mountainous areas (except the South of Germany) (DTU Wind Energy et al., 2021). These natural resource occurrences are determining CDR options availability as well as future changes in energy supply by illustrating requirements for expansion in installations and infrastructure (Simon et al., 2022). Corresponding to PV potential, storage options needed for CO₂ are mostly allocated in the northern half of the country, with some locations also in the center and South of Germany (Müller and Reinhold, 2011).

The energy intensive industries are located mostly in the West and South of Germany and in several highly agglomerated regions, which coincide with the density of population (GTAI 2020; BBSR 2021). These agglomerations also correspond to the highest emissions, which is where CO₂ storage should be located to minimize transport. However, capacities for that are not matching the geographical location of emitters (Emissionshandelsstelle, 2018). For the CDR concepts presented in the preceding sections, a regional allocation scheme that illustrates explicitly the implementation potential in Germany can be developed (Table 3). This scheme is based on the current status of biomass and renewable energy availability, type of area (terrestrial or marine) and degree of urbanization. In this table, concerning the geographic distinction, the country has been split into five main areas: the north, east, south, west, and center. Generally, the cardinal direction provided by the regional classification and the distinction according to federal states should be understood only as a fluid concept and not as a fixed distinction, since resources and potentials cannot be measured by administrative boundaries. Assigning the CDR options to the mentioned regions further depends on technological flexibility, scale of the options deployment, degree of decentralization, and the nature of the concept itself (e.g., marine options are not implementable on land). The latter also informs the additional distinction of the area type

in Table 3, as urban and rural areas are characterized by different implementation abilities (e.g., concepts with need for agricultural products are relatively infeasible to implement in highly urbanized regions). Additionally, marine areas are introduced to capture the needs of concepts which use offshore-based technologies or marine CDR processes.

The applicability of the regional disaggregation is marked by either a ‘+’, which stands for moderate implementation in the specific area that may be limited on certain conditions, ‘++’ stands for high implementation potential.

For BECCS, different options depend strongly on suitable biomass availability. As agricultural and forestry residues and waste are widely occurring feedstocks, it is difficult to set clear regional restrictions for implementation of technologies based on these resources. Among BECC concepts, an exception can be macroalgae- and paludiculture-based concepts, which have stronger limitations as they can only work in marine or rural areas with specific biophysical conditions (e.g., suitability for restoring peatland). DACC implementation is connected to the specific renewable energy potential and thus follows along the power potentials of either wind (relatively higher potential in the north) or PV (relatively higher potential in the south). For larger, centralized DACC-facilities one of the most important location factors is the availability of renewable energy in sufficient quantities. Therefore we assume these plants will follow the potential of renewable energy sources, with a secondary preference for less expensive construction land in rural areas (HeSS et al., 2020). On the other hand, decentralized HVAC-integrated DACC-systems primarily require suitable buildings in which they can be implemented. The selection of renewable energy supply must be decided on a more local, case-by-case basis. On-site generation of renewables has to be complemented with other energy sources, such as industrial waste heat, which is more readily available near industrial and urban centers (Dittmeyer et al., 2022; Dittmeyer et al., 2019).

If there are further specifications of the type of region where a concept can be implemented, it is noted in brackets in Table 3. For instance, with biogas for CHP, regions of deployment in Germany are generally not restricted to either north, south, etc., but in urban areas the option depends on bio-waste, and in rural regions, agriculture is a prerequisite for implementation.

Overall, it is important to account for the different perception of concepts that are implementable and spatially diffused (Rhoden et al., 2021). Especially considering the expansion of renewable energy, and depending on the context of a concept, the regional effect on the landscape, and thus on the need of environmental conditions, can differ strongly.

4.4.3 Setting the CO₂ removal potential in context

Beyond the different bottlenecks and hurdles for implementation, in order to understand the potential contribution of CDR options to reaching net-zero CO₂ emissions, the estimated CO₂ removal potentials should be compared with the actual CO₂ emissions in Germany. In 2020, Germany emitted 644 Mt CO₂, mostly coming from the energy sector (211 Mt CO₂), industry sector (163 Mt CO₂), and transport sector (144 Mt CO₂) (UBA, 2021). Noteworthy in this context is that energy production by fossil fuel combustion across sectors amounts to over 90% of current CO₂ emissions in Germany.

If Germany would achieve its 88% reduction in emissions relative to 1990 by 2040, this amounts to annual emission of 130 Mt CO₂, which would have to be entirely eliminated or compensated for within 5 years (KSG, 2021). While central DAC units could theoretically provide 150 Mt CO₂ capture per year if limited by area demand alone, constraining DAC by energy provision limits its potential to about 16 Mt CO₂ (Ariadne Report, 2021). No other CDR option alone can provide the necessary order of magnitude of carbon removal to compensate for 130 Mt CO₂/year. In total, BECC options could provide about 62 MtCO₂, half of which would be provided by biomass CHP. This option however, would need large amounts of woody biomass as feedstock. As for the enhancement of natural carbon sinks, we find that enhanced rock weathering, afforestation and peatland rewetting are the options which show the highest CDR potentials (5.8, 3.5 and 3.4 Mt CO₂/year, respectively). In total, we assess the CDR potential of the five selected NSE options in Germany to be in the order of magnitude of 15 Mt CO₂/year. Our overall estimated CDR potential in the year 2050 amounts to about 240 Mt CO₂/year, which is reduced to 91 Mt CO₂/year if the central DAC option were constrained by energy supply. While single CDR options are constrained differently and therefore single potentials vary, our estimate of the overall CDR potential agrees well with the order of magnitude of 103-116 Mt CO₂/year identified in the Ariadne Report (2021).

This conclusion clearly illustrates that CO₂ removal can only compensate for a very small share of today's emissions in Germany. Moreover, the maturity of the options illustrates that most of the CDR options might only be deployed in 5-10 years' time. In other words, in the coming decade, the focus should be laid on mitigating emissions in the first place rather than relying on negative emission technologies for removing emissions after they have been emitted. In Figure 3, we present the potentials of analyzed CDR concepts, along with their relation to current German CO₂ emissions and projected residual emissions in 2050.

4.4.4 Limitations and further research demand

The definition and description of exemplary CDR concepts was performed with experts in the different fields, using the - to our knowledge - best available information. However, we know that also within the expert fields there are uncertainties in the optimized design and performance of the concepts, which is also affecting the data quality of our fact sheets. Larger data collections can help to reduce these uncertainties in the future, and we propose to use this study as a starting point to broaden the database of CDR concepts for CO₂ removal in Germany.

Additionally, in our assessment we focused mainly on technical and CO₂ removal related criteria. For implementation of CDR concepts, a broader view on societal and political aspects is necessary. With regard to economic, environmental or social aspects, the fact sheets will need more harmonization, e.g., by commonly agreed indicators (see Fridahl et al., 2020, Förster et al., 2022).

We also did not consider interactions between the CDR concepts, especially when it comes to their upscaling. In general, for each concept, competition by increased market potential is facilitating market penetration and ensures cost-efficiency. In technologies, further innovation support enables efficiency gains and cost reductions (Hepburn et al., 2019). Among that, concepts can compete for land and resources, and the deployment of one option may reduce the potential of implementation of another concept. This makes it essential that a regionally specific CDR portfolios are developed in order to avoid possibly conflicting solutions.

4.5 Conclusion

CDR is discussed as a relevant measure to reach the temperature goals of the Paris Agreement not only globally but also in national contexts. Different CDR measures are available and their implementation depends on site specific conditions, such as biophysical conditions, existing infrastructure and regulations. In our study, we investigated near-to-market-options for CDR in Germany, which we depicted in 13 concepts and systematically described in fact sheets (see Supplementary Materials). These concepts are based on the current situation and allow incremental implementation of CDR options during the next decade. The CDR concepts cover technical, hybrid, and natural sink enhancement options with CO₂ removal in a range from 34 tonnes (Baltic Sea seagrass meadows) to 3 megatonnes CO₂ (biomass combustion CHP) per concept, and with costs ranging from -45

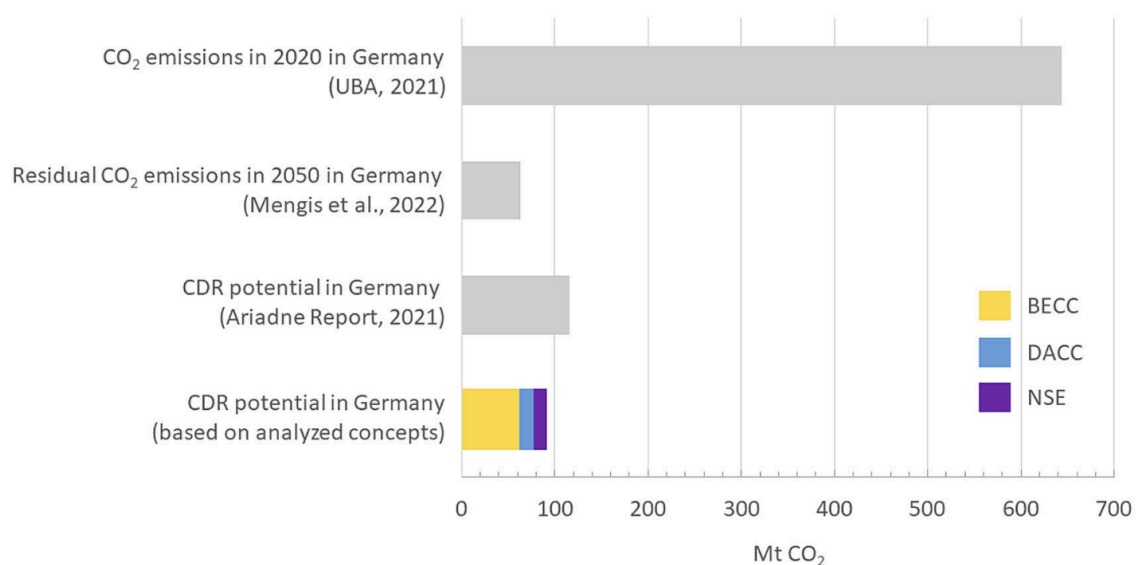


Figure 4.3: CDR potential of analyzed concepts in comparison with estimates of current CO₂ emissions in Germany (UBA 2021), projected residual emissions for 2050 (Mengis and Kalhori et al., 2022) and CDR potential in Germany (Ariadne Report, 2021). BECC: based on all analyzed BECC concepts, likely requiring imports of woody biomass. DAC: based on decentralized DAC concept, excluding centralized DAC due to energy constraints. NSE: based on all analyzed NSE concepts. The indicated potentials for BECC and DAC do not include possible constraints by the feasibility of geological CO₂ storage.

(minimal estimate for cover crops; Fuss et al., 2018) to 800 (maximal estimate for DACC; HeSS et al., 2020) per tonne of CO₂ removed (see Supplementary Materials for details). With their elaboration in fact sheets, a substantial database has been generated which can be further used in climate research and policy actions, such as research and demonstration of CDR options, as well as climate and energy scenario development.

With regard to the overall CO₂ removal potential, 10 of the 13 CDR concepts provide technical removal potential of at least 1 million tonnes CO₂ per year, so a combination of concepts is necessary to achieve the necessary impact for the climate targets. Options with the highest CO₂ removal potentials are: DACC farms (150 Mt CO₂/year), BECC: biomass combustion with CHP (29.9 Mt CO₂/year), DACC combined with HVAC systems (15 Mt CO₂/year), BECC: pyrolysis (14 Mt CO₂/year), BECC: biogas CHP (12.6 Mt CO₂/year), NSE: enhanced rock weathering (5.82 Mt CO₂/year), NSE: afforestation of cropland (3.49 Mt CO₂/year), NSE: peatland rewetting (3.35 Mt CO₂/year), and NSE: cover crops (2.34 Mt CO₂/year). Our overall, maximized estimation of CDR potential of analyzed options in 2050 varies from 91 to 240 Mt CO₂/year, mostly depending on the scale of deployment of DACC farms. However, it should be noted that this potential can further decline, e.g., if the future availability of biomass for BECC application decreases, there are further constraints in renewable energy supply for DACC or limitations in CO₂ storage. Compared to Germany's total actual CO₂ emissions of 644 Mt CO₂ (data from 2020; UBA, 2021) and the estimated hard-to-abate emissions of 36 - 63 Mt CO₂ in 2050 (Ariadne Report, 2021, Mengis and Kalhori et al., 2022), it seems that CDR could theoretically provide sufficient potential to counterbalance the residual emissions. However, it should not be considered as a primary mitigation measure, but as a complementary option following emission reductions and avoidance.

Taking biophysical conditions and infrastructure into account, northern Germany seems preferable for many concepts. Necessary next steps needed to enable their successful implementation and include consideration of economic aspects, societal perception and political frameworks (Nemet et al., 2018; Cherry et al., 2018). Therefore, in general, a comprehensive framework like the SDGs can foster political action to deployment and give guidance to a German approach to bring technology concepts to the market (see also Honegger et al., 2020). Participatory processes and a focus on good governance can relieve some of the barriers to implementation (Honegger et al., 2018). They need to be applied highly region-specific as the federal structure of the political background and the geographical feasibility potentials of technologies (centralized or decentralized) differ strongly and require careful place-based consideration. Specifically for the hybrid and technical carbon

dioxide removal options (BECCS and DACCS), implementation strongly depends on the availability of carbon storage options, which are currently constrained by laws in Germany and can only be unlocked by changing the current regulations on carbon storage.

4.6 References

- Archer, D. (2005). Fate of fossil fuel CO₂ in geologic time. *J. Geophys. Res. Oceans* 110:C9. doi: 10.1029/2004JC002625
- Archer, D. and Brovkin, V. (2008). The millennial atmospheric lifetime of anthropogenic CO₂. *Clim. Change*, 90:3, 283–297. doi: 10.1007/s10584-008-9413-1
- Ariadne Report (2021). Deutschland auf dem Weg zur Klimaneutralität 2045. Szenarien und Pfade im Modellvergleich. Luderer, G., Kost, C. and Sörgel, D. (Eds.). October, 2021. doi: 10.48485/pik.2021.006.
- Babin, A., Vaneekhaute, C. and Iliuta, M.C. (2021). Potential and challenges of bioenergy with carbon capture and storage as a carbon-negative energy source: A review. *Biomass Bioenergy* 146:105968. doi: 10.1016/j.biombioe.2021.105968
- BBSR (2021) INKAR –Indikatoren und Karten zur Raum- und Stadtentwicklung. Bundesinstitut für Bau-, Stadt- und Raumforschung (BBSR), Bonn. Available online at: <https://www.inkar.de/> (accessed on: November 2, 2021)
- Beerling, D. J., Kantzas, E. P., Lomas, M. R., Wade, P., Eufrazio, R. M., Renforth, P. et al. (2020). Potential for large-scale CO₂ removal via enhanced rock weathering with croplands. *Nature* 583:7815, 242–248. doi: 10.1038/s41586-020-2448-9
- Bellamy, R. and Osaka, S. (2020). Unnatural climate solutions? *Nat. Clim. Chang.* 10, 98–99. doi: 10.1038/s41558-019-0661-z
- BGR (2017) Karte der Bergbau- und Speicherbetriebe (BergSP), Stand 31.12.2017, 48. Auflage, zusammengestellt vom Referat L 2.7 des Landesamt für Bergbau, Energie und Geologie Hannover, veröffentlicht von den Bergbehörden der Länder und der Bundesanstalt für Geowissenschaften und Rohstoffe
- Billig, E., Decker, M., Benzinger, W., Ketelsen, F., Pfeifer, P., Peters, R., et al. (2019). Non-fossil CO₂ recycling - The technical potential for the present and future utilization for fuels in Germany. *J. CO₂ Util.* 30, 130–141. doi: 10.1016/j.jcou.2019.01.012
- BioKraftQuG (2006). Biofuels Quota Act. Gesetz zur Einführung einer Biokraftstoffquote durch Änderung des Bundes-Immissionsschutzgesetzes und zur Änderung energie- und stromsteuerrechtlicher Vorschriften (Biokraftstoffquotengesetz). BGBl I, 3180. Available online at: https://www.bgbl.de/xaver/bgbl/start.xav?start=//%5B@attr_id=%27bgbl106s3180.pdf%27%5D#__bgbl_%2F%2F%5B%40attr_id%3D%27bgbl106s3180.pdf%27%5D__1658772578431 (accessed on: July 28, 2022)
- Birdsey, R., Duffy, P., Smyth, C., Kurz, W. A., Dugan, A. J. and Houghton, R. (2018). Climate, economic, and environmental impacts of producing wood for bioenergy. *Environ. Res. Lett.* 13. doi: 10.1088/1748-9326/aab9d5
- BNetzA (2021). Kraftwerksliste Bundesnetzagentur, Stand 19.01.2021. Available online at: https://www.bundesnetzagentur.de/SharedDocs/Downloads/DE/Sachgebiete/Energie/Unternehmen_

Institutionen/Versorgungssicherheit/Erzeugungskapazitaeten/Kraftwerksliste/Kraftwerksliste_2021_1.xlsx?__blob=publicationFile&v=4 (accessed on: November 2, 2021)

Bobsien, I.C., Hukriede, W., Schlamkow, C., Friedland, R., Dreier, N., Schubert, P.R., et al. (2021). Modeling eelgrass spatial response to nutrient abatement measures in a changing climate. *Ambio* 50, 400-412. doi: 10.1007/s13280-020-01364-2

Bonn, A., Allott, T., Evans, M., Joosten, H., Stoneman, R. (2016). Peatland restoration and ecosystem services: an introduction, In: Bonn, A., Joosten, H., Evans, M., Stoneman, R., Allott, T. (Eds.), *Peatland Restoration and Ecosystem Services: Science, Policy and Practice*, Ecological Reviews. Cambridge University Press, Cambridge, 1–16. doi: 10.1017/CBO9781139177788.002

Boysen, L. R., Lucht, W., Gerten, D., Heck, V., Lenton, T. M., and Schellnhuber, H. J. (2017). The limits to global-warming mitigation by terrestrial carbon removal. *Earths Fut.* 5, 463–474. doi: 10.1002/2016EF000469

Buck, H.J. (2016). Rapid scale-up of negative emissions technologies: social barriers and social implications. *Clim. Change* 139:2, 155-167. doi: 10.1007/s10584-016-1770-6.

Buck, B.H. and Buchholz, C.M. (2004). The offshore-ring: A new system design for the open ocean aquaculture of macroalgae. *J. Appl. Phycol.* 16, 355–368. doi: 10.1023/B:JAPH.0000047947.96231.ea

Bui, M., Adjiman, C.S., Bardow, A., Anthony, E.J., Boston, A., Brown, S. et al. (2018). Carbon capture and storage (CCS): the way forward. *Energy Environ. Sci.* 11:1062, doi: 10.1039/c7ee02342a

Cherry, C., Scott, K., Barrett, J. and Pidgeon, N. (2018). Public acceptance of resource-efficiency strategies to mitigate climate change. *Nat. Clim. Change* 8, 1007-1012. doi:10.1038/s41558-018-0298-3

Chen, F. and Morosuk, T. (2021). Exergetic and Economic Evaluation of CO₂ Liquefaction Processes. *Energies* 14. doi: 10.3390/en14217174

Chung, I.K., Oak, J.H., Lee, J.A., Shin, J.A., Kim, J.G. and Park, K.S. (2013). Installing kelp forests/seaweed beds for mitigation and adaptation against global warming: Korean Project Overview. *ICES J. Mar. Sci.* 70, 1038–1044. doi: 10.1093/icesjms/fss206

Cox, E., Pidgeon, N., and Spence, E. (2021). But They Told Us It Was Safe! Carbon Dioxide Removal, Fracking, and Ripple Effects in Risk Perceptions. *Risk Anal.* 0:0. doi: 10.1111/risa.13717

Daggash, H.A., Fajardy, M., Heptonstall, P., Mac Dowell, N., Gross, R. (2019). Bioenergy with carbon capture and storage, and direct air carbon capture and storage: Examining the evidence on deployment potential and costs in the UK. UKERC Technology and Policy Assessment, April 2019. Available online at: <https://d2e1qxpsswcpqz.cloudfront.net/uploads/2020/05/UKERC-TPA-Negative-Emissions-V3-Final.pdf> (accessed on: November 2, 2021)

DESTATIS (2018). Land- und Forstwirtschaft, Fischerei - Bodennutzung der Betriebe (Struktur der Bodennutzung), Fachserie 3 Reihe 2.1.2. Retrieved from Wiesbaden, Germany. Available online at: https://www.statistischebibliothek.de/mir/receive/DEHeft_mods_00070848 (accessed on: November 2, 2021)

Deutsche WindGuard GmbH (2020). Status des Offshore-Windenergieausbaus in Deutschland – Erstes Halbjahr 2020. Available online at: https://www.windguard.de/id-1-halbjahr-2020.html?file=files/cto_layout/img/unternehmen/windenergiestatistik/2020/Status%20des%20Offshore-Windenergieausbaus_Halbjahr%202020.pdf (accessed on: November 2, 2021)

Deutz, S. and Bardow, A. (2021). Life-cycle assessment of an industrial direct air capture process based on temperature–vacuum swing adsorption. *Nat. Energy* 6:2, 203–213. doi: 10.1038/s41560-020-00771-9.

Dittmeyer, R., Klumpp, M., Kant, P., and Ozin, G. (2019). Crowd oil not crude oil. *Nat. Commun.* 10:1, 1818. doi: 10.1038/s41467-019-09685-x.

DOE, (2011). *Technology Readiness Assessment Guide*. Department of Energy (DOE). Washington, DC. U.S. Available online at: <https://www.directives.doe.gov/directives-documents/400-series/0413.3-EGuide-04> (accessed November 3, 2021).

Donnison, C., Holland, R.A., Hastings, A., Armstrong, L.M., Eigenbrod, F., and Taylor, G. (2020). Bioenergy with Carbon Capture and Storage (BECCS): Finding the win-wins for energy, negative emissions and ecosystem services-size matters. *GCB Bioenergy* 2020:00, 1-19. doi: 10.1111/gcbb.12695

Dooley, K., Harrould-Kolieb, E., and Talberg, A. (2020). Carbon-dioxide Removal and Biodiversity: A Threat Identification Framework. *Glob. Policy* 12:S1. doi: 10.1111/1758-5899.12828.

Dooley, K. and Kartha, S. (2018). Land-based negative emissions: risks for climate mitigation and impacts on sustainable development. *Int. Environ. Agreements* 18:1, 79-98. doi: 10.1007/s10784-017-9382-9.

Drax Group (2018). Drax closer to coal-free future with fourth biomass unit conversion. Available online at: https://www.drax.com/press_release/drax-closer-coal-free-future-fourth-biomass-unit-conversion/ (accessed on: October 19, 2021)

Drucksache 19/25295, 2020; Antrag der Abgeordneten Dr. Lukas Köhler, Frank Sitta, Grigorios Aggelidis, Olaf in der Beek, Judith Skudelnj, et al. und der Fraktion der FDP. 55+5 - Ein ambitioniertes EU-Klimaziel mit Negativemissionstechnologien ermöglichen. Available online at: <https://dserver.bundestag.de/btd/19/252/1925295.pdf> (accessed on: November 2, 2021)

Drucksache 19/30724, 2021 Antwort der Bundesregierung auf die Kleine Anfrage der Abgeordneten Dr. Lukas Köhler, Frank Sitta, Grigorios Aggelidis et al. und der Fraktion der FDP. CO₂-Speicherung als Voraussetzung für Klimaneutralität. Available online at: <https://dserver.bundestag.de/btd/19/307/1930724.pdf> (accessed on: November 2, 2021)

DTU Wind Energy, The World Bank, Vortex (2021). *Global Wind Atlas*. Available online at: <https://globalwindatlas.info/area/Germany> (accessed on: November 2, 2021)

Dütschke, E. (2011). What drives local public acceptance—Comparing two cases from Germany. *Energy Procedia* 4, 6234-6240. doi: 10.1016/j.egypro.2011.02.636.

Dynarski, K. A., Bossio, D. A. and Scow, K. M. (2020). Dynamic Stability of Soil Carbon: Reassessing the “Permanence” of Soil Carbon Sequestration. *Front. Environ. Sci.* 8, doi: 10.3389/fenvs.2020.514701

EEG (2000). *German Renewable Energy Act. Gesetz für den Vorrang Erneuerbarer Energien, Erneuerbare-Energien-Gesetz. BGBl I 2000, 305.* Available online at: https://www.bgbl.de/xaver/bgbl/start.xav?start=%2F%2F*%5B%40attr_id%3D%27bgbl100s0305.pdf%27%5D#__bgbl__%2F%2F*%5B%40attr_id%3D%27bgbl100s0305.pdf%27%5D__1658772437646 (accessed on: July 28, 2022)

EEG (2021). *German Renewable Energy Act*. Available online at: https://www.gesetze-im-internet.de/eeg_2014/ (accessed on: November 3, 2021)

Emissionshandelsstelle (2018). *Installations covered by ETS in Germany 2018*, Deutsche Emissionshandelsstelle, Available online at: https://www.dehst.de/SharedDocs/downloads/EN/installation_lists/2018.pdf (accessed on: November 2, 2021)

Eriander, L., Infantes, E., Olofsson, M., Olsen, J.L., and Moksnes, P.O. (2016). Assessing methods for

restoration of eelgrass (*Zostera marina* L.) in a cold temperate region. *J. Exp. Mar. Biol. Ecol.* 479, 76-88. doi: 10.1016/j.jembe.2016.03.005

Erlach, B., Hennig, C. and Schünemann, F. (2019). Biomasse im Spannungsfeld zwischen Energie- und Klimapolitik. Strategien für eine nachhaltige Bioenergienutzung. Stellungnahme Februar 2019. Herausgeber: Nationale Akademie der Wissenschaften Leopoldina, acatech –Deutsche Akademie der Technikwissenschaften, Union der deutschen Akademien der Wissenschaften.

Eurostat Press Office (2015). Erste Bevölkerungsschätzungen. EU-Bevölkerung zum 1. Januar 2015 auf 508,2 Millionen gestiegen. Available online at: <https://ec.europa.eu/eurostat/documents/2995521/6903514/3-10072015-AP-DE.pdf/1dc02177-b1d7-47ed-8928-66fec35e2e36#:~:text=Am%201.,Januar%202014> (accessed on: October 5, 2021)

Fasihi, M., Efimova, O., and Breyer, C. (2019). Techno-economic assessment of CO₂ direct air capture plants. *J. Clean. Prod.* 224, 957–980. doi: 10.1016/j.jclepro.2019.03.086.

Fernand, F., Israel, A., Skjermo, J., Wichard, T., Timmermans, K.R., Golberg, A. (2017). Offshore macroalgae biomass for bioenergy production: Environmental aspects, technological achievements and challenges. *Renew. Sustain. Energy Rev.* 75, 35–45. doi: 10.1016/j.rser.2016.10.046

FNR (2018). Rohstoffmonitoring Holz. Fachagentur Nachwachsende Rohstoffe (FNR). Available online at: https://www.fnr.de/fileadmin/allgemein/pdf/broschueren/Broschuere_Kurzfassung_Rohstoffmonitoring_Web.pdf (accessed on: November 3, 2021)

FNR (2020). Basisdaten Bioenergie Deutschland 2021. Fachagentur Nachwachsende Rohstoffe (Ed.), Gülzow, 2021. Available online at: https://www.fnr.de/fileadmin/Projekte/2020/Mediathek/broschuere_basisdaten_bioenergie_2020_web.pdf (accessed on: November 4, 2021)

Förster, J., Beck, S., Borchers, M., Gawel, E., Korte, K., Markus, T. et al. (2022). Framework for Assessing the Feasibility of Carbon Dioxide Removal Options Within the National Context of Germany. *Front. Clim.* 4:758628. doi: 10.3389/fclim.2022.758628

Fridahl, M., Hansson, A., and Haikola, S. (2020). Towards Indicators for a Negative Emission Climate Stabilization Index: Problems and Prospects. *Climate* 2020:8, 75; doi: 10.3390/cli8060075

Fuss, S., Lamb, W. F., Callaghan, M. W., Hilaire, J., Creutzig, F., Amann, T., et al. (2018). Negative emissions—Part 2: costs, potentials and side effects. *Environ. Res. Lett.* 13:063002. doi: 10.1088/1748-9326/aabf9f

Gao, G., Burgess, J., Wu, M., Wang, S. and Gao, K. (2020). Using macroalgae as biofuel: current opportunities and challenges. *Bot. Mar.*, 63:4, 355-370. doi: 10.1515/bot-2019-0065

GCCSI Report (2019) Global Status of CCS 2019. Available online at: <https://www.globalccsinstitute.com/resources/publications-reports-research/global-status-of-ccs-report-2019/> (accessed on: November 2, 2021)

Geden, O., and Schenuit, F. (2020). Unconventional Mitigation. Carbon Dioxide Removal as a New Approach in EU Climate Policy. SWP Research Paper 2020/RP 08, doi: 10.18449/2020RP08

Geden, O., Scott, V., and Palmer, J. (2018). Integrating carbon dioxide removal into EU climate policy: prospects for a paradigm shift. *WIREs Clim. Change* 9:e521. doi: 10.1002/wcc.521

Gerwin, W., Repmann, F., Galatsidas, S., Vlachaki, D., Gounaris, N., Baumgarten, et al. (2018). Assessment and quantification of marginal lands for biomass production in Europe using soil-quality indicators. *Soil* 4:4, 267-290. doi: 10.5194/soil-4-267-2018

Gignac, R., and H. D. Matthews. Allocating a 2C cumulative carbon budget to countries. *Environ. Res. Lett.* 10:7. doi: 10.1088/1748-9326/10/7/075004

Graves, C., Sune D. Ebbesen, S.D., Mogensen, M., and Lackner, K.S. (2001). Sustainable hydrocarbon fuels by recycling CO₂ and H₂O with renewable or nuclear energy. *Renew. Sust. Energ. Rev.* 15:1, 1-23. doi: 10.1016/j.rser.2010.07.014

Griffiths, P., Nendel, C., and Hostert, P. (2019). Intra-annual reflectance composites from Sentinel-2 and Landsat for national-scale crop and land cover mapping. *Remote Sens. Environ.* 220, 135-151. doi: 10.1016/j.rse.2018.10.031

GTAI (2020). The Automotive Industry in Germany. Germany Trade and Invest (GTAI), Berlin. Available online at: [https://www.gtai.de/resource/blob/64100/07f5613dd96b786a118a106788e3b988/20200812_IO_Automotive_Web%20\(1\).pdf](https://www.gtai.de/resource/blob/64100/07f5613dd96b786a118a106788e3b988/20200812_IO_Automotive_Web%20(1).pdf) (accessed on: November 2, 2021)

Günther, A., Barthelmes, A., Huth, V., Joosten, H., Jurasinski, G., Koebsch, F. et al. (2020). Prompt rewetting of drained peatlands reduces climate warming despite methane emissions. *Nat. Commun.* 11, 1644. doi: 10.1038/s41467-020-15499-z

Hahn, A., Szarka, N., and Thrän, D. (2020). German Energy and Decarbonization Scenarios: “Blind Spots” With Respect to Biomass-Based Carbon Removal Options. *Front. Energy Res.* 8:130. doi: 10.3389/fenrg.2020.00130

Hepburn, C., Adlen, E., Beddington, J. Carter, E.A., Fuss, S., Mac Dowell, N., et al. (2019) The technological and economic prospects for CO₂ utilization and removal. *Nature* 575, 87–97. doi: 10.1038/s41586-019-1681-6

HeSS, D., Klumpp, M., and Dittmeyer, R. (2020). Nutzung von CO₂ aus Luft als Rohstoff für synthetische Kraftstoffe und Chemikalien. Verkehrsministerium Baden-Württemberg. Karlsruher Institut für Technologie. Available online at: <https://vm.baden-wuerttemberg.de/fileadmin/redaktion/m-mvi/intern/Dateien/PDF/29-01-2021-DAC-Studie.pdf> (accessed on: March 1, 2021).

HI-CAM (2020). Factsheet No. 04. Direct Air Capture. Helmholtz Klima Initiative. Hermann von Helmholtz-Gemeinschaft Deutscher Forschungszentren e.V. Berlin. Available online at: https://www.helmholtz-klima.de/sites/default/files/medien/dokumente/Factsheet%2004_Direct%20Air%20Capture.pdf (accessed on: November 2, 2021)

Hills, T.P., Sceats, M., Rennie, D., and Fennell, P. (2017). LEILAC: Low Cost CO₂ Capture for the Cement and Lime Industries. *Energy Procedia* 114, 6166-6170, doi: 10.1016/j.egypro.2017.03.1753.

Honegger, M., Derwent, H., Harrison, N., Michaelowa, A. and Schäfer, S. (2018). Carbon Removal and Solar Geoengineering: Potential implications for delivery of the Sustainable Development Goals. (New York, Carnegie Climate Geoengineering Governance Initiative. Available online at: https://www.c2g2.net/wp-content/uploads/C2G2-Geoeng-SDGs_20180521.pdf (accessed on: November 3, 2021)

Honegger, M., Poralla, M., Michaelowa, A., and Ahonen, H.-M. (2021). Who Is Paying for Carbon Dioxide Removal? Designing Policy Instruments for Mobilizing Negative Emissions Technologies. *Front. Clim.* 3:50. doi: 10.3389/fclim.2021.672996.

Honegger, M., Michaelowa, A., and Roy, J. (2020). Potential implications of carbon dioxide removal for the sustainable development goals. *Clim. Policy* 21:5. doi: 10.1080/14693062.2020.1843388.

Höhne, N., den Elzen, M., and Escalante, D. (2014). Regional GHG reduction targets based on effort sharing: a comparison of studies. *Clim. Policy* 14:1, 122–47. doi: 10.1080/14693062.2014.849452

Höhne, N., Galleguillos, C., Kornelis, B., Harnisch, J., and Phylipson, D. (2003) Evolution of Commitments Under the UNFCCC: Involving Newly Industrialized Economies and Developing Countries (Berlin, Germany: Ecofys/Federal Environmental Agency). Available online at: <https://www.umweltbundesamt.de/sites/default/files/medien/publikation/long/2235.pdf> (accessed on: November 3, 2021).

Infantes, E., Eriander, L., and Moksnes, P.O. (2016). Eelgrass (*Zostera marina*) restoration on the west coast of Sweden using seeds. *Mar. Ecol. Prog. Ser.* 546, 31-45. doi: 10.3354/meps11615

Infantes, E. and Moksnes, P.O. (2018). Eelgrass seed harvesting: Flowering shoots development and restoration on the Swedish west coast. *Aquat. Bot.* 144, 9-19. doi: 10.1016/j.aquabot.2017.10.002

IPBES-IPCC (2021). Scientific Outcome of the IPBES-IPCC co-sponsored workshop on biodiversity and climate change. Available online at: https://ipbes.net/sites/default/files/2021-06/2021_IPCC-IPBES_scientific_outcome_20210612.pdf (accessed on: November 3, 2021)

IPCC (2005). IPCC Special Report on Carbon Dioxide Capture and Storage. Prepared by Working Group III of the Intergovernmental Panel on Climate Change, [Metz, B., O. Davidson, H. C. de Coninck, M. Loos, and L. A. Meyer (eds.)]. Cambridge University Press, Cambridge, United Kingdom and New York, NY, USA, 442 pp.

IPCC (2018). Global Warming of 1.5°C. An IPCC Special Report on the impacts of global warming of 1.5°C above pre-industrial levels and related global greenhouse gas emission pathways, in the context of strengthening the global response to the threat of climate change, sustainable development, and efforts to eradicate poverty [Masson-Delmotte, V., Zhai, P., Pörtner, H. O., Roberts, D., Skea, J., Shukla, P. R. et al. (Eds.)] Global warming of 1.5 °C, (IPCC Special Report), Geneva : Intergovernmental Panel on Climate Change, 93-174.

IPCC (2021). Climate Change 2021: The Physical Science Basis. Contribution of Working Group I to the Sixth Assessment Report of the Intergovernmental Panel on Climate Change. Masson-Delmotte, V., Zhai, P., Pirani, A, Connors, S.L., Péan, C., Berger, S. et al. (Eds.). Cambridge University Press.

Joosten, H. (2009). The Global Peatland CO₂ Picture. Peatland status and emissions in all countries of the world. Draft. Available online at: <https://unfccc.int/sites/default/files/draftpeatlandco2report.pdf> (accessed on: November 2, 2021).

Joosten, H., and Clarke, D. (2002). Wise use of mires and peatlands - Background and principles including a framework for decision-making. International Mire Conservation Group and International Peat Society.

Joosten, H., Sirin, A., Couwenberg, J., Laine, J., Smith, P. (2016). The role of peatlands in climate regulation. In: Bonn, A., Allott, T., Evans, M., Joosten, H., and Stoneman, R. (Eds.), Peatland Restoration and Ecosystem Services. Cambridge University Press, Cambridge, 63–76. doi: 10.1017/CBO9781139177788.005

Kabisch, N., Stadlet, J., Korn, H., and Bonn, A. (2016). Nature-based solutions to climate change mitigation and adaptation in urban areas. Bonn, Bundesamt für Naturschutz (BfN)/Federal Agency for Nature Conservation, BfN-Skripte 446. ISBN 978-3-89624-183-2

Kearns, K., Liu, H., and Consoli, C. (2021). GCCSI Report: Technology Readiness and Costs of CCS. Available online at: <https://www.globalccsinstitute.com/resources/publications-reports-research/technology-readiness-and-costs-of-ccs/> (accessed on: November 2, 2021)

Kearns, J., Teletzke, G., Palmer, J., Thomann, H., Kheshgi, H., Chen, Y-H.H., et al. (2017). Developing

a Consistent Database for Regional Geologic CO₂ Storage Capacity Worldwide. *Energy Procedia* 114, 4697–4709. doi: 10.1016/J.EGYPRO.2017.03.1603.

Keith, D.W., Holmes, G., St. Angelo, D., and Heidel, K. (2018). A Process for Capturing CO₂ from the Atmosphere. *Joule* 2, 1573–1594. doi: 10.1016/j.joule.2018.05.006.

Kemna, R., and Moreno Acedo, J. (2014). Average EU building heat load for HVAC equipment. VHK. Available online at: https://ec.europa.eu/energy/sites/ener/files/documents/2014_final_report_eu_building_heat_demand.pdf (accessed on: October 28, 2020).

Kempka, T., Lucia, M. de, and Kühn, M. (2014). Geomechanical integrity verification and mineral trapping quantification for the Ketzin CO₂ storage pilot site by coupled numerical simulations. *Energy Procedia* 63, 3330–3338. doi: 10.1016/j.egypro.2014.11.361

Kim, D.-G., and Kirschbaum, M.U.F. (2015). The effect of land-use change on the net exchange rates of greenhouse gases: A compilation of estimates. *Agric. Ecosyst. Environ.* 208, 114-126. doi: 10.1016/j.agee.2015.04.026

Kim, J.K., Yarish, C., Hwang, E.K., Park, M., and Kim, Y. (2017). Seaweed aquaculture: Cultivation technologies, challenges and its ecosystem services. *Algae* 32, 1–13. doi: 10.4490/algae.2017.32.3.3

Knopf, S. and May, F. (2017). Comparing methods for the estimation of CO₂ storage capacity in saline aquifers in Germany: regional aquifer based vs. structural trap based assessments. *Energy Procedia* 114, 4710-4721. doi: 10.1016/j.egypro.2017.03.1605

KSG (2021) Bundes-Klimaschutzgesetz (KSG). Available online at: https://www.bmu.de/fileadmin/Daten_BMU/Download_PDF/Klimaschutz/ksg_aendg_2021_bf.pdf (accessed on: November 2, 2021)

Kuzyakov, Y., Bogomolova, I. and Glaser, B. (2014). Biochar stability in soil: Decomposition during eight years and transformation as assessed by compound-specific 14C analysis. *Soil Biol. Biochem.* 70, 229-236. doi: 10.1016/j.soilbio.2013.12.021

Kuzyakov, Y., Subbotina, I., Chen, H., Bogomolova, I. and Xu, X. (2009). Black carbon decomposition and incorporation into soil microbial biomass estimated by 14C labeling. *Soil Biol. Biochem.* 41:2, 210-219. doi: 10.1016/j.soilbio.2008.10.016

KVBG (2020) Kohleausstiegsgesetz Gesetz zur Reduzierung und zur Beendigung der Kohleverstromung und zur Änderung weiterer Gesetze. Available online at: https://www.bundesrat.de/SharedDocs/drucksachen/2020/0301-0400/392-20.pdf?__blob=publicationFile&v=1 (accessed on: November 3, 2021)

KSpG (2012). Gesetz zur Demonstration der dauerhaften Speicherung von Kohlendioxid (Kohlendioxid-Speicherungsgesetz - KSpG). Available online at: <https://ra.de/gesetze/kspg> (accessed on: November 3, 2021)

Leedham, E.C., Hughes, C., Keng, F.S.L, Phang, S.-M., Malin, G., and Sturges, W.T. (2013). Emission of atmospherically significant halocarbons by naturally occurring and farmed tropical macroalgae. *Biogeosciences* 10:6, 3615-3633. doi: 10.5194/bg-10-3615-2013

Lehmann, J., Czimczik, C., Laird, D. and Sohi, S. (2009). Stability of biochar in soil. In: Lehmann, J. and Joseph, S. (Eds.), *Biochar for environmental management - science and technology*, 183-205.

Lehmann, J., Gaunt, J. and Rondon, M. (2006). Bio-char sequestration in terrestrial ecosystems -a review. *Mitig. Adapt. Strateg. Glob. Chang.* 11, 403–427. doi: 10.1007/s11027-005-9006-5.

Lehmann, J. and Joseph, S. (Eds.) (2015). *Biochar for Environmental Management: Science, Technology and Implementation*, 2nd ed. Routledge, London and New York. doi:

10.4324/9781849770552.

Leng, L., Huang, H., Li, H., Li, J., and Zhou, W. (2019) Biochar stability assessment methods: A review. *Sci. Total Environ.* 647, 210-222. doi:10.1016/j.scitotenv.2018.07.402

Linzenich, A., Arning, K., Offermann-van Heek, J., Ziefle, M. 2019. Uncovering attitudes towards carbon capture storage and utilization technologies in Germany: Insights into affective-cognitive evaluations of benefits and risks. *Energy Res. Soc. Sci.* 48, 205-218. doi: 10.1016/j.erss.2018.09.017

Low, S., and Schäfer, S. (2020). Is bio-energy carbon capture and storage (BECCS) feasible? The contested authority of integrated assessment modeling. *Energy Res. Soc. Sci.* 60:101326. doi: 10.1016/j.erss.2019.101326

MacDicken, K. (2013). Forest Resources Assessment Working Paper 180. FAO: Rome. Available at: <http://www.fao.org/docrep/017/ap862e/ap862e00.pdf> (accessed on: November 3, 2021)

Marbà, N., AriasOrtiz, A., Masqué, P., Kendrick, G.A., Mazarrasa, I., Bastyan, G.R., et al. (2015). Impact of seagrass loss and subsequent revegetation on carbon sequestration and stocks. *J. Ecol.* 103:2, 296-302. doi: 10.1111/1365-2745.12370

Martens, S., Kempka, T., Liebscher, A., Möller, F., Schmidt-Hattenberger, C., Streibel, M., et al. (2015). Field Experiment on CO₂ Back-production at the Ketzin Pilot Site. *Energy Procedia* 76, 519–527. doi: 10.1016/j.egypro.2015.07.902

Matthews, H., Gillett, N., Stott, P. and Zickfeld, K. (2009). The proportionality of global warming to cumulative carbon emissions. *Nature* 459, 829–832. doi: 10.1038/nature08047

Matthews, H.D., Tokarska, K.B., Rogelj, J. et al. (2021). An integrated approach to quantifying uncertainties in the remaining carbon budget. *Commun. Earth Environ.* 2:7. doi: 10.1038/s43247-020-00064-9

Mengis, N., Kalthori, A., Simon, S., Harpprecht, C., Baetcke, L., Prats-Salvado, E., et al. (2022). Net-zero CO₂ Germany - A retrospect from the year 2050. *Earths Future* 10. doi: 10.1029/2021EF002324

Mengis, N., Simon, S., Thoni, T., Stevenson, A., Goerl, K., Steuri, B., et al. (2021). Net-Zero-2050 Cluster: Defining the German carbon budget. Project briefing #2, ver. 2, October 2021. Available online at: https://www.netto-null.org/imperia/md/assets/net_zero/dokumente/2_carbonbudget_2021_10_web.pdf (accessed on: November 3, 2021).

Merk, C., Klaus, G., Pohlers, J., Ernst, A., Ott, K., and Rehdanz, K. (2019). Public perceptions of climate engineering: Laypersons' acceptance at different levels of knowledge and intensities of deliberation. *GAIA* 28:4, 348-355(8). doi: 10.14512/gaia.28.4.6

Meyer, M. A. and Früh-Müller, A. (2020). Patterns and drivers of recent agricultural land-use change in Southern Germany. *Land Use Policy* 99, 104959. doi: 10.1016/j.landusepol.2020.104959

Minx, J. C., Lamb, W. F., Callaghan, M. W., Fuss, S., Hilaire, J., Creutzig, F., et al. (2018). Negative emissions - Part 1: research landscape and synthesis. *Environ. Res. Lett.* 13:063001. doi: 10.1088/1748-9326/aabf9b

Moksnes, P.O., Eriander, L., Infantes, E. and Holmer, M. (2018). Local regime shifts prevent natural recovery and restoration of lost eelgrass beds along the Swedish west coast. *Estuaries Coast.* 41:6, 1712-1731. doi: 10.1007/s12237-018-0382-y

Montingelli, M.E., Tedesco, S., and Olabi, A.G. (2015). Biogas production from algal biomass: a review. *Renew. Sust. Energ. Rev.* 43, 961-972. doi: 10.1016/j.rser.2014.11.052

Moosdorf, N., Renforth, P., and Hartmann, J. (2014). Carbon dioxide efficiency of terrestrial enhanced

weathering. *Environ. Sci. Technol.* 48:9, 4809-4816. doi: 10.1021/es4052022

Morrow, D.R., Thompson, M.S., Anderson, A., Batres, M., Buck, H.J., Dooley, K., et al. (2020). Principles for Thinking about Carbon Dioxide Removal in Just Climate Policy. *One Earth* 3:2, 150-153. doi: <https://doi.org/10.1016/j.oneear.2020.07.015>

Müller, C. and Reinhold, K. (Eds.) (2011). *Geologische Charakterisierung tiefliegender Speicher- und Barrierehorizonte in Deutschland – Speicher-Kataster Deutschland – Schriftenr. dt. Ges. Geowiss., Heft 74; Hannover. ISSN 1860-1782*

Müller, P., Ladiges, N., Jack, A., Schmiedl, G., Kutzbach, L., Jensen, K., et al. (2019). Assessing the long-term carbon-sequestration potential of the semi natural salt marshes in the European Wadden Sea. *Ecosphere* 10:1, doi:10.1002/ecs2.2556

Nellemann, C., Corcoran, E., Duarte, C. M., Valdés, L., De Young, C., Fonseca, L., et al. (Eds) (2009). *Blue Carbon. A Rapid Response Assessment.* United Nations Environment Programme, GRID-Arendal. Available online at: <https://www.grida.no/publications/145> (accessed on: November 3, 2021)

Nemet, G. F., Callaghan, M. W., Creutzig, F., Fuss, S., Hartmann, J., Hilaire, J., et al. (2018). Negative emissions - Part 3: Innovation and upscaling. *Environ. Res. Lett.* 13:063003. doi: 10.1088/1748-9326/aabff4

Orsted Media Relations (2016). Denmark's largest power station replaces coal with wood pellets. Available online at: <https://orsted.com/en/media/newsroom/news/2017/10/denmarks-largest-power-station-replaces-coal-with-wood-pellets> (accessed on: October 19, 2021)

Oschlies, A., and G. Klepper (2017) Research for assessment, not deployment, of Climate Engineering: The German Research Foundation's Priority Program SPP 1689, *Earth's Future* 5, 128–134, doi:10.1002/2016EF000446.

Otto, D., and Gross, M. (2021). Stuck on coal and persuasion? A critical review of carbon capture and storage communication. *Energy Res. Soc. Sci.* 82, 102306. doi: 10.1016/j.erss.2021.102306.

Patuzzi, F., Basso, D., Vakalis, S., Antolini, D., Piazzzi, S., Benedetti, V., et al. (2021). State-of-the-art of small-scale biomass gasification systems: An extensive and unique monitoring review. *Energy* 223, 120039. doi: 10.1016/j.energy.2021.120039

Poeplau, C., and Don, A. (2015). Carbon sequestration in agricultural soils via cultivation of cover crops –A meta-analysis. *Agric. Ecosyst. Environ.* 200, 33-41. doi: 10.1016/j.agee.2014.10.024

Pozo, C., Galán-Martín, Á., Reiner, D.M. et al. (2020). Equity in allocating carbon dioxide removal quotas. *Nat. Clim. Chang.* 10, 640–646. doi: 10.1038/s41558-020-0802-4

Prognos, Öko-Institut, Wuppertal-Institut (2021). *Klimaneutrales Deutschland 2045. Wie Deutschland seine Klimaziele schon vor 2050 erreichen kann. Langfassung.* Hg. v. Stiftung Klimaneutralität, Agora Energiewende, Agora Verkehrswende. Available online at: https://static.agora-energiewende.de/fileadmin/Projekte/2021/2021_04_KNDE45/A-EW_209_KNDE2045_Zusammenfassung_DE_WEB.pdf (accessed on: November 3, 2021)

Rauch, R., Hrbek, J. and Hofbauer, H. (2014). Biomass gasification for synthesis gas production and application, *Wiley Interdiscip. Rev. Energy Environ.* 3:4, 343-362. doi: 10.1002/wene.97

Rhoden, I., Vögele, S., Ball, C., Simon, S., Mengis, N., Baetcke, L., et al. (2021). Spatial Heterogeneity - Challenge and Opportunity for Net-Zero Germany. Report, in press. Helmholtz Climate Initiative. Available online: https://www.netto-null.org/imperia/md/assets/net_zero/dokumente/2021_netto-null_spatial-heterogeneity.pdf (accessed on: July 28, 2022)

Rogelj, J., Shindell, D., Jiang, K., Fifita, S., Forster, P., Ginzburg, V., et al. (2018). Mitigation Pathways Compatible with 1.5°C in the Context of Sustainable Development. In: Masson-Delmotte, V., Zhai, P., Pörtner, H. O., Roberts, D., Skea, J., Shukla, P. R., et al. (Eds.), Global warming of 1.5 °C, (IPCC Special Report), Geneva, Intergovernmental Panel on Climate Change, 93-174.

Rydin, H. and Jeglum, J.K., (2013). Peatland habitats. In: *The Biology of Peatlands*. Oxford University Press, New York, NY, USA, 1–17.

Sanchez, D. L., Johnson, N., McCoy, S. T., Turner, P. A. and Mach, K.J. (2018). Near-term deployment of carbon capture and sequestration from biorefineries in the United States. *Proc. Natl. Acad. Sci. U. S. A.*, 115:19, 4875–4880. doi: 10.1073/pnas.171969511

Scheftelowitz, M., and Thrän, D. (2016). Biomasse im EEG 2016: Hintergrundpapier zur Situation der Bestandsanlagen in den verschiedenen Bundesländern. Available online at: https://www.dbfz.de/fileadmin/user_upload/Referenzen/Statements/Hintergrundpapier_Biomasse_EEG2016.pdf (accessed on: November 3, 2021)

Schenuit, F., Colvin, R., Fridahl, M., McMullin, B., Reisinger, A., Sanchez, D.L., et al. (2021). Carbon Dioxide Removal Policy in the Making: Assessing Developments in 9 OECD Cases. *Front. Clim.* 3:638805. doi: 10.3389/fclim.2021.638805

Schlesinger, W.H. (2018). Are wood pellets a green fuel? *Science* 359, 1328–1329. doi: 10.1126/science.aat2305

Scholwin, F., and Siegert, G. (2020). Biogas aus Paludikulturen. Produktionsweg, Hintergründe, Klimaschutzwirkung. Institut für Biogas, Kreislaufwirtschaft und Energie. Greifswald Moor Centrum. Greenpeace Energy eG. Available online at: https://green-planet-energy.de/fileadmin/docs/publikationen/Studien/201109_GPE-Studie_zu_Paludi_final.pdf (accessed on: November 3, 2021)

Shell Canada Ltd. Report (2019). Quest Carbon Capture and Storage Project, 2019 Annual Status Report. Available online at: <https://open.alberta.ca/dataset/f74375f3-3c73-4b9c-af2b-ef44e59b7890/resource/92e474c0-b043-4c8f-8693-1336447933d0/download/energy-quest-annual-status-report-alberta-energy-regulator-2019.pdf> (accessed on: November 3, 2021)

Simon, S., Xiao, M., Harpprecht, C., Sasanpour, S., Gardian, H., Pregger, T. A. (2022). Pathway for the German Energy Sector Compatible with a 1.5 °C Carbon Budget. *Sustainability* 14, 1025. doi: 10.3390/su14021025

Smith, E., Morris, J., Kheshgi, H., Teletzke, G., Herzog, H. and Paltsev, S. (2021). The cost of CO₂ transport and storage in global integrated assessment modeling. *Int. J. Greenh. Gas Control* 109. doi: 10.1016/j.ijggc.2021.103367.

Smith, L.J., and Torn, M.S. (2013). Ecological limits to terrestrial biological carbon dioxide removal. *Clim. Change* 118, 89–103. doi: 10.1007/s10584-012-0682-3

Spence, E., Cox, E. and Pidgeon, N. (2021). Exploring cross-national public support for the use of enhanced weathering as a land-based carbon dioxide removal strategy. *Clim. Change* 165: 23. doi: 10.1007/s10584-021-03050-y

Stottrop, D., and Flühöh, C. (2007). Büroflächenbestand-Grundlagen, Daten und Methoden. Hg. v. Prof. Dr. Karl-Werner Schulte und Prof. Dr. Stephan Bone-Winkel. International Real Estate Business School (IREBS), Universität Regensburg. Regensburg.

Tanneberger, F., Able, S., Couwenberg, J., et al. (2021). Towards net-zero CO₂ in 2050:

An emission reduction pathway for organic soils in Germany. *Mires Peat* 27:5, 17. doi: 10.19189/MaP.2020.SNPG.StA.1951.

Tanneberger, F., Appulo, L., Ewert, S., Lakner, S., Ó Brolcháin, N., Peters, J. et al. (2020). The Power of Nature-Based Solutions: How Peatlands Can Help Us to Achieve Key EU Sustainability Objectives. *Adv. Sustain. Syst.* 5. doi: 10.1002/adsu.202000146

Tanneberger, F., Birr, F., Couwenberg, J. Kaiser, M., Luthardt, V., Nerger, M. et al. (2022). Saving soil carbon, greenhouse gas emissions, biodiversity and the economy: paludiculture as sustainable land use option in German fen peatlands. *Reg. Environ. Change* 22, 69. doi: 10.1007/s10113-022-01900-8

Tcvetkov, P., Cherepovitsyn, A., and Fedoseev, S. (2019). Public perception of carbon capture and storage: A state-of-the-art overview. *Heliyon* 5:12, doi: 10.1016/j.heliyon.2019.e02845.

The World Bank (2019). Global Solar Atlas 2.0, Solar resource data: Solargis. Available online at: <https://solargis.com/maps-and-gis-data/download/germany> (accessed on: November 3, 2021).

Thoni, T., Beck, S., Borchers, M., Förster, J., Görl, K., Hahn, A., et al. (2020). Deployment of Negative Emissions Technologies at the National Level: A Need for Holistic Feasibility Assessments, *Front. Clim.* 2, 590305. doi: 10.3389/fclim.2020.590305.

Thrän, D. (2019). Interdisziplinäres Bewertungsinstrument für Bioenergie-Entwicklungspfade. Materialien zur Analyse Biomasse im Spannungsfeld zwischen Energie- und Klimapolitik. Potenziale –Technologien –Zielkonflikte. Schriftenreihe Energiesysteme der Zukunft, München. Available online at: https://www.leopoldina.org/uploads/tx_leopublication/2019_ESYS_Materialien_Bioenergie.pdf (accessed on: November 4, 2021)

Thrän, D. and Schindler, H. (2021). Umrüstung von Kohlekraftwerken auf Biomasse. DBFZ Positionspapier, Deutsches Biomasseforschungszentrum gGmbH (DBFZ), Juni 2021. Available online at: https://www.dbfz.de/fileadmin/user_upload/Referenzen/Statements/2021_Position_Kohlekraftwerke.pdf (accessed on: November 2, 2021)

Trepel, M., Pfadenhauer, J., Zeitz, J., and Jeschke, L. (2017) Part II: Germany. In: Joosten H, Tanneberger F, Moen A (Eds.) *Mires and peatlands of Europe: status, distribution and conservation*. Schweizerbart Science Publishers, Stuttgart, 413–424. ISBN 978-3-510-65383-6

Tripathi, M., Sahu, J., and Ganesan, P. (2016). Effect of process parameters on production of biochar from biomass waste through pyrolysis. *Renew. Sust. Energ. Rev.* 55, 467-481. doi: 10.1016/j.rser.2015.10.122

UBA (2021). Previous year's estimate of German greenhouse gas emissions for 2020. Umweltbundesamt (UBA) Dessau, 15.03.2021. Available online at: https://www.umweltbundesamt.de/sites/default/files/medien/361/dokumente/2021_03_10_trendtabellen_thg_nach_sektoren_v1.0.xlsx (accessed on: November 2, 2021).

UNFCCC (2015). Paris Agreement. Available online at: <https://unfccc.int/process-and-meetings/the-paris-agreement/the-paris-agreement> (accessed on: February 19, 2021).

UNEP (2017). The Emissions Gap Report 2017: A UN Environment Synthesis Report. Nairobi: United Nations Environmental Program. Available online at: https://wedocs.unep.org/bitstream/handle/20.500.11822/22070/EGR_2017.pdf?sequence=1&isAllowed=y (accessed on: November 3, 2021).

Waller, L., Rayner, T., Chilvers, J., Gough, C.A., Lorenzoni, I., Jordan, A., et al. (2020). Contested framings of greenhouse gas removal and its feasibility: Social and political dimensions. *Wiley Interdiscip.*

Rev. Clim. Change. doi: 10.1002/wcc.649.

Wallquist, L., Seigo, S.L.O., Visschers, V.H.M., and Siegrist, M. (2012). Public acceptance of CCS system elements: A conjoint measurement. *Int. J. Greenh. Gas Control.* 6, 77-83. doi: 10.1016/j.ijggc.2011.11.008.

Wartenberg, R., Feng, L., Wu, J.J., Mak, Y.L., Chan, L.L., Treffer, T.C, et al. (2017). The impacts of suspended mariculture on coastal zones in China and the scope for integrated multi-trophic aquaculture. *Ecosyst. Health Sustain.* 3:6, 1340268. doi: 10.1080/20964129.2017.1340268

Wichtmann, W., Schröder C., and H. Joosten (2015). *Paludikultur — Bewirtschaftung nasser Moore für regionale Wertschöpfung, Klimaschutz und Biodiversität.* Schweizerbart Science Publishers, Stuttgart. ISBN 978-3-510-65282-2

Wieding, J., Stubenrauch, J., and Ekardt, F. (2020). Human rights and precautionary principle: limits to geoengineering, SRM, and IPCC scenarios. *Sustainability* 12:8858. doi: 10.3390/su12218858

Wolske, K.S., Raimi, K.T., Campbell-Arvai, V., and Hart, P.S. (2019). Public support for carbon dioxide removal strategies: the role of tampering with nature perceptions. *Clim. Change* 152:3-4, 345-361. doi: 10.1007/s10584-019-02375-z.

Zickfeld, K., Azevedo, D., Mathesius, S., and Matthews, H.D. (2021). Asymmetry in the climate–carbon cycle response to positive and negative CO₂ emissions. *Nat. Clim. Chang.* 11, 613–617 (2021). doi: 10.1038/s41558-021-01061-2

Ziegler, R., Wichtmann, W., Abel, S., Kemp, R., Simard, M., and Joosten, H. (2021). Wet peatland utilisation for climate protection –An international survey of paludiculture innovation. *Cleaner Engineering and Technology* 5, 100305. doi: 10.1016/j.clet.2021.100305.

Ziska F, Quack B, Abrahamsson K, Archer, S.D., Atlas, E., Bell, T., et al. (2013). Global sea-to-air flux climatology for bromoform, dibromomethane and methyl iodide. *Atmos. Chem. Phys.* 13:17, 8915-8934. doi: 10.5194/acp-13-8915-2013

Chapter 5

Conclusion and Outlook

5.1 Summary and Conclusion

The amplified recognition of Carbon Dioxide Removal (CDR) methodologies underscores their pivotal role in counteracting climate change anomalies (IPCC, 2022). Ocean-based CDR approaches, also termed as ocean NETs (Net Emission Technologies), exploiting the ocean's robust carbon sequestration capability, exhibit significant promise. A pivotal endeavor in advancing these ocean-based CDR approaches is the identification of proficient carbon carriers, proficient in carbon capture with reduced environmental ramifications and superior maneuverability. Subsequently, macroalgae have attracted substantial attention due to their elevated photosynthetic performance and carbon-rich biomass, their propensity to thrive without occupying agricultural land, and the entrenched breeding and cultivation protocols (Chung et al., 2013; Bach et al., 2021). Within this thesis, the comprehension of ocean-based CDR employing macroalgae was expanded, herein termed as macroalgae-based CDR. The investigation and assessment of macroalgae-based CDR are executed through numerical modeling. By embedding a macroalgae growth model within an Earth system model, a thorough assessment encompassing the facets of carbon sequestration capacity, the interplay between oceanic carbon sequestration and the global carbon cycle, as well as the potential ancillary impacts on marine biogeochemistry, was conducted.

In Chapter 2, we investigated the theoretical CDR efficacy and the biogeochemical implications of macroalgae open-ocean mariculture and sinking (MOS) as an macroalgae-based CDR methodology. Employing a synergistic approach by incorporating a macroalgae growth model into an Earth system model, University of Victoria Earth System Model (UVic ESCM), the study simulated the potential of macroalgal mariculture in the open-

ocean surface, and subsequent rapid sinking of carbon-rich macroalgal biomass to the profound seafloor, assuming no remineralization during the descent. Additionally, the enhancement of MOS with Artificial Upwelling (AU) was examined, revealing a significant increase in carbon capture and sequestration. Projected globally from 2020 to 2100 under a moderate-emissions pathway (RCP 4.5), the data illustrated that MOS could sequester 270 PgC, further amplified to 447 PgC with AU, although the oceanic carbon stock only increased by 171.8 PgC (283.9 PgC with AU) due to Earth system feedbacks. The discernible effects of MOS on pelagic ecosystems encompassed a reduction in Phytoplankton Net Primary Production (PNPP) due to nutrient competition and canopy shading, along with alterations in Oxygen-Minimum Zones (OMZs) both at mid-layers and the seafloor. Moreover, a notable alteration in the global carbon cycle was observed, highlighting a reduction in atmospheric and terrestrial carbon reservoirs, while augmenting the oceanic carbon reservoir. Although effects were largely reversible post cessation of MOS, a complete recovery was not observed by year 3000. A sensitivity analysis further disclosed that in the absence of remineralization, all MOS-captured carbon is permanently stored in the ocean, albeit at the cost of long-term nutrient depletion in surface waters, thus reducing PNPP. Collectively, the findings underscore the substantial theoretical CDR potential of MOS as an ocean-based strategy; however, they also delineate significant repercussions on marine ecosystems and biogeochemical cycles, potentially leading to a reorganization of marine trophic structures across extensive oceanic expanses.

In Chapter 3, we evaluated another macroalgae-based CDR strategy titled Nearshore Macroalgae Aquaculture for Carbon Sequestration (N-MACS) by facilitating macroalgae cultivation with biomass harvesting in nearshore ocean surfaces. This chapter assessed the CDR potential of N-MACS alongside its implications on the global carbon cycle, marine biogeochemistry, and marine ecosystems. The macroalgae model, initially established in the UVic ESCM in Chapter 1, was adapted to nearshore areas to simulate the cultivation and harvest of macroalgae biomass, aligning with the span of Exclusive Economic Zones (EEZs). The simulations indicate that coastal N-MACS holds the potential to sequester approximately 0.7 to 1.1 GtC yr⁻¹. Nevertheless, a notable downside emerged, where N-MACS significantly curtails marine net primary productivity by phytoplankton (PNPP) due to nutrient depletion and canopy shading, offsetting about 30% of the N-MACS CDR capacity. This reduction in surface PNPP, in turn, diminishes organic carbon export from the euphotic zone to the deep ocean, subsequently elevating dissolved oxygen levels and reducing denitrification in current oxygen minimum zones in upwelling regions. The effects triggered by harvesting-induced phosphate (PO₄) removal exhibited a lasting impact, per-

sisting for centuries even after ceasing N-MACS operations. The findings from this chapter not only contribute to a deeper understanding of the N-MACS approach but also underscore the necessity for a balanced evaluation of its ecological impacts, hinting at pivotal areas for further research and refinement in the quest for viable CDR strategies.

In Chapter 4, the focus shifts to applying macroalgae-based CDR within a specific context, proposing its use in BECC–Macroalgae farming for biogas production as part of Germany’s Net-Zero 2050 target (concept 6 among 13 selected CDR concepts). Macroalgae, with its rapid growth and favorable biochemical composition, is identified as a viable feedstock for third-generation biofuels. The marine environment, especially offshore, is suggested for cultivation, thereby conserving arable land and freshwater resources. This chapter also highlights the maturity of macroalgae cultivation technologies, primarily in Asian nations, and explores potential expansion in Germany’s North Sea exclusive economic zone (EEZ), integrated with offshore wind farms. Furthermore, coupling this approach with Integrated Multi-Trophic Aquaculture (IMTA) could mitigate eutrophication and enhance bio-remediation and aquaculture productivity. The chapter concludes with the potential of retrofitting biogas plants on Germany’s North Sea coast with CCS units, facilitating the removal of approximately 0.79 Mt CO₂ per year, thus integrating carbon removal with sustainable energy and ecological benefits.

In this dissertation, through numerical simulations utilizing an Earth system model, we conducted a systematic evaluation of the macroalgae-based CDR methodologies from the perspectives of marine biogeochemistry and the global carbon cycle. We examined this method under 1) various deployment locations from the open ocean to nearshore areas; 2) in combination with artificial upwelling, and 3) through a case study within the Exclusive Economic Zone (EEZ) of Germany as a conceptual CDR option.

Our findings, in conjunction with previous research, further indicate that macroalgae-based CDR entails a significant trade-off: a suppression in marine primary production by plankton. This suppression is primarily caused by the canopy shading effect and nutrient competition of macroalgae. This repercussion on NPP, in turn, limits the CDR efficiency of macroalgae-based strategies. The perturbation to marine primary productivity may induce cascading effects, potentially instigating alterations to marine food webs and ecosystems as a whole. Nutrients, particularly in the surface ocean, serve as a kind of ‘currency’ in all ocean-based biotic CDR approaches that aim to enhance the biological carbon pump. Utilizing these nutrients for the desired export and storage of biomass can impoverish the remaining marine ecosystem.

While our analyses are predicated on certain idealized assumptions, and the execution

techniques and frameworks of such marine CDR methods may diverge from the concepts presented herein in future endeavors, the preliminary explorations in our estimations and simulations are poised to contribute to subsequent in-depth investigations. Concurrently, Our findings, in conjunction with previous studies concerning CDR and other climate mitigation strategies, further indicate that no singular solution emerges as a panacea for the climate change crisis. This advocates the emergency for accelerating and amplifying research and implementation of diverse mitigation and adaptation strategies, alongside fostering more rigorous and synergistic collaborations globally.

5.2 Outlook

The inquiries conducted in this dissertation underscore the necessity for an enriched understanding of macroalgae-based CDR methods. As we navigate a period that demands immediate and efficient climate action to mitigate the escalating impacts of anthropogenic emissions, the improvement and optimization of such environmentally-sustainable CDR approaches become utterly pivotal. This urgent need highlights the substantial potential that macroalgae-based CDR methods hold, given their natural ability to both capture CO₂ and offer extra environmental benefits. However, tapping into this potential requires thorough evaluation and assessment of the related methods, extending from biological underpinnings of macroalgae to the technological and logistical frameworks required for large-scale implementation.

From a modeling perspective, there are several areas that warrant improvement. Refining the macroalgae model is crucial for accurately simulating macroalgae growth and its interaction with surrounding marine ecosystems. Specifically, the incorporation of dynamic stoichiometric ratios (C:N:P) in biomass within the model can offer a more realistic portrayal of nutrient cycling and macroalgae physiology, thereby enhancing the model's robustness and reliability in predicting the outcomes of macroalgae-based CDR approaches (Van Der Molen et al., 2018; Broch and Slagstad, 2012). The consideration of potential iron limitation on macroalgae growth is also noteworthy (Paine et al., 2023). Furthermore, extending the modeling to encompass the generation of various chemicals from macroalgae and assessing their role within the CDR scheme could be enlightening. For instance, macroalgae generate recalcitrant dissolved and particulate organic matter (DOM and POM), releasing them into the ocean, which could significantly augment the ocean carbon pool (Pedersen et al., 2021; Watanabe et al., 2020; Chen et al., 2020). By integrating observational or lab-measured data, modeling the quantity and fate of these carbon mate-

rials will foster a more robust evaluation of the method. Conversely, certain macroalgae species emit halocarbons, a greenhouse gas, which could potentially diminish the CDR efficiency (Baker et al., 2001; Jia et al., 2021; Tegtmeier et al., 2012). Moreover, integrating the existing or refined macroalgae models into Earth system models or regional ocean models with enhanced resolutions could also aid in the evaluation and assessment of macroalgae-based CDR. Higher resolution models will yield a more nuanced depiction of oceanic and atmospheric processes, crucial for complements the current studies by providing additional insight into the efficacy and impacts of macroalgae-based CDR strategies on global or regional marine biogeochemistry and the carbon cycle (e.g., Berger et al.; Arzeno-Soltero et al.).

On a broader strategic level, the goal is to expand the area of macroalgae farms for CDR while reducing competition with nutrient-rich ocean surfaces and associated human activities like fisheries. The vast Low Nutrient-Low Chlorophyll (LNLC) regions, including the subtropical gyres in the North and South Atlantic (Antoine et al., 1996), stand out as competitive locations for macroalgae-based CDR. These regions provide a compromise between maximizing CDR potential and minimizing interference with existing oceanic activities and ecosystems. Overcoming the nutrient deficiency in surface waters within these regions could be achieved through the implementation of artificial upwelling in conjunction with seaweed farms (see Chapter 2), pumping nutrient-rich deep water to promote seaweed growth in the farms. Concurrently, the floating seaweed species, *Sargassum*, epitomizes an ideal candidate. Possessing an entirely pelagic life cycle, rapid growth rates, high carbon to nutrient biomass ratios (C:N of around 50, Lapointe et al.), and the potential to produce recalcitrant carbon-rich biomass (Sichert et al., 2020), pelagic *Sargassum* holds promise for carbon sequestration. The sequestered carbon can be permanently stored or at least retained on the seafloor for an extended duration. Additionally, the harvested biomass could be processed using CDR methods such as Bioenergy with Carbon Capture and Storage (BECCS). The recent recurrence of the Great Atlantic Sargassum Belt (GASB) and the golden wave in the East China Sea serve as natural analogues (Wang et al., 2019; Smetacek and Zingone, 2013), illustrating the potential for executing macroalgae-based CDR by leveraging the synergy between *Sargassum* and subtropical gyres. Furthermore, to mitigate the impacts of long-term nutrient removal, the nutrients extracted within the harvested macroalgae biomass could potentially be reintroduced to the ocean. This approach not only facilitates a cyclical nutrient process but also exemplifies a sustainable strategy to bolster the efficacy of macroalgae-based CDR. The model and methodologies rooted in this dissertation possess the potential for application in evaluating this specific macroalgae-

based CDR approach.

5.3 References

- David Antoine, Jean-Michel André, and André Morel. Oceanic primary production: 2. Estimation at global scale from satellite (Coastal Zone Color Scanner) chlorophyll. *Global Biogeochemical Cycles*, 10(1):57–69, 1996. ISSN 1944-9224. doi: 10.1029/95GB02832. URL <https://onlinelibrary.wiley.com/doi/abs/10.1029/95GB02832>. _eprint: <https://onlinelibrary.wiley.com/doi/pdf/10.1029/95GB02832>.
- Isabella B. Arzeno-Soltero, Benjamin T. Saenz, Christina A. Frieder, Matthew C. Long, Julianne DeAngelo, Steven J. Davis, and Kristen A. Davis. Large global variations in the carbon dioxide removal potential of seaweed farming due to biophysical constraints. *Communications Earth & Environment*, 4(1):1–12, June 2023. ISSN 2662-4435. doi: 10.1038/s43247-023-00833-2. URL <https://www.nature.com/articles/s43247-023-00833-2>. Number: 1 Publisher: Nature Publishing Group.
- Lennart T. Bach, Veronica Tamsitt, Jim Gower, Catriona L. Hurd, John A. Raven, and Philip W. Boyd. Testing the climate intervention potential of ocean afforestation using the Great Atlantic Sargassum Belt. *Nature Communications*, 12(1):2556, May 2021. ISSN 2041-1723. doi: 10.1038/s41467-021-22837-2. URL <https://www.nature.com/articles/s41467-021-22837-2>.
- J.M. Baker, W.T. Sturges, J. Sugier, G. Sunnenberg, A.A. Lovett, C.E. Reeves, P.D. Nightingale, and S.A. Penkett. Emissions of CH₃Br, organochlorines, and organoiodines from temperate macroalgae. *Chemosphere - Global Change Science*, 3(1):93–106, January 2001. ISSN 14659972. doi: 10.1016/S1465-9972(00)00021-0. URL <https://linkinghub.elsevier.com/retrieve/pii/S1465997200000210>.
- Manon Berger, Lester Kwiatkowski, David T Ho, and Laurent Bopp. Ocean dynamics and biological feedbacks limit the potential of macroalgae carbon dioxide removal. *Environmental Research Letters*, 18(2):024039, February 2023. ISSN 1748-9326. doi: 10.1088/1748-9326/acb06e. URL <https://iopscience.iop.org/article/10.1088/1748-9326/acb06e>.
- Ole Jacob Broch and Dag Slagstad. Modelling seasonal growth and composition of the kelp *Saccharina latissima*. *Journal of Applied Phycology*, 24(4):759–776, August 2012. ISSN 0921-8971, 1573-5176. doi: 10.1007/s10811-011-9695-y. URL <http://link.springer.com/10.1007/s10811-011-9695-y>.

- Siwang Chen, Kai Xu, Dehua Ji, Wenlei Wang, Yan Xu, Changsheng Chen, and Chaotian Xie. Release of dissolved and particulate organic matter by marine macroalgae and its biogeochemical implications. *Algal Research*, 52:102096, December 2020. ISSN 22119264. doi: 10.1016/j.algal.2020.102096. URL <https://linkinghub.elsevier.com/retrieve/pii/S2211926420309644>.
- Ik Kyo Chung, Jung Hyun Oak, Jin Ae Lee, Jong Ahm Shin, Jong Gyu Kim, and Kwang-Seok Park. Installing kelp forests/seaweed beds for mitigation and adaptation against global warming: Korean Project Overview. *ICES Journal of Marine Science*, 70(5):1038–1044, September 2013. ISSN 1095-9289, 1054-3139. doi: 10.1093/icesjms/fss206. URL <https://academic.oup.com/icesjms/article/70/5/1038/644026>.
- IPCC. Summary for policymakers. In H. O. Pörtner, D. C. Roberts, M. Tignor, E. S. Poloczanska, K. Mintenbeck, A. Alegría, M. Craig, S. Langsdorf, S. Löschke, V. Möller, A. Okem, and B. Rama, editors, *Climate Change 2022: Impacts, Adaptation and Vulnerability. Contribution of Working Group II to the Sixth Assessment Report of the Intergovernmental Panel on Climate Change*. Cambridge University Press, Cambridge, UK and New York, NY, USA, 2022. doi: 10.1017/9781009325844.001. URL https://www.ipcc.ch/report/ar6/wg2/downloads/report/IPCC_AR6_WGII_SummaryForPolicymakers.pdf.
- Yue Jia, Birgit Quack, Robert D. Kinley, Ignacio Pisso, and Susann Tegtmeier. Potential environmental impact of bromoform from *Asparagopsis* farming in Australia. preprint, Gases/Atmospheric Modelling/Troposphere/Chemistry (chemical composition and reactions), November 2021. URL <https://acp.copernicus.org/preprints/acp-2021-800/acp-2021-800.pdf>.
- B. E. Lapointe, R. A. Brewton, L. W. Herren, M. Wang, C. Hu, D. J. McGillicuddy, S. Lindell, F. J. Hernandez, and P. L. Morton. Nutrient content and stoichiometry of pelagic Sargassum reflects increasing nitrogen availability in the Atlantic Basin. *Nature Communications*, 12(1):3060, May 2021. ISSN 2041-1723. doi: 10.1038/s41467-021-23135-7. URL <https://www.nature.com/articles/s41467-021-23135-7>.
- Ellie R. Paine, Philip W. Boyd, Robert F. Strzepek, Michael Ellwood, Elizabeth A. Brewer, Guillermo Diaz-Pulido, Matthias Schmid, and Catriona L. Hurd. Iron limitation of kelp growth may prevent ocean afforestation. *Communications Biology*, 6(1):1–9, June 2023. ISSN 2399-3642. doi: 10.1038/s42003-023-04962-4. URL <https://www.nature.com/articles/s42003-023-04962-4>. Number: 1 Publisher: Nature Publishing Group.
- Mf Pedersen, K Filbee-Dexter, NI Frisk, Z Sárossy, and T Wernberg. Carbon sequestration potential increased by incomplete anaerobic decomposition of kelp detritus. *Marine Ecology Progress Series*, 660:53–67, February 2021. ISSN 0171-8630, 1616-1599. doi: 10.3354/meps13613. URL <https://www.int-res.com/abstracts/meps/v660/p53-67/>.

- Andreas Sichert, Christopher H. Corzett, Matthew S. Schechter, Frank Unfried, Stephanie Markert, Dörte Becher, Antonio Fernandez-Guerra, Manuel Liebeke, Thomas Schweder, Martin F. Polz, and Jan-Hendrik Hehemann. Verrucomicrobia use hundreds of enzymes to digest the algal polysaccharide fucoidan. *Nature Microbiology*, 5(8):1026–1039, May 2020. ISSN 2058-5276. doi: 10.1038/s41564-020-0720-2. URL <https://www.nature.com/articles/s41564-020-0720-2>.
- Victor Smetacek and Adriana Zingone. Green and golden seaweed tides on the rise. *Nature*, 504(7478):84–88, December 2013. ISSN 1476-4687. doi: 10.1038/nature12860. URL <https://www.nature.com/articles/nature12860>. Number: 7478 Publisher: Nature Publishing Group.
- S. Tegtmeier, K. Krüger, B. Quack, E. L. Atlas, I. Pisso, A. Stohl, and X. Yang. Emission and transport of bromocarbons: from the West Pacific ocean into the stratosphere. *Atmospheric Chemistry and Physics*, 12(22):10633–10648, November 2012. ISSN 1680-7324. doi: 10.5194/acp-12-10633-2012. URL <https://acp.copernicus.org/articles/12/10633/2012/>.
- Johan Van Der Molen, Piet Ruardij, Karen Mooney, Philip Kerrison, Nessa E. O’Connor, Emma Gorman, Klaas Timmermans, Serena Wright, Maeve Kelly, Adam D. Hughes, and Elisa Capuzzo. Modelling potential production of macroalgae farms in UK and Dutch coastal waters. *Biogeosciences*, 15(4):1123–1147, February 2018. ISSN 1726-4189. doi: 10.5194/bg-15-1123-2018. URL <https://bg.copernicus.org/articles/15/1123/2018/>.
- Mengqiu Wang, Chuanmin Hu, Brian B. Barnes, Gary Mitchum, Brian Lapointe, and Joseph P. Montoya. The great Atlantic *Sargassum* belt. *Science*, 365(6448):83–87, July 2019. ISSN 0036-8075, 1095-9203. doi: 10.1126/science.aaw7912. URL <https://www.science.org/doi/10.1126/science.aaw7912>.
- Kenta Watanabe, Goro Yoshida, Masakazu Hori, Yu Umezawa, Hirotada Moki, and Tomohiro Kuwae. Macroalgal metabolism and lateral carbon flows can create significant carbon sinks. *Biogeosciences*, 17(9):2425–2440, May 2020. ISSN 1726-4189. doi: 10.5194/bg-17-2425-2020. URL <https://bg.copernicus.org/articles/17/2425/2020/>.

A. Supporting Information for Chapter 2

Appendix

A.1 MOS validations

A.1.1 MOS yield calculation

For the convenience of calculation, we assume that, when MOS occupies a surface grid cell, the area is covered by parallel cultivation ropes (lines) with an interval distance of d (see Table 2.1 and Fig. A.1). The total length of the cultivation lines (L_{MOS} , in meters) of MOS in the grid cell is then

$$L_{\text{MOS}} = S_{\text{MOS}} \div d, \quad (\text{A.1})$$

where S_{MOS} (m^{-2}) is the area of ocean surface occupied by MOS. Accordingly, the conversion between macroalgal biomass yield on ropes (Y_{rope} in kg DW m^{-1}) or in fields (Y_{field} in kg DW m^{-2}) can be calculated as follows:

$$Y_{\text{rope}} = Y_{\text{field}} \times d. \quad (\text{A.2})$$

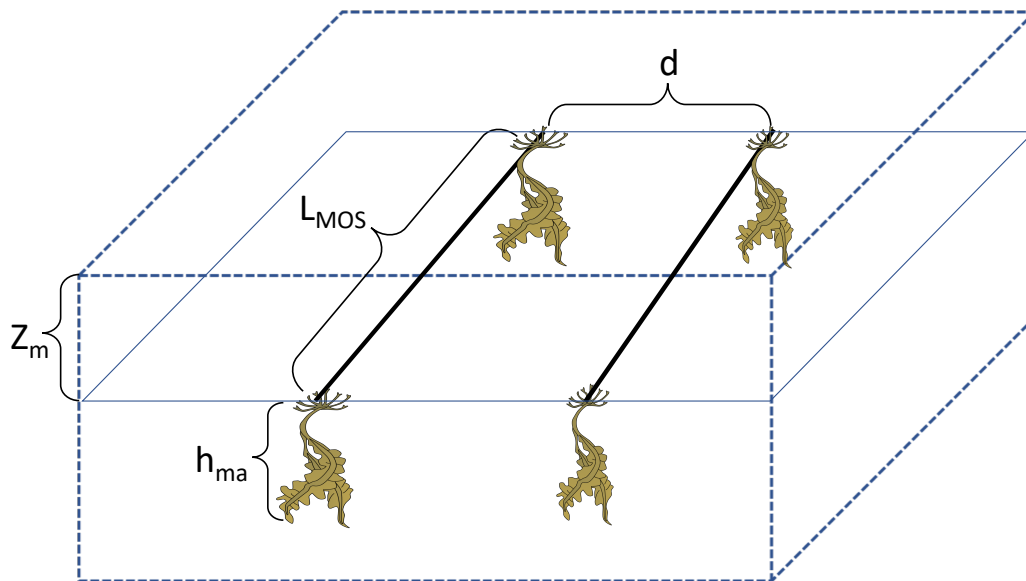


Figure A.1: Sketch of key features of MOS.

A.1.2 MOS NPP

A.2 Impacts of MOS on global biogeochemistry

Code & Data Availability

The model codes are available online at https://git.geomar.de/jiajun-wu/wu_esd_cdr_mos.

The data used to generate the contents, tables and figures are available online at <https://data.geomar.de/downloads/20.500.12085/d88214cc-43aa-40d4-be40-f26aa346e8fa/>

Acknowledgements

We thank Wolfgang Koeve, Nadine Mengis, Karin Kvale and Fabian Reith for the helpful discussions. We thank Susann Tegtmeier, Birgit Quack and Yue Jia for the discussions about generation of halocarbons from macroalgae cultivation.

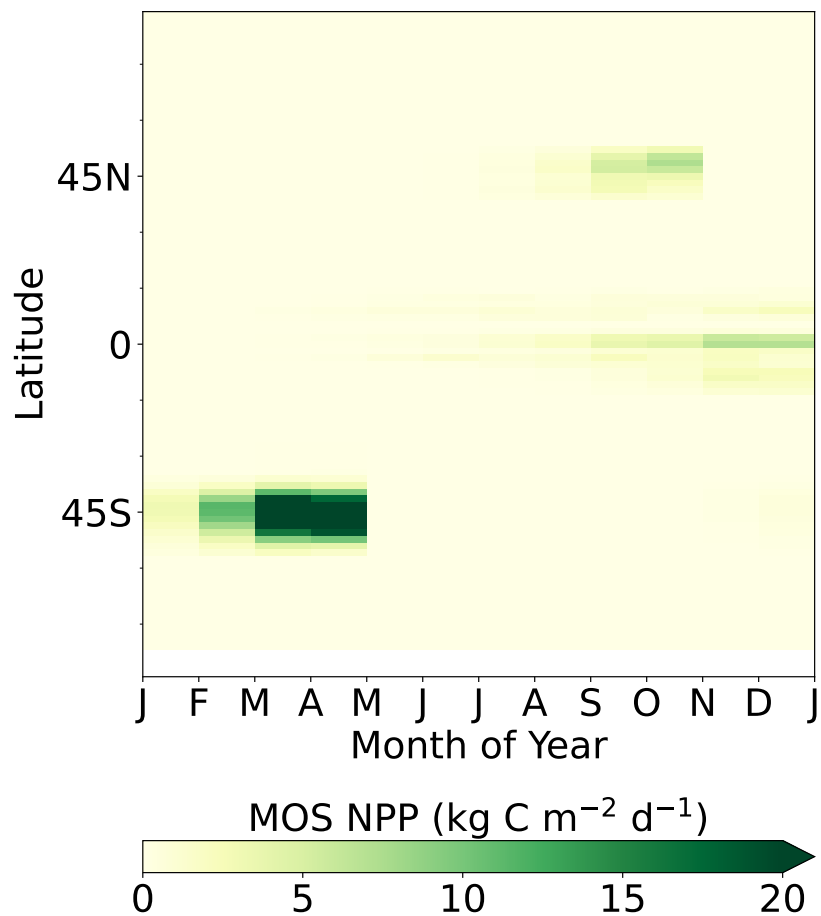


Figure A.2: Hovemoeller plot of latitudinally and vertically integrated MOS NPP. High NPP are found in the Southern Ocean. The change of MOS NPP follows the seasonal solar radiation in UVic ESCM.

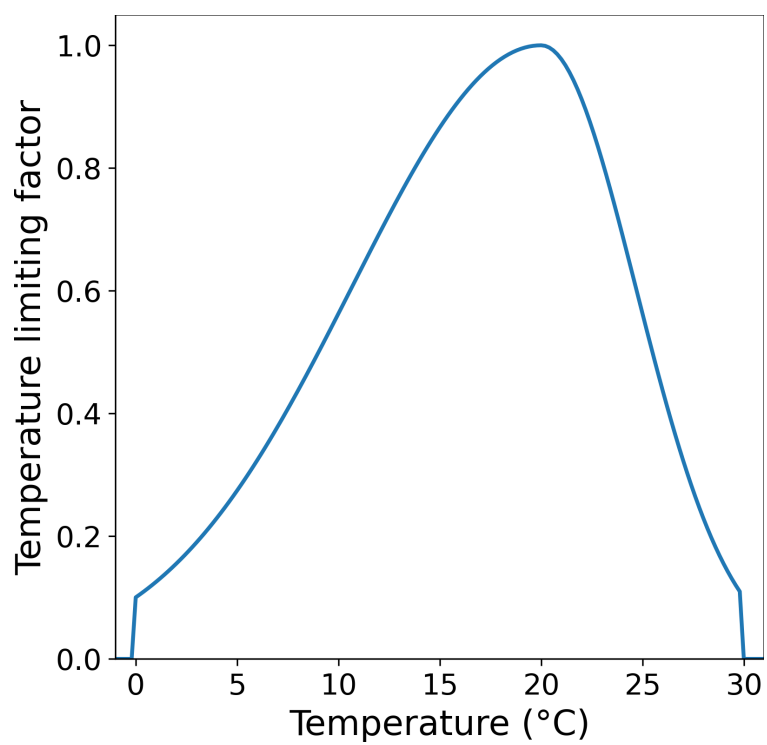


Figure A.3: Temperature optimum curve of the macroalgae in MOS.

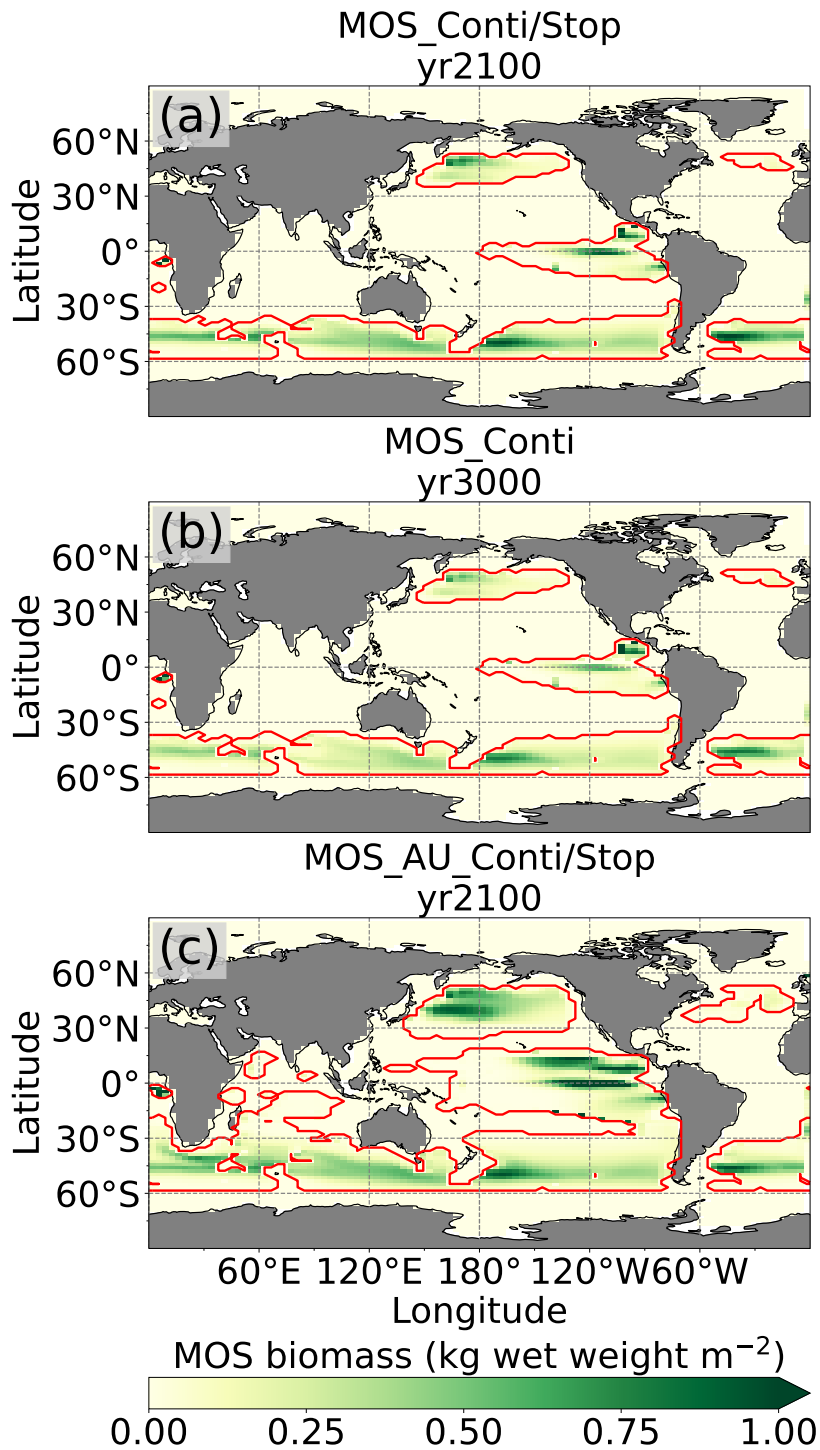


Figure A.4: MOS biomass distributions. Red lines contour the maximum MOS-occupied area during the previous years. The annual macroalgal biomass of MOS in this figure is an average over a 10 year period, which includes times of low and high biomass due to the sinking of biomass. Thus, the biomass shown here is less than the biomass shown in Fig. 2.2.

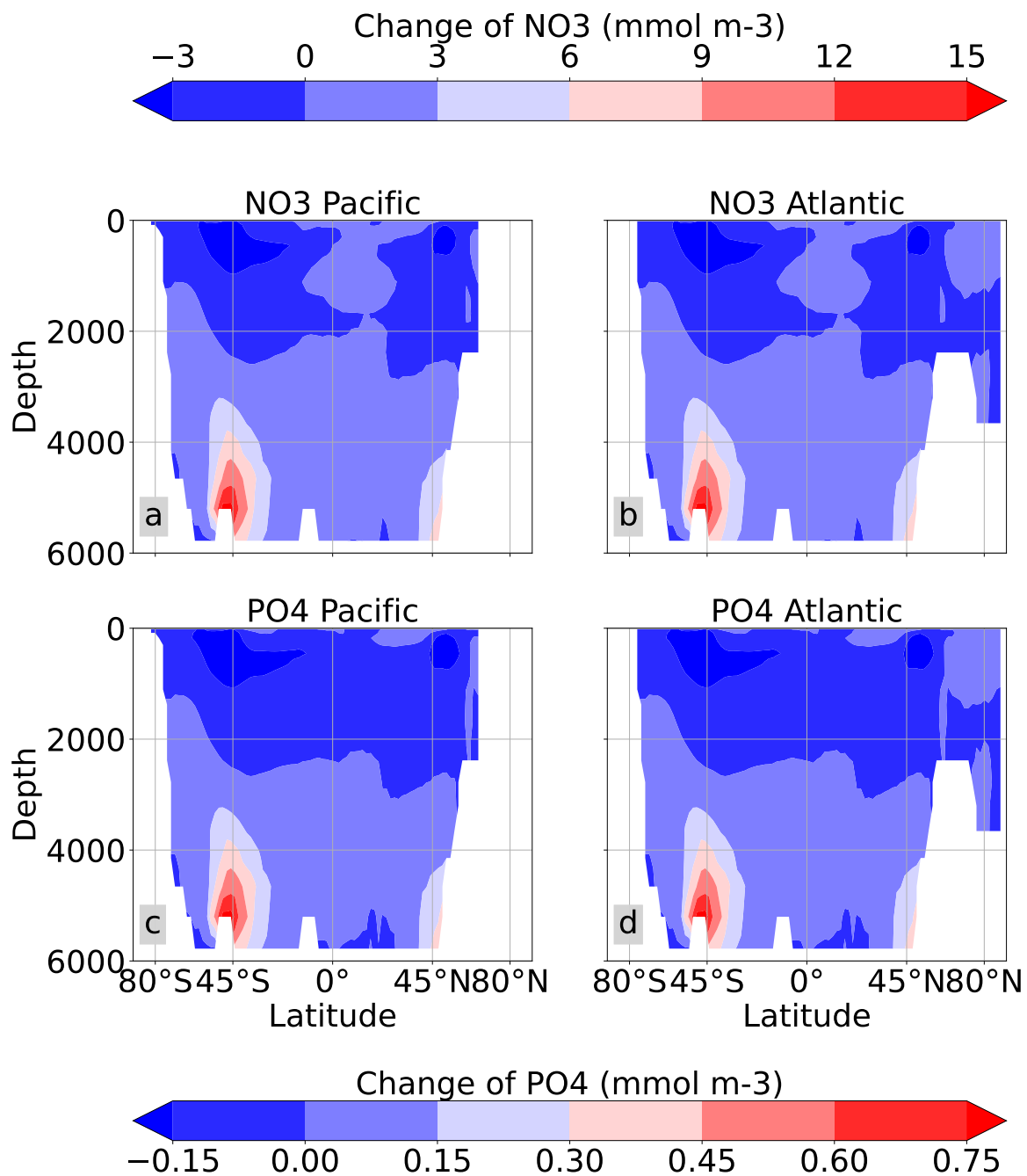


Figure A.5: Nutrients horizontal-distribution changes in the Pacific & Atlantic basins (MOS_Conti) relative to RCP 4.5 at year 2100. The nutrients trapping by MOS can be observed on the upper layers at, e.g., the Southern Ocean and mid-high latitudes in the Northern Hemisphere. The nutrients are enriched at the ocean bottom by the remineralization of MOS biomass, especially in the Southern Ocean deep waters.

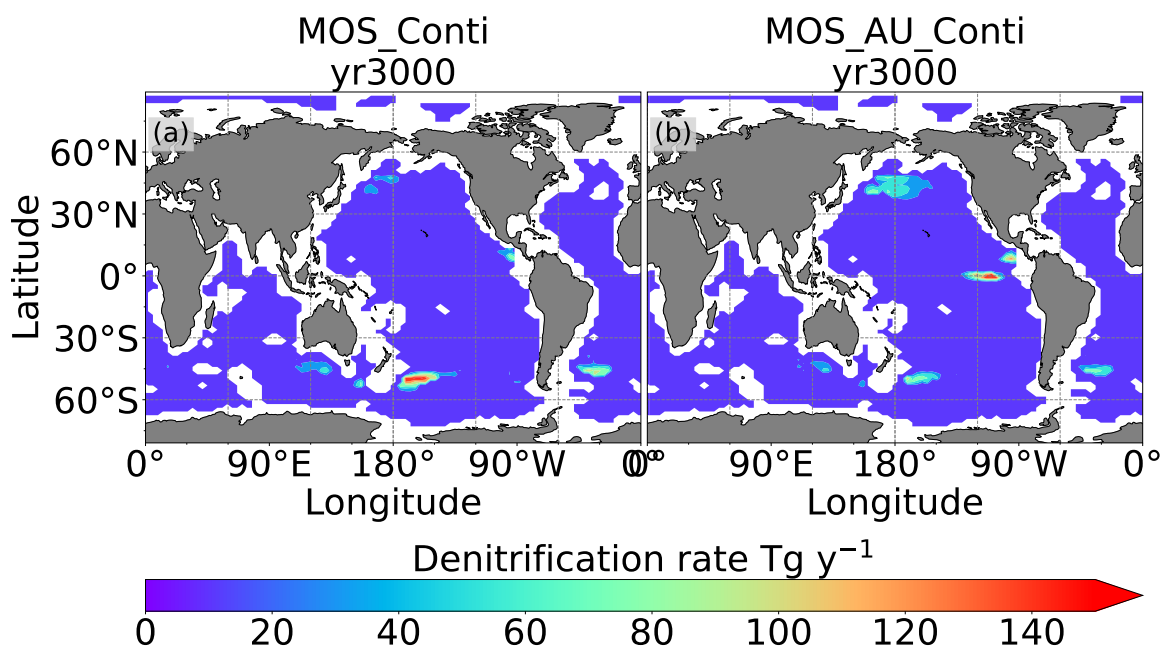


Figure A.6: Denitrification rate at depth 3000–6000 m in year 3000, where the oxygen level is lower than $5\ \mu\text{mol}\ m^{-3}$, caused by the remineralization of continuously sunken MOS biomass.

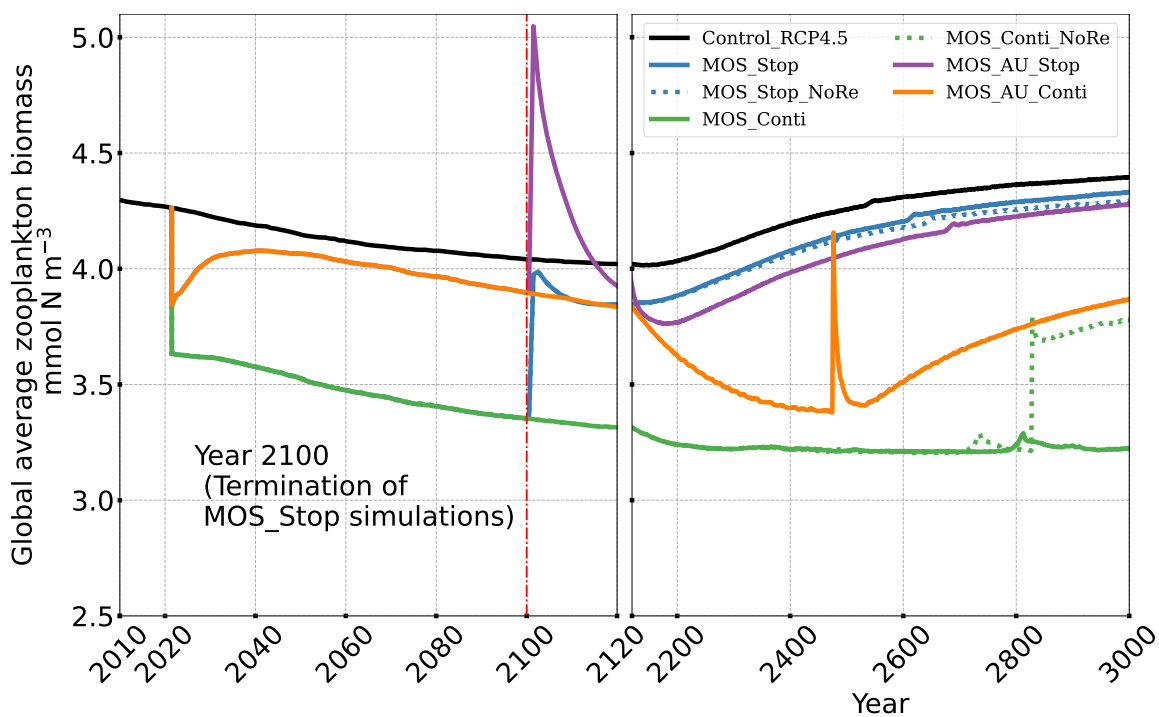


Figure A.7: Plot of global averaged biomass of zooplankton.

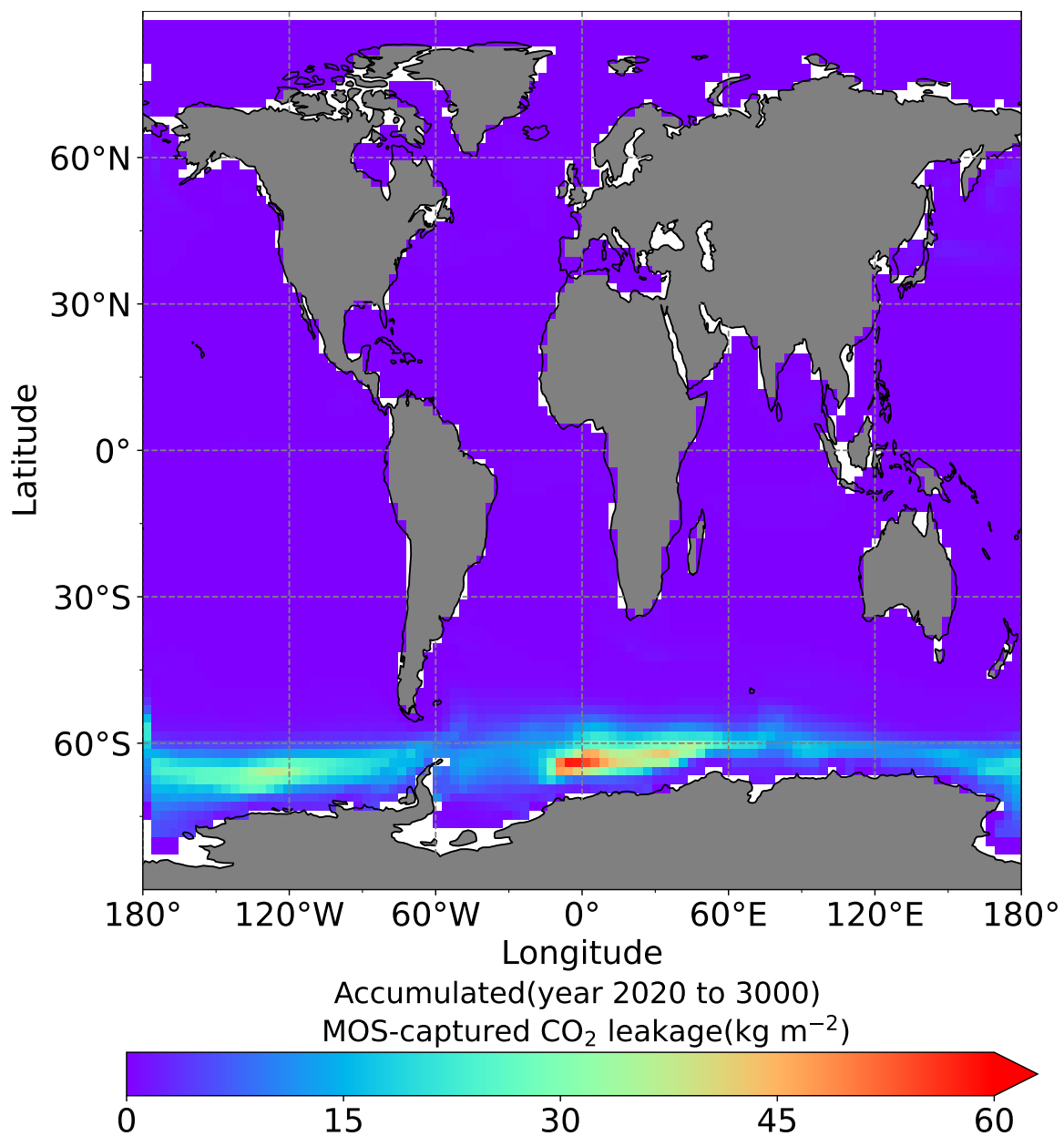


Figure A.8: Cumulative (year 2020 to 3000) leakage of MOS-captured carbon in the simulation MOS_Stop.

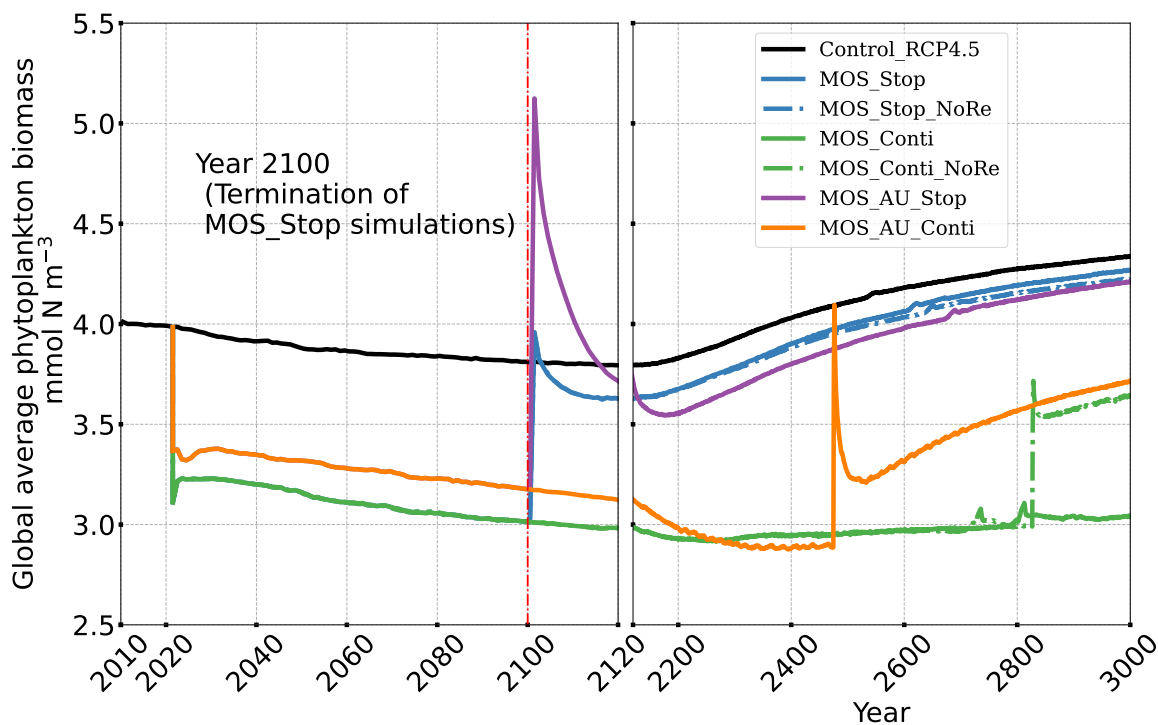


Figure A.9: Plot of global averaged phytoplankton biomass.

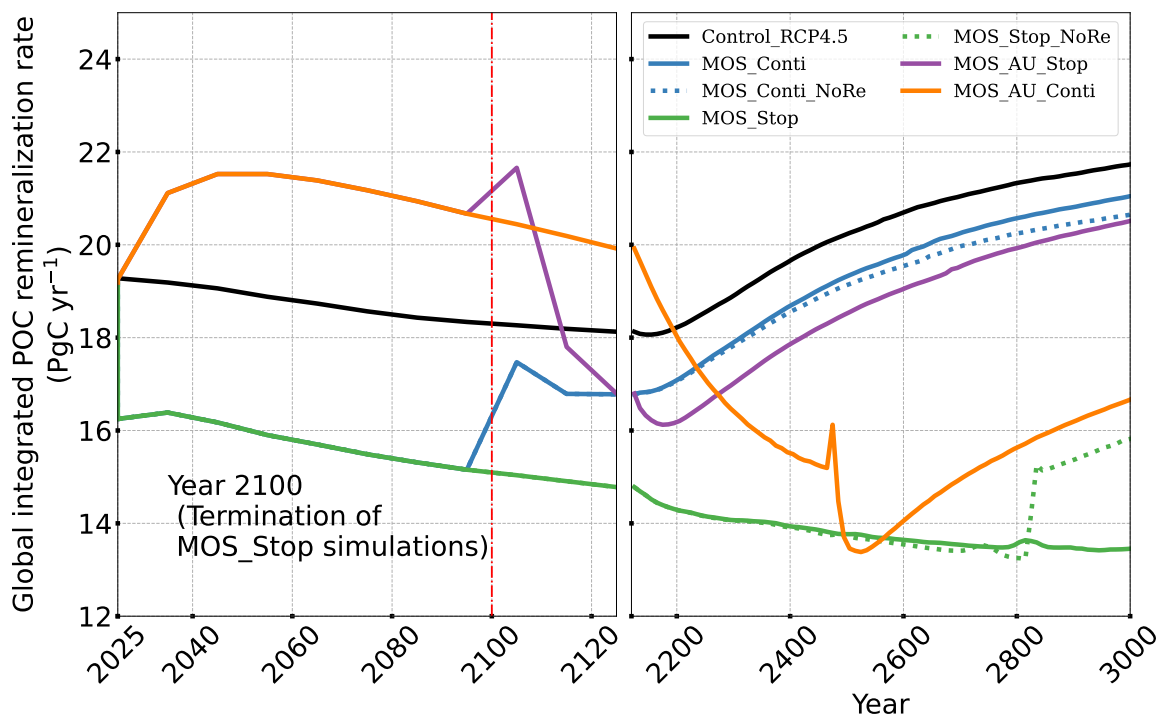


Figure A.10: Plot of upper-ocean 0–2000 m averaged detritus remineralization rate.

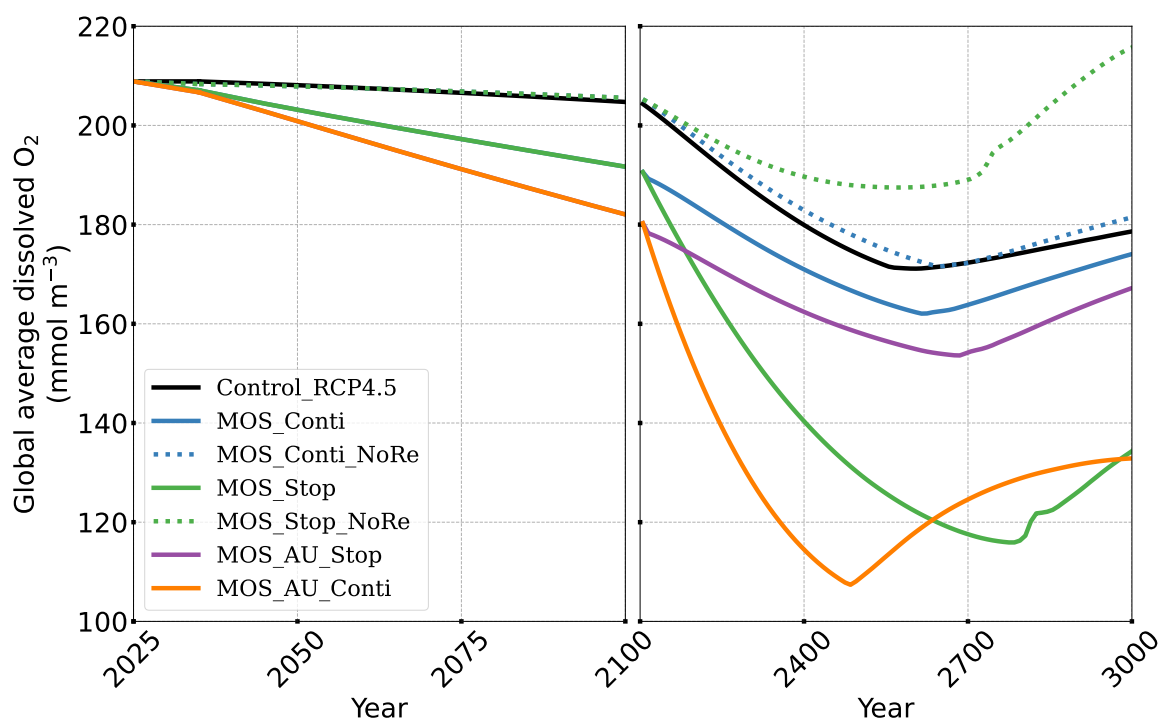


Figure A.11: Upper-ocean 3000–6000 m averaged dissolved-oxygen concentrations.

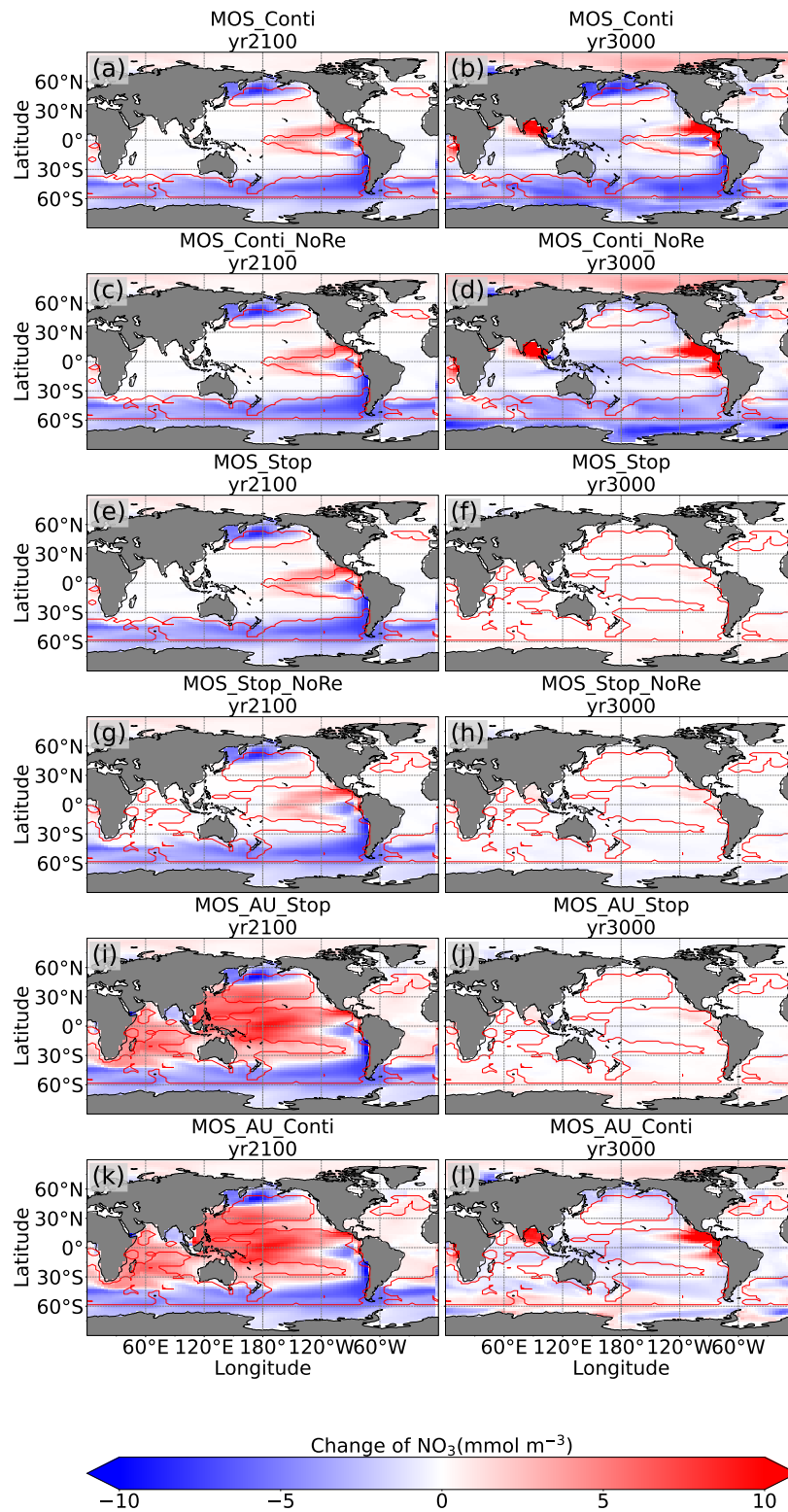


Figure A.12: Redistributions of NO_3 avg. 0–200 m depth relative to RCP 4.5.

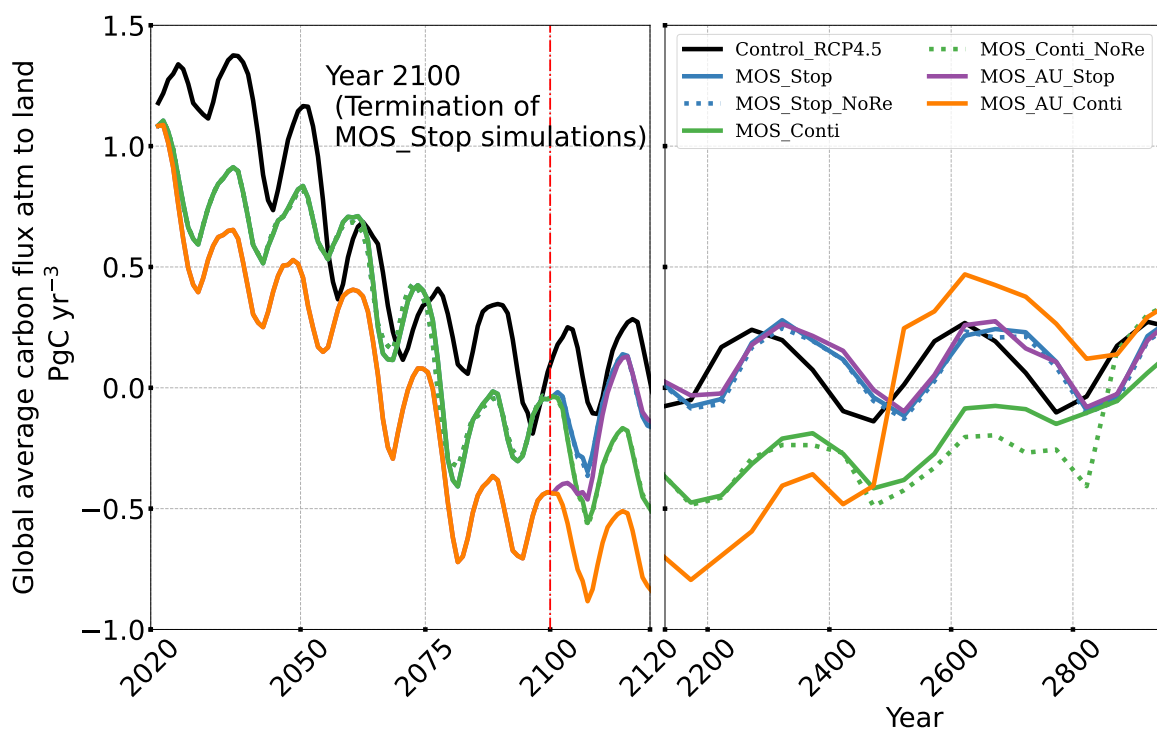


Figure A.13: Global averaged carbon flux from atmosphere to land.

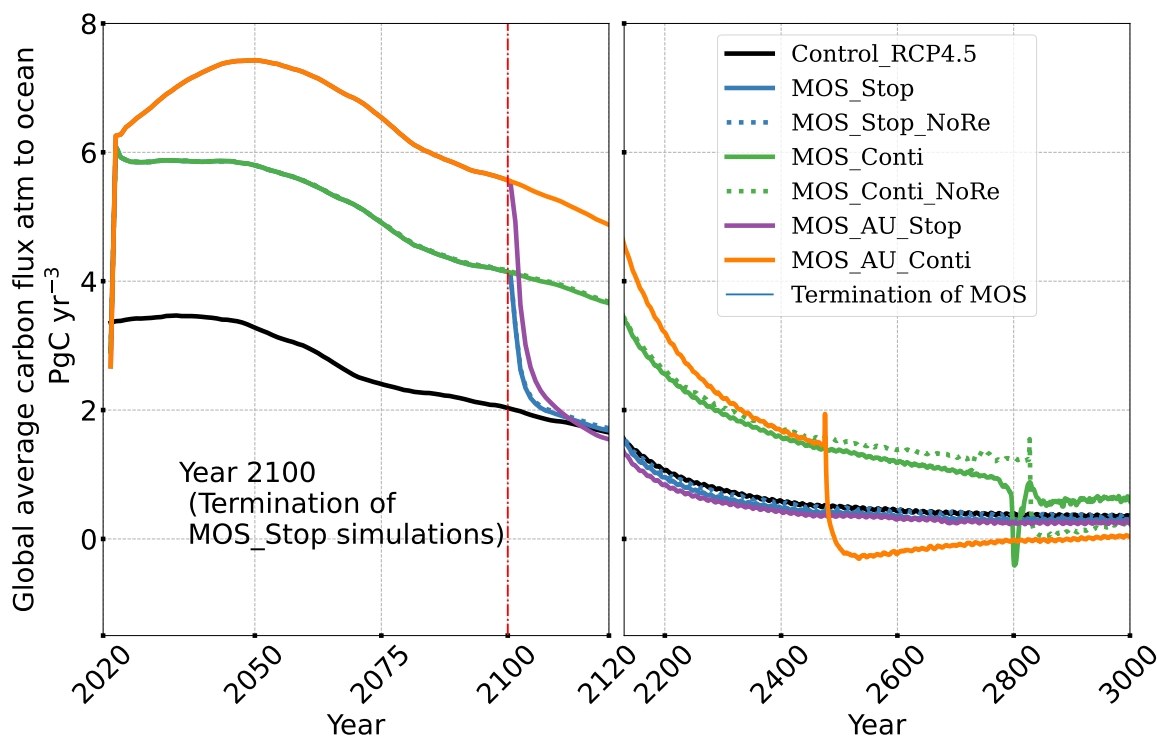


Figure A.14: Global averaged carbon flux from atmosphere to ocean.

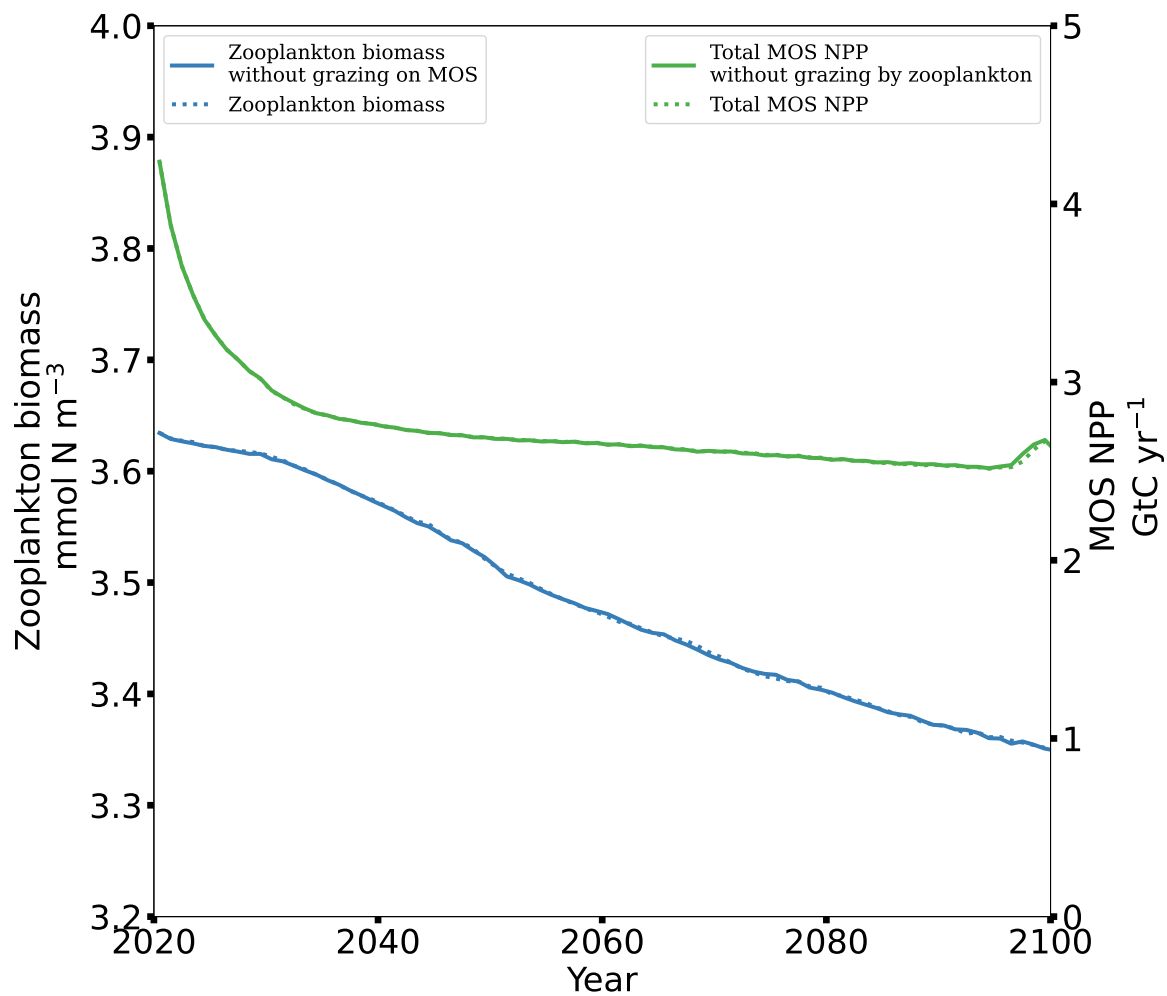


Figure A.15: Global profiles of zooplankton biomass (left y axis) and macroalgal NPP of MOS (right y axis) with and without zooplankton grazing on macroalgae. The “zooplankton” communities do not have large effects, via grazing, on macroalgae NPP or its own biomass.

B. Supporting Information for Chapter 3

Appendix

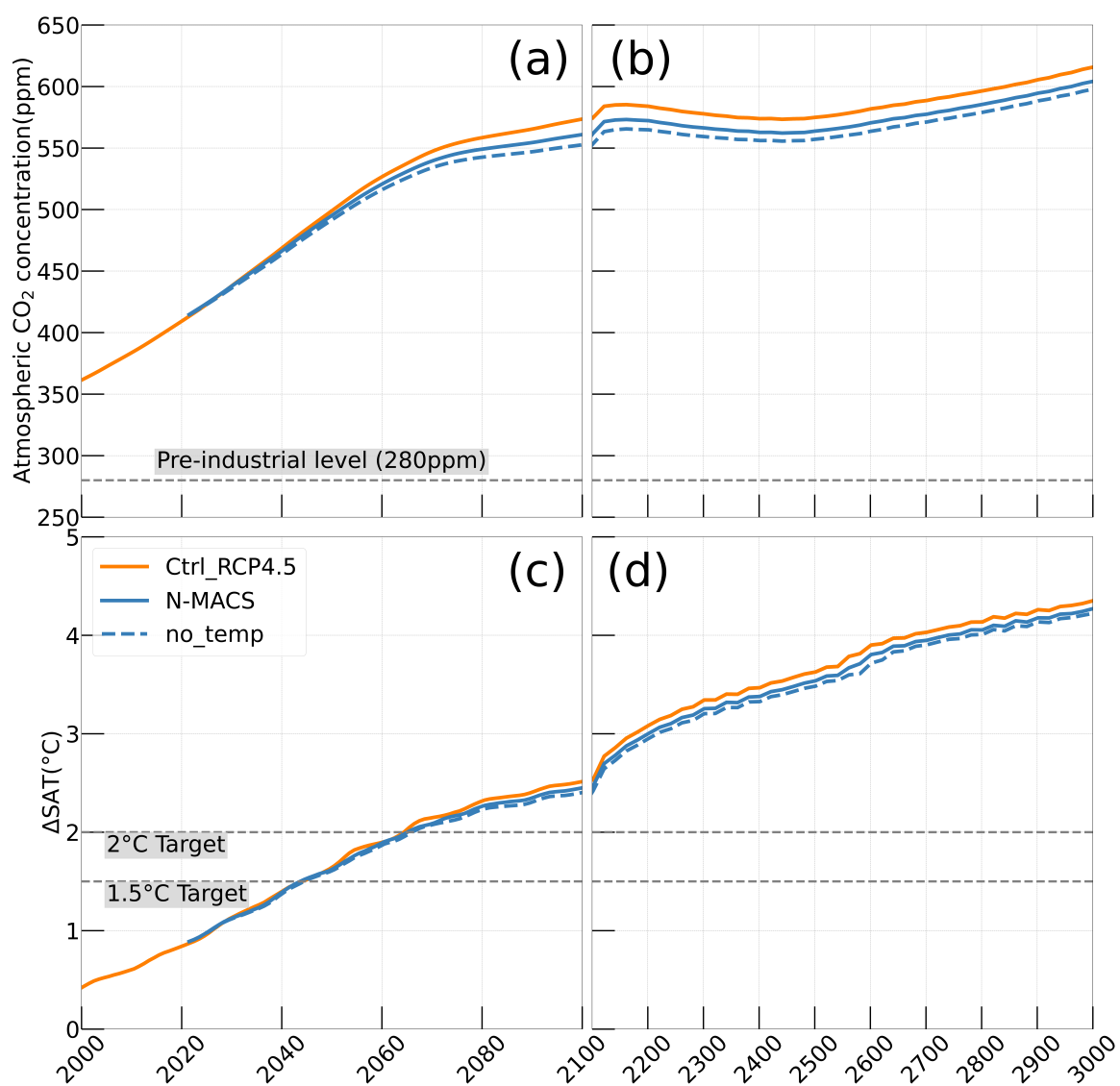


Figure A1: Global temporal evolution of atmospheric CO₂ concentration and surface averaged temperature (SAT)

Table A1: Macroalgae biomass annual productivity ($\text{t DW km}^{-2} \text{ yr}^{-1}$) in N-MACS regions.

	N-MACS	No_Temp
Mean of all N-MACS areas	97.02	155.10
Significant N-MACS areas	165.25	229.67
Northeast Asia	143.67	214.37
South America	413.46	610.10
Oceania	60.75	77.49
South Africa	196.54	205.14

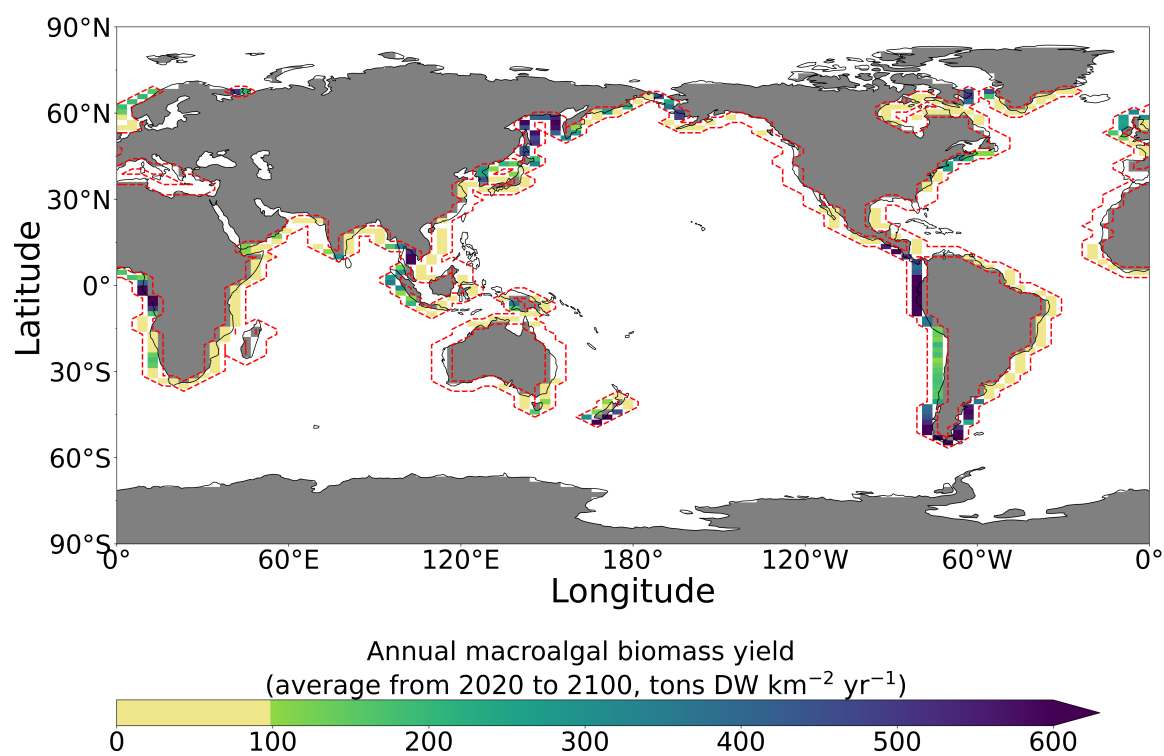


Figure A2: Annual macroalgae biomass yield (averaged from year 2020 to year 2100) of sensitivity simulation without temperature limiting factor. Dashed red lines outline the initial seeding locations in year 2020. Yellowish areas indicate relatively lower yield (≤ 100 tonnes DW per km^2 per year).

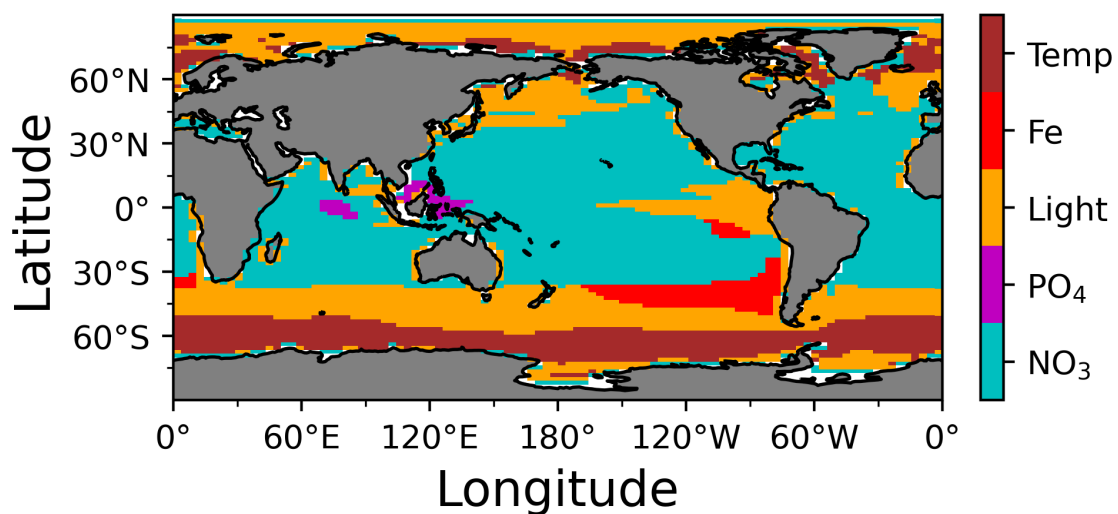


Figure A3: The most limiting growth factor for ordinary phytoplankton in N-MACS simulation from 2020 to 2100.

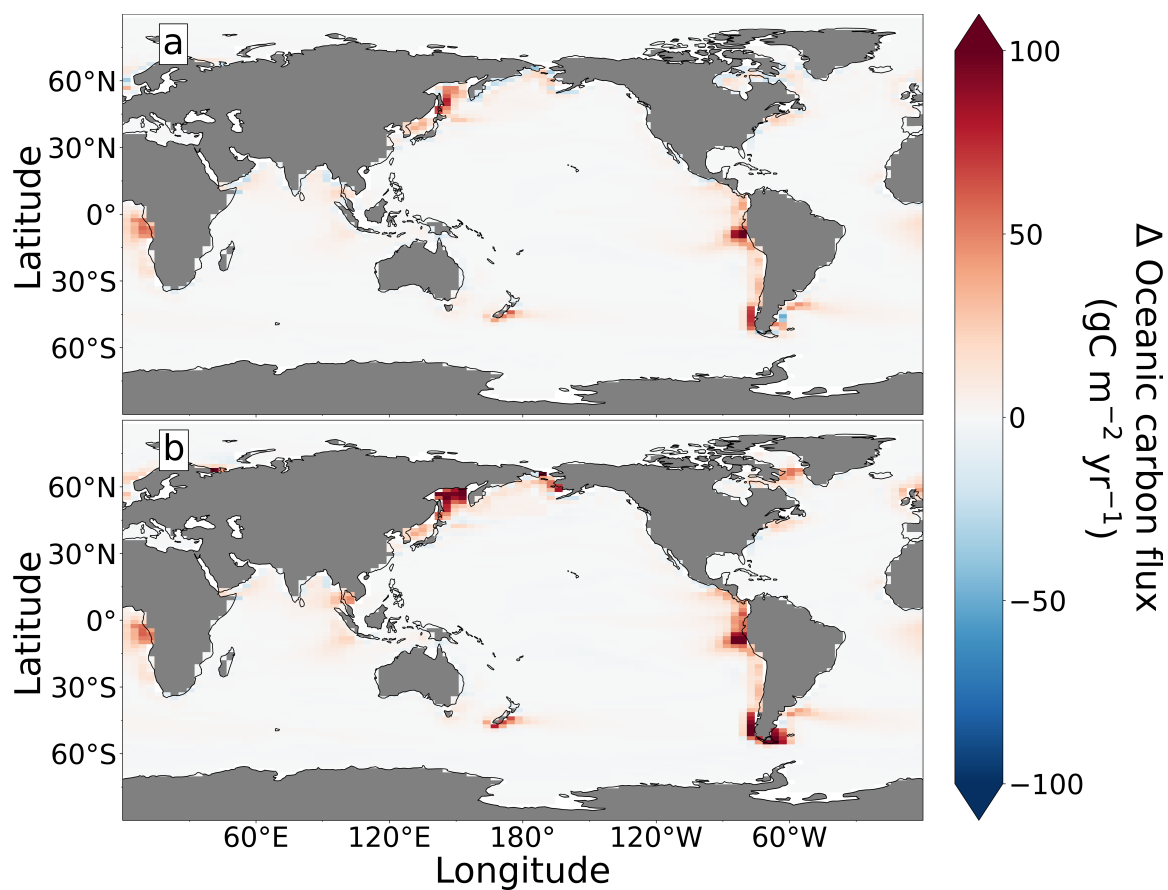


Figure A5: Yearly averaged variations in global oceanic carbon flux between 2020 and 2100, comparing (a) N-MACS and (b) No_Temp relative to RCP4.5 scenario. Positive values indicate net oceanic carbon uptake from the atmosphere.

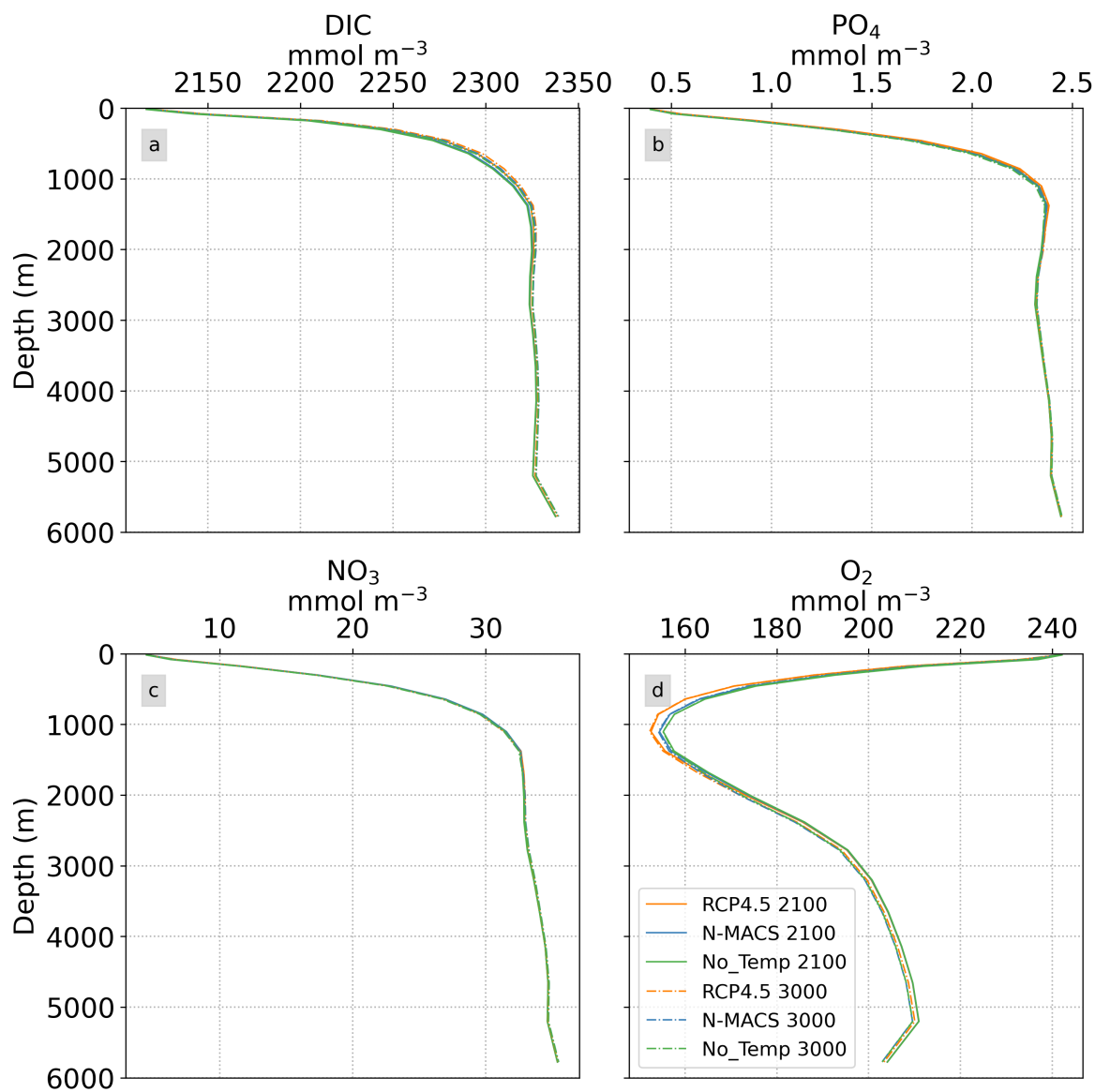


Figure A4: Globally averaged vertical profiles of dissolved inorganic carbon (DIC), dissolved phosphate (PO_4), dissolved nitrate (NO_3), and dissolved oxygen (O_2).

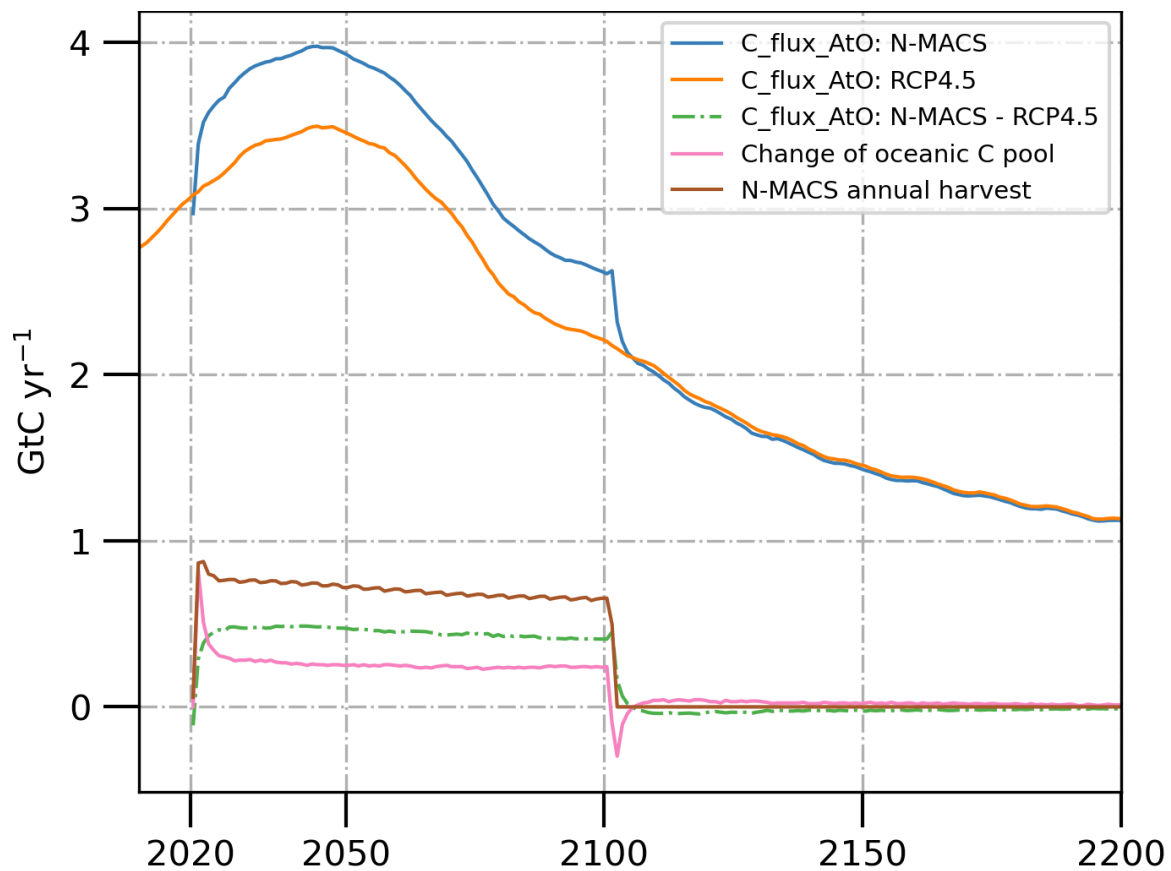


Figure A6: Global profile of air-sea carbon fluxes, N-MACS harvested biomass and oceanic carbon reservoir (GtC yr⁻¹).

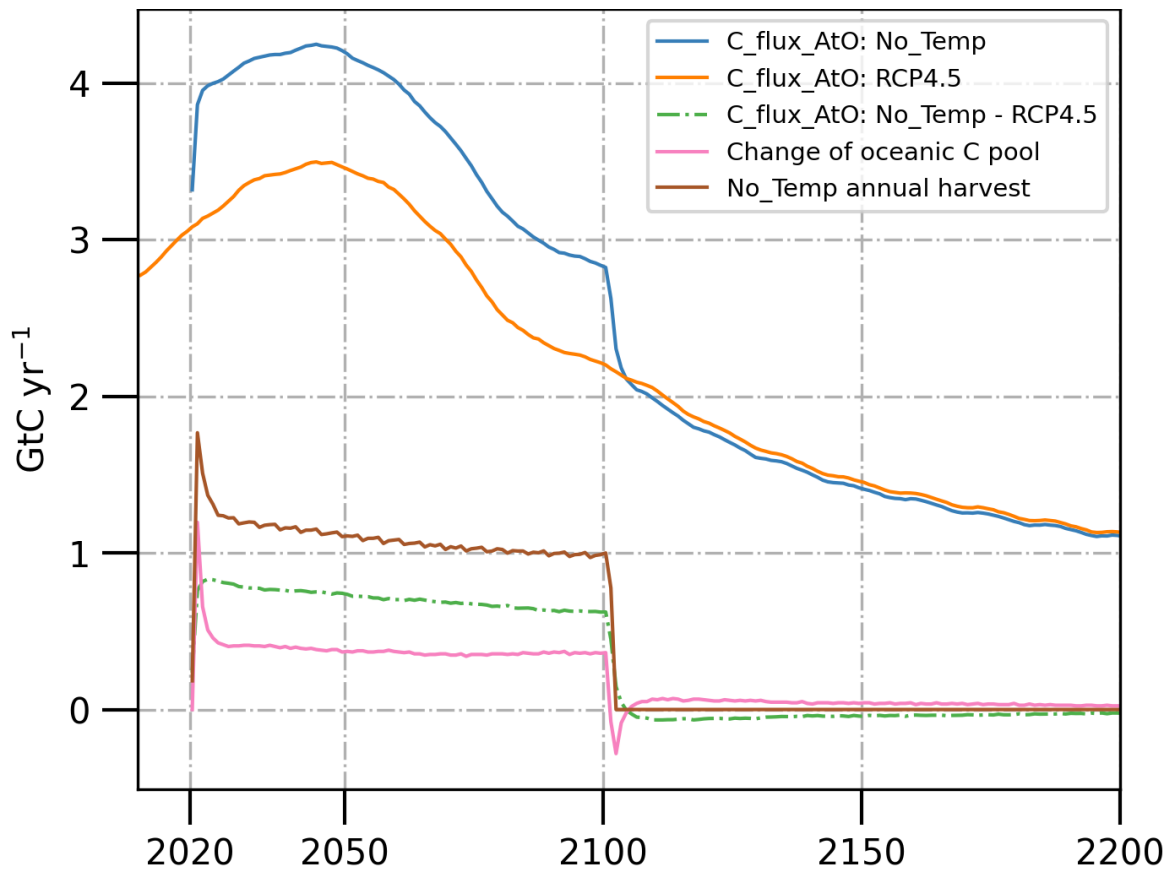


Figure A7: Global profile of air-sea carbon fluxes, No_Temp harvested biomass and oceanic carbon reservoir (GtC yr⁻¹).

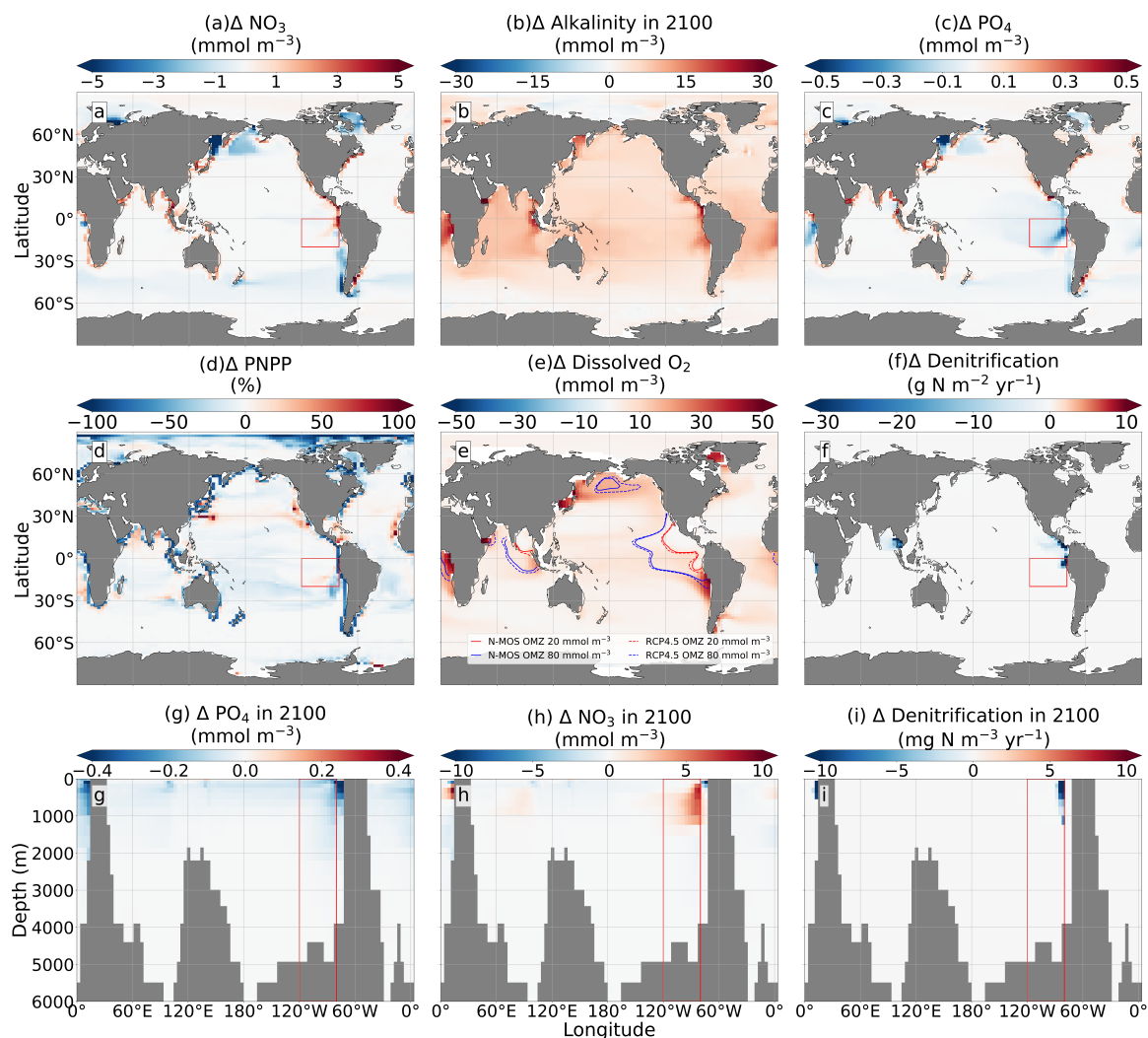


Figure A8: Changes relative to RCP4.5 caused by the deployment of No_Temp (data averaged from year 2020 to 2100, except for **d** which represents data in 2100): **a**: Nitrate distribution in the ocean's surface layer (top 50m); **b**: Alkalinity in the ocean's surface layer; **c**: Phosphate distribution in the surface layer; **d**: Phytoplankton net primary production (PNPP); **e**: Dissolved oxygen concentrations and oxygen minimum zones (OMZs) at a depth of 300m; **f**: Oceanic denitrification rates; Regions within red rectangles (between latitudes 20°S to 0° and longitudes 80°W to 120°W) indicate latitudinal averaged data relative to the Ctrl_RCP4.5: **g**: Phosphate concentrations, **h**: Nitrate concentrations, **i**: Annual denitrification rates.

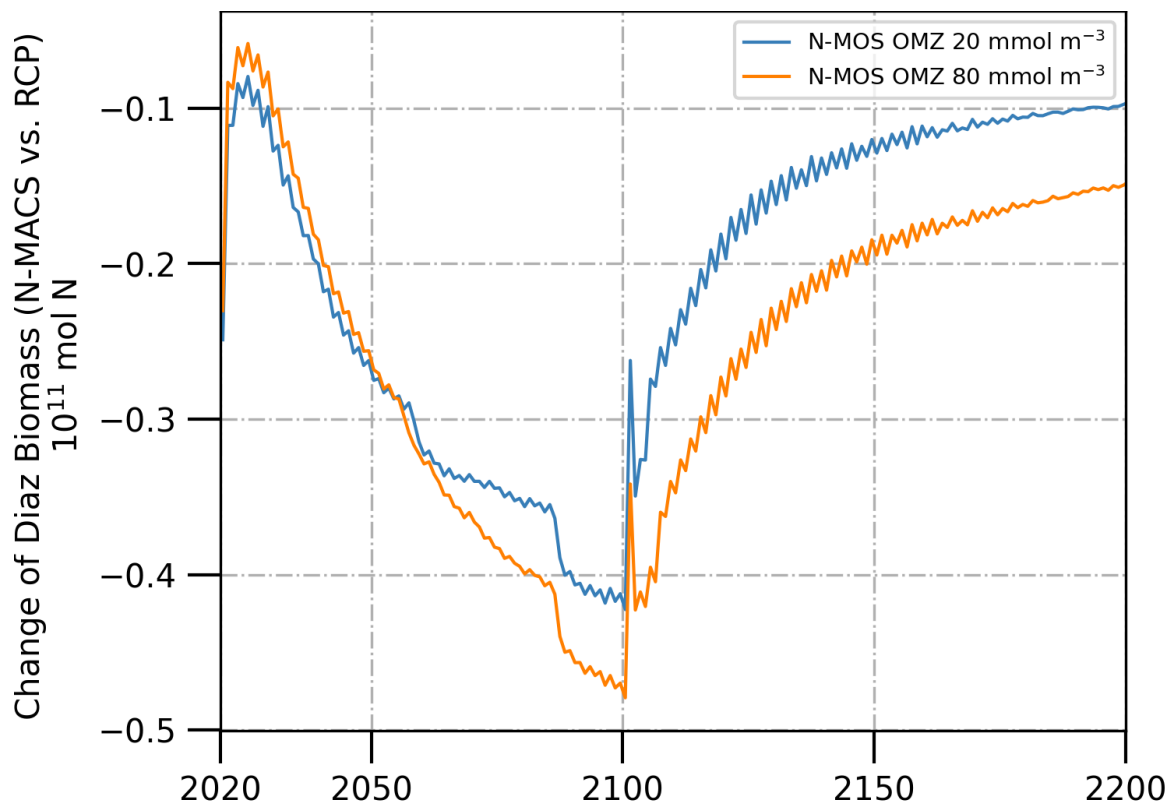


Figure A9: Globally integrated diazotroph biomass of N-MACS (bluish line) and No_Temp (greenish line) relative to RCP4.5.

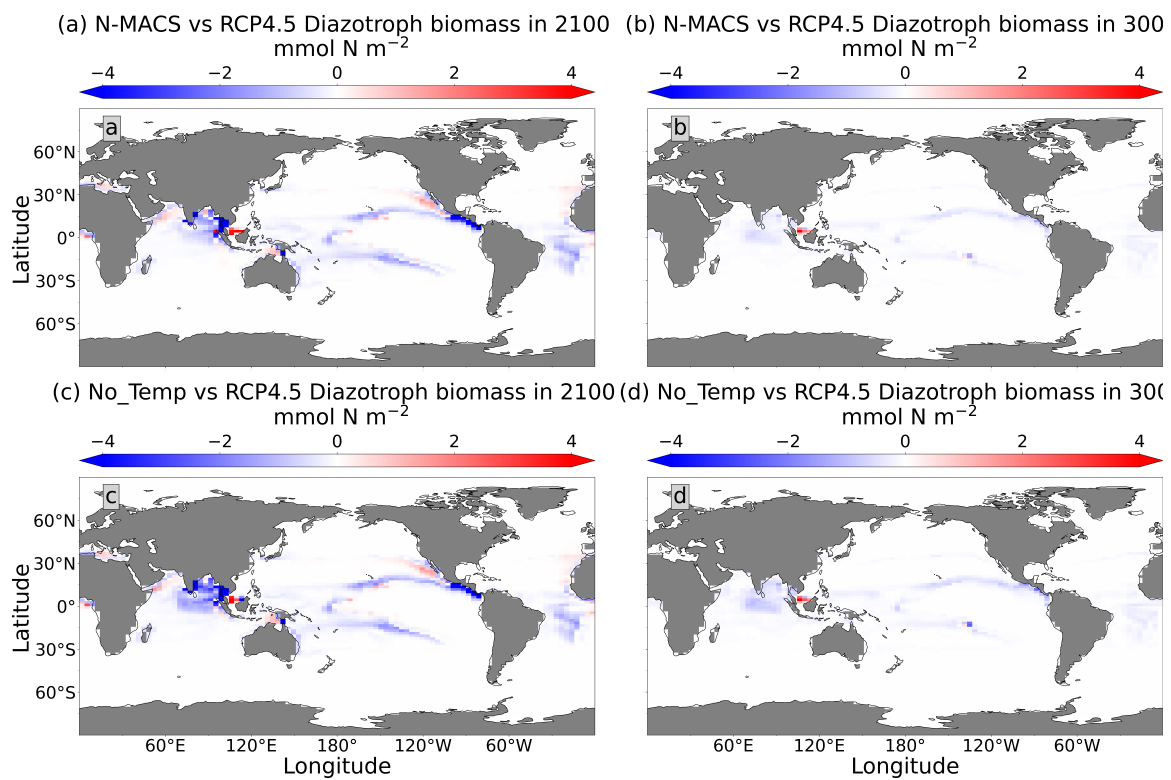


Figure A10: Variation in global vertically integrated diazotrophs biomass (mmol N m⁻²): N-MACS vs. RCP4.5 at year 2100 (a) and 2200 (b); No_Temp vs. RCP4.5 at year 2100 (c) and 2200 (d).

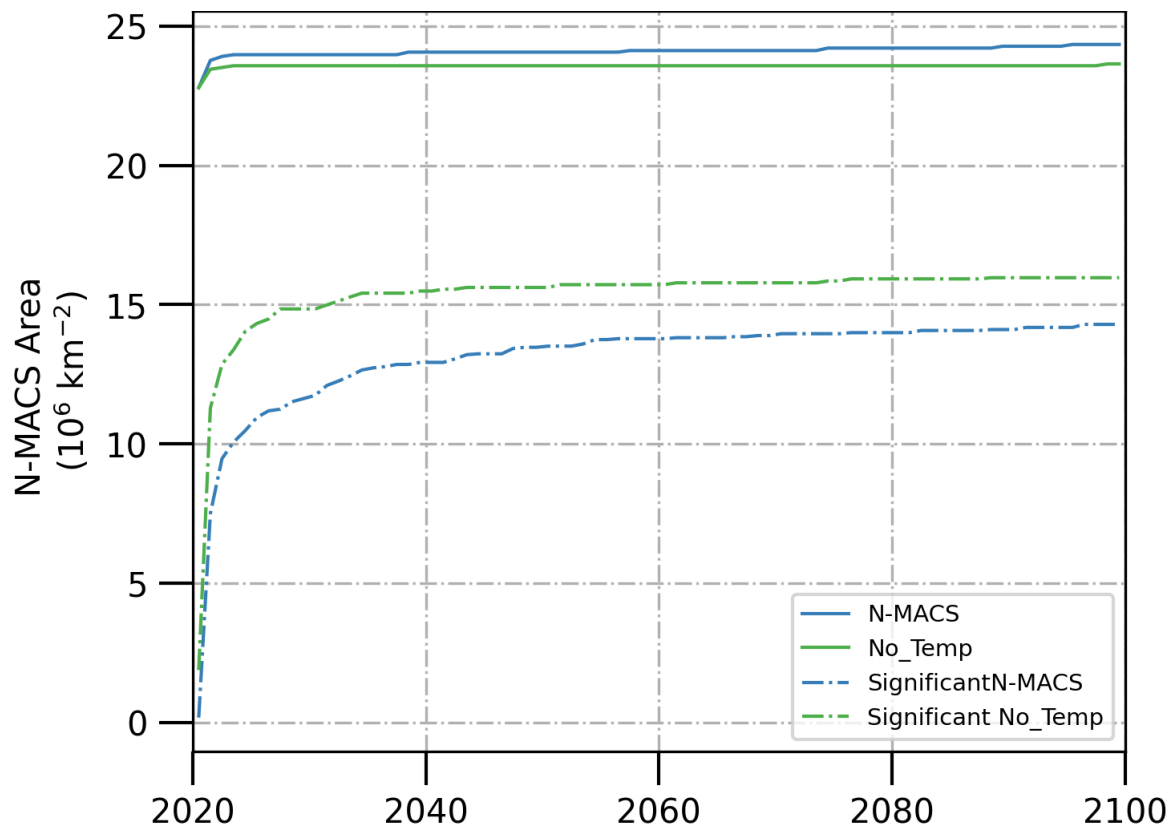


Figure A11: The globally assumed total occupied areas (solid lines) and significant production areas (dashed lines) areas of N-MACS (green tones) and No_Temp (blue tones) simulations.

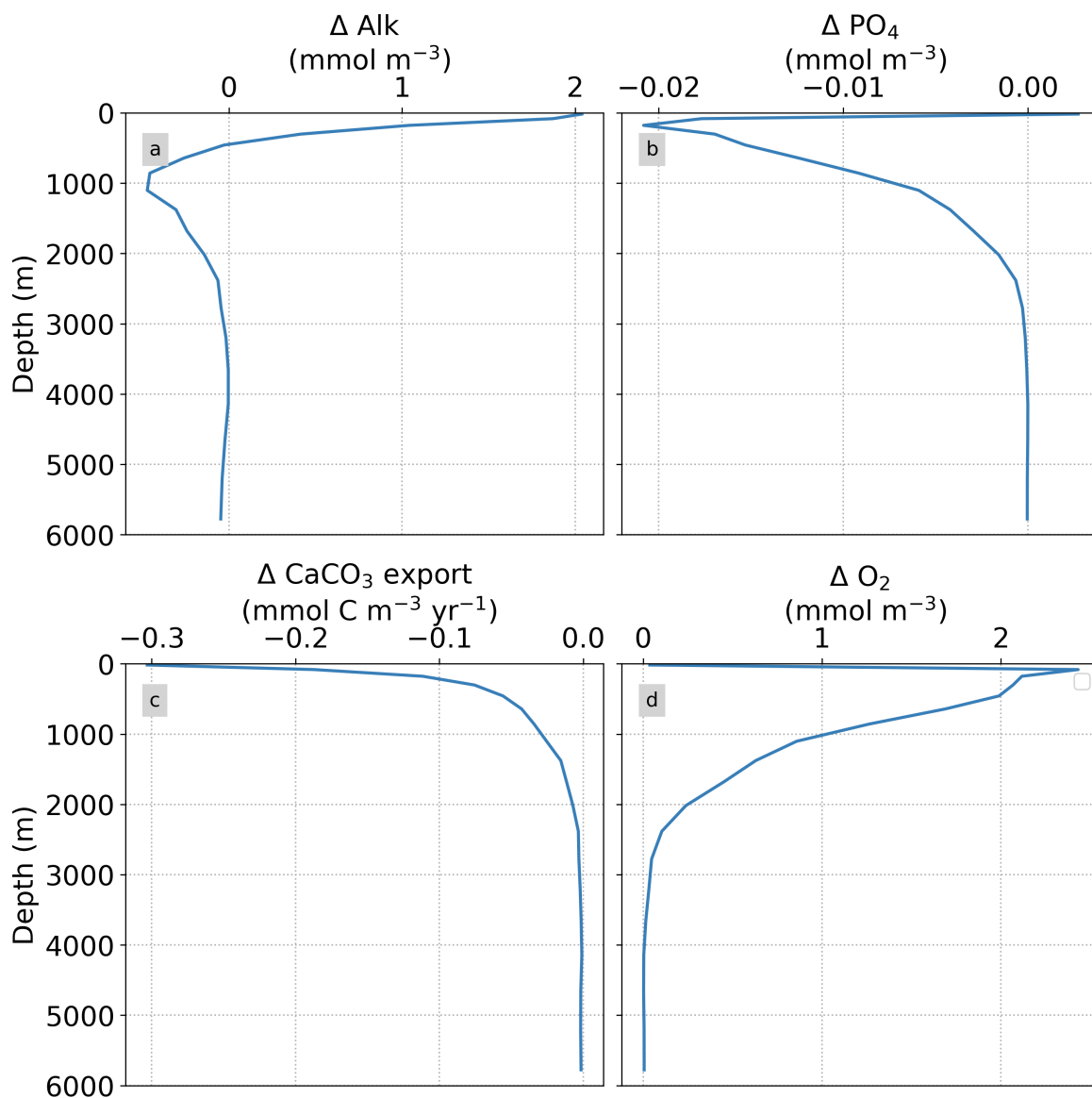


Figure A12: Vertical profiles comparing global horizontal averages of (a) alkalinity, (b) phosphate, (c) carbonate export, and (d) dissolved oxygen between N-MACS and RCP4.5 in 2100.

C. Supporting Information for Chapter 4

The Supplementary Material for this article can be found online at: <https://www.frontiersin.org/articles/10.3389/fclim.2022.810343/full#supplementary-material>

List of Figures

1.1	Simplified schematic of the global carbon cycle. Numbers represent reservoir mass in PgC (1 PgC = 10^{15} gC) and annual carbon exchange (in Pg yr ⁻¹). Black numbers and arrows indicate reservoir mass and exchange fluxes estimated for the time prior to the Industrial Era. Red arrows and numbers indicate annual anthropogenic fluxes averaged over the 2000–2009 time period. Reprinted from Figure 6.1 in Ciais et al. (2013)	8
1.2	An illustrative diagram showcasing the conceptual approaches of Ocean-based Carbon Dioxide Removal (CDR), or Ocean Negative Emission Technologies (Ocean NETs). The artwork is credited to Rita Erven, Ocean-NETs/GEOMAR	18
2.1	Schematic illustrating the biogeochemical fluxes and physical impacts of MOS on nutrients (NO ₃ and PO ₄), oxygen, dissolved inorganic carbon (DIC), ordinary phytoplankton (P _O in green), diazotrophs (P _D in pale brown) and zooplankton (Z).	57
2.2	Annual vertically integrated macroalgae biomass of MOS (a) and MOS-AU (b) in year 2024. Solid red lines outline the MOS-occupied area at year 2024 in both, while dashed red lines outline the initial MOS seeding area at year 2020 in (a). The simulated MOS area generally covers the NO ₃ -rich ocean surface (a) and can be expanded with nutrients supplemented by AU (b), making it larger than the estimated adequate area for macroalgae in previous studies Lehahn et al., 2016; Froehlich et al., 2019). Results for Areas I (blue circle), II (yellowish pentagon) and III (cyan rectangle) are discussed in the text and displayed in Fig. 2.3. Braces indicate the belts of N, M and S with various seeding strategies of macroalgae (Table 2.2), which are designed to avoid winter periods.	72

2.3	Vertically integrated macroalgae NPP simulated by experiment MOS (solid lines) for year 2024 and with representative Areas I (dark blue circle), II (yellow pentagon) and III (cyan rectangle) highlighted by rectangles with corresponding colors in Fig. 2.2. The NPP of macroalgae of experiment MOS_AU (dashed) shows an enhancement of NPP as expected.	73
2.4	Simulations of (a, b) annual global mean atmospheric CO ₂ concentration and (c, d) surface-averaged temperature relative to the pre-industrial (average of year 1850 to year 1900) level of 13.18 °C (Δ SAT). Under RCP 4.5 scenario, MOS reaches the 2 °C target in conjunction with AU, while the 1.5 °C cannot be met in all MOS simulations. Note that MOS is terminated whenever pre-industrial concentrations of atmospheric CO ₂ are reached, as seen for MOS_AU_Conti (solid orange) and MOS_Conti_NoRe (dotted blue) in (b, d) . Both atmospheric CO ₂ and Δ SAT remain lower than control after MOS termination.	78
2.5	Temporal evolution of globally integrated sunken macroalgal biomass on the seafloor. Biomass generally increases with fertilization by AU. In the idealized zero-remineralization simulations, all sunken macroalgal biomass remains on the seafloor, and globally integrated sunken macroalgal biomass shows a monotonous increase.	79
2.6	Global and basin-wide averaged vertical profiles of various model tracers in year 2100 and year 3000 under the RCP 4.5 emission scenario. In general, MOS (except for the zero-remineralization one) transports DIC and nutrients in the surface layer to the deep ocean. The oxygen levels are increased in the mid layers due to the declined downward organic-particle flux (Sect. 2.4.3), but they are decreased in the deep ocean as a result of the remineralization of sunken biomass. These impacts are strengthened when MOS is deployed continuously and/or in conjunction with AU.	80
2.7	Vertically integrated annual PNPP in year 2100. (a, b) MOS minus Control_RCP 4.5, with red boundaries contouring the MOS-occupied area; (c) Control_RCP 4.5; (a) illustrates a decline in PNPP in MOS-occupied areas accompanied by a “halo” of enhanced PNPP surrounding MOS areas, particularly in the ETP caused by the leakage of residual nutrients (Sect. 2.4.3). These impacts on PNPP are amplified in MOS_AU (b)	82

- 2.8 Proportion of MOS NPP in the global oceanic NPP by year 2100 ($\text{MOS_NPP}/(\text{MOS_NPP} + \text{PNPP}) \times 100$). Note that the NPP values are converted to carbon using the respective C:N ratio. The MOS_NPP generally amounts to more than 70 % of total oceanic NPP where MOS is deployed, indicating an obvious NPP shift from phytoplankton PNPP to MOS_NPP. 84
- 2.9 Temporal evolution of globally integrated PNPP (**a1, a2**); downward POC flux at 2 km depth (**b1, b2**). The termination runs branch off of the continuous ones in year 2100 and are identical up to that point. Through the 21st century, MOS reduces PNPP and POC export due to canopy shading and competition for nutrients. Obvious rebounds followed by quick decline can be observed right after terminations of MOS. 85
- 2.10 Dissolved O_2 concentration distribution in year 2100 at 300 m depth (**a, c, e**) and at the seafloor (**b, d, f**); lines delineate boundaries of OMZs at any location within the water column with less than 80 mmol m^{-3} oxygen (dashed white) and less than 20 mmol m^{-3} oxygen (solid red). At 300 m depth, elevated dissolved-oxygen levels in MOS simulations are caused by the decline in POC export (**c**); exceptions are the reduced oxygen concentrations in regions outside the MOS_AU deployment (**e**). On the seafloor, remineralization of sunken biomass creates several new low-oxygen areas (**d, f**). 87
- 2.11 Dissolved O_2 concentrations at depth ~ 300 m (left panel) and the ocean bottom (right panel) in year 3000: contour lines indicate boundaries of OMZs with less than 80 mmol m^{-3} oxygen (dashed white) and less than 20 mmol m^{-3} oxygen (solid red). Continuous MOS deployment further shrinks the OMZ at 300 m depth (**e, g, i**) but expands them at the bottom (**f, j**), except for the zero-remineralization one in (**h**). 89
- 2.12 Zonally averaged MOS-captured carbon outgassing in the simulation (**a**) MOS_Conti and (**b**) MOS_Stop. When conveyed back to the surface, the DIC from MOS remineralization participates in the air-sea exchange (Sect. 2.2.2). MOS-C outgassing starts in year 2100 when MOS is terminated (**a**) or after year 2300 when MOS is continuously deployed. The outgassing mainly happens in the Southern Ocean. The outgassing is strengthened around year 2800 when a Southern Ocean deep-convection event accelerates the upwelling of deep waters with high concentrations of remineralized DIC (Sect. 2.4.4). 92

- 3.1 Annual macroalgae biomass yield (averaged from year 2020 to year 2100). Dashed red lines outline the initial seeding locations in year 2020. Regions with high macroalgae productivity include: Coasts of North Western Pacific (near northern China, Japan and Korean Peninsula), South Eastern Pacific (coasts of South America), South Eastern Atlantic (mid-south Africa coast), coast of New Zealand, and South Eastern of Australia. Yellowish areas indicate relatively lower yield (≤ 100 tonnes DW per km² per year). 118
- 3.2 Differences in simulated oceanic properties in year 2100 after continuous N-MACS deployment from 2020 to 2100, with respect to Ctrl_RCP4.5 without N-MACS deployment (data averaged over this period, except for **d** and **e** representing data in 2100): **a**: Surface-layer nitrate (top 50m); **b**: Surface-layer alkalinity; **c**: Surface-layer phosphate; **d**: Phytoplankton net primary production (PNPP); **e**: Dissolved oxygen concentrations and oxygen minimum zones (OMZs) at a depth of 300m; **f**: Oceanic denitrification rates. Subfigures **g**, **h** & **i** represent latitudinally averaged data from 20°S to 0°, relative to the Ctrl_RCP4.5 scenario depicted in subfigures **a**, **c**, & **f** (highlighted by red rectangular regions between latitudes 20°S to 0° and longitudes 80°W to 120°W): **g**: Phosphate concentrations, **h**: Nitrate concentrations, **i**: Annual denitrification rates. 123
- 3.3 Temporal evolution of globally integrated nutrients, Phytoplankton Net Primary Production (PNPP), and Particulate Organic Carbon (POC) Export at 2,000m depth: Comparison of N-MACS (solid blue), No_Temp (dashed blue), and Ctrl_RCP4.5 Baseline Simulation (orange). Insets in each panel extend the timeline to the year 3000. **a** & **c**: Permanent removal of PO₄ from the surface, **b** & **d**: Surface NO₃ levels and global NO₃ trends (increase in N-MACS, decrease in No_Temp). **e**: Surface PNPP (see also Fig.3.2d). **f**: The export of POC at 2,000m depth. **g**: The averaged O₂ concentration at 300m depth. **h**: Globally integrated Nitrogen fixation. 124

4.1	Overview of the selected CDR options. Circled numbers correspond to the numbering of CDR concepts in the paper and represent following options: 1 - BECC: biomass combustion CHP; 2 - BECC: biogas CHP; 3 - BECC: paludiculture for biogas CHP; 4 - BECC: macroalgae for biogas CHP; 5 - BECC: pyrolysis for biocoal production; 6 - BECC: gasification for biofuels production; 7 - DACC: centralized; 8 - DACC: decentralized; 9 - NSE: peatland rewetting; 10 - NSE: afforestation of cropland; 11 - NSE: SOC, cover crops; 12 - NSE: SOC, ERW; 13 - NSE: seagrass meadows Baltic Sea; 14 - geological storage solutions.	147
4.2	Overview of CO ₂ removal potential of selected options. A: Scalability of options expressed as a number of units available for deployment by 2050 and CO ₂ removal potential. B: Amount of CO ₂ removed per unit of energy generated by BECC technologies. C: Amount of CO ₂ removed per unit of energy used by DACC technologies. D: Amount of CO ₂ removed per hectare by NSE options.	162
4.3	CDR potential of analyzed concepts in comparison with estimates of current CO ₂ emissions in Germany (UBA 2021), projected residual emissions for 2050 (Mengis and Kalhori et al., 2022) and CDR potential in Germany (Ariadne Report, 2021). BECC: based on all analyzed BECC concepts, likely requiring imports of woody biomass. DACC: based on decentralized DACC concept, excluding centralized DACC due to energy constraints. NSE: based on all analyzed NSE concepts. The indicated potentials for BECC and DACC do not include possible constraints by the feasibility of geological CO ₂ storage.	172
A.1	Sketch of key features of MOS.	196
A.2	Hovemoeller plot of latitudinally and vertically integrated MOS NPP. High NPP are found in the Southern Ocean. The change of MOS NPP follows the seasonal solar radiation in UVic ESCM.	197
A.3	Temperature optimum curve of the macroalgae in MOS.	198
A.4	MOS biomass distributions. Red lines contour the maximum MOS-occupied area during the previous years. The annual macroalgal biomass of MOS in this figure is an average over a 10 year period, which includes times of low and high biomass due to the sinking of biomass. Thus, the biomass shown here is less than the biomass shown in Fig. 2.2.	199

A.5	Nutrients horizontal-distribution changes in the Pacific & Atlantic basins (MOS_Conti) relative to RCP 4.5 at year 2100. The nutrients trapping by MOS can be observed on the upper layers at, e.g., the Southern Ocean and mid–high latitudes in the Northern Hemisphere. The nutrients are enriched at the ocean bottom by the remineralization of MOS biomass, especially in the Southern Ocean deep waters.	200
A.6	Denitrification rate at depth 3000–6000 m in year 3000, where the oxygen level is lower than $5 \mu\text{mol m}^{-3}$, caused by the remineralization of continuously sunken MOS biomass.	201
A.7	Plot of global averaged biomass of zooplankton.	201
A.8	Cumulative (year 2020 to 3000) leakage of MOS-captured carbon in the simulation MOS_Stop.	202
A.9	Plot of global averaged phytoplankton biomass.	203
A.10	Plot of upper-ocean 0–2000 m averaged detritus remineralization rate.	203
A.11	Upper-ocean 3000–6000 m averaged dissolved-oxygen concentrations.	204
A.12	Redistributions of NO_3 avg. 0–200 m depth relative to RCP 4.5.	205
A.13	Global averaged carbon flux from atmosphere to land.	206
A.14	Global averaged carbon flux from atmosphere to ocean.	206
A.15	Global profiles of zooplankton biomass (left y axis) and macroalgal NPP of MOS (right y axis) with and without zooplankton grazing on macroalgae. The “zooplankton” communities do not have large effects, via grazing, on macroalgae NPP or its own biomass.	207
A1	Global temporal evolution of atmospheric CO_2 concentration and surface averaged temperature (SAT)	210
A2	Annual macroalgae biomass yield (averaged from year 2020 to year 2100) of sensitivity simulation without temperature limiting factor. Dashed red lines outline the initial seeding locations in year 2020. Yellowish areas indicate relatively lower yield (≤ 100 tonnes DW per km^2 per year).	211
A3	The most limiting growth factor for ordinary phytoplankton in N-MACS simulation from 2020 to 2100.	212
A5	Yearly averaged variations in global oceanic carbon flux between 2020 and 2100, comparing (a) N-MACS and (b) No_Temp relative to RCP4.5 scenario. Positive values indicate net oceanic carbon uptake from the atmosphere.	212

A4	Globally averaged vertical profiles of dissolved inorganic carbon (DIC), dissolved phosphate (PO ₄), dissolved nitrate (NO ₃), and dissolved oxygen (O ₂).	213
A6	Global profile of air-sea carbon fluxes, N-MACS harvested biomass and oceanic carbon reservoir (GtC yr ⁻¹).	214
A7	Global profile of air-sea carbon fluxes, No_Temp harvested biomass and oceanic carbon reservoir (GtC yr ⁻¹).	215
A8	Changes relative to RCP4.5 caused by the deployment of No_Temp (data averaged from year 2020 to 2100, except for d which represents data in 2100): a : Nitrate distribution in the ocean's surface layer (top 50m); b : Alkalinity in the ocean's surface layer; c : Phosphate distribution in the surface layer; d : Phytoplankton net primary production (PNPP); e : Dissolved oxygen concentrations and oxygen minimum zones (OMZs) at a depth of 300m; f : Oceanic denitrification rates; Regions within red rectangles (between latitudes 20°S to 0° and longitudes 80°W to 120°W) indicate latitudinal averaged data relative to the Ctrl_RCP4.5; g : Phosphate concentrations, h : Nitrate concentrations, i : Annual denitrification rates.	216
A9	Globally integrated diazotroph biomass of N-MACS (bluish line) and No_Temp (greenish line) relative to RCP4.5.	217
A10	Variation in global vertically integrated diazotrophs biomass (mmol N m ⁻²): N-MACS vs. RCP4.5 at year 2100 (a) and 2200 (b); No_Temp vs. RCP4.5 at year 2100 (c) and 2200 (d).	218
A11	The globally assumed total occupied areas (solid lines) and significant production areas (dashed lines) areas of N-MACS (green tones) and No_Temp (blue tones) simulations.	219
A12	Vertical profiles comparing global horizontal averages of (a) alkalinity, (b) phosphate, (c) carbonate export, and (d) dissolved oxygen between N-MACS and RCP4.5 in 2100.	220

List of Tables

1.1	Conversions between the weight of carbon (C) and carbon dioxide (CO ₂) for commonly used units. The conversion factor is based on the molecular weight ratio of CO ₂ (44.01 g/mol) to C (12.01 g/mol), approximately 3.67.	3
2.1	Model parameters.	66
2.2	Latitudinal division of MOS deployment regions.	68
2.3	Description of the model experiments. “Stop” represents the termination of the simulation in year 2100; “Conti” represents the continuous MOS deployment till year 3000; “AU” represents artificial upwelling; NoRe represents zero remineralization of sunken macroalgal biomass; CN represents the molar C:N ratio of macroalgal biomass (MR _{C:N} in Table 2.1).	70
2.4	Properties of globally implemented MOS. Selected areas are from data of year 2024, whereas belt areas are values averaged from 2020 to 2024. Areal NPP rates and “Biomass yield” refer to the respective MOS area. The observational data come from the references.	74

2.5	Model simulations under the RCP 4.5 emission scenario. MOS-C represents the carbon sequestered via MOS. C_{atm} , C_{oc} and C_{ter} stand for atmospheric, oceanic and terrestrial carbon reservoirs respectively. ΔSAT stands for surface-averaged temperature relative to 13.18°C, the pre-industrial.	76
3.1	Summary table of N-MACS simulations. Significant N-MACS area is area with ≥ 100 tonnes DW per km ² per year. The changes are N-MACS variations relative to Ctrl_RCP4.5. . . .	117
4.1	Fact sheet design and description of individual parameters. . .	159
4.2	Overview of the CDR concepts considered in the study with current scale and estimated time of deployment of CDR options. Estimation of implementation time for concepts 1-8 has been performed assuming allowance for CO ₂ storage either on German territory under a German law (which currently is unfeasible due to restrictions in KSpG (2012)), or transportation of CO ₂ for storage in other countries.	163
4.3	Distribution patterns of CDR options.	167
A1	Macroalgae biomass annual productivity (t DW km ⁻² yr ⁻¹) in N-MACS regions.	211

Acknowledgements

行路难，行路难，多歧路，今安在？
长风破浪会有时，直挂云帆济沧海。

— 唐·李白

I would like to express my sincere gratitude to my supervisors, Prof. Dr. Andreas Oschlies and Dr. David P. Keller, for their unwavering support and guidance since my Master studies and throughout my PhD studies. Their invaluable advice and encouragement have been instrumental in shaping the direction of my research and the development of my skills as a scientist. I have been incredibly fortunate to have had the opportunity to work with such exceptional mentors, who have been not only brilliant scientists but also generous and kind colleagues. I extend my gratitude to my thesis committee for their diligent evaluation of both my thesis and its defense.

I am also deeply grateful to my BM colleagues, who have created a supportive and stimulating research environment that has made my work a truly collaborative and enriching experience. Their willingness to share their expertise, their constructive feedback, and their friendship have been indispensable to me, and I feel privileged to have been a part of such a dynamic and inspiring community. Especially I would like to thank Dr. Tianfei Xue, Dr. Wanxuan Yao, Dr. Wolfgang Koeve, Dr. Nadine Mengis, Dr. Karin Kvale, Dr. Christopher Somes, Dr. Fabian Reith and Vanessa Lampe for their selfless help in the past years. In addition, I would like to thank Pr. Dr. Victor Smetacek and my lovely colleagues from the research group of Dr. Mar Fernandez-Mendez at AWI.

My heartfelt thanks also go to my adorable friends: Dr. Chi Guan, Dr. Ruiyan

Zhang, Dr. Bei Su, Dr. Yanan Zhao, Dr. Te Liu, Dr. Jialin Zhou, Dr. Min Luo and Wenbin Cui, Runsheng Chen, Kang Ding, Ding Jin, Yujia Jin & Jingwen Zou, Yimei Zhang, Li Zhou. They have been a constant source of encouragement, happiness, and comfort throughout the ups and downs of my PhD journey. Their unwavering support and love have made all the difference, and I will always cherish the memories we have created together.

Last but not least, I want to express my deepest gratitude to my parents, who have been my rock and my inspiration in all aspects of my life. Special gratitude should be given to my wife, who has supported me all the time. Their unconditional love, sacrifice, and encouragement have sustained me through the challenges and successes of my PhD, and I could not have accomplished this without them. I dedicate this thesis to them with all my heart.

To my deeply loved Grandfather: I know that you're with me the only way that you can be, until I'm in your arms again.

亲爱的姥爷：我没有让您失望，我还会继续努力下去。当我们再次拥抱彼此，就永远不再分离！

Erklärung

Hiermit erkläre ich an Eides statt, dass die vorliegende Arbeit mit dem Titel ‘A Model-based Assessment of Ocean Carbon Sequestration with Macroalgae Mariculture’ von mir selbstständig angefertigt wurde. Es wurden keine weiteren Quellen als die zitierten Referenzen und die Beratung meiner Betreuer verwendet. Die Arbeit ist unter Einhaltung der Regeln guter wissenschaftlicher Praxis der Deutschen Forschungsgemeinschaft entstanden. Sie wurde weder im Rahmen eines Prüfungsverfahrens an anderer Stelle vorgelegt noch veröffentlicht. Ich erkläre mich damit einverstanden, dass diese Arbeit an die Bibliothek des GEOMAR sowie die Universitätsbibliothek der Christian-Albrechts-Universität zu Kiel weitergeleitet wird. Keiner meiner akademischen Grade wurde mir jemals entzogen.

Jiajun Wu

Kiel, February 2024